

Novel Organoalanes in Organic Synthesis and Mechanistic Insight in Conjugate Addition

DARREN WILLCOX, MSci

Thesis submitted to the University of Nottingham for the
degree of doctor of Philosophy

March 2014

Abstract

This thesis describes the development of novel aluminium hydrides ($\text{HAlCl}_2 \cdot \text{L}_n$) and organoalanes ($\text{Cl}_2\text{AlCH=CHR}$ and ClMeAlCH=CHR) for organic synthesis, as well as exploring the mechanism by which copper-catalysed conjugate addition proceed with diethylzinc and triethylaluminium.

In Chapter 1, the mechanism of copper-catalysed conjugate addition of diethylzinc to cyclohexenone and nickel-catalysed 1,2-addition of trimethylaluminium to benzaldehyde has been studied. The kinetic behaviour of the systems allows insight into which metal to ligand ratio provides the fastest rest state structure of the catalyst to enter the rate determining step. The ligand order in these reactions (derived from these ligand optimisation plots) provides information about the molecularity within the transition state.

In Chapter 2, the synthesis of somewhat air-stabilised aluminium hydrides and their subsequent use in palladium-catalysed cross-coupling is described. Stabilised aluminium hydrides of the type $\text{HAlCl}_2 \cdot \text{L}_n$, $[\text{HAl}(\text{O}^t\text{Bu})_2]$ and $[\text{HAl}(\text{N}^i\text{Bu}_2)]_2$ were synthesised. The hydroalumination of terminal alkynes was optimal using *bis*(pentamethylcyclopentdienyl) zirconocene dichloride, resulting in a highly regio- and stereo-

chemical synthesis of alkenylalanes which undergo highly efficient palladium-catalysed cross-coupling with a wide range of sp^2 -electrophiles.

Chapter 3, describes conjugate addition chemistry of $CIXAICH=CHR$ ($X = Cl$ or Me) under phosphoramidite/copper(I) conditions ($X = Me$). Highly enantioselective additions to cyclohexenones (89-98+% ee) were attained. A highly efficient racemic addition of the alkenylalanes ($X = Cl$) to alkylidene malonates occurs without catalysis.

Finally, Chapter 4 includes all the experimental procedures and the analytical data for the compounds prepared in the subsequent chapters.

Contents

Abstract.....	2
Acknowledgements.....	8
<i>Abbreviations</i>	10
<i>Mechanistic insight in conjugate addition by ligated cuprates</i>	11
<i>1.0 Introduction</i>	12
<i>1.1 General introduction</i>	12
<i>1.1.1 Conjugate addition of stoichiometric organocopper reagents</i>	12
<i>1.1.2 Catalytic Ligated cuprates</i>	15
<i>1.1.3 Mechanistic investigations of copper-catalysed conjugate addition</i>	25
1.2 Aims of research.....	30
1.3 Results and Discussions	32
<i>1.3.1 The kinetic protocol</i>	32
<i>1.3.2 Reproducibility of kinetic runs</i>	37
<i>1.3.3 Ligand effect in conjugate addition</i>	39
<i>1.3.4 Effect of the copper source</i>	49
<i>1.3.5 Effect of the terminal organometallic reagent</i>	51
<i>1.3.6 Ligand rate dependencies</i>	53

The results from Table 4 show that the number of ligands in the fastest rest state of the catalyst which enters into the transition state (ligand optimisation plot) is generally higher than the number of ligands in the transition state (ligand order).

However, this is not the case for trimethylphosphine, where the rest state of the catalyst is akin to the transition state.	55
1.3.7. <i>Non-linear studies</i>	55
1.3.8. <i>Method of continuous variation analysis</i>	59
1.3.9. <i>Conjugate addition of Grignard reagents to α,β-unsaturated esters</i>	62
1.3.10. <i>Nickel-catalysed 1,2-addition to aromatic aldehydes</i>	64
1.4 <i>Conclusions</i>	66
Chapter 2	68
<i>Synthesis of air-stabilised alanes and application in hydroalumination chemistry</i>	68
2.1 <i>Introduction</i>	69
2.1.1 <i>Aluminium hydrides</i>	69
2.1.2 <i>Synthesis of alkenylalanes</i>	75
2.1.3 <i>Cross coupling of alkenylalanes</i>	83
2.2 <i>Aims of research</i>	87
2.3 <i>Results and Discussion</i>	89
2.3.1 <i>Synthesis of aluminium hydrides</i>	89
2.3.2 <i>Hydroalumination of alkynes</i>	96
2.3.2.1 <i>Palladium catalysed Negishi coupling</i>	100
2.3 <i>Conclusions</i>	110
Chapter 3	111
<i>Conjugate addition of alkenylaluminum reagents to α,β-unsaturated carbonyl compounds</i>	111
3.1 <i>Introduction</i>	112
3.1.1 <i>Conjugate addition to diactivated carbonyls</i>	112

3.1.2 Uncatalysed conjugate addition of alkenylalanes to enones	116
3.1.3 Copper-catalysed conjugate addition of alkenyl organometallics.....	117
3.2 Aim of research.....	128
3.3 Results and discussions	129
3.3.1 Conjugate addition to alkylidene malonates	129
3.3.2 Copper-catalysed conjugate addition of alkenylalanes	133
3.3.3. ACA to trisubstituted enones	150
3.4. Conclusion	154
Chapter 4	155
Experimental Section	155
General remarks.....	156
General procedure 1: Kinetic studies using phosphorus ligands	158
General procedure 2: Kinetic studies Using SIMES.....	158
General procedure 3: Kinetic studies of Triethylaluminium with phosphoramidite ligands	160
General procedure 4: Kinetic studies of the conjugate addition of ethylmagnesium bromide to methyl crotonate	161
General procedure 5: Kinetic studies of nickel-catalyzed 1,2-addition of trimethylaluminium to benzaldehyde	162
General procedure 6: Phosphoramidite synthesis	166
General Procedure 7: Synthesis of Aryl SimplePhos ligands	170
General Procedure 8: synthesis of alkyl SimplePhos ligands	176
General procedure 9: Synthesis of dichloroalane adducts ^{51b}	182

<i>General Procedure 10: Cp*₂ZrCl₂-catalysed hydroalumination-cross coupling</i>	191
<i>General Procedure 11: ²H{¹H} and ¹H NMR monitoring of hydroalumination</i>	192
<i>General procedure 12: Zirconium-catalysed hydroalumination and conjugate addition</i>	224
<i>General procedure 13: volatile alkyne hydroalumination and conjugate addition</i>	230
<i>General procedure 14: Zirconium-catalysed hydroalumination and conjugate addition (neat conditions)</i>	232
<i>References</i>	256

Acknowledgements

There are many people I need to thank, without whom none of this would have been possible. First of all my supervisor Prof. Simon Woodward for giving me the chance to work as part of his group and for his continuous encouragement, inspiration, enthusiasm and professionalism. The next thank you goes to Prof. Luis Verios for all the DFT work carried out, without which understanding the kinetics work would have been highly challenging. I should also like to thank Prof. Alexandre Alexakis in Geneva for the kind donation of ligands, for which I am very grateful.

During my three years study I have worked with some great people, the past and present members of the Woodward group, to whom I owe a big thank you for creating a great working environment and helping me to grow as a chemist. These people are: Dr. Andrej Vinogradov, Dr. Xiaoping Tang, Dr. Daniel Glynn, Dr. Matthias Welker, Dr. Martta Asikainen, Dr. Rosie Crampton, Dr. Phil Andrews, Dr. Laurence Burroughs, Dr. Benoit Wahl, Dr. Chris Latham, Melchior Cini, Dorrit Tyack, Marc Magre, Marc Civit and Humaira Gondal. I would also like to thank all the technical and analytical staff from the University of Nottingham especially: Adrienne Davis, Kevin Butler, Shazad Aslam, Mick Copper, Graham Coxhill,

Dane Toplis, Jim fyfe, Eric Delea and Chris McGowen at the stores and Sue for supplying well need cups of tea and coffee.

Many thanks go to my close friends for their tremendous support during the three years: Jan Saska, Phil Andrews and Jessica Bellamy.

Last but by no means last I would like to give an especially big thank you to my fiancée Sarah Thornalley, who has supported and encouraged me so much throughout my PhD, and also my family for all the support.

Abbreviations

ACA	Asymmetric Conjugate Addition
acac	Acetylacetonate
BINOL	1,1'-Binaphthol
Cy	Cyclohexyl
DABAL-Me ₃	Bis(trimethylaluminum)-1,4-diazabicyclo[2.2.2]octane adduct
DABCO	1,4-diazabicyclo[2.2.2]octane
DFT	Density functional theory
DIBAL-H	Diisobutylaluminium hydride
DOSY	Diffusion-ordered spectroscopy
dppp	Diphenylphosphinopropane
e.e.	Enantiomeric excess
E ⁺	Electrophile
E _{act}	Activation energy
GC	Gas chromatography
HOMO	Highest occupied molecular orbital
HPLC	High performance liquid chromatography
L	A generalised monodentate Ligand
L.A.C	Ligand accelerated catalysis
LUMO	Lowest unoccupied molecular orbital
MCV	<i>Method of continuous variation</i>
MHz	Mega hertz
NHC	<i>N</i> -heterocyclic carbene
ppm	Parts per million
TADDOL	$\alpha,\alpha,\alpha,\alpha$ -tetraphenyl-1,3-dioxolane-4,5- dimethanol
TMEDA	<i>N,N</i> - tetramethylethylene diamine

Chapter 1

Mechanistic insight in conjugate addition by ligated cuprates

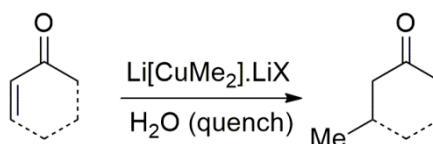
1.0 Introduction

1.1 General introduction

Since the seminal discovery of 1,4-nucleophilic addition to α,β -unsaturated carbonyl compounds by Arthur Michael,¹ applications of conjugate additions have become fundamental procedures for the synthesis of carbon-carbon and carbon-heteroatom bonds. The formation of carbon-carbon bonds especially is often carried out using organocopper compounds either as stoichiometric cuprates, or in catalytic amounts. As this is the major theme of this thesis it is appropriate to present an overview of this area.

1.1.1 Conjugate addition of stoichiometric organocopper reagents

The first examples of conjugate additions to α,β -unsaturated carbonyl compounds date from the early 1950s and used stoichiometric amounts of cuprates, mainly lithium cuprates (Gilman reagents), as the nucleophiles (**Scheme 1**).²



Scheme 1 Representative cuprate addition to enones.

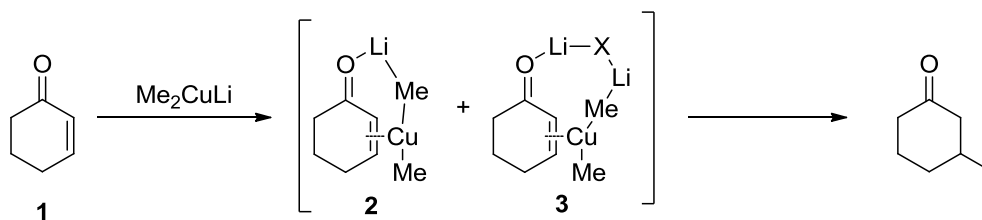
In order to add an organo-group in an enantioselective manner, either the organocopper reagent needs to be chiral

and enantioenriched or an external chiral Lewis acid must be added. The former can be achieved by synthesising a heterocuprate bearing a covalently bound chiral alkoxy-, amino or sulfur ligand to act as an asymmetric 'dummy ligand', which remains coordinated to the copper throughout the transformation.³

Initial kinetic studies by Krauss⁴ on the mechanism of conjugate addition of Gilman-type cuprates to enones indicated that the reaction follows first order kinetics in terms of enone but a more complex order with respect to the cuprate. Krause and co-workers noticed that when an excess of cuprate was used, the reaction still followed first-order kinetics.⁵ The authors concluded that the mechanism involves a reversible cuprate-enone complex which is followed by the conversion of the intermediate into the product through a unimolecular pathway.

The intermediate complex between the cuprate and enone has been investigated in several NMR studies.⁶ In all of these reports a common feature is that there is a lengthening of the C=C π -bond upon formation of the copper- π -complex. Additionally, in all cases the lithium atom is coordinated to the carbonyl oxygen. When Bertz and co-workers probed the addition of $\text{Me}_2\text{CuLi} \cdot \text{LiX}$ (X = bromide or chloride) to cyclohexenone **1** *via* rapid injection NMR, two cuprate-enone

π -complexes were detected for which they proposed structures **2** and **3** (**Scheme 2**).

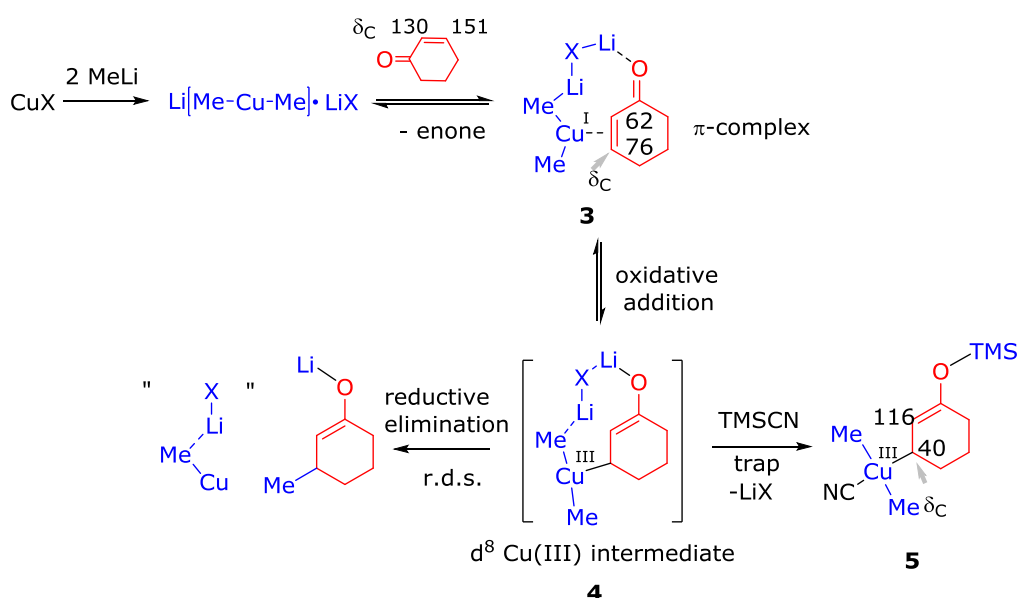


Scheme 2 Proposed π -complexes in conjugate additions of Gilman's reagent to cyclohexenone.

These two species were identified by carbon-13 NMR where a downfield shift in the carbonyl resonance by up to 10 ppm and a large upfield shift of around 60 ppm or greater for the olefin carbons was detected. This chemical shift difference in the olefinic region was attributed to the partial rehybridisation of the alkene sp^2 carbon centres into sp^3 centres.

Although computational evidence was presented for a copper(III) intermediate **4** in such 1,4-additions (**Scheme 3**), it initially remained undetected. However, in 2007 Bertz and co-workers demonstrated the presence of this key intermediate, using the rapid injection NMR technique, carrying out the same reaction in **Scheme 2** in the presence of trimethylsilyl cyanide.⁷ This technique allowed the spectroscopic characterisation of a transient copper(III) species. An upfield shift was observed from 76 ppm in the π -

complex **3** to 40 ppm in the copper(III) alkyl complex, which is considered indicative of a copper(III)-C_{alkyl} species like **5** (**Scheme 3**).



Scheme 3 Carbon-13 NMR elucidation of a copper(III)

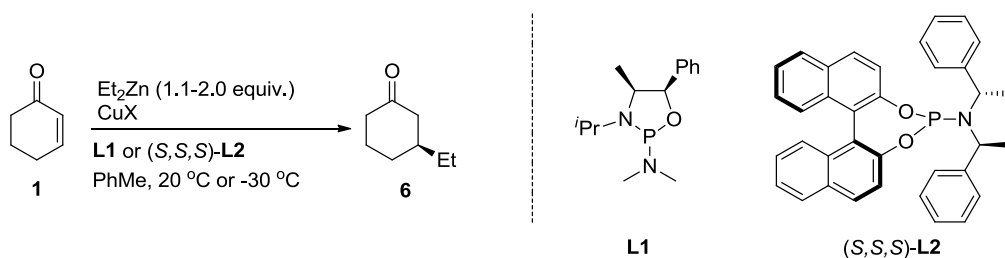
intermediate. The numbers on structures refer to ^{13}C chemical shifts

An excellent review concerning the reactions and mechanisms of organocopper reagents, was published in 2012, covers in detail the approaches used to characterise intermediates in stoichiometric cuprate chemistry is available.⁸

1.1.2 Catalytic Ligated cuprates

In order to facilitate the transition from enantioselective stoichiometric cuprate additions to the use of only catalytic amounts of copper salts and chiral ligands, the application of ligand accelerated catalysis (L.A.C.) is deemed essential.⁹ Typically, copper(I)-catalytic systems are under dynamic

ligand exchange and the presence of strongly rate accelerating external ligands can lead to the formation of a highly kinetically advantaged catalyst. The first major breakthrough for copper-catalysed conjugate addition arose when dialkylzinc based systems were used to replace Gilman-type cuprates. In the early 1990s Alexakis and co-workers reported the first use of diethylzinc in 1,4-additions to cyclohexenone in the presence of a catalytic amount of copper and a chiral ligand (**L1**) (**Scheme 4**).¹⁰ Although only a low enantioselectivity was achieved (32%), this pioneering work is of high importance as the reaction quickly became a benchmark for the testing of new ligands. Finally, the introduction of phosphoramidite ligands, for example **L2** by Feringa and co-workers¹¹ led to routine attainment of extremely high levels of enantioselectivity (>98%), cementing copper's place as a metal of choice for asymmetric conjugate additions. Previously only rhodium complexes had afforded such high levels of enantioselectivity.¹²



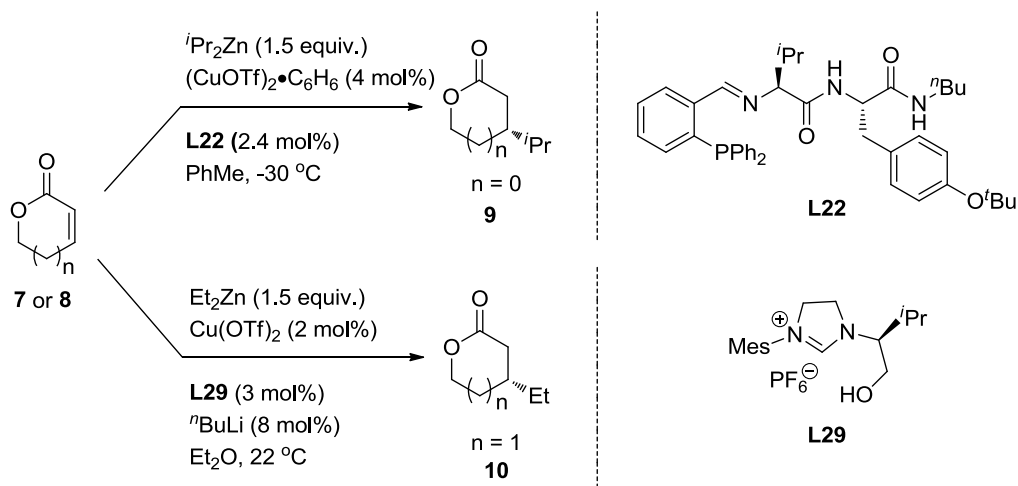
Scheme 4. Initial examples of catalytic conjugate addition of diethylzinc.

1.1.2.1 Choice of primary organometallic reagent

Prior to the 1990s, lithium cuprates were the typical nucleophiles for conjugate addition. However cuprates can also be synthesised from many other primary organometallic systems, including: magnesium, zinc, aluminium, zirconium and others.¹³ It is therefore appropriate to give a brief overview of the most common organometallic reagents used in copper-catalysed conjugate additions.

Since the seminal work by Alexakis, dialkylzinc reagents remain a common choice for conjugate addition due to their low background reactivity in the absence of catalytic additives. This lower dialkylzinc background reactivity means that many functional groups tolerate the presence of alkylzinc units such that functionalised organozinc reagents can be used to attain high enantioselective additions without chemoselectivity issues.^{11,14} One disadvantage of diorganozinc reagents is that only a small selection of them is commercially available: diethylzinc, dimethylzinc, di-*n*-butylzinc, diisopropylzinc and diphenylzinc. Functionalised organozinc reagents can however be readily synthesised from either organoiodide/diethylzinc exchanges or *via* hydroboration/transmetallation processes. Although all diorganozinc reagents can be used in conjugate addition chemistry, commercially available diethylzinc is the one most commonly employed. Dimethylzinc is seldomly used,

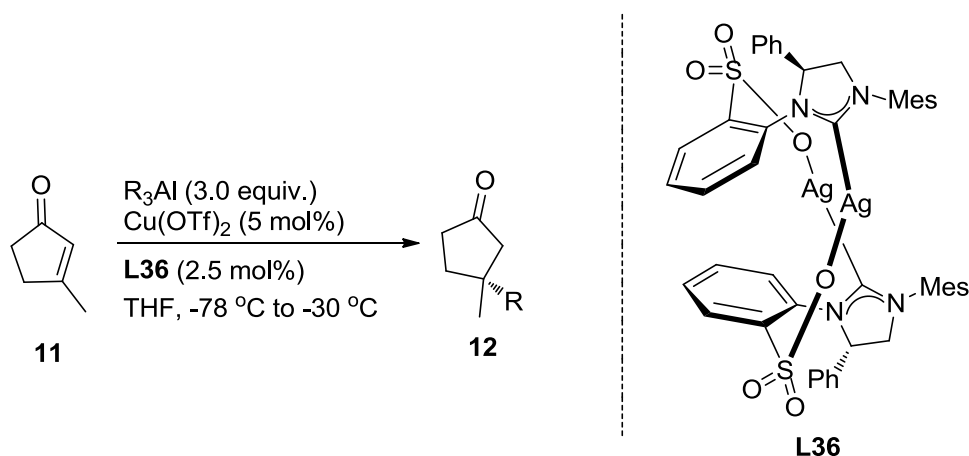
even though comparable enantioselectivities to diethylzinc additions can be achieved. Its limited use is due to its stronger zinc-carbon bond which lowers the innate reactivity and highly increased reaction times are normally required even for relatively activated substrates, such as enones. One drawback to the inherent lower reactivity of diorganozinc based systems is that there are very few examples of additions to substrates with lower reactivity than simple enones, such as α,β -unsaturated esters (**Scheme 5**).^{15,16}



Scheme 5 ACA reactions of dialkylzincs to challenging substrates.

Triorganoaluminium reagents have recently become a popular choice of organometallic for conjugate addition reactions as they have a higher reactivity than the corresponding dialkylzincs. Like dialkylzinc reagents, the commercial availability of triorganoaluminium reagents is limited. Only trimethylaluminium, triethylaluminium, tri-*n*-propylaluminium, tri-*n*-butylaluminium, triisobutylaluminium,

tri-*n*-hexylaluminium and tri-*n*-octylaluminium are readily available. Due to the enhanced reactivity of triorganoaluminium reagents they can undergo copper-catalysed ACA reactions with a range of Michael acceptors, including challenging trisubstituted enones (**Scheme 6**).¹⁷ This enhancement of reactivity is due to the higher Lewis acidity of aluminium compared to zinc (prior coordination of the enone carbonyl is believed to be important in substrate activation). Unlike dimethylzinc, trimethylaluminium is highly active in conjugate addition and is the main choice when installing a methyl group into target compounds.



Scheme 6 Use of trialkylaluminium reagents in catalytic ACA reactions.

All early attempts at asymmetric catalytic conjugate addition (prior to 1990) were based on the seminal work by Kharash¹⁸ who used Grignard reagents, but these provided only limited stereoselectivities.¹⁹ This limited success was due to the high background reactivity of the unligated magnesium cuprate coupled to the poor L.A.C. effects shown in the

ligand/solvent combinations initially used. The major advantages of using Grignard reagents is their ready commercial availability coupled to their ease of preparation. Unfortunately, unless an appropriate ligand is chosen, uncatalysed 1,2- or 1,4-addition reactions dominate the reaction manifold. The choice of optimal ligands for catalytic asymmetric Grignard reagents are different to those used for other organometallics, typically diphosphines or *N*-heterocyclic carbenes (NHCs) ligands are preferred.

The family of organometallics that can be used for copper-catalysed ACA chemistry is still growing, with organozirconium,^{20, 21} and organoboron²² reagents being recent examples.

1.1.2.2 Ligands

The ligands used for efficient copper-catalysed conjugate addition are crucial, not only for enantioselectivity, but for also maximising competition against background (racemic) reaction contributions. The major types of ligands used for conjugate addition are phosphorus-based (phosphites, phosphoramidites and phosphines) or NHCs. Due to the vast number of ligands, only a brief discussion will be given here as there are several excellent reviews covering the area.²³

The most popular ligands used in copper(I)-catalysed conjugate additions are phosphoramidites (**Figure 1**). These

are based on a rigid (often chiral) C₂-symmetric diol or phenol together with an amine. Either component can be the asymmetric element.²⁴

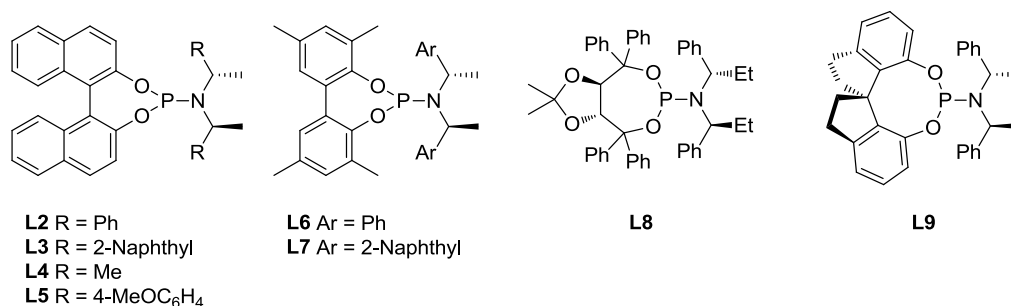


Figure 1 Representative phosphoramidites.

On changing the rigid backbone of the phosphoramidite ligands to simple aryl or alkyl substituents, phosphinamines are derived (**Figure 2**). These are sometimes referred to as SimplePhos ligands. These have been noted to give catalysts of improved activity and sometimes superior enantioselectivity over phosphoramidites.²⁵

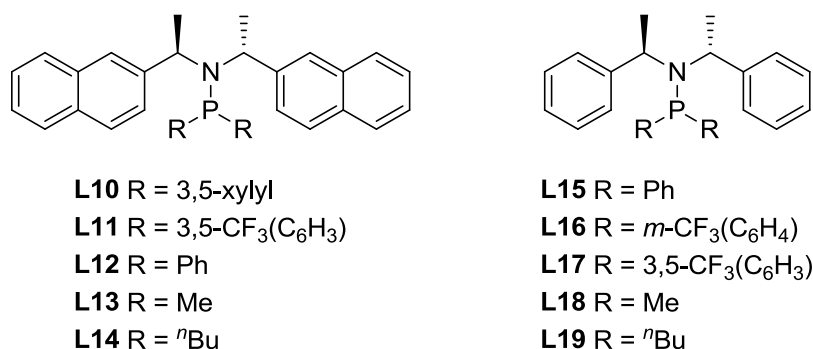


Figure 2 Representative SimplePhos ligands.

Phosphine ligands have been successfully used in copper-catalysed conjugate addition but their use is generally restricted than phosphoramidites (**Figure 3**). Monodentate phosphines perform better with dialkylzinc or

trialkylaluminium reagents.^{15,26,27} Bidentate phosphines are of greater utility when Grignard reagents are used resulting in catalysts delivering high enantioselectivities, particularly in the case of α,β -unsaturated esters (e.g. use of **L28**).²⁸

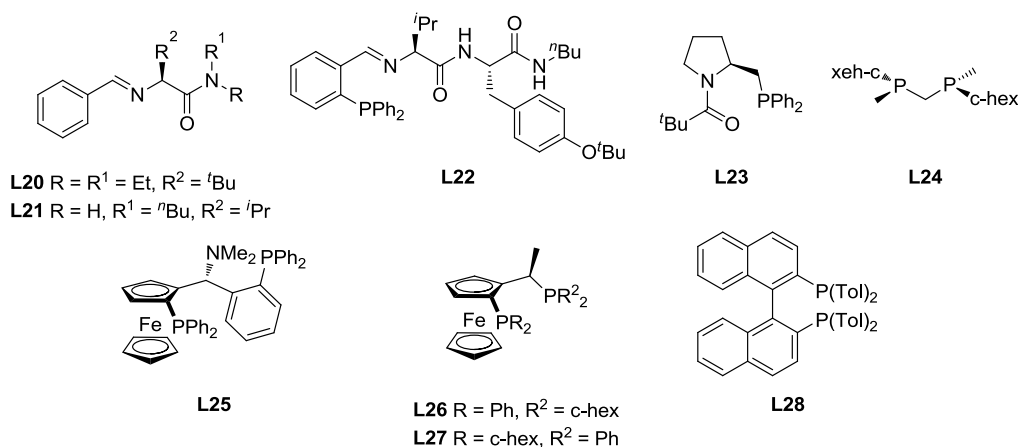


Figure 3 Representative monodentate and bidentate phosphine ligands.

Another class of ligands that can be used in conjugate additions of carbon nucleophiles are NHCs (**Figure 4**). The first reported use of these ligands was by Woodward and Fraser,²⁹ with the first enantioselective procedure reported by Alexakis.³⁰ Since these initial reports, many chiral NHC ligands have been used in conjugate addition, including NHC ligands with secondary coordination sites.¹⁶ When Grignard reagents are used, the NHC precursor (typically an imidazolium salt) can be used directly, but when dialkylzinc or trialkylaluminium reagents are used, a silver precursor (such as **L34-L37**) is required due to the slow rate of deprotonation of the imidazolium precursor.^{17, 31}

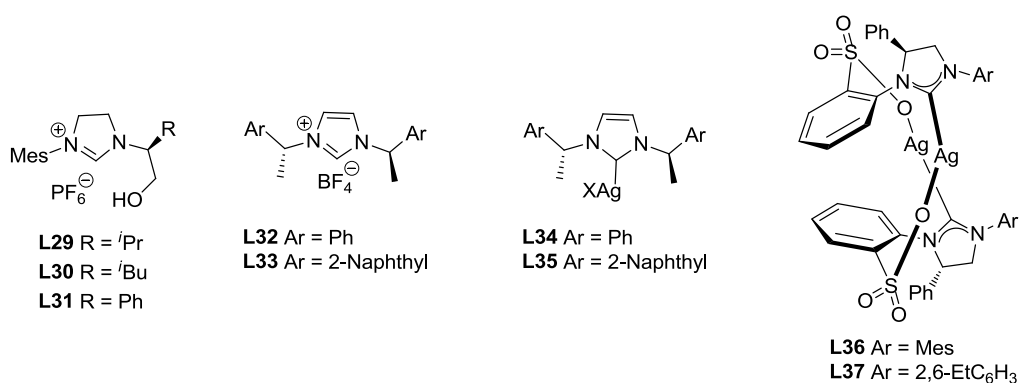


Figure 4 Representative NHC ligand precursors.

1.1.2.3 Substrate scope

There are many classes of Michael acceptor substrate that can be used for conjugate asymmetric addition and several reviews have been published concerning this topic in the period 1992-2014.²³ The most popular substrates are cyclic and acyclic enones, nitroolefins and α,β -unsaturated esters.

Within the cyclic enone family, cyclohexenone (**1**) is the most extensively studied. Such enones are highly reactive due in part to their conformation being locked *s-trans*. Other cyclic enones that have been used are substituted in the α -position to the carbonyl (**16** and **17**), in the β -position (**18** to **22**) and also in the 4-position (**23**). These substrates are potentially useful for kinetic resolutions, the formation of β,β -quaternary centres and buttressed tertiary centres respectively. Cyclic dienones have also been deployed resulting in high enantioselectivities (up to 98%) based on C=C enone differentiation. Acyclic enones are more demanding substrates as they can undergo *s-cis* and *s-trans* conformational

interconversion (**26** to **29**). Typically rather different ligands to those used for cyclic enones are required (**Figure 5**).

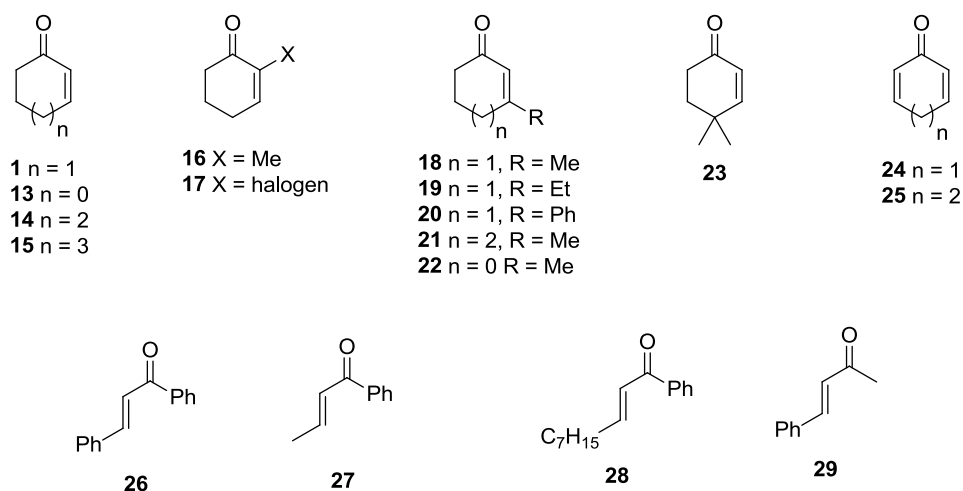


Figure 5 some representative enones.

Nitroolefins (**30** to **34**) have also been successfully used in copper-catalysed conjugate addition reactions (**Figure 6**). The 1,4-products generated are synthetically useful moieties, as the nitro group can be transformed into many other functional groups such as aldehydes, amines etc. Lactones (**7** and **8**), chromones (**35**), lactams (**36** and **37**), piperidones (**38**) and α,β -unsaturated esters (**39** and **40**) (**Figure 6**) have also all been used in conjugate addition resulting in products with high optical purity. The products from these latter reactions are important building blocks in total synthesis.

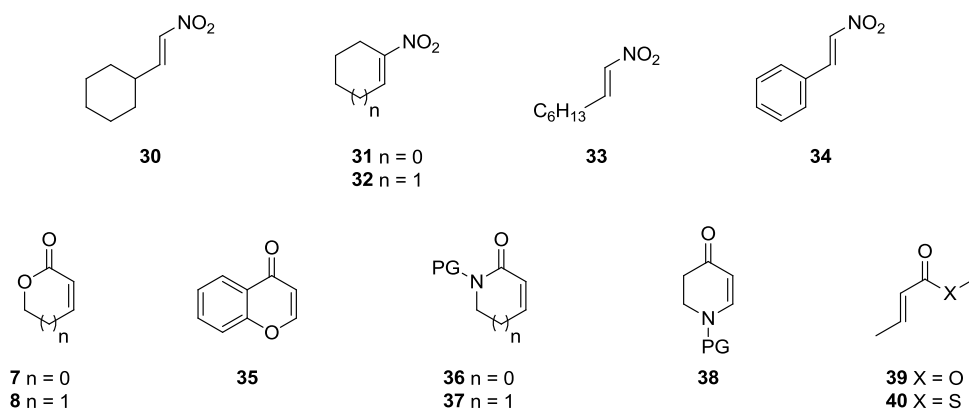
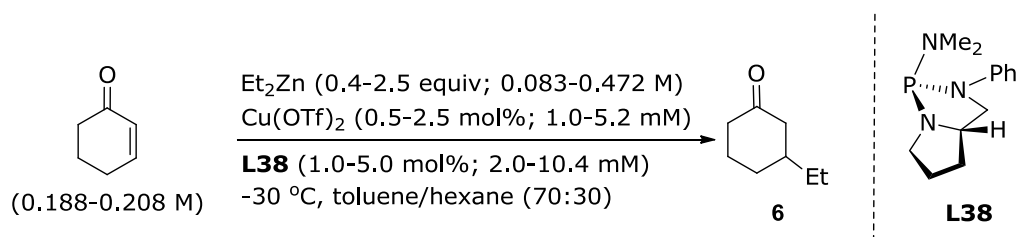


Figure 6 Representative nitroolefins, lactones, chromones, lactams, piperidones and unsaturated ester substrates for ACA reactions.

1.1.3 Mechanistic investigations of copper-catalysed conjugate addition

Various mechanistic tools have been applied in order to shed light on the mechanism(s) of copper-promoted conjugate addition. However, most of these have focussed on simple 'ligandless' Gilman-type cuprates.⁸ These are of less relevance to the work in this thesis, so here we focus on the literature covering ligated copper catalysts. Obtaining accurate kinetic data and reaction orders for copper-catalysed conjugate addition by ligated cuprates is challenging. Schröder and co-workers attempted to identify the reaction order of the catalyst for the copper-catalysed conjugate addition of diethylzinc to cyclohexenone in terms of both the catalyst and diethylzinc.³² In these series of experiments, the ratio of copper to ligand **L38** was fixed at 1:2 (**Scheme 7**). In this

case the order of the ACA reaction with respect to the ligand cannot be determined.



Scheme 7 Schröder's kinetic study.

On closer inspection of this work, there are some potential issues with the data collection: i) smooth continuous decay of the enone was not always observed, due to rapid quenching of the kinetic aliquots not always being attained; ii) before the first data point was collected, a significant conversion of the enone had already occurred (>40%) in some cases. The primary data was fitted to pseudo-first order behaviour, even in cases when neither limiting reagent was in large excess. On the basis of these kinetic results, it was proposed that the reaction was first order in both catalyst and diethylzinc. Reductive elimination of a copper(III) species derived from **42** was suggested to be the rate-determining step. The presence of two zinc species in the transition state is based on observations that stoichiometric cuprates require a 2:1 ratio of organometallic to $\text{Cu}(\text{I})$ halide for successful conversion.³³ It was suggested from these studies that species **41** would be most in accord with the first order kinetics in diethylzinc, due

to rapid association of the cuprate with a second zinc. The number of copper centres and ligands present in the putative π -complex cannot be determined from Schröder's studies. Structures having one **41**, two **42** or three **43** ligands leading to a key rate-determining copper(III) intermediate have all been proposed in the wider literature (**Figure 7**).³²

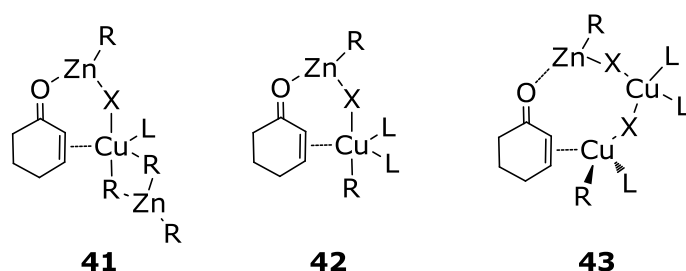
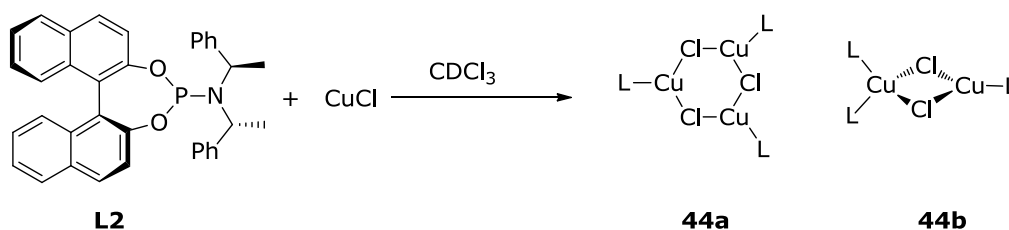


Figure 7 Proposed π -complexes for ACA of organozinc reagents.

Thus far, no direct kinetic or NMR data has been presented to discriminate between **41**, **42** and **43**, and all three are just proposals. Gschwind and co-workers suggested that **43** was the key π -complex based on diffusion-ordered NMR (DOSY) studies, which correlates the volume of the complex to the number of ligands attached to the copper centre. The studies were carried out on the pre-catalytic mixtures of copper(I) chloride and **L2**.³⁴ At a copper(I) chloride to **L2** ratio of 1:1, the major species present is an undefined trimer (CuClL2)₃ **44a**. When the concentration of the ligand is increased, a tetrahedral-trigonal dimer, $\text{Cu}_2\text{Cl}_2(\text{L2})_3$ **44b** is observed

(**Scheme 8**). This species is in equilibrium with others *via* ligand association processes.

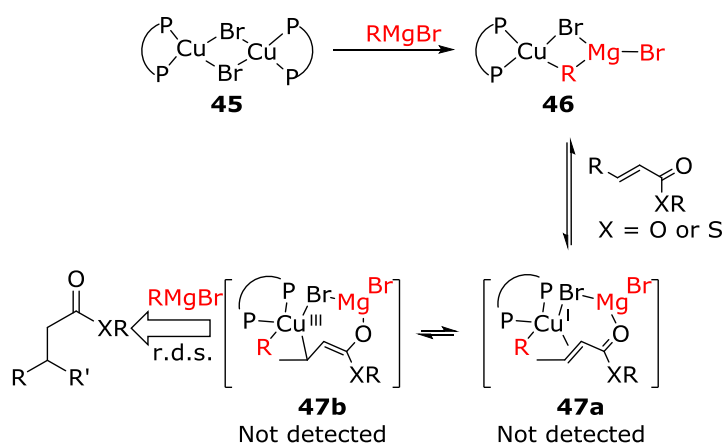


Scheme 8 The main structures determined *via* DOSY experiments.

Presently, these NMR studies have not been extended to real catalytic mixtures containing terminal organometallics by Gschwind.

Feringa and co-workers studied the kinetics of the conjugate addition of ethylmagnesium bromide to α,β -unsaturated esters and thioesters.³⁵ These systems have been the subject of kinetic analyses using the crystallographically characterised dimer **45** as the catalyst precursor. The overall reaction was fitted to second order kinetics (rate \propto [enone][RMgX]) but showed first order dependence in total copper concentration. Additionally, ^1H and ^{31}P NMR studies were used to characterise the intermediates present in solution. When methylmagnesium bromide was added to **45**, there was rapid conversion to monomer **46** plus a minor, unidentified species (**Scheme 9**). When the α,β -unsaturated ester was added to **46**, a π -complex proposed to be **47a** is

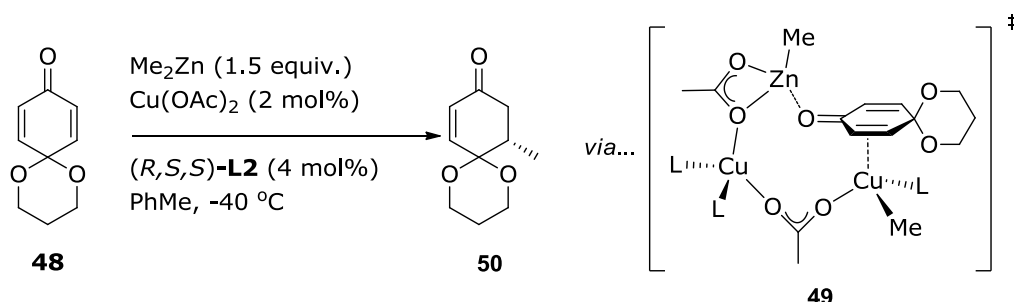
formed. However, unlike stoichiometric lithium cuprates, neither this π -complex nor the copper(III) intermediate **47b** are detectable by NMR spectroscopy. Therefore, support for the formation of a copper(III) intermediate over a direct carbocupration pathway came only from the (Z) to (E) isomerisation of initially geometrically pure Michael acceptors that is observed in these systems. This was thus taken to indicate a reversible back reaction from **47b**, leading to (Z) to (E) conversion in the starting material *via* (E/Z)-**47a** (Scheme 9).



Scheme 9. Proposed catalytic cycle for the addition of RMgBr to α,β -unsaturated esters and thioesters.

Computational studies have also been used help elucidate the reaction coordinate in ligated copper-catalysed conjugate addition. Woodward and co-workers probed the validity of π -complexes **41**, **42** and **43** using DFT.³⁶ This was achieved by looking at the conjugate addition of dimethylzinc to acetal **48** in the presence of copper(II) acetate and **L2**

(**Scheme 10**). Computational screening of **41**, **42** and **43** (among others) was carried out and indicated that complex **49**, analogous to **43**, is highly favoured. From this study, two common themes emerged: penta-coordinate phosphoramidite ligated copper(I) species were all highly energetically unfavourable and structure **41** could not be attained, even though docking of additional zinc to the π -complex is facile, due to the interaction between the copper and zinc units being too weak.



Scheme 10 π -complex identified *via* DFT using PBE1PBE hybrid functional and a VDZP basis set.

1.2 Aims of research

Given that ACA reactions rely almost exclusively on ligand accelerated catalysis by $\text{M}_a[\text{Cu}_b\text{R}_c\text{X}_d\text{L}_e]$ ligated cuprates (R and X are anionic transferable and non-transferable groups respectively, **L** = a donor ligand and $\text{M} = \text{ZnR}$, AlR_2 or MgX ; a-e are integers), it is surprising that so few publications deal with discovery of optimal ligated copper catalysts through

reaction rate studies. The principle aim for this part of our research was to answer two questions: firstly “can a kinetic study be used to define an optimal $[RCuL_n]^m$ catalyst quickly?”; and secondly; “is there any significance to the copper to ligand ratio measured in such experiments?”.

1.3 Results and Discussions

1.3.1 *The kinetic protocol*

Typical approaches for the determination of both mechanism and structure do not give quantitative information on catalyst stoichiometry as a function of ligand properties. Plots $\ln(k_1)$ vs. $[\mathbf{L}]/[\text{Cu}]$ were selected as $\ln(k_1)$ is directly related to the overall reaction's activation energy such that the maximum of the parabola indicates an optimal copper:ligand system composition for product turnover (**Figure 8**). The degree of parabola curvature also gives some indication of the degree of speciation in the catalytic mixture. In one limiting case a sharp peak at a single $[\mathbf{L}]/[\text{Cu}]$ value is expected if essentially just one, fast acting, catalytic species is present. Conversely, a very flat profile is expected if numerous species with similar $k_n[\text{Cu}_a\mathbf{L}_b]$ values can access product turnover from various compositions. For a range of ligands, such plots (ligand optimisation plot) might provide insight into how the steric and electronic factors of the ligands affect the catalyst, aiding further optimisation and mechanistic understanding. To the best of our knowledge, such an approach has appeared not to have been carried out. Additionally, the tangent to the slope of such plots should

provide an estimate of the ligand molecularity in the transition state

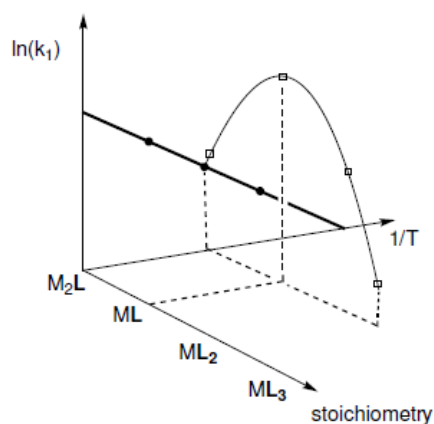


Figure 8. A representative Arrhenius plot (•) and its corresponding projection onto the stoichiometry of the catalyst (□).

For this approach to work three stringent criteria must be met: (i) ligand exchange must be fast compared to the catalysed reaction – or an equivalent mechanism must operate to provide a diverse catalyst library, (ii) $k(\text{M:L}_{\text{optimal}}) > k(\text{M:L}_{\text{rest}})$ must be true for the entire metal to ligand range studied, (iii) the fit of the primary kinetic data to a single appropriate model over the metal to ligand range must be accurate. Fortunately, all of these criteria are often fulfilled in asymmetric catalysis. For this technique to be used in an effective manner, the simple protocol outlined below (**Figure 9**) was followed.

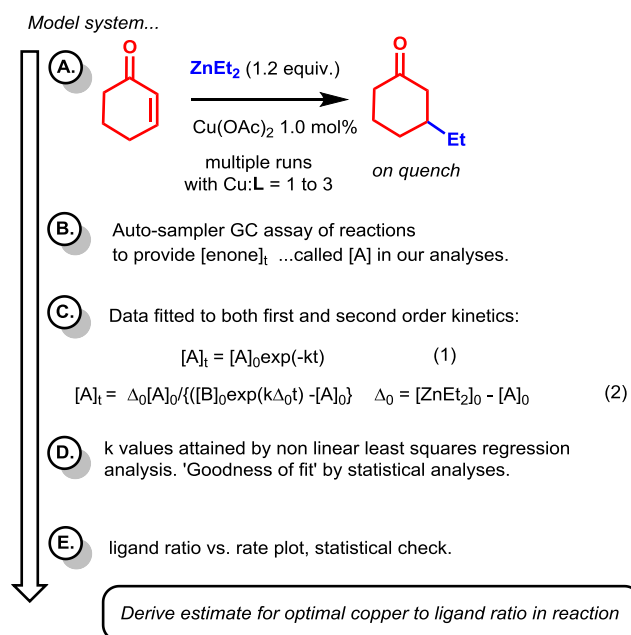
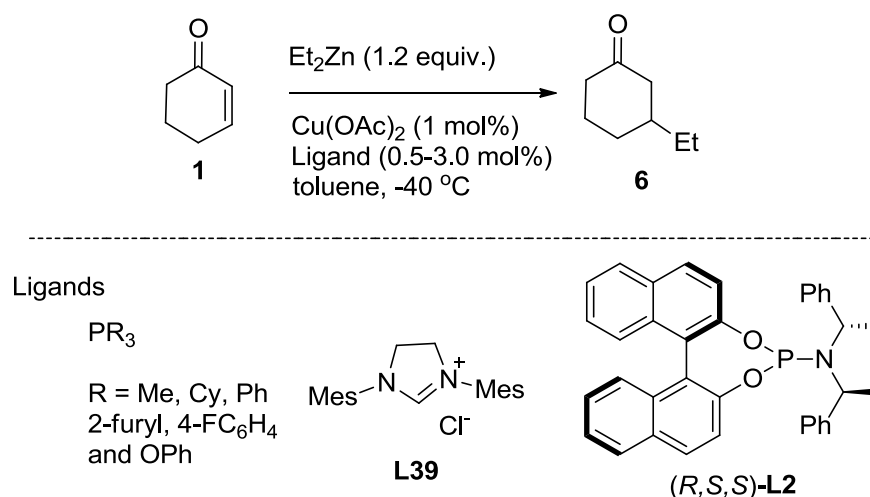


Figure 9. Standard procedure for the ligand optimisation plot.

The initial step of the procedure involves the addition of all the reagents, including the internal standard, followed by the enone for each copper to ligand ratio to be analysed. At specific time intervals aliquots were removed from the reaction mixture under a stream of dry argon using a pre-cooled pipette (liquid nitrogen) and then quenched with acid and analysed by GC. The raw data obtained was then used to plot a decay curve (in excel) for the starting material for both a first and second order dependence. The rate constants are then obtained using a non-linear least squares regression analysis (SOLVER in excel). From the derived rate constants a plot of the natural logarithm of the rate constant against the mole percentage of ligand allowed a copper to ligand ratio to be determined.

The technique was applied to the conjugate addition of diethylzinc to cyclohexenone (**Scheme 11**). It is critical that only one parameter is changed at any given time, therefore the concentration of the copper source (0.00256 M), diethylzinc (0.308 M), enone (0.256 M) and internal standard (0.014 M) were kept constant as was the temperature of the reaction (-40 °C). This means that the only parameter to change was the concentration of the ligand in the reaction mixture.



Scheme 11 The standard reaction protocol for the kinetic analysis.

The analysis of organometallic systems can be problematic, for example, it was noted that simple pseudo first order logarithmic plots can hide higher order kinetics.³⁷ We were anxious to avoid such issues.

After the kinetic runs had been carried out, the primary data were fitted to both first and second order rate (near

equal concentrations) equations. The k_{obs} values for these were then obtained using the non-linear least squares regression package SOLVER in Excel.³⁸ Once these were calculated, the quality of the data was assessed using a statistical package (Solver Stat.) to give R^2 'goodness of fit' data for each of the kinetic models and the average of the fits were taken to see which model fits the experimental data the best (**Table 1**, see also step C **Figure 9**). The values highlighted in bold represent the chemical model best fitted.

Ligand	Range studied/ mol % (No. of runs)	R^2 average for 1 st order fit	R^2 average for 2 nd order fit
L39	1-2.5 (4)	0.868	0.929
PMe₃	1-2.5 (4)	0.966	0.957
PCy₃	1-2.5 (4)	0.973	0.949
P(2-Furyl)₃	0.5-2.5 (5)	0.949	0.895
P(4-FC₆H₄)₃	0.5-2 (4)	0.960	0.918
PPh₃	1-2.5 (4)	0.927	0.830
P(OPh)₃	1-3 (4)	0.970	0.900
(R,S,S)-L2	1.5-3 (4)	0.964	0.895

Table 1. 'Goodness of fit' (R^2) of primary kinetic data to first and second order kinetics for the reaction shown in **Scheme 11**.

1.3.2 Reproducibility of kinetic runs

The paucity of published kinetic studies on copper(I)/ligand-catalysed additions of organometallics to enones is not without reason. Sampling by Krause's aliquot procedure (the normal approach) is susceptible to a number of issues, including: (i) lack of innate precision in organometallic concentration and purity issues through their time-dependant modification by traces of oxygen and water, (ii) the high lability and air sensitivity of phosphine-ligated cuprates (compared to stoichiometric Gilman-type cuprates), and (iii) the presence of competing oxygen induced radical background 1,4-addition reactions. The technical difficulties mentioned above are clearly demonstrated in the most sensitive of the systems we studied: copper(II) acetate/triphenylphosphine (1 mol%/1.5 mol%). While separate triphenylphosphine runs easily provide acceptable fits to either pseudo first order (Equation 1 in **Figure 9**) or second order near equal concentration (Equation 2 in **Figure 9**) models, unless special precautions are taken duplicate runs typically provide non reproducible rate constants with large error bars (**Figure 10**).

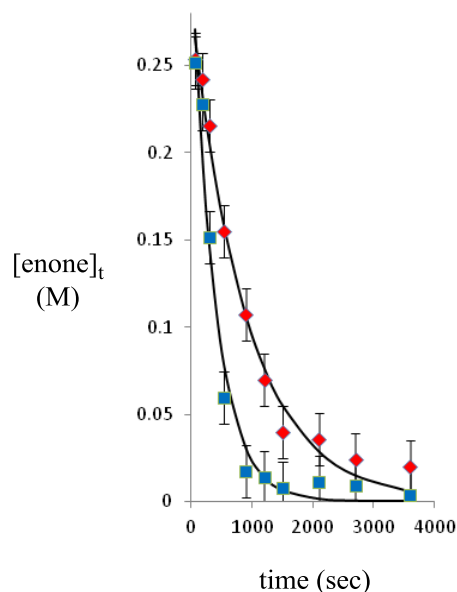


Figure 10 Reproducibility issues in the most labile systems.

Extensive trials revealed that the reproducibility issues within **Figure 10** could be minimised by: (i) sampling under argon (as opposed to nitrogen), (ii) use of more strongly ligated copper-ligand combinations than *in situ* copper(I) acetate/triphenylphosphine (e.g. increasing cuprate Lewis acidity or ligand donor power), (iii) avoiding $[\text{Ligand}]/[\text{copper}] < 1$ regimes, where complex behaviour was often observed, (iv) conducting all runs with identical organometallic batches over a short period of time for all ligands trialled – ensuring at the least valid *relative* comparisons and (v) plotting $\ln(k_1)$ vs. mol% **L** to allow identification of the fastest Copper:**Ligand** catalyst combination within the ratios investigated. Such parabolic plots were found to be somewhat self-compensating of minor

reproducibility in the primary data and led to much more robust fastest copper:**Ligand**_(fast) determinations (often even across different reagent batches). Finally, the use of the copper(II) precursors was not an issue as reduction *in situ* to copper(I) salts was found to be rapid (typically >99% completed within 180 sec.).

1.3.3 Ligand effect in conjugate addition

The ligands we have analysed fall into two groups: those attached to strong σ -donor and those ligated by strong π -acceptors.

The results obtained from following the protocol of **Figure 9** were used to generate ligand optimisation plots which will allow the determination of the estimated copper:ligand ratio which provides the fastest overall rate for σ -donor ligands studied and these are summarised in **Table 2**.

The results showed that when strong σ -donor ligands (those with low χ_d values in the literature) such as tricyclohexylphosphine and trimethylphosphine, are used the copper to ligand ratios tend to be higher than that for weaker σ -donor ligands (those with higher χ_d values)

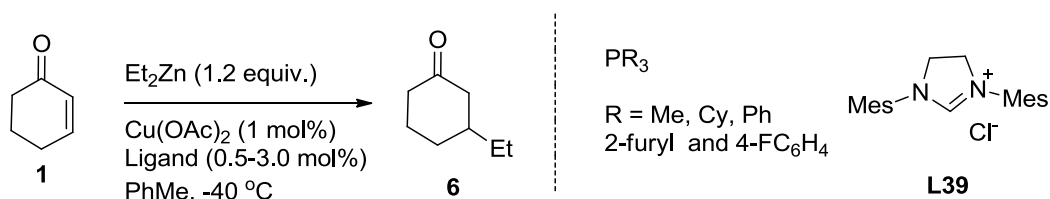


Table 2. 1,4-addition of diethylzinc to cyclohexenone using σ -donor ligands.

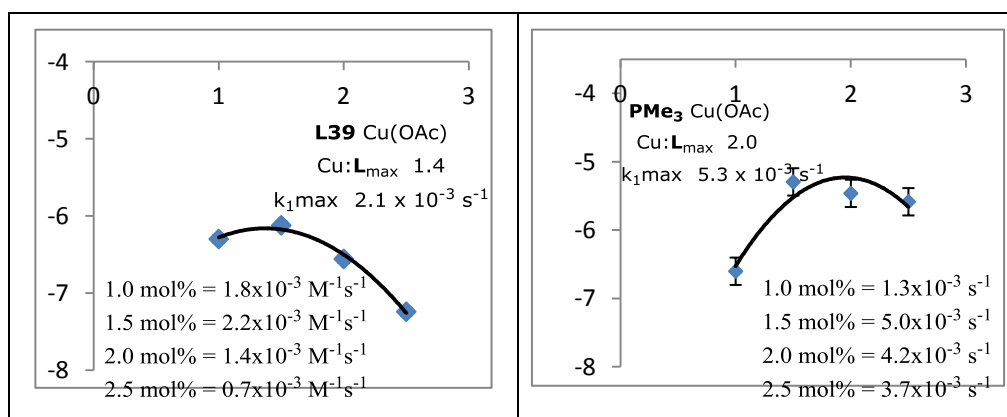
Entry	Ligand	σ -donor value (χ_d) ^[a]	π -donor value (π_p) ^[a]	copper to ligand ratio
1	L39	-	-	1:1.4
2	PMe₃	8.55	0	1:2.0
3	PCy₃	1.40	0	1:2.0
4	PPh₃	13.25	0	1:1.7
5	P(2-furyl)₃	-	-	1:1.3
6	P(<i>p</i>-FC₆H₄)₃	15.7	0	1:1.2

[a] Using the QALE approach for defining relative σ -donor/ π -acceptor ability. Small χ_d values correlate with strong σ -donors; non zero values of π_p indicate π -acceptor ability.³⁹

From Table 1 the 'goodness of fit' (R^2) data for NHC precursor **L39** indicates that the reaction best follows second order kinetics, *i.e.* a dependence on both the enone and zinc concentration (bottom equation in C in **Figure 9**). The free carbene (**L39** deprotonated with potassium *t*-butoxide) was also tested so a comparison with **L39** could be conducted. When the imidazolium species **L39** was used, the reaction proceeded cleanly (not much scatter in the primary kinetic data), conversely when the free carbene was employed the

reaction proceeded much slower and poor kinetic plots resulted. A possible explanation for this is that when imidazolium **L39** was used, it was deprotonated cleanly by the diethylzinc. Alternatively, when **L39** is pre-deprotonated with potassium *t*-butoxide, *t*-butanol is formed as a by-product and this changes the speciation of the active catalyst. Due to the level of scattering observed in the primary kinetic data, it was not possible to generate a meaningful ligand optimisation plot and only salt **L39** was used.

The value of the copper to ligand obtained from the ligand optimisation plot for **L39** indicates that there are 1.4 ligands attached to per copper centre (**Figure 11**). This is in line with the predicted transition state proposed by Gschwind from the NMR studies which suggests that it could take the form of **51** (**Figure 12**).³⁴ However, the error on this estimate is quite high (± 0.2). When 0.5 mol% ligand was tried the paucity of the data was too great to obtain meaningful rate constants



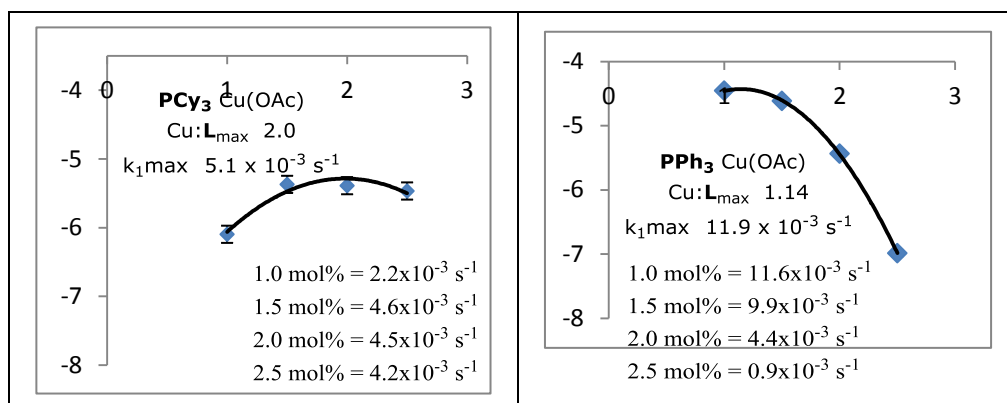


Figure 11. Comparative copper(II) acetate:L optimisation plots for the systems studied (at -40 °C). X-axes: mol% L per 1 mol% copper precursor used; y-axes: ln(k₁). For: a) **L39**, b) trimethylphosphine, c) tricyclohexylphosphine and d) triphenylphosphine.

When strong σ -donor phosphine ligands are employed (entries 2 and 3 in **Table 2**), the reaction mechanism is different to that of **L39**, with the 'goodness of fit' of the primary kinetic data is better on fitting a first order kinetic model. From the derived ligand optimisation plot, the copper to ligand ratios for trimethylphosphine and tricyclohexylphosphine suggests that the most populated rest state species in the reaction mixture which leads to 1,4-addition contain a Cu(PAlkyl)₃)₂ unit. Assuming that copper(I) attains a maximum coordination number of 4 then structures **52** and **53** seem the most likely arrangements leading up to

the transition state if reductive elimination of a Cu^{III} -like transition state is the rate determining step (**Figure 12**).

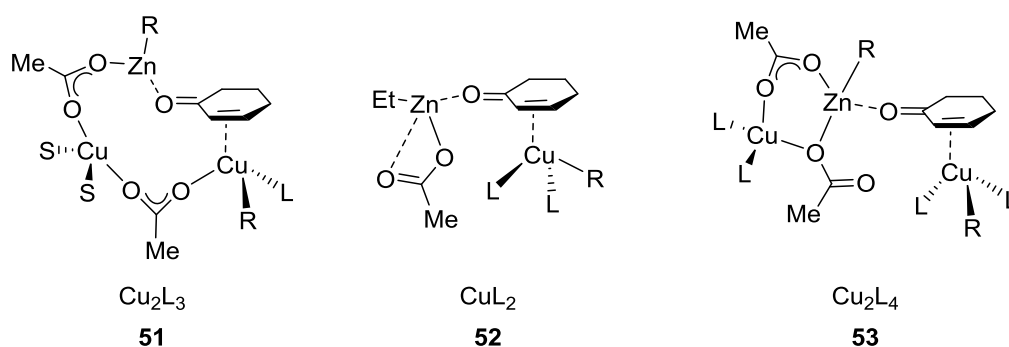


Figure 12. Possible π -complexes proposed *via* DFT calculations.

When tri(2-furyl)phosphine and tri(4-fluorophenyl)phosphine are used as ligands (entries 5 and 6 in Table 2), the R^2 data indicates that these ligands best fit an overall first order reaction rate, *i.e.* dependent on enone concentration only. From the ligand optimisation plots a range of values for the predicted catalyst rest state structure is obtained. Within the error bar of the reaction (± 0.2), these values suggest that these catalysts have similar structures to **51**. It is also evident that the amount of π -acceptor character influences the strength of the bond between the phosphine and the copper centre. The copper to phosphorus bond is significantly weaker than that of the corresponding σ -donor ligands resulting in a more labile system and greater scatter is observed in the ligand optimisation plots.

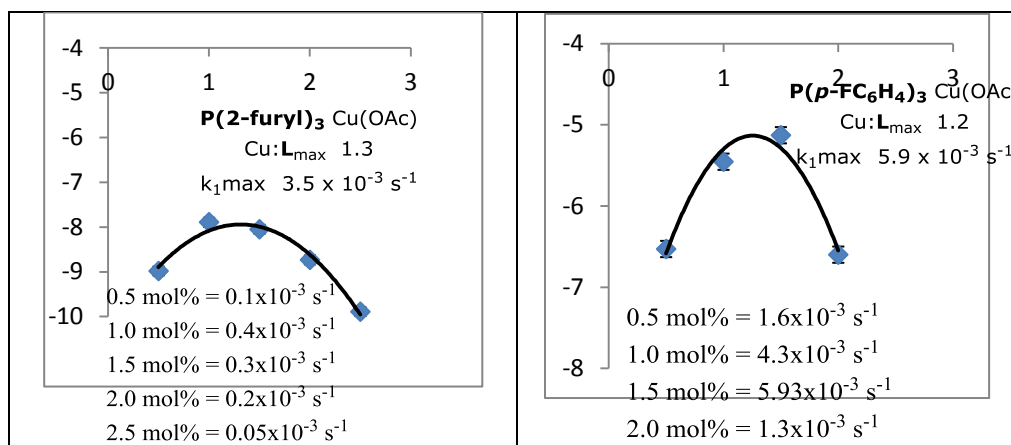


Figure 13. Comparative $\text{Cu}(\text{OAc})_2\text{:L}$ optimisation plots for the systems studied (at -40°C). X-axes: mol-% **L** per 1 mol-% copper precursor used; y-axes: $\ln(k_1)$. For: a) tri(2-furanyl)phosphine and b) tris(4-fluorophenyl)phosphine.

To help with the elucidation of these π -complexes, we collaborated with Prof. Verios who ran DFT calculations for us using trimethylphosphine as a model ligand.⁴⁰ A viable structure that could be identified was **53**, which provides a lower energy route for conjugate addition which matches the experimentally observed stoichiometry. When the reaction involving the Cu_2L_4 stoichiometry was modelled, it was found that the reaction occurred in three steps. The initial step involves the addition of an external trimethylphosphine ligand *via* a dissociative process, which creates a higher energy intermediate. This is followed by the dissociation of the acetate linker from the copper centre containing the 'R' group,

which is then followed by the addition of the methyl group across the olefin double bond, resulting in a lower energy state (**Figure 14**).

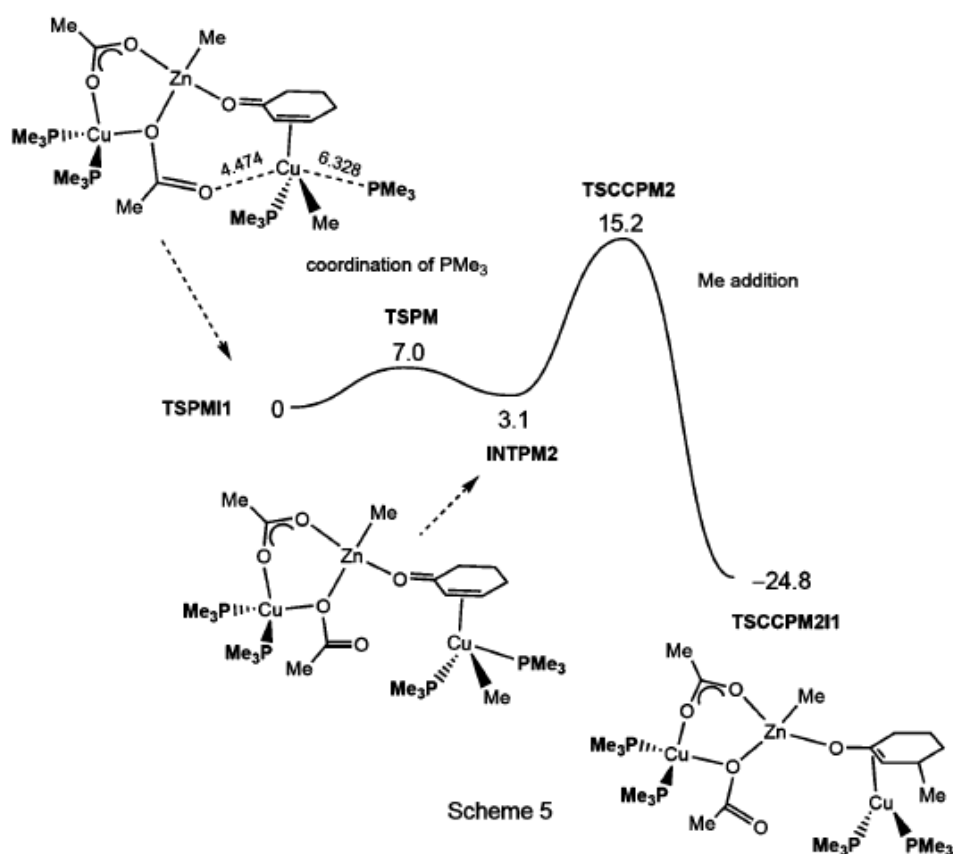


Figure 14. Free energy profile (B3LYP, kcal mol⁻¹) for the methyl addition to cyclohexenone, with a Cu₂L₄ stoichiometry.

When strong π -acceptor phosphorus ligands were employed, the 'goodness of fit' on the primary kinetic data shows that the best fits was to overall first order kinetics. From the data it was evident that the higher the π -acceptor capability of the ligand (higher values of πp) the higher the number of ligands seem to be in the rest-state of the catalyst (**Table 3**).

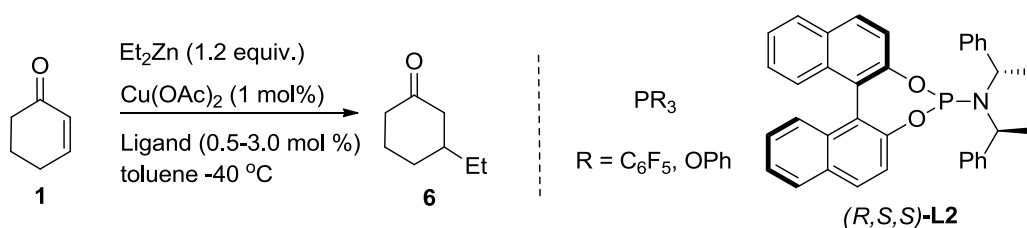


Table 3. 1,4-addition to cyclohexenone using π -acceptor ligands.

Entry	Ligand	σ -donor value (χ_d) ^[a]	π -donor value (π_p) ^[a]	copper to ligand ratio
1	P(C₆F₅)₃	34.80	4.10	N/A
2	P(OPh)₃	23.60	4.10	1.0:2.3
3	(R,S,S)-L2	-	-	1.0:3.3

[a] Using the QALE approach for defining relative σ -donor/ π -acceptor ability. Small χ_d values correlate with strong σ -donors; non zero values of π_p indicate π -acceptor ability.³⁷

When tris(pentafluorophenyl) phosphine (entry 1, Table 3) was employed in the reaction, it was evident that the reaction was far too slow to be of any use, because after one hour the reaction had not reached the optimal three half lives normally required for accurate kinetic analysis. Because of this it was not possible to obtain a ligand optimisation plot for this ligand.

For ligand **(R,S,S)-L2**, the Cu:**L_{fastest}** studies indicate that a wide range of speciation in the reaction mixture with a slight preference for coordinatively saturated $\text{XCu}(\text{L2})_3$ (X = ethyl, acetate) as the catalytic rest state when $[\text{L2}]/[\text{Cu}] > 1$ (**Figure 15a**). A Cu_2L_2 motif for the rest state is, we believe,

the most likely. One potential structure is **51** (S = any credible 2-electron donor; *e.g.* toluene solvent, enone O-ligation, ethylzinc acetate, *etc.*). Given that rapid copper-ligand exchange is a known feature of such catalysts such a model is in accord with literature experimental data including the observation that potentially chelating substrates are frequently excellent substrates for ACA reactions, whereas substrates akin to **16** with R > Me are poorly represented in successful ACA transformations. Coordination vs. steric repulsion to the second copper centre in **51** (with displacement of one S) would be in line with these observations. Structure **51** is identical to the suggestion of Gschwind when S = **L2**. Given the fast exchange of ligands in these complexes, capture of additional **L2** by **51** is certainly possible. However, based on the kinetic evidence presented here, additional P-ligation in selective transition state is neither vital for turnover nor is it a major component in the r.d.s. The role of these additional phosphoramidites seems to be small additional conformational biasing within structure of **51** leading to the minor NLEs seen in section **1.3.7** and the maximisation of ee for additions when $[\mathbf{L2}]/[\text{Cu}]$ is >1. We sought evidence to support solvent interaction with transition state **51**. Dichloromethane is known to bind copper(I) centres more effectively than toluene and crystallographically

characterised examples are known. To the best of our knowledge no equivalent binding of dichloromethane to zinc(II) centres has been reported. In line with solvent exchange into transition state **51**, increasing the concentration of dichloromethane in the toluene solvent from 0.02 to 2.0 M results in a tenfold increase in reaction rate.

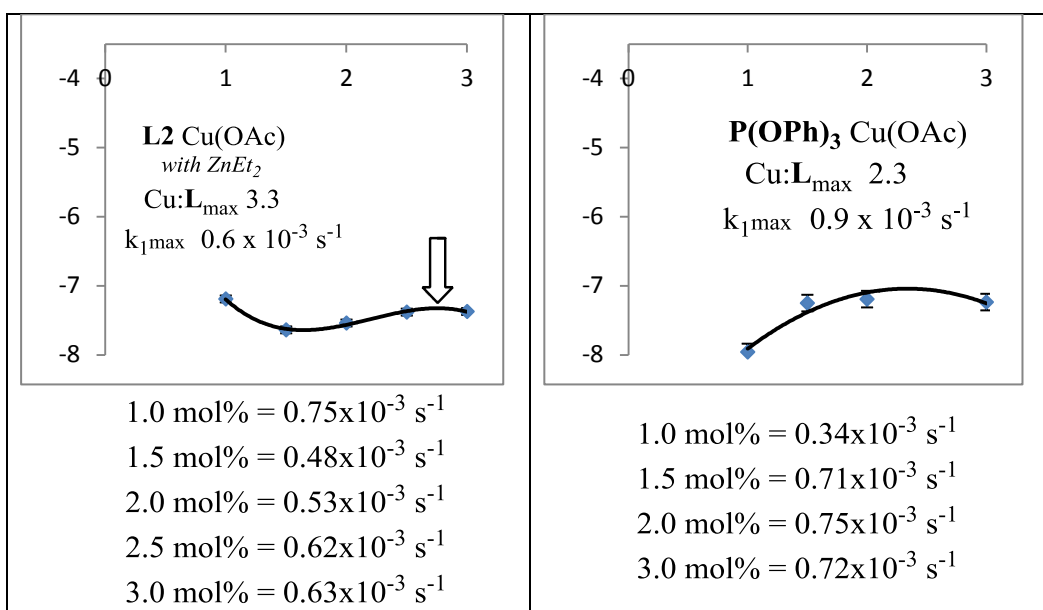


Figure 15. Comparative $\text{Cu}(\text{OAc})_2\text{:L}$ optimisation plots for the systems studied (at -40°C). X-axes: mol% **L** per 1 mol% copper precursor used; y-axes: $\ln(k_1)$. For: a) (*R,S,S*)-**L2** and b) triphenylphosphite.

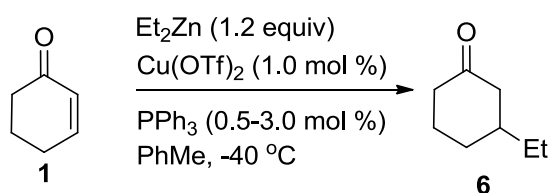
From copper to ligand studies for triphenylphosphite, a structure based on **51** is the transition state precursor, but with a slight propensity for an $\text{EtCu}(\text{triphenylphosphite})_2$ catalyst rest state. In all cases involving π -acceptor ligands,

slightly higher ratios were observed in comparison to σ -donor ligands. For these ligands it is clear from the curvature of the ligand optimisation plot, they bind copper(I) much less strongly than the σ -donor ligands, thus leading to a slightly increased error bar in the stoichiometry.

It is suggested that π -acceptor ligands lower the energy barrier for reductive elimination to occur from a transient copper(III) species derived from **51**, **52** and **53**, therefore increasing the reaction rate. However, in the DFT calculations, no copper(III) intermediates could be identified and the reaction coordinate is more akin to carbocupration of the enone.

1.3.4 Effect of the copper source

The Lewis acidity of the cuprate was also subjected to the same kinetic analysis under the same conditions previously mentioned. The highly labile *in situ* generated copper(I) acetate was changed to the more Lewis acidic copper(I) triflate which was generated *in situ*. Triphenylphosphine was the ligand of choice because it allowed a direct comparison between the two copper salts (**Scheme 12**).



Scheme 12. Standard reaction conditions when using copper(II) triflate as the copper source.

After closely examining the 'goodness of fit' of the primary kinetic data, it was evident that the overall reaction best fits first order kinetics, *i.e.* having only a dependence on enone concentration. Although the error bar on the copper(II) acetate/triphenylphosphine data is too high to allow any but the most general comparison (values of copper: $L_{\text{fast}} \sim 1.7$ and $k_{1\text{max}} \sim 1 \times 10^{-3} \text{ s}^{-1}$ were determined) it is clear that increasing the Lewis acidity of the cuprate does not alter the speciation compared to the acetate moiety (copper: $L_{\text{fast}} \sim 1.7$) but significantly increases its reactivity ($k_{1\text{max}} \sim 7.5 \times 10^{-3} \text{ s}^{-1}$). For the copper(II) triflate/triphenylphosphine system the Gschwind Cu_2L_3 core seems be the bulk rest state but whether this is maintained in the transition state for conjugate addition or behaviour akin to **52** is attained, cannot be deduced due to the quality of the data. However, it is clear that the zinc(II) triflate counter-cation provides very significant rate acceleration. Coordination of ethylzinc triflate (generated during catalyst formation) to the ligation sites of **51** (or a related structure) would be expected to significantly affect the

binding affinity of the enone to the adjacent copper-ethyl site. Finally, it is important to note that our data do not provide information on the number of zinc atoms in the transition state.

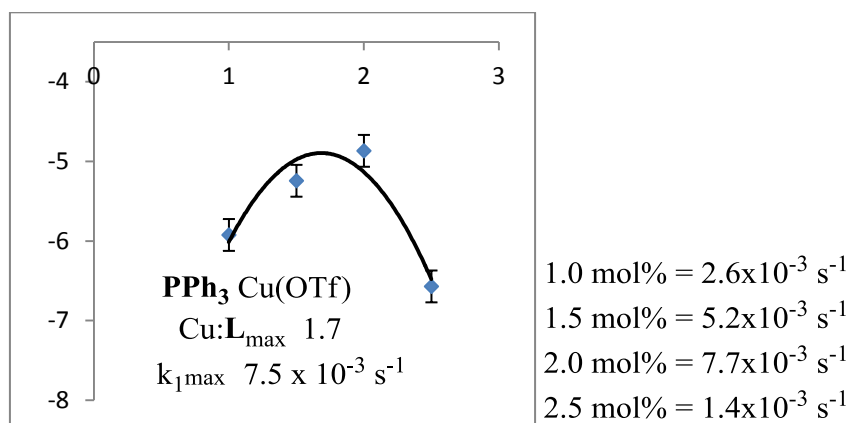
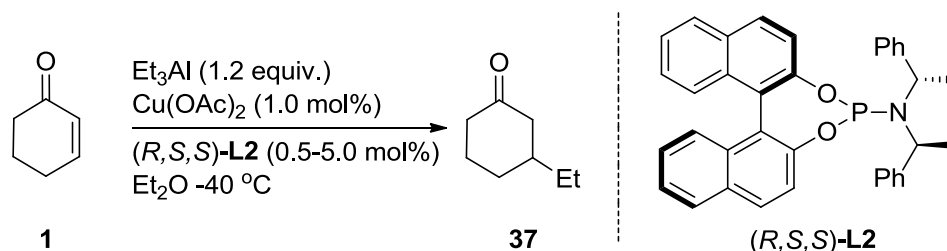


Figure 16. Comparative copper(II)triflate/triphenylphosphine optimisation plot (at $-40\text{ }^{\circ}\text{C}$). X-axes: mol-% **L** per 1 mol-% copper precursor used; y-axes: $\ln(k_1)$.

1.3.5 Effect of the terminal organometallic reagent

The effect of the terminal organometallic nucleophile was also examined by changing the terminal organometallic from diethylzinc to triethylaluminium. In order to directly compare the nature of the π -complex for the aluminium species, the conditions needed to be kept the same as for that of diethylzinc. To do this the concentration of copper(II) acetate (0.00256 M), triethylaluminium (0.364 M) and internal standard (0.014 M) were kept constant throughout all of the

runs, the ligand was fixed as (*R,S,S*)-**L2** and the solvent of choice was diethylether (**Scheme 13**). Diethyl ether was chosen as the solvent over toluene because toluene led to rapid oligomerisation of cyclohexenone.



Scheme 13. Standard reaction conditions for the addition of triethylaluminium to cyclohexenone.

The ligand optimisation plot data, based on first order kinetics, provides a copper:**L2**_{fast} ~2.4 ligands per copper. Based on the curvature of the ligand optimisation plot for this system it is closely analogous to that of diethylzinc/**L2**. Therefore we predict a structure based on **51** but with the ZnEt unit replaced by AlEt_2 as the intimate precursor to the ACA transition state. Based on the $\text{Cu}:\text{L}_{\text{fast}}$ data speciation within the catalyst pool is high but the major components are $\text{EtCu}(\text{L2})_n$ ($n = 2,3$).

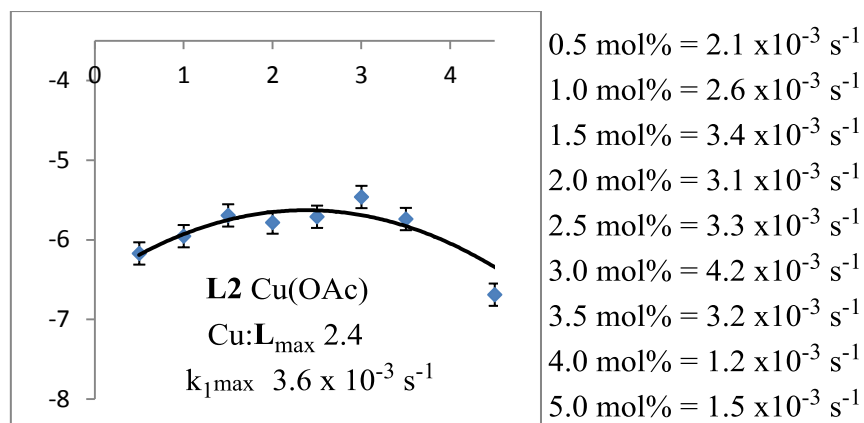


Figure 17. Comparative copper(II) acetate/(*R,S,S*)-**L2** optimisation plot (at -40 °C). X-axes: mol-% **L** per 1 mol-% copper precursor used; y-axes: $\ln(k_1)$.

1.3.6 Ligand rate dependencies

It is clear from the ligand optimisation plots for all systems studied, that only trimethylphosphine, tricyclohexylphosphine, triphenylphosphite, **L2** (both with diethylzinc and triethylaluminium) and copper triflate/triphenylphosphine gave reliable data to estimate the r.d.s ligand dependency. The 1,4-addition rate dependency on the ligand concentration for these systems is non-linear – at concentrations above $k_{1\max}$ the overall rate falls due to the presence of increasing concentrations of catalytically inactive, presumably coordinatively saturated, species. It is highly desirable to estimate the value of n in $\{\text{rate} \propto [\mathbf{L}]^n\}$ is determined as this would shed light on the number ligands present at the critical rate determining step of these ligated cuprate catalysts. To

the best of our knowledge such information has remained kinetically undetermined. To attain initial estimates of the ligand reaction orders we have applied linear fits to the initial slopes of the 1 mol% to the **L_{fast}** mol% data from the ligand optimisation plots. (Except for run e where the 1 mol-% data point was excluded). The values attained from this simple analysis are given in **Table 4**. The error bar on these average ligand order rate dependencies is quite high – we estimate it to be ± 0.2 . Nevertheless, the numbers derived here are important as no other values are available in the literature. An alternative approach to attaining $[L]^n$ involved the fitting of tangents to the midpoint of the rise of the $\ln(k_{1\max})$ data against parabolic fits of $\ln([L])$ and this gave similar results (within error) except for the copper triflate/triphenylphosphine system. This was the only case where the attained values were very different (triphenylphosphine order of 1.9 vs. 2.6) for these two different approaches. The copper triflate/triphenylphosphine system was the most labile from which reproducible data could be attained and it is clearly at the limits of our technique with an unacceptable error.

Table 4. data derived from the ligand optimisation plots

Ligand	Size, V_{Bur} /% ^[a]	Best rate ratio ^[b] Cu: L _{fast}	Ligand order ^[b] [L] ⁿ
PMe ₃	27.3	2.0	2.2
PCy ₃	38.8	2.0	1.2
PPh ₃ {+ Cu(OTf) ₂ } ^[e]	34.8	1.7	var. ^[e]
P(OPh) ₃	36.5	2.3	1.1
L2	34.9 ^[f]	3.3	0.4
L2 {with AlEt ₃ } ^[h]	34.9 ^[f]	2.4	0.4

[a] Literature values were used or calculated by the method of Cavallo for the LAuCl complex (with Bond radii scaled by 1.17, $R_{\text{sphere}} = 3.5 \text{ \AA}$, and $d(\text{M-L}) = 2.0 \text{ \AA}$);^[7] lower % V_{Bur} corresponds to less steric demand for **L**. [b] The maximum error bars on the Cu:**L** ratios giving the fastest overall reaction and ligand reaction orders are estimated at ± 0.2 .

The results from **Table 4** show that the number of ligands in the fastest rest state of the catalyst which enters into the transition state (ligand optimisation plot) is generally higher than the number of ligands in the transition state (ligand order). However, this is not the case for trimethylphosphine, where the rest state of the catalyst is akin to the transition state.

1.3.7. Non-linear studies

Non-Linear Effect (NLE) study of **L4** where strong deviations from linearity were *not* observed in the addition of diethylzinc to cyclohexenone using copper(II) triflate. To allow a direct

comparison an NLE study on **L2** using diethylzinc under our exact conditions was conducted (**Figure 18a**) – as this is absent in the literature. There is only a slight positive NLE deviation across the entire range of ligand enantiopurity. The apparent first order rate constant of the reaction with copper: (*R,S,S*)-**L2** = 2 at -40 °C was determined to be $7.9 \times 10^{-4} \text{ s}^{-1}$ for a sample of (*R,S,S*)-**L2** with 50% ee. This value is broadly similar to that for the equivalent run using 100% ee (*R,S,S*)-**L2** ($5.3 \times 10^{-4} \text{ s}^{-1}$ page 48). Within the maximum error on the single rate determinations (ca. $4 \times 10^{-4} \text{ s}^{-1}$), the data suggests that the NLE most probably derives from a slight kinetic advantage for a heterochiral species over its homochiral equivalent and *not* from any ‘reservoir effect’ – where a very significant decrease in the rate is expected due to the population loss of the catalytically competent species. To support these ideas a brief Arrhenius study was made of the 50% ee (*R,S,S*)-**L2** system between -35 and -45 °C. To conduct this, the rate constants were derived according to **Figure 9**, and a linear trendline fitted and the activation parameters obtained. A reaction E_{act} of $15 \pm 2.7 \text{ kcal mol}^{-1}$ was determined. The accuracy of the data did not warrant extraction of ΔH^\ddagger and ΔS^\ddagger but the activation energy is very similar to other reported dialkylzinc/enone systems.³⁶ Finally, it has been suggested that below Cu:**L** ratios of 1:1.5 the

enantioselectivity delivered by **L2** falls dramatically – but no figure is provided in widely available literature as far as we can determine. When copper(II) acetate: (*R,S,S*)-**L2** values of 1 mol%:0.5 mol% were used the conjugate addition product was attained with a final ee value 96%, the same as that (94%) attained with literature ‘optimal’ copper:ligand ratios of 1:2 within the error for the ee determination ($\pm 3\%$ maximum, and generally better than $\pm 2\%$). In general, in all of our kinetic runs the ee values ($96 \pm 2\%$) for the diethylzinc 1,4-addition product was independent of both the copper: (*R,S,S*)-**L2** ratio used in the reaction and the time of sampling. The simplest explanation of this behaviour is that a single identical entity is responsible for the stereoselective transition state, and that this is extracted by self-assembly from the rest-pool of entities through ligand acceleration effects. This condition is vital for our analysis of the copper:ligand ratios in the various transition states proposed here. Deviations in the diethylzinc/(*R,S,S*)-**L2**/copper(II) acetate ee data were generally observed in the first 180 seconds when Cu^{II} reduction and catalyst genesis is not quite complete. We also determined the NLE of the triethylaluminium addition (**Figure 18b**). This shows essentially linear behaviour up to 50% ee ligand purity and then a significant negative deviation; however, kinetic data in the latter regime were not attained.

Nevertheless, we could show that the enantioselectivity for the 1,4-addition ($79\pm3\%$) final product were again invariant over a range of copper: (*R,S,S*)-**L2** ratios (2:1 to 1:3) at the endpoint of the reaction. However, in the triethylaluminium/(*R,S,S*)-**L2** system the ee value of the product showed time dependance (rising from $<54\%$ to $79\pm3\%$ ee over the first 9 minutes (ca. 90%) of conversion in all cases). Because of these observations it cannot be guaranteed that the asymmetric addition arises from a single entity with the (*R,S,S*)-**L2** molecularity of **Table 4**.

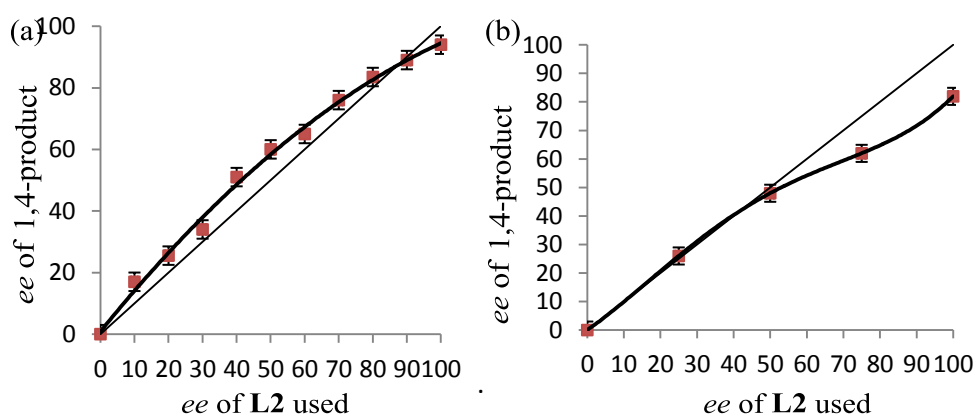


Figure 18. Non Linear Effects (NLEs) for copper(II) acetate (1 mol %) and Feringa's phosphoramidites (**L2**) (2 mol %) catalysed additions of (a) diethylzinc (in toluene); (b) triethylaluminium (in diethyl ether). The maximum error bars on the ee determination are $\pm 3\%$.

1.3.8. Method of continuous variation analysis

Job's plots are commonly used to determine metal-to-ligand ratios in complex formation reactions. In this technique, the total amount of ligand and metal are fixed, whereas the individual amounts of ligand and metal are varied continuously. A physical property is measured and a plot of the physical property versus mole fraction of the metal yields a curve with ascending, then descending branches whose sides meet at a maximum. This maximum denotes the optimum mole fraction of the metal at which complete complex formation occurs. However, Job's plots for organometallic chemistry are poorly represented.

As well as conducting ligand optimisation plots, A Job's plot analysis was also conducted according to **Figure 9** where a fixed amount of ligand and copper (4.5 mol% total) was used while varying the mole fraction of both within this totality. Due to the shallow maxima in π -acceptor ligands the speciation of triphenylphosphine, triphenylphosphite, *tris*(*para*-fluorophenyl) phosphine were analysed *via* the Job's plot method along with **L39 (Figure 19)**.

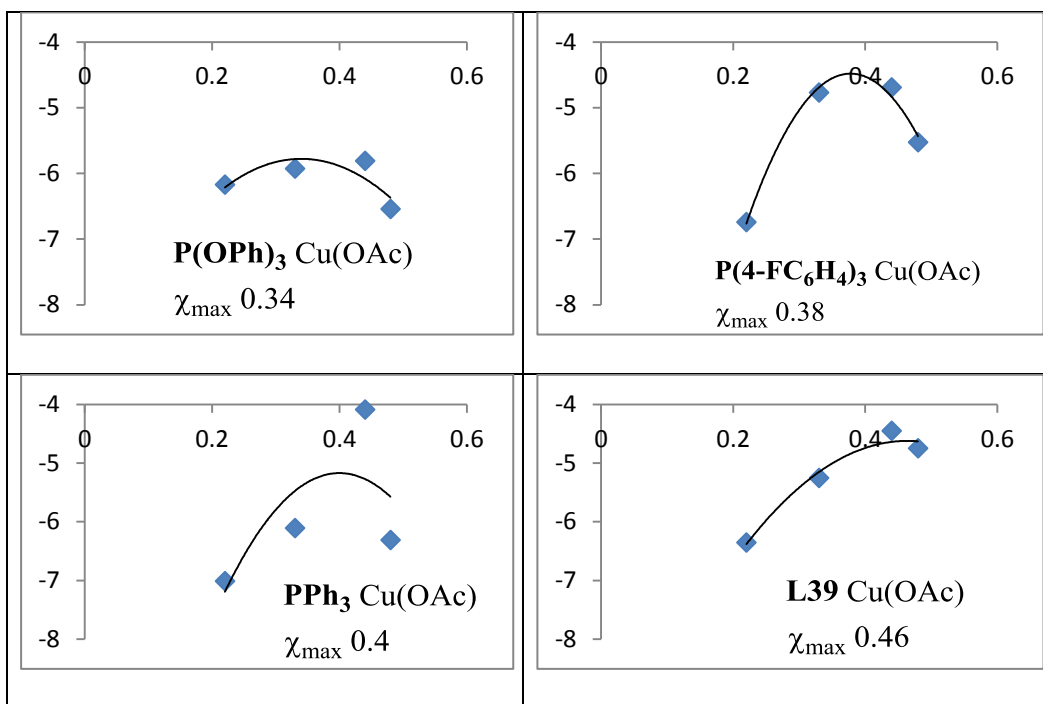


Figure 19 Job's plots for copper(II) acetate and a) **L39**, b) tris(4-fluorophenyl)phosphine c) triphenylphosphine and d) triphenylphosphite. X-axes: mole fraction of copper and ligand; y-axes: $\ln(k_1)$

For both the triphenylphosphite and *tris*(para-fluorophenyl)phosphine systems, the traditional Job's continuous variations plot provided a copper: triphenylphosphite ratio of 1:1.9 and a copper:*tris*(para-fluorophenyl)phosphine ratio of 1:1.6. The fit of the primary kinetic data in both the ligand optimisation plots and the Job's plots are comparable (R^2_{ave} 0.97 vs. 0.99) for triphenylphosphite indicating a similar maximum error of ± 0.2 in the derived copper:Ligand ratio. Thus, while there are

numerous species in the catalytic 'rest state pool' of this system the most populous, by both techniques, is $\text{XCu}\{\text{P}(\text{OPh})_3\}_2$ or $\text{XCu}\{\text{P}(4\text{-FC}_6\text{H}_4)_3\}_2$ ($\text{X} = \text{OAc}$ or Et).

The kinetic analyses require a regime where the rate of ligand exchange between 'rest state species' is significantly faster than the rate determining step for conversion of enone to 1,4-addition product. While this is known to be the case for *P*-ligands we have used, the same cannot be assured for Cu-NHC species where build-up of a small 'non exchanging $\text{XCu}(\text{SIMes})_2$ pool' cannot be discounted. A kinetic Job's plot of the behaviour of **L39** also suggested this might be the case as it provided Cu:**L39** of 1:1.2 (± 0.2 max error) as the most populous rest state species. A paucity of data at ligand loadings between 0-1 mol-% prevented realistic estimates of the carbene ligand r.d.s. reaction order. Although we could not reliably determine the ligand order for reactions based on **L39** (due to a lack of reproducible data at $[\text{L39}]/[\text{Cu}] < 1$) the involvement of (**L39**)Cu-Et seems likely, based on the maximum at Cu:**L39** of 1.4 and 1.2 (both ± 0.2) observed in the ligand optimisation and Job's plots.

Unfortunately the paucity of the kinetic data for the triphenylphosphine system leads to a poor fit in the Job's plot analysis and therefore no meaningful data can be obtained.

1.3.9. Conjugate addition of Grignard reagents to α,β -unsaturated esters

The conjugate addition of ethylmagnesium bromide to methyl crotonate was also studied using the ligand ratio vs. rate plot technique outlined in **Figure 9 (Table 5)**.

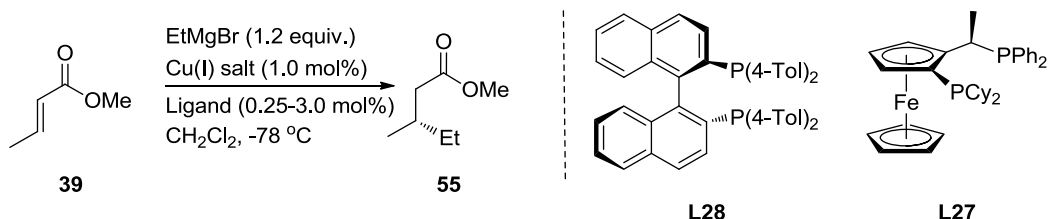


Table 5. Copper-catalysed 1,4-addition of ethylmagnesium bromide to methyl crotonate.

Entry	Cu salt	Ligand	Cu: n ^o of Ligands
1	CuI	L28	1.0:1.1 (slow) & 1.0:1.2
2	CuBr.SMe ₂	L27	-

These were carried out using the same bottle of Grignard reagent and freshly distilled methyl crotonate, with fixed concentrations of the copper salt (0.00323 M), ethylmagnesium bromide (0.387 M), internal standard (0.013 M) and methyl crotonate (0.323 M). The reaction temperature was also kept constant (-78 °C). The primary kinetic data indicated that the overall reaction neither followed simple first order kinetics (dependence on enone concentration), nor second order kinetics (dependence on enone and Grignard concentration). The reaction could only be fitted to an overall double first order kinetic model (equation 2), potentially

indicating that there are two catalytically active species present, each following separate first order kinetics. This suggestion concurs with the phosphorus NMR study carried out by Feringa, in which he found there were two distinct species present which have different chemical shifts to one another.³⁵

$$[A]_t = ([A]_0 \exp(-k_{\text{obs}}t))_{\text{fast}} + ([A]_0 \exp(-k_{\text{obs}}t))_{\text{slow}} \quad (2)$$

Where $[A]_0$ is the initial enone concentration, $[A]_t$ is the calculated enone concentration, k_{obs} is the observed rate constant and t is the time.

Unfortunately, no meaningful kinetic data could be obtained for the use of **L27**, due to the active catalyst being far too fast at -78 °C, and the majority of the starting material had been converted to product in less than 5 minutes. For this reason, there were not enough data points to obtain an initial rate from the data. Because of this our attention was turned to another catalyst system which was reported in the literature by Loh, in which copper(I) iodide and (*S*)-tolyl-BINAP (**L28**) were used (entry 1, **Table 5**).⁴¹

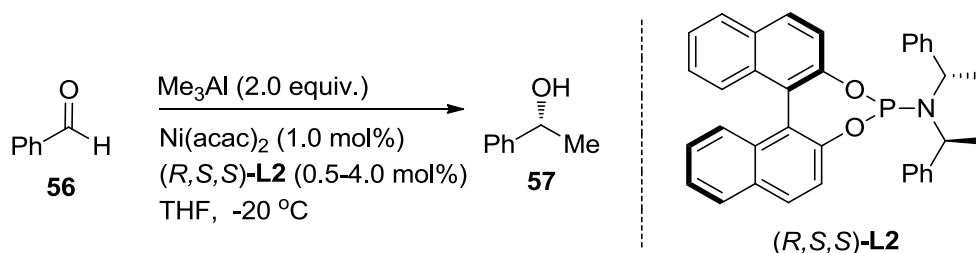
This catalytic system reacted slowly enough to provide meaningful kinetic data at -78 °C. From the ligand ratio vs. rate plot a copper to ligand ratio could be obtained for both the fast and slow reacting catalysts. The fast reacting catalyst has a stoichiometry of one copper to two phosphorus donors,

which is consistent with the π -complex proposed by Feringa.³⁵

The slow reacting catalyst has a copper to ligand ratio of 1.0:1.2, which indicates that the structure of the π -complex is slightly different, and that this π -complex possibly contains a dinuclear copper species. However, no structure has yet been proposed for this observation.

1.3.10. Nickel-catalysed 1,2-addition to aromatic aldehydes

While we have concentrated primarily on 1,4-additions of terminal organometallics, we believe that the ligand optimisation plot technique has the potential for wider use. Therefore, the technique has been extended to probe the mechanism of 1,2-addition of trimethylaluminium to benzaldehyde under nickel(II) acetoacetate catalysis in the presence of **L2** (**Scheme 14**).



Scheme 14. Standard reaction conditions for the addition of trimethylaluminium to benzaldehyde.

Analysis of the data collected *via* **Figure 9** showed that the overall reaction follows zero order kinetics, *i.e.* no dependence on the nucleophile or aldehyde (equation 4).

$$[A]_t = [A]_0 - k_{\text{obs}}t \quad (4)$$

Where $[A]_t$ is the calculated concentration of benzaldehyde, $[A]_0$ is the initial concentration of benzaldehyde, k_{obs} is the observed rate constant and t is the time.

From the reaction rate data obtained, a ligand optimisation plot was derived and the stoichiometry of the nickel to ligand ratio was found to be 1.0:1.0. This is in accord with the proposed transition state structure **58** (**Figure 20**). When more traditional optimisation procedures, based on enantiopurity of the product alcohol, were used, these proved unhelpful, as the alcohol's enantioselectivity is independent of the nickel to **L2** stoichiometry.⁴²

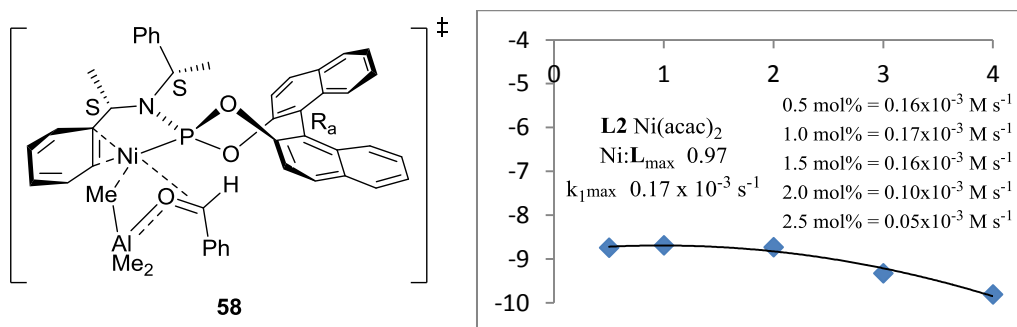


Figure 20. a) Proposed transition state in the nickel-catalysed addition of trimethylaluminium to benzaldehyde; b) ligand optimisation plot at -20 °C X-axes: mol-% **L** per 1 mol-% copper precursor used; y-axes: $\ln(k_1)$.

What was also evident from the primary data is that when the ligand concentration exceeds 2 mol percent, the activity of the catalyst drops dramatically, due to coordinate poisoning of the nickel species.

1.4 Conclusions

The kinetic behaviour of catalytic copper(II) acetate (1 mol-%) and ligands (at ranges from 0.5 mol-% to 3 mol-%) for the addition of diethylzinc to cyclohexenone have been investigated. Diethylzinc addition promoted by copper(II) triflate (1 mol-%) and triphenylphosphine (1-2.5 mol-%), triethylaluminium addition by Feringa's phosphoramidite (at ranges from 0.5 mol-% to 3 mol-%), ethylmagnesium bromide addition by diphosphine ligands to enoates and nickel-phosphoramidite catalysed addition to trimethylaluminium to benzaldehyde have also been investigated. Non-linear dependency of the reaction rate constant as a function of the ligand concentration is observed with rate constant maxima at copper to ligand ratios of 1.4-3.3 for a fixed $[\text{Cu}^I]$ of 1 mol-%. Ligand orders were also determined for a select few catalyst systems the average ligand orders are: $[\text{PMe}_3]^2$, $[\text{PCy}_3]^1$, $[\text{P(OPh)}_3]^1$ and $[\text{L2}]^{0.5}$ within the error (± 0.2) on the determinations. These numbers

are in accord with known substrate dependencies, non-linear effect studies and other mechanistic data.

Chapter 2

Synthesis of air-stabilised alanes and application in hydroalumination chemistry

2.1 Introduction

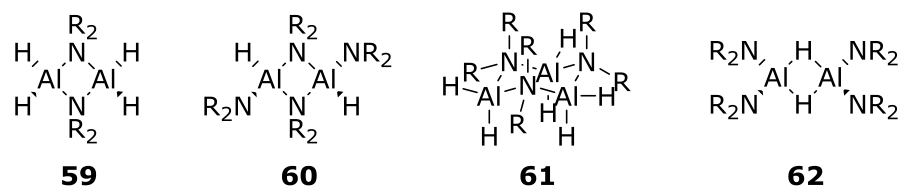
2.1.1 Aluminium hydrides

Alanes are neutral aluminium compounds which possess aluminium-hydrogen bonds. By this definition anionic 'ate' species containing anionic hydrides (such as the ubiquitous lithium aluminium hydride AlH_4^-) are excluded and not further discussed in detail. Numerous alanes have been characterised, of which the major types are summarised in **Figure 21**.

AlH_3	R_2NAIH_2 or $(\text{R}_2\text{N})_2\text{AlH}$	$(\text{RNAIH})_n$	$(\text{RO})\text{AlH}_2$ or $(\text{RO})_2\text{AlH}$	XAlH_2 or X_2AlH	RAIH_2 or R_2AlH
Alane	Amidoalanes	Imidoalanes	Alkoxyalanes	Haloalanes	Organoalanes

Figure 21 Major classes of alanes.

The structural chemistry of amidoalanes is dominated by the formation of oligomers of $\text{AlH}_n(\text{NR}_2)_{3-n}$ ($n = 1-2$). Such monomers can be bonded either typically by Al-N-Al bonds as in **59**, **60** and **61** or atypically *via* hydride bridges **62** when very sterically encumbering groups are present (**Figure 22**). The Lewis acidity at the aluminium centre implied by these empirical formulae of the monomers underpins the vast majority of the chemistry of amidoalanes and this is moderated by the donor properties (steric and electronic) of the amido group.⁴³

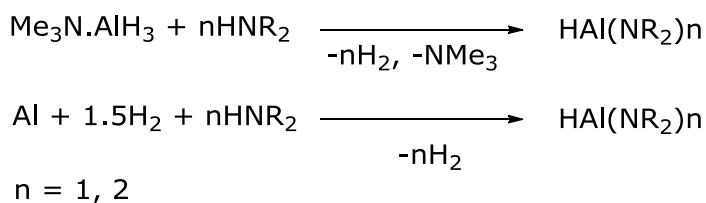


R = Me, piperidino, tmp

Figure 22 Structures of amidoalanes.

If sterically unencumbered dimethylamide units are present, both **60** and **61** can be formed, depending upon the aggregation. Dimer **60** has an Al-N bond length of 1.966 Å for the bridged amide and 1.804 Å for the terminal amide but the Al-H bond length is undefined.⁴⁴ The trimer **61** has an Al-N bond length is 1.936 Å with an Al-H bond length of 1.55 Å.⁴⁵ When extremely bulky amines are used such as 2,2,6,6-tetramethylpiperidine, only motif **62** is formed, with an Al-N bond length of 1.835 Å and a 1.68 Å Al-H bond.⁴⁶

Amidoalanes are typically synthesized *via* the reaction of secondary amines with a source of alane (AlH₃) in molar ratios of 1:1 for the dihydride **59** or 2:1 for the monohydride **60** or **61** (**Scheme 15**). Another approach to preparing such amidoalanes is *via* the reaction of elemental aluminium and hydrogen under ultra high pressures (3000-4000 psi) in the presence of the corresponding secondary amine. This approach has recently been targeted as a potential method for hydrogen storage. A wide variety of these amidoalanes have been synthesised and their structures and chemistry explored.



Scheme 15 Synthesis of amidoalanes.

Imidoalanes exhibit high degrees of oligomerisation. The Al-H containing sub-unit tends to aggregate into cubic tetramers-**63**, hexagonal prismatic hexamer-**64** or even higher oligomers (**Figure 23**).⁴⁷ The synthetic approaches to these alanes are very similar to that of amidoalanes: a source of alane (AlH_3) is reacted in the presence of a primary amine in a molar ratio of 1:1.⁴⁶

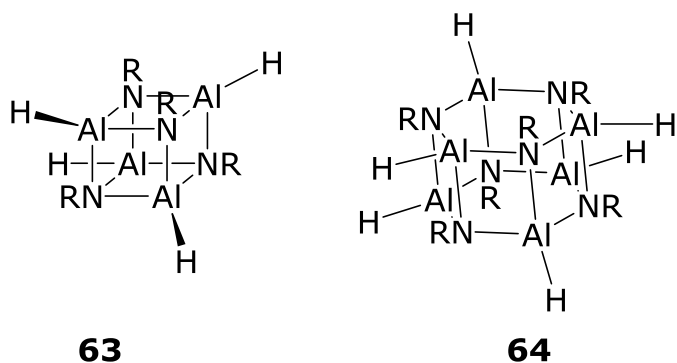


Figure 23 Structure of imidoalanes.

Alkoxyalanes, typically adopt a dimeric structure, in which the alkoxide substituents occupy the two bridging positions, thus forming a M_2O_2 central ring (**Figure 24**). When the alkoxide moiety is *t*-butoxy, both **65** and **66** can exist.⁴⁸ When the dihydride is formed, **65** is commonly observed, in which the bond length of $\text{Al}-\text{O}^t\text{Bu}$ is *ca.* 1.81 Å, with an Al-H

bond length of 1.55 Å. When the monohydride is formed, **66** is observed, with the bridging Al-O-Al having a bond length of about 1.82 Å, while a shorter bond length of 1.67 Å is observed for the terminal Al-OR (in the case R = *tert*-butoxide). An Al-H bond length was also determined at 1.51 Å.

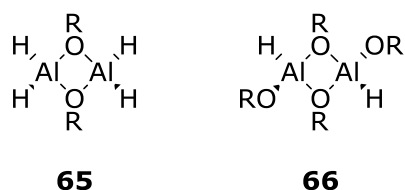
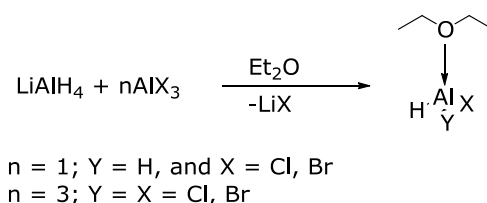


Figure 24 Common structures for alkoxyalanes.

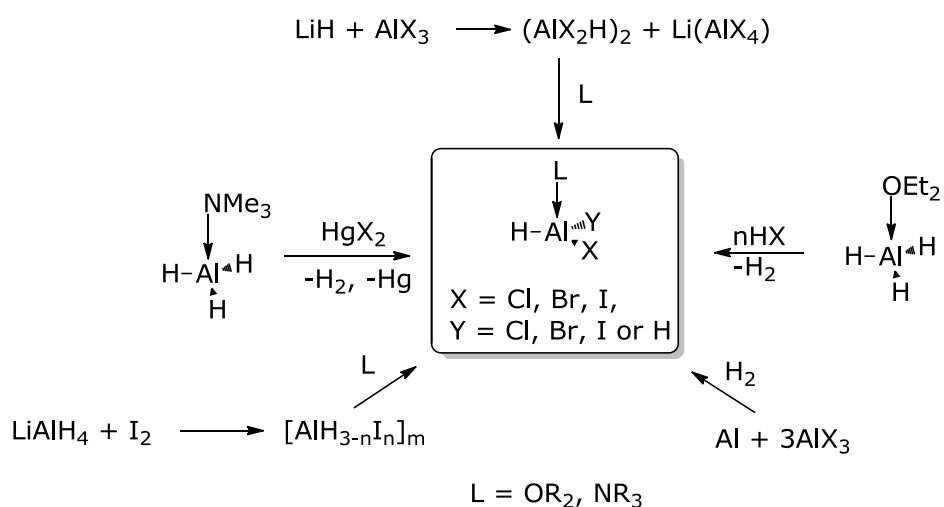
Haloalanes are rather underrepresented in the literature but both monohaloalanes (H_2AlX) and dihaloalanes (HAlX_2 , where $\text{X} = \text{F}, \text{Cl}, \text{Br}, \text{I}$) are known.⁴⁹ The first reported attempted structure of a Lewis base adduct of such haloalanes was due to Semenenko in 1973 (**Scheme 16**).⁵⁰ However, no bond length data could be obtained due to disorder in the crystal structure between the hydrides and chlorides.



Scheme 16 First reported synthesis of haloalanes.

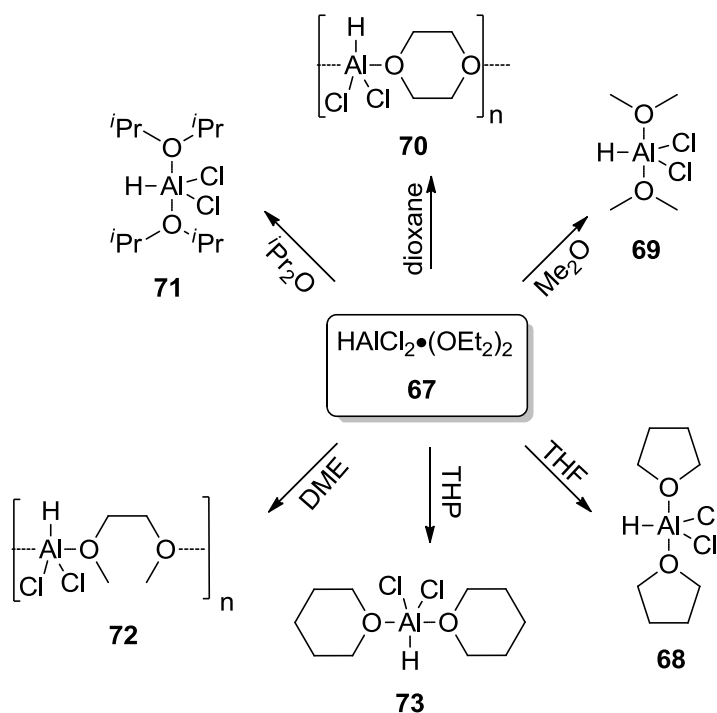
The early synthesis of haloalanes involves reactions of an alane adduct with either anhydrous hydrogen halides or mercuric halides giving moderate to good yields (up to 50%). Another approach is the reaction of lithium hydride with the

corresponding aluminium trihalide in the presence of a Lewis base, giving the haloalane in up to 60% yield. Haloalanes can be synthesised directly from a reaction between aluminium powder, aluminium trihalide and hydrogen gas. Unfortunately, this procedure required elevated temperatures (80-150 °C) and elevated pressures (up to 10,000 psi), but good yields of the haloalanes were attained (**Scheme 17**).⁵¹



Scheme 17 early syntheses of haloalanes.

Oxygen-containing Lewis base adducts of haloalanes can be synthesized by the same approach of Semenenko (**Scheme 16**) followed by the addition of the corresponding oxygen-donor ligand.⁵² For the tetrahydrofuran adduct the solvent was simply changed from diethyl ether to tetrahydrofuran.⁵² During this study the authors noted it was possible to do a halide-hydride redistribution from alane and two equivalents of aluminium trihalide in tetrahydrofuran (**Scheme 18**).



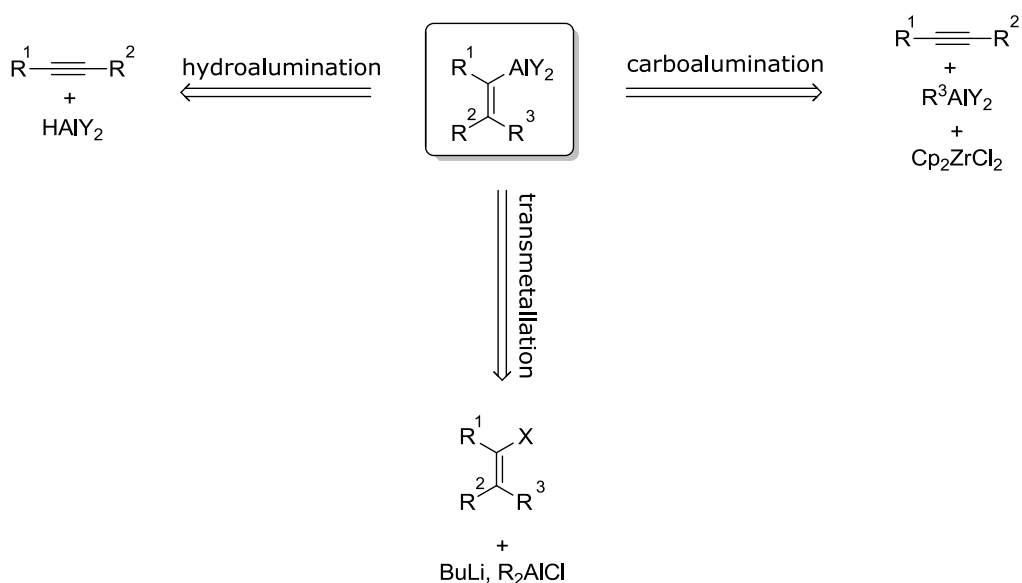
Scheme 18 Synthesis of oxygen Lewis base adducts of dichloroalane.

Recently, it has been shown that it is possible to synthesise haloalanes stabilised by NHC ligands. This can be achieved in two ways: i) by a ligand substitution of a labile and volatile donor on the alane (e.g. $\text{AlH}_3 \cdot \text{NMe}_3$) with the deprotonated NHC,⁵³ or by a hydride-halide exchange of a pre-existing aluminium halide NHC complex.⁵⁴

By replacing hydrides on the aluminium centre with heteroatom containing groups (halides, amino, alkoxy-groups) the reactivity of the remaining hydrides is reduced due to the inductive effects of these groups. Due to this tunability of the alane both alkoxy- and amidoalanes have been widely utilised in organic synthesis.

2.1.2 Synthesis of alkenylalanes

The synthesis of alkenylalanes can be achieved *via* three routes: i) transmetallation from alkenyllithiums or Grignard reagents; ii) hydroalumination of alkynes and iii) alkyne carboalumination (**Scheme 19**).

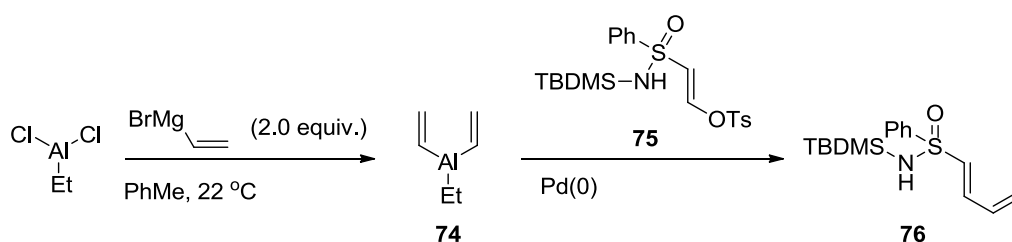


Scheme 19 Protocols for alkenylalane synthesis.

2.1.2.1 Transmetalation procedures

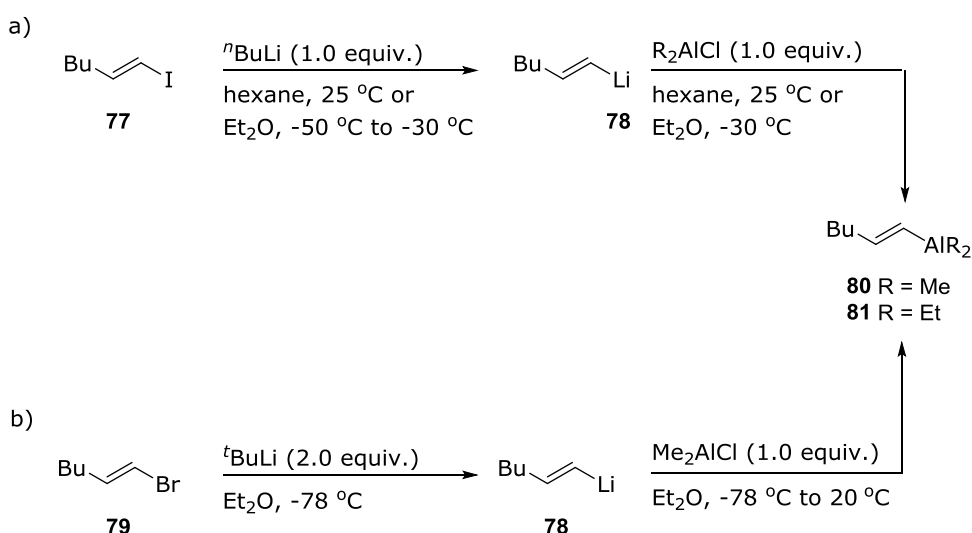
The synthesis of alkenylalanes *via* transmetalation from organolithium and Grignard precursors is surprisingly underrepresented in the literature. Such approaches were first reported by Paley and Snow in 1990.⁵⁵ Vinylmagnesium bromide was reacted with ethylaluminium dichloride and the intermediate alkenyl alane subsequently cross-coupled (**Scheme 20**). The authors noted that the use of dimethyl-

and diethylvinyl alanes were unsuccessful in the cross-coupling.



Scheme 20 first synthesis of vinylalanes *via* transmetalation.

Carreño and co-workers reported the synthesis of alkenylalanes from alkenyl iodides.⁵⁶ Initial lithium-iodine exchange followed by reaction with dimethylaluminium chloride in hexane at ambient temperature afforded **80**. Alexakis reported a similar procedure using diethylether as solvent. However, this latter approach required a more complicated temperature control protocol (**Scheme 21**).



Scheme 21 Synthesis of alkenylalanes from alkenyl halides.

Due to the lack of commercially available alkenyl iodides, a modified procedure was also reported by Alexakis and co-

workers based on alkenyl bromides. Initially alkenylbromides are reacted with *t*-butyllithium (2 equivalents) in diethyl ether; this was followed by a transmetallation onto dimethylaluminium chloride to yield the corresponding alkenylalane (**Scheme 21**).

2.1.2.2 Hydroalumination

Hydroalumination can be defined as the *syn* addition of an aluminium hydride across an unsaturated carbon-carbon bond *via* a formal [2+2] cycloaddition. Woodward-Hoffman analysis of hydroalumination reactions show that this process is thermally allowed (**Figure 25**).

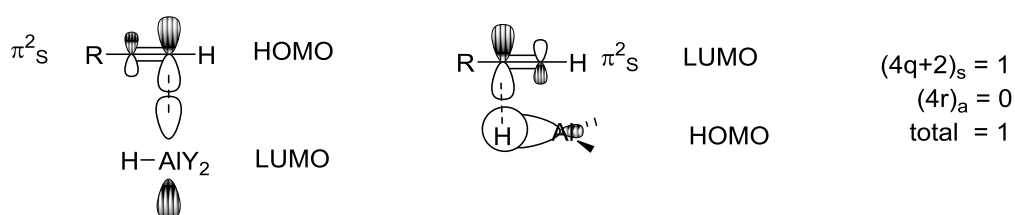
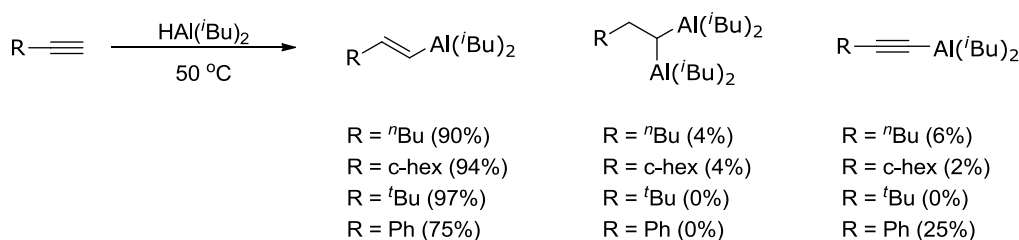


Figure 25 Woodward-Hoffman analysis of hydroalumination.

2.1.2.2.1 Uncatalysed hydroalumination

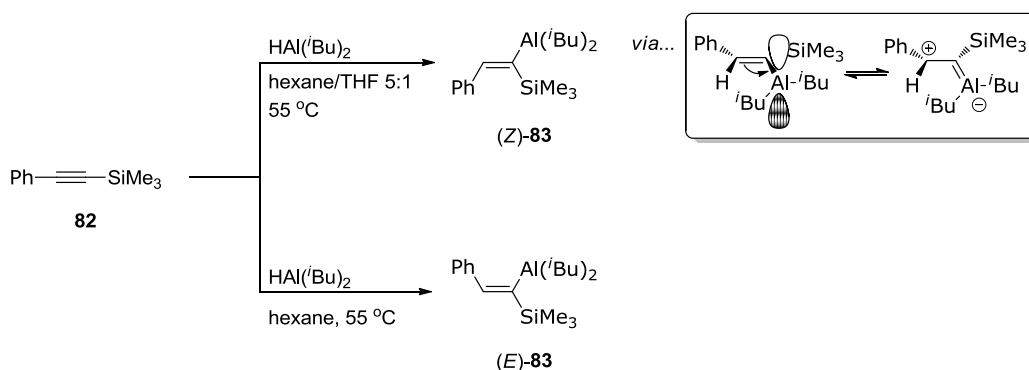
Wilke and Müller⁵⁷ reported the first hydroalumination of terminal alkynes using diisobutylaluminium hydride under both neat conditions and in hydrocarbon solvents. Depending upon the nature and branching of the substituent on the alkyne, competing metallation and over-hydroalumination is also observed. If *n*-alkyl substituents are present in the alkyne,

only low levels of undesired products are detected. If electron-withdrawing or conjugated substituents are present, such as phenyl, 2-cyclohexene, then the alkynyl proton becomes more acidic leading to significant amounts of acetylides and the reaction is poor overall (**Scheme 22**).⁵⁸



Scheme 22 Uncatalysed hydroalumination and associated side reactions.

One approach to avoid the formation of aluminium acetylides in the presence of acidic alkynyl protons was due to Eisch.⁵⁹ In this pioneering work, Eisch and co-worker reported the thermal hydroalumination of silyl-substituted alkynes resulting in a regioselective addition with the aluminium α to the silicon (**Scheme 23**). The regioselectivity observed could be explained by the stabilisation of the partial negative charge into the low lying σ^* orbital on the silicon or the stabilisation of a beta positive charge through the carbon-silicon σ bond.



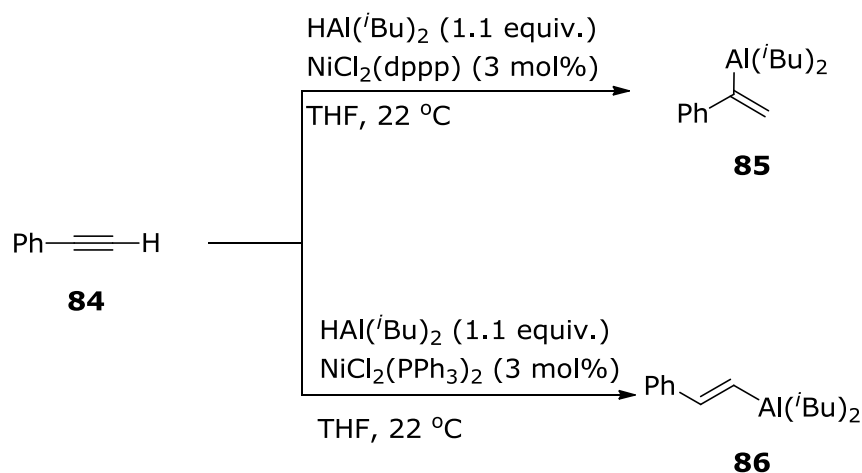
Scheme 23 Hydroalumination of silyl-substituted alkynes.

Eisch noted that the solvent played a major part in the stereoselectivity of the reaction. When coordinating solvents were used, a *syn*-addition across the triple bond was observed but when non-coordinating solvents were used, an *anti*-addition was observed. This stereochemical outcome was attributed to a destabilisation of the double bond, formed in an initial *syn*-addition, *via* the unoccupied *p*-orbital on the aluminium followed by isomerisation to minimise the steric interactions between the trimethylsilyl group and the *iso*-butyl group. Whereas in coordinating solvents (such as tetrahydrofuran), the empty *p*-orbital is coordinated and unable to participate in stabilising the β -positive charge (**Scheme 23**).

2.1.2.2.2 Nickel-catalysed hydroalumination

Eisch and co-workers discovered that nickel salts, in particular nickel acetylacetonate, could catalyse the

hydroalumination of terminal alkynes.⁶⁰ Recently, Hoveyda and co-workers revisited this work in order to find a protocol that could be used for the hydroalumination of terminal alkynes bearing electron withdrawing or conjugated substituents. After screening a range of commercial nickel salts, it was found that, dichloro(1,3-*bis*(diphenylphosphino)propane)nickel ($\text{NiCl}_2(\text{dppp})$) would furnish the α , internal alkenylalane with excellent regioselectivities of $\alpha/\beta >98:2$, whereas *bis*(triphenylphosphine)nickel(II) dichloride ($\text{NiCl}_2(\text{PPh}_3)_3$) would generate the more synthetically useful β -alkenylalane, but the regioselectivity decreased to α/β 7:93 (**Scheme 24**).⁶¹

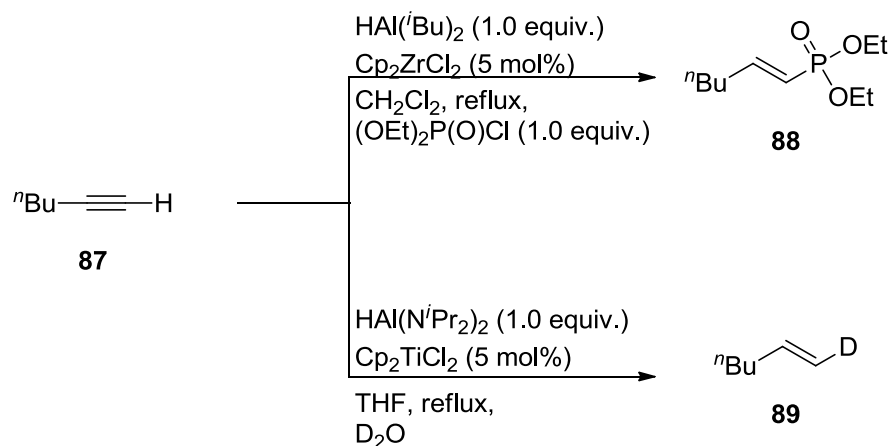


Scheme 24 Nickel catalysed hydroalumination.

2.1.2.2.3 Titanium and zirconium catalysed hydroalumination

Taapken and co-workers demonstrated that terminal alkynes can undergo hydroalumination with

diisobutylaluminium hydride in the presence of *bis*(cyclopentadienyl)zirconocene dichloride.⁶² This reaction was carried out in refluxing dichloromethane for 24 hours, followed by treatment with diethylchlorophosphate to give **88** (**Scheme 25**). Additionally, Ashby and Noding showed that *bis*(diisopropylamino)alane, in the presence of either *bis*(cyclopentadienyl)titanocene dichloride or titanium tetrachloride, was able to undergo hydroalumination with internal and terminal alkynes to generate the corresponding olefin in near quantitative yields. When the reaction was quenched with deuterium oxide high levels of deuterium incorporation was observed (**Scheme 25**).⁶³

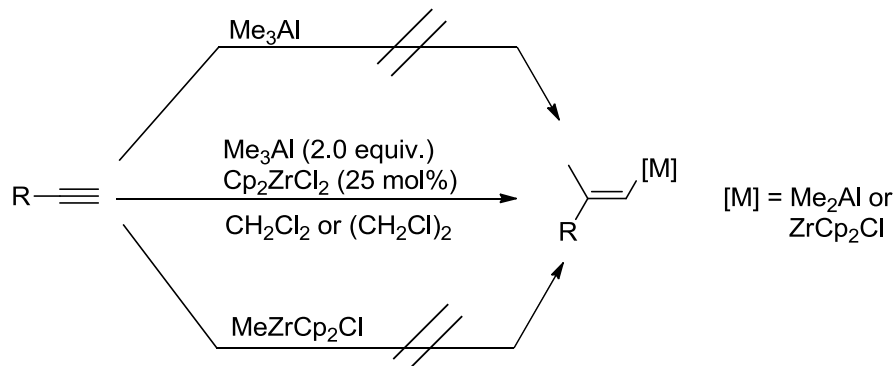


Scheme 25 Titanium and zirconium catalysed hydroalumination.

2.1.2.3 Zirconium-catalysed carboalumination

The first examples of carboalumination of alkynes were a thermal reaction between trialkylalanes and gaseous acetylene to generate (*Z*)-selective alkenyldialkylalanes.⁶⁴

The first zirconium-catalysed carboalumination was reported by Negishi in 1978 where group four transition metals were shown to be active for methylmetallation of both terminal and internal alkynes.⁶⁵ This process is extremely general in terms of the alkyne used, however, both trimethylaluminium and zirconocene dichloride needs to be present for this reaction to proceed. If trimethylaluminium or MeZrCp_2Cl are used independently, no reaction occurs (**Scheme 26**).⁶⁶ This approach followed by subsequent functionalisation has been used in the synthesis of natural isoprenoids for example: geraniol, monocyclofarnesol, and farnesol.⁶⁷



Scheme 26 Zirconium catalysed carboalumination.

Wipf and co-workers reported a modified procedure for the zirconium-catalysed carboalumination of alkynes. Addition of up to 2.0 equivalents of water was noticed to promote a dramatic increase in the carboalumination rate even at -70°C . This rate acceleration was exclusive to water because when alcohols, hydrogen sulfide, silanols *etc*, were tried, the effect

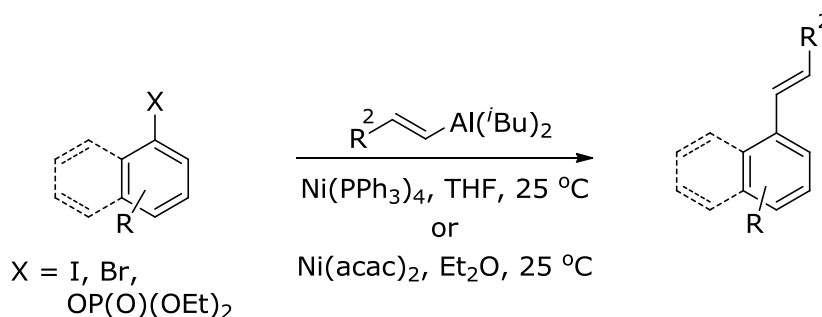
was not observed. The authors proposed that a ligand exchange occurs at zirconium, to create a catalytically active oxo-bridged dimer.⁶⁸

2.1.3 Cross coupling of alkenylalanes

Cross-coupling of terminal organometallic reagents with electrophiles under either palladium or nickel catalysis has become one of the most important and studied classes of reactions in organic synthesis. The organometallic reagents employed are typically: organoboron (Suzuki), organosilicon (Hiyama), organotin (Stille), organomagnesium (Kumada) and organozinc (Negishi). The use of organoaluminium reagents is significantly underrepresented and is typically described as a sub-set category of various Negishi-type couplings.

The first reported examples of a tandem hydroalumination and cross coupling procedure was reported by Negishi and Baba, in which alkenylalanes were reacted with aryl iodides or bromides⁶⁹ or alkenyl halides⁷⁰ in the presence of catalytic *tetrakis*(triphenylphosphine)nickel to generate the substituted styryl compound and the 1,4-dienes respectively in good to moderate yields at 25 °C. The authors also noted that the use of *tetrakis*(triphenylphosphine)palladium could also generate the desired products but at a slower rate. Kumada and co-workers showed that it was possible to

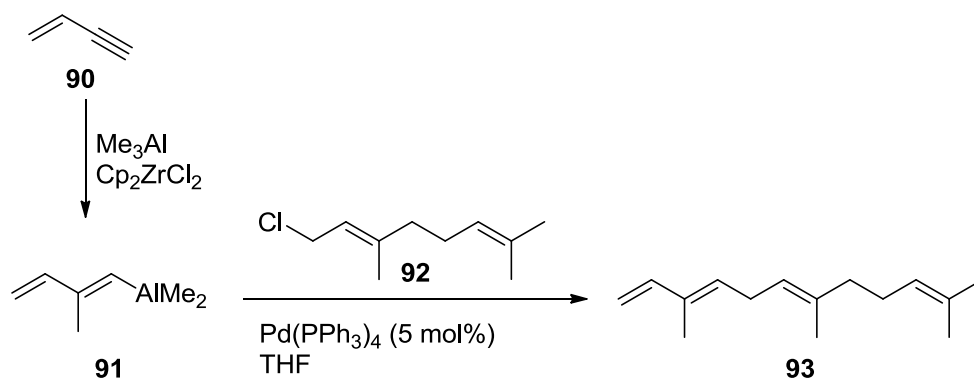
conduct cross-coupling reactions using nickel(II) acetylacetonate as a pre-catalyst with aryl phosphonates as the coupling partner at ambient temperature (**Scheme 27**).⁷¹



Scheme 27 Cross coupling of alkenylalanes.

Under Negishi's initial cross-coupling conditions, the coupling of alkenylalanes to alkenyl halides only gave low yields of the desired product. In order to increase the yields for the cross-coupling of alkenylalanes to alkenyl halides, the addition of different additives for the coupling to 1-bromo-2-iodoethene was explored. It was found the addition of a zinc salt had an accelerating effect on the reaction.⁷² Recently (2004), Negishi reported that the use of indium trichloride as a co-catalyst could dramatically increase the yield of the corresponding coupling products.⁷³

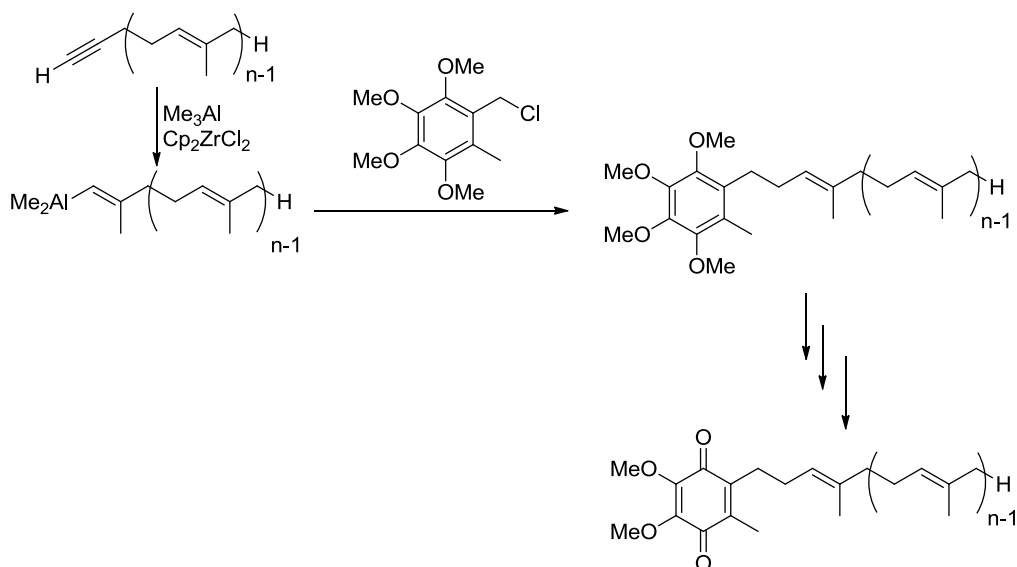
In the early 1980s Negishi and co-workers reported the use of zirconium-catalysed carboalumination followed by a palladium catalysed cross coupling onto allylic electrophiles to generate the corresponding skipped dienes, such as α -farnesene in 86% yield (**Scheme 28**).⁷⁴



Scheme 28 Palladium cross-coupling to allylic halides.

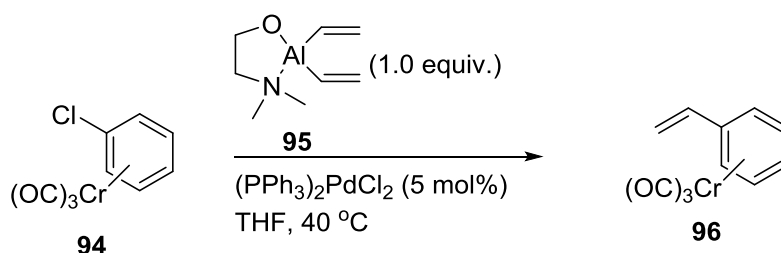
Although there are many cross-coupling protocols that can be used for benzylic halides, very few describe the use of alkenylalanes. An initial example was attained by Negishi and co-workers using alkenylalanes generated *via* carboalumination and subsequent palladium cross-coupling with benzyl bromide or chloride to generate allylated arenes in high yields (up to 93%).⁷⁵ In the late 1990s it was found that alkenylalanes generated by the thermal hydroalumination would undergo efficient nickel-catalysed cross coupling in good to excellent yields. Lipshutz showed that this protocol could be used to synthesise ubiquinones (CoQ_n) and demethylated ubiquinones *via* either carboalumination or hydroalumination of the corresponding alkyne (**Scheme 29**).⁷⁶ Very recently (2012), Gau and co-workers showed that alkenylalanes generated *via* hydroalumination could undergo an efficient nickel catalysed cross coupling at room temperature, to a wide range of benzyl halides containing electron-donating and electron-withdrawing groups with excellent yields. It was also

shown that benzyl chlorides would efficiently undergo the cross-coupling with excellent yields.⁷⁷



Scheme 29 Application of nickel-catalysed alane cross-coupling.

In the early 2000s Schumann and Schmalz showed that stabilised alkenylalanes could be used in palladium-catalysed cross-coupling of both haloarenes and chloroarene-chromium tricarbonyl complexes. The corresponding styryl compound was generated in high yields (up to 98%) using 5-10 mol% *bis*(triphenylphosphine)palladium dichloride. This reaction proceeds well for aryl halides containing ethers and esters but when haloanilines were used no reaction occurred (**Scheme 30**).⁷⁸

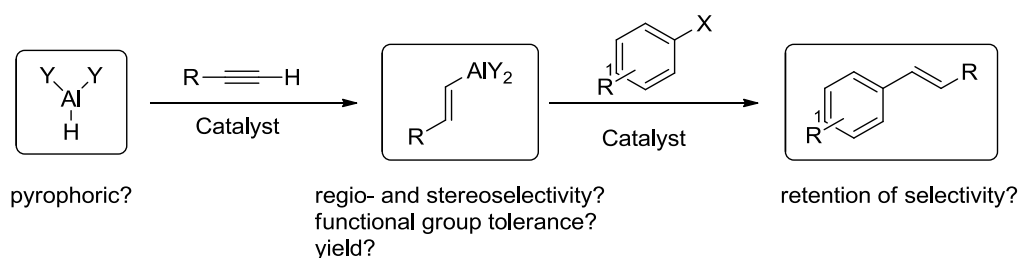


Scheme 30 cross-coupling of a chloroaryl-chromium tricarbonyl complex.

2.2 Aims of research

Diisobutylaluminium hydride is an organoaluminium hydride which is used widely in many aspects of organic synthesis. Although diisobutylaluminium hydride is cheap and commercially available, neat diisobutylaluminium hydride is a pyrophoric liquid which requires air-sensitive techniques for safe usage. Due to its pyrophoric nature, neat samples need to be transported *via* sea freight, which can take long periods of time to arrive from US production facilities. Additionally the steric demand of the *iso*-butyl groups can mean that transmetallation on to ligated transition metals is generally slow. Finally, the *iso*-butyl group can itself be a transferrable group resulting in competing transfer (*iso*-butyl or hydride *via* b-elimination from *iso*-butyl). The aim of this research was to synthesise aluminium hydrides having small, non-transferrable groups attached to aluminium preferably with reduced

pyrophoricity. The latter was envisaged to be achieved by dimer formation or the addition of an external stabilising ligand. A couple of classes of aluminium hydrides that could deliver on some of these requirements were the haloalanes (in particular dichloroalane), di-*t*-butoxyalane and diisopropylamidoalane. Once the pyrophoricity was addressed, the alane would be tried in hydroalumination of alkynes to see if the alkenylalanes could be generated cleanly in high yields and subsequently applied in a Negishi-type coupling (Scheme 31).

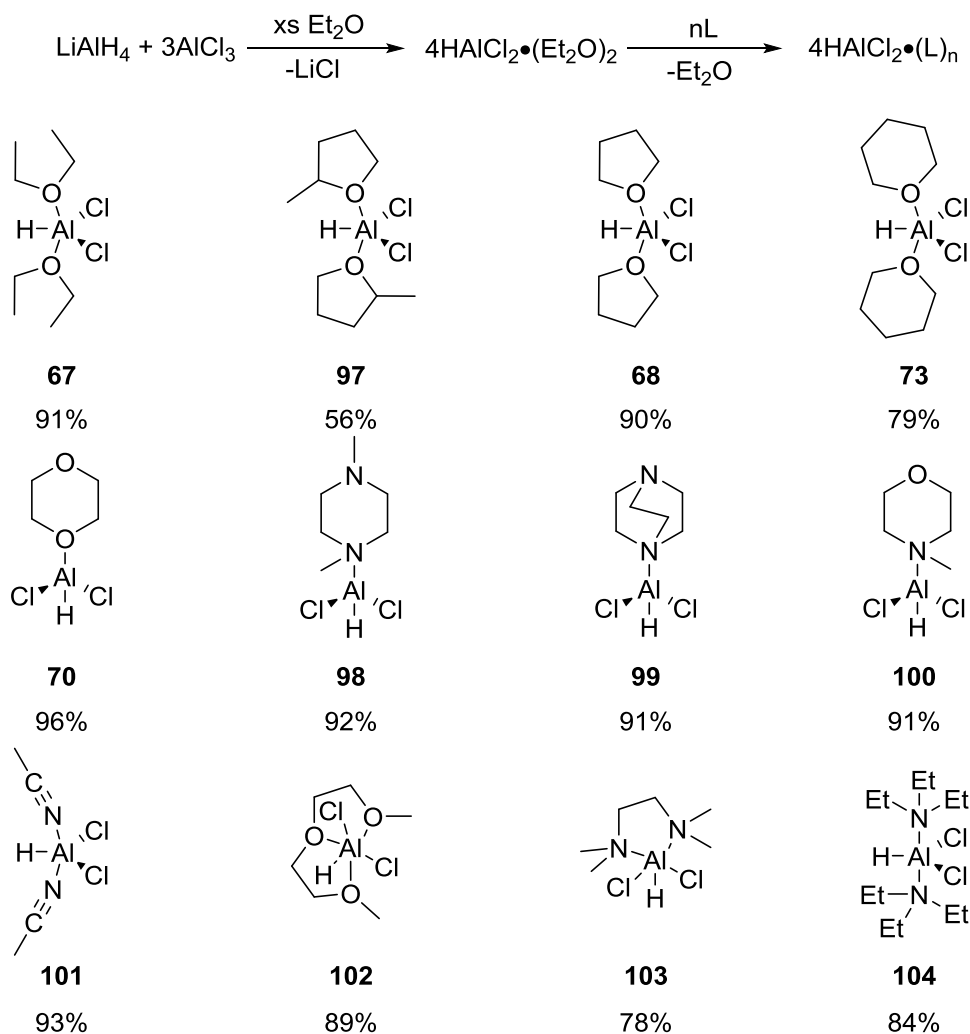


Scheme 31 Aims of this research.

2.3 Results and Discussion

2.3.1 Synthesis of aluminium hydrides

Dichloroalanes were synthesised *via* the procedure of Flagg and Schmidt,⁵² in which lithium aluminium hydride is dissolved in diethyl ether and a solution of aluminium trichloride in diethyl ether added. After stirring for 15 minutes, the lithium chloride by-product was removed by cannula filtration to give an ethereal solution of dichloroalane, which on solvent removal yielded the *bis*(diethyl ether) complex. Unfortunately, the *bis*(diethyl ether) adduct **67** is a pyrophoric liquid. However, coordinated diethyl ether is somewhat labile and therefore this adduct was a useful precursor for the synthesis of other species. The addition of other Lewis base donors to an ethereal solution of dichloroalane•*bis*(diethyl etherate) afforded a wide range of new Lewis base adducts quickly and in excellent yields. Only nitrogen and oxygen Lewis base adducts are shown in **Scheme 32**. Sulfur-donor adducts were tried but due to poor sulfur coordination to the aluminium, the diethyl ether was not displaced.



Scheme 32 Synthesis of Lewis base adducts of dichloroalane.

The physical properties of the individual corresponding adducts formed were difficult to predict. For example, the *bis*(tetrahydrofuran) adduct of dichloroalane was isolated as a colourless, free flowing powder, with the *bis*(2-methyl tetrahydrofuran) adduct was a low melting solid (m.p. 24-26 °C). Changing the ether ring size significantly affected the nature of the alane. Adducts containing tetrahydrofuran rings (**68** and **97**) were appreciably easier to handle than their corresponding liquid pyran analogue (**73**). When Lewis bases

containing two potential sites of coordination were reacted with dichloroalane•*bis*(diethyl etherate) (providing **70**, **98**, **99** and **100**) all the adducts were obtained in excellent yields with the adduct precipitating from the solution immediately upon addition of the Lewis base. These ligands presumably form polymeric structures which are insoluble in diethyl ether. All of the alanes of **Scheme 32** can be synthesised on large scales (~50 grams).

Spectroscopic characterisation for these dichloroalane adducts was limited by their reactivity and intrinsic NMR properties. The hydride NMR resonances for these compounds were not always visible. This is not unusual as the reduced symmetries of these Lewis base complexes leads to strong quadrupolar relaxation by the aluminium centre (^{27}Al , $I = 5/2$, 100%). This relaxation and associated coupling often results in much broadened Al-H signals that can be very difficult to observe. Nevertheless, except for a select few of the alanes (**67** and **73**) Al-H stretches could be identified by IR spectroscopy (**Table 6**).

Table 6 Spectroscopic data for dichloroalane adducts.

Entry	Adduct	IR ν Al-H (cm^{-1})	^1H NMR (ppm) ^a
1	67	-	0.91, 3.62, 4.30 (Al-H)
2	68	1845	3.97, 1.38
3	73	-	1.18, 1.29, 3.80
4	70	1884	3.42
5	98	1797	0.34, 0.48 ^b
6	99	1930	- ^c
7	100	1843	1.94, 2.28, 3.18
8	102	1899	1.46, 1.63, 1.71

a) NMR spectrum in deuterated benzene; b) NMR spectrum in deuterated tetrahydrofuran due to insolubility in benzene; c) insoluble in all solvents.

From the IR spectra, the Al-H stretching modes have an increased wavenumber with the presence of the two chlorides with respect to alane (1801 cm^{-1}) except for **98**. Ashby⁷⁹ has proposed that the addition of inductively electron withdrawing groups (such as chlorides) on an alane lowers the electron density at aluminium leading to greater Al-H covalency (less hydridic character for H). This can be seen in the increased $\nu(\text{Al-H})$ values for most of the adducts. The reason for the anomalous behaviour of **98** is not understood.

It is worth noting that the chemical shifts of the Lewis base donors attached to the aluminium exhibit shifts compared to the free Lewis base. For example, the ^1H resonances of free diethyl ether moiety in deuterated benzene are δ_{H} 1.11 (CH_3) and (3.26) (OCH_2), whereas when the ether is coordinated to aluminium, the chemical shifts change $\Delta\delta_{\text{H}}$ - 0.2 (CH_3) and $\Delta\delta_{\text{H}}$ +0.36 (OCH_2). The latter observation is

consistent with the decreased electron density at the methylene group α to the oxygen when the latter is coordinated to the Lewis acidic alane.

2.3.1.1 Air-stability of alanes

Having achieved a rapid and simple procedure for the reliable synthesis of dichloroalane adducts their stability, and potentially pyrophoric nature, was explored. Aluminium hydrides like many other metal hydrides react quantitatively with hydrolytic solvents (alcohols, water, acids) to produce hydrogen gas. The volume of hydrogen gas can be directly measured providing a convenient method for determining the purity, concentration (when in solution) and air-stability of these hydrides. Each individual alane adduct of **Scheme 32** was weighed out (in a glove box) into a sealed Schlenk tube. This provided a standard, for the pure dichloroalane adduct species - so that the sample could be assumed to be pure. Subsequently, for each alane, a range of samples were exposed to laboratory air for increasing times (testing every 15 minutes). Their 'handling time' was defined as the period when >90% of the alane purity remained by hydrogen evolution. For comparison lithium aluminium hydride was also tested which remained >90% for at least 3 hours (**Table 7**).

Table 7 handling time of dichloroalane adducts

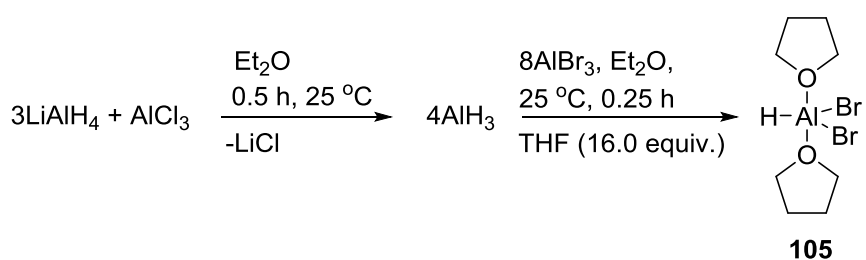
Entry	Alane	Handling time (min) ^a
1	LiAlH ₄	>3 h
2	68	30
3	70	45
4	99	30
5	100	<15
6	102	15
7	[HAL(O ^t Bu) ₂] ₂	30 ^b
8	HAL(N ⁱ Pr ₂) ₂	30 ^b

a) Handling time is defined as the period when the alane is 90-100% pure; b) carried out by Dr. A. Vinogradov, personal communication.

The results showed that none of the dichloroalane adducts, or di-*t*-butoxyalane and diisopropylamidoalane were as air stable as lithium aluminium hydride, which has an appreciably long handling time (entry 1). However, all of these alanes showed increased air-stability compared to diisobutylaluminium hydride (pyrophoric). When the polymeric dichloroalane (dioxane) adduct (**70**) was tested the handling time was 45 minutes (entry 3); presumably its improved stability is due to its polymeric nature. Dichloroalane adducts of *bis*(tetrahydrofuran) **68**, (DABCO) **98** and also di-*t*-butoxyalane all showed increased handling times of 30 minutes (entries 2, 4 and 7). Dichloroalane (diglyme) adducts showed a small level of air-stability (entry 6) whereas the *N*-methylmorpholine adduct showed very little air stability and was hydrolysed in air in less than 15 minutes (entry 5). Dichloroalane adducts **68**, **70** and **99**, as well as di-*t*-butoxyalane and diisopropylamidoalane, could all be stored

under standard Schlenk conditions under argon. Their increased air-stability allows these reagents to be promptly weighed out on the bench without any special protocols for one off reactions.

For comparison, the dibromoalane•*bis*(tetrahydrofuran) adduct was also prepared. However, a different route to that used for dichloroalane•*bis*(tetrahydrofuran) was needed due to the solubility of the lithium bromide by-product in diethyl ether. Dibromoalane•*bis*(tetrahydrofuran) was prepared by pre-forming the alane etherate adduct which could be separated from lithium chloride *via* cannula filtration, prior to ligand redistribution upon addition of aluminium tribromide (**Scheme 33**). The melting point of this adduct was lower than the chloride adduct (58-60 °C compared to 74-76 °C).



Scheme 33 Synthesis of dibromoalane•*bis*(tetrahydrofuran).

Although dichloroalane adducts **68**, **70** and **99**, di-*t*-butoxyalane and diisopropylamidoalane all showed somewhat increased air-stability, dichloroalane•*bis*(tetrahydrofuran) **68** was taken forward to use in the rest of our studies. This choice was based on: convenience of synthesis, its low molecular

weight, and the compatibility of tetrahydrofuran with many catalytic processes.

2.3.1.2 Summary of alane synthesis

Dichloroalane derivatives are shown to be somewhat air-stabilised aluminium hydrides which are easily accessible on large scales (up to 50 grams) (**Figure 26**). It is possible to weigh these reagents on the bench and to still use them without loss of alane activity - provided this is done promptly.



$\text{HAICl}_2 \cdot (\text{THF})_2$



neat DIBAL-H

Figure 26 Dichloroalane•bis(tetrahydrofuran) in air (left) vs. neat diisobutylaluminium hydride in air (right).

2.3.2 Hydroalumination of alkynes

With conditions in hand to synthesise large quantities of dichloroalane•bis(tetrahydrofuran), the hydroalumination of terminal alkynes was explored. Conditions to generate the corresponding alkenylalane dichloride with optimal regio-chemo-selectively and high yield needed to be found. A range of transition metals, which have previously found to be effective in hydroalumination chemistry, was screened *via* a

high throughput gas chromatography procedure. The hydroalumination of 1-decyne with dichloroalane•bis(tetrahydrofuran) was employed, to see what yields of the corresponding 1-decene could be achieved (**Table 8**).

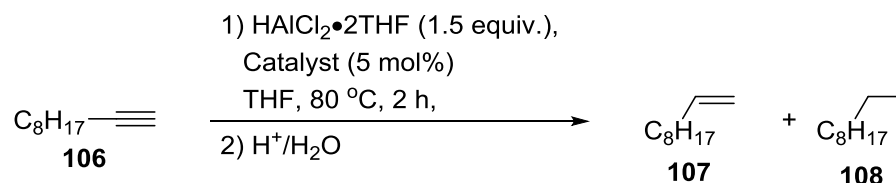


Table 8 hydroalumination catalyst screen.^a

Entry	Catalyst	Yield of decene (%) ^b	Yield of decane (%) ^b
0	none	6	1
1	ZrCl ₄	51	23
2	TiCl ₄ .2THF	78	20
3	Cp ₂ TiCl ₂	85	13
4	Cp ₂ ZrCl ₂	86	13
5	Cp* ₂ TiCl ₂	80	1
6	Cp* ₂ ZrCl ₂	84	15
7	Ni(dppp)Cl ₂	93	6
8	Ni(PPh ₃) ₂ Cl ₂	98	2

a) reaction carried out on a 0.5 mmol scale; b) determined by GC with dodecane as internal standard after quench.

The results showed that without any catalyst present, a very low background reaction occurred. When tetrachloro derivatives of group 4 metals were used, moderate yields of 1-decene was obtained with moderate levels of over reduction (entries 1 and 2). Near quantitative yields of 1-decene was obtained when nickel catalysts were used (entries 7 and 8), with only small amounts of over hydroalumination to decane observed. High yields of 1-decene were observed when

cyclopentadienyl derived substituents were present on the catalyst with higher amounts of over reduction compared to the nickel catalysts (entries 3 to 6).

To evaluate the regioselectivity of the hydroalumination, the reaction was quenched with deuterium oxide. $^2\text{H}\{^1\text{H}\}$ NMR studies revealed the point(s) of attachment of any aluminium organometallic formed through the hydroalumination catalysis. As the ^2H NMR spectrum was proton decoupled, trials showed that relative integration of the remaining singlets was an excellent way to monitor chemo and regioselectivity (**Table 9**). Extensive studies of nickel(II) pre-catalysts were avoided due to several reports and our own preliminary studies indicating that when nickel catalysts are used, such reactions frequently provide low levels of deuterium incorporation. This is attributed to a radical hydrogen abstraction from the tetrahydrofuran resulting in the corresponding reduced product, but *not* the formation of the required alkenylaluminium reagent.

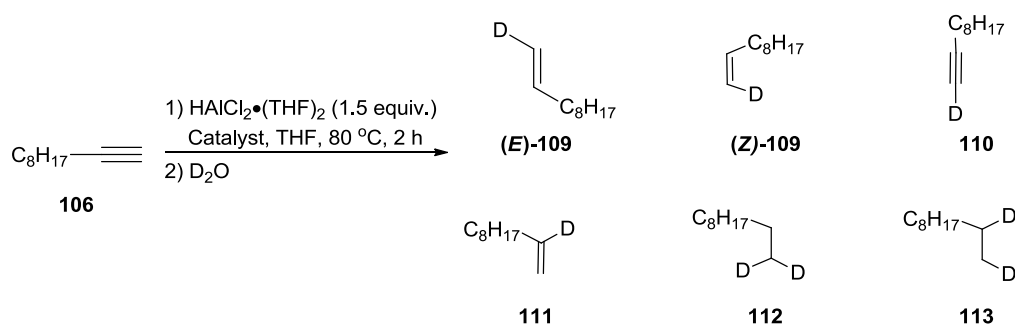


Table 9 Regioselectivity of hydroalumination determined by ^2H NMR.^a

Run	Catalyst ^b	(E)- 109	(Z)- 109	110	111	112	113 ^b
1	Cp ₂ TiCl ₂ (5 mol%)	53	2	0	42	1	2
2	Cp ₂ ZrCl ₂ (5 mol%)	74	0	15	5	5	0
3	Cp* ₂ TiCl ₂ (5 mol%)	75	3	0	6	14	3
4	Cp* ₂ ZrCl ₂ (5 mol%)	87	0	1	2	7	3
5	Cp* ₂ ZrCl ₂ (2 mol%)	82	0	0	2	11	2
6	Cp* ₂ ZrCl ₂ (1 mol%)	82	0	0	2	15	2
7	Cp* ₂ ZrCl ₂ (0.5 mol%)	75	0	0	3	18	3

a) Reactions carried out on 1 mmol scale; b) By $^2\text{H}\{^1\text{H}\}$ NMR spectroscopy on D₂O quenched reaction mixture.

What was pleasing to note from this procedure was the results observed were in agreement with the catalyst screen in **Table 8**. Titanocene dichloride was highly active but showed poor regioselectivity leading to high quantities of **111** (entry 1). Simple zirconocene dichloride inhibited the activity, providing poorer and variable conversions but all with high regioselectivity favouring (E)-**109** but significant amount of

acetylide **110** was also detected (entry 2). Speculation into this variable conversion could be due to the formation of stable dichloroalane adducts, perhaps related to $\text{Cp}_2\text{Zr}(\mu\text{-H})(\mu\text{-H}_2\text{AlCl}_2)\text{ZrCp}_2$.

Bis(pentamethylcyclopentadienyl)titanium dichloride had two undesirable features: firstly, with dichloroalane it gave unclear reactivity generating (Z)-**109**, **111**, **112**, **113** and hydrogen transfer products (entry 3); secondly, its literature preparation is problematic and low yielding leading to very uninviting costs for its purchase. Fortunately, *bis*(pentamethylcyclopentadienyl)zirconium dichloride pre-catalyst is highly potent for terminal alkyne hydroalumination using dichloroalane (entry 4), the only significant by-product being some **112**. It is also noted that the amount of catalyst for this transformation could be decreased to 1 mol percent without any significant drop in conversion and regioselectivity (entries 5 and 6), However, when 0.5 mol percent catalyst was used the regioselectivity decreased to 75% with increased amounts of the over reduction product **112** (entry 7).

2.3.2.1 Palladium catalysed Negishi coupling

Having a protocol in place for the highly regioselective formation of (*E*)-alkenylalanes, conditions were explored in order to apply these reagents in cross-coupling. Fortunately, very little optimisation was required for this protocol, as the

conditions that were optimal were analogous to the cross-coupling of DABAL-Me₃.⁸⁰ When carrying out the initial screening on the cross coupling of styrylaluminium dichloride the addition of DABCO to form the DABAL-(alkenyl)Cl₂ reagent *in situ* led to a maximised yield of the desired (*E*)-product (**Table 10**).

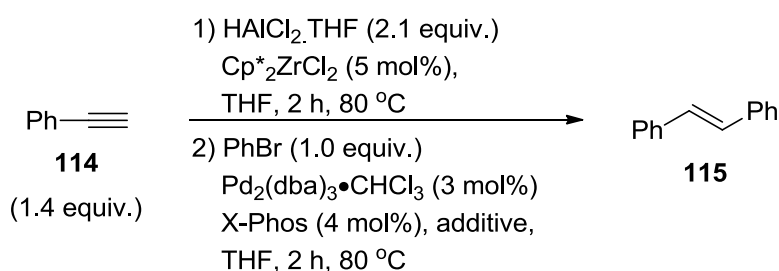


Table 10 A screening of additive effects.^a

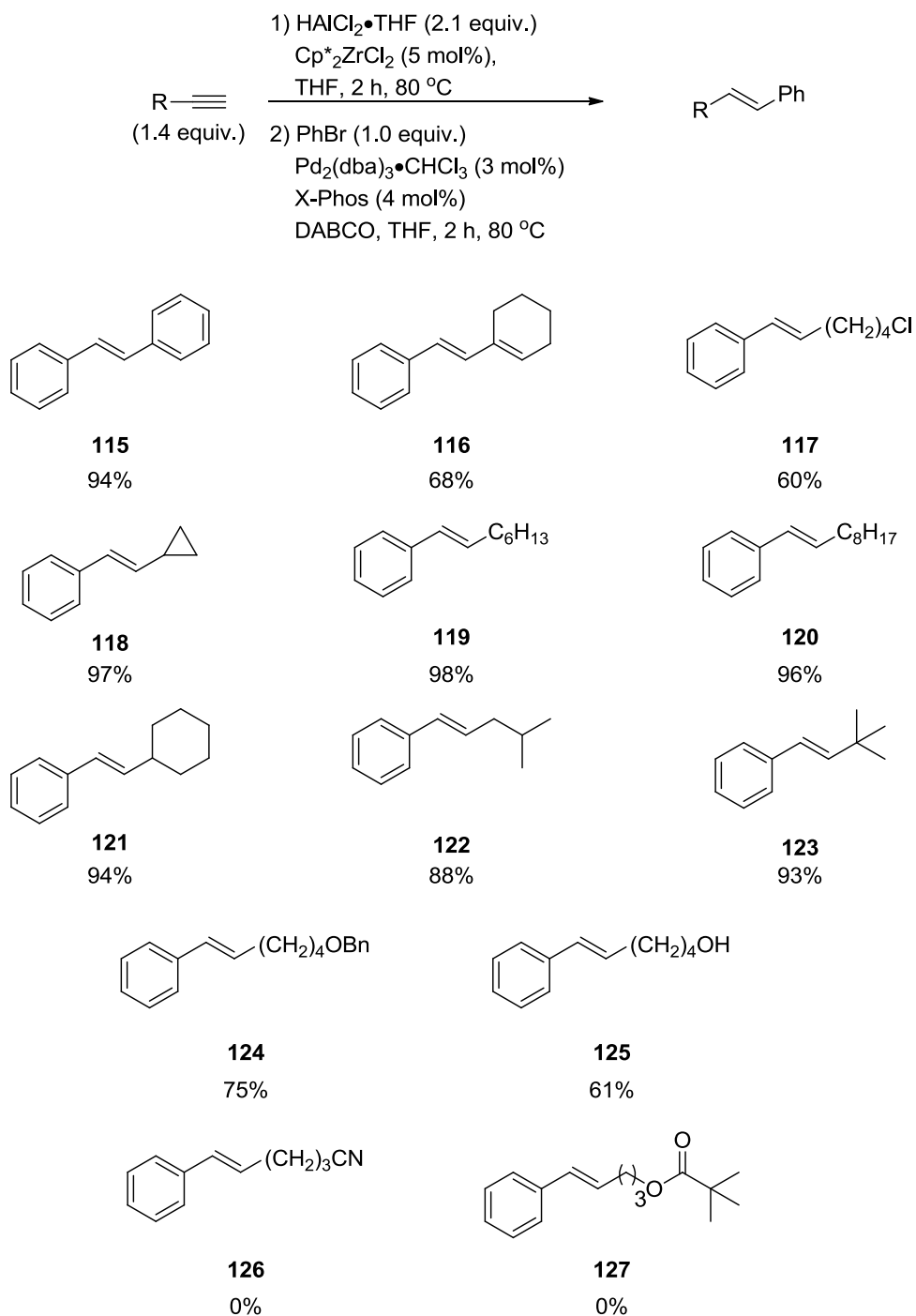
Entry	Additive	Yield (%) ^b
1	None	81
2	DABCO ^c	94

a) reaction performed on a 2 mmol scale; b) determined by GC; c) 0.5 equiv used with respect to alkyne.

Satisfyingly, the presence of neither the zirconium catalyst nor small amounts of **112** inhibited the coupling and the presence of a co-activator was not required.

2.3.2.2 Scope and limitation of alkenylalane

The generality of this optimal procedure with a range of alkynes was next tested (**Scheme 34**).



Scheme 34 Alkenylalane screen in palladium-catalysed cross-coupling reaction.

The results showed that alkynes which are typically problematic under diisobutylaluminium hydride hydroalumination (*i.e.* those which contain acidic protons or

halides), underwent hydroalumination with dichloroalane and subsequent cross-coupling which yielded the alkenylarenes, **115**, **116**, **117** and **118** in good to moderate yields (up to 94%). Alkyl alkynes underwent tandem hydroalumination/cross-coupling giving the expected products in excellent yields. Non-branched alkynes produced coupled products in up to 98% yield (**119** and **120**) and alkynes which contained different levels of branching were also coupled in excellent yields (**121**, **122** and **123**). When alkynes bearing pendent alcohol groups were subjected to hydroalumination with 1.5 equivalents of dichloroalane•*bis*(tetrahydrofuran), with respect to the alkyne, under *bis*(pentamethylcyclopentadienyl)zirconium dichloride catalysis followed by cross-coupled with bromobenzene the major product that was isolated was the olefin. This arises from alkyne hydroalumination but without any subsequent cross-coupling. When the amount of alane was doubled to 3 equivalents, the cross-coupling took place in the presence of an indium(III) chloride co-catalyst, **125** was isolated in 61% yield. The indium(III) chloride was chosen as it had been previously used for the cross-coupling of alkenylalanes with successful results but its role is unknown. When the benzyl protected alkynol was used product **124** was obtained in 75% yield with only 1.5 equivalents of dichloroalane. When the

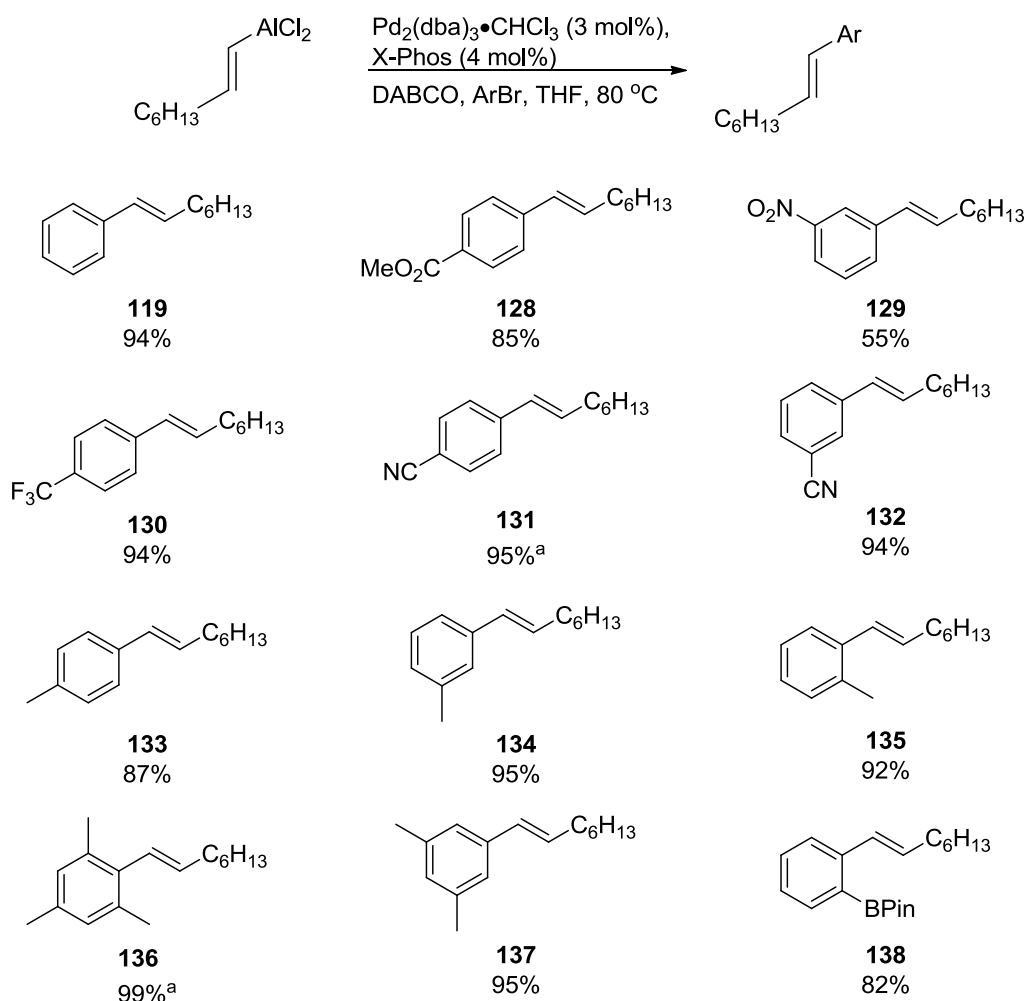
pivoyl ester and the nitrile functionalised alkynes were employed, none of the desired products were obtained. In the case of the pivoyl ester, only the free alkynol was observed, which indicated that the rate of ester cleavage is greater than the rate of catalysed hydroalumination. In the case of the nitrile alkyne, no reaction was observed in the hydroalumination reaction which might be attributed to the formation of a Lewis base adduct with the zirconium catalyst deactivating it.

2.3.2.3 Scope and limitations of electrophilic coupling partner

The generality of the optimal procedure was examined using (*E*)-octenylaluminium dichloride as a fixed nucleophilic coupling partner with various aryl and heteroaryl halides (**Scheme 35**).

Aryl bromides that contain other potentially electrophilic centres such as esters, nitriles and nitro- groups all underwent cross-coupling in excellent yields (up to 95%). However, the nitro substituted aryl halide gave **129** in lower yields (55%). When the position of the nitrile substituent was altered, the yield of the product was not affected (**131** and **132**). When aryl halides that contain carbonyl groups more reactive than an ester moiety were used, none of the desired cross-coupled product was observed. Aryl halides containing slightly

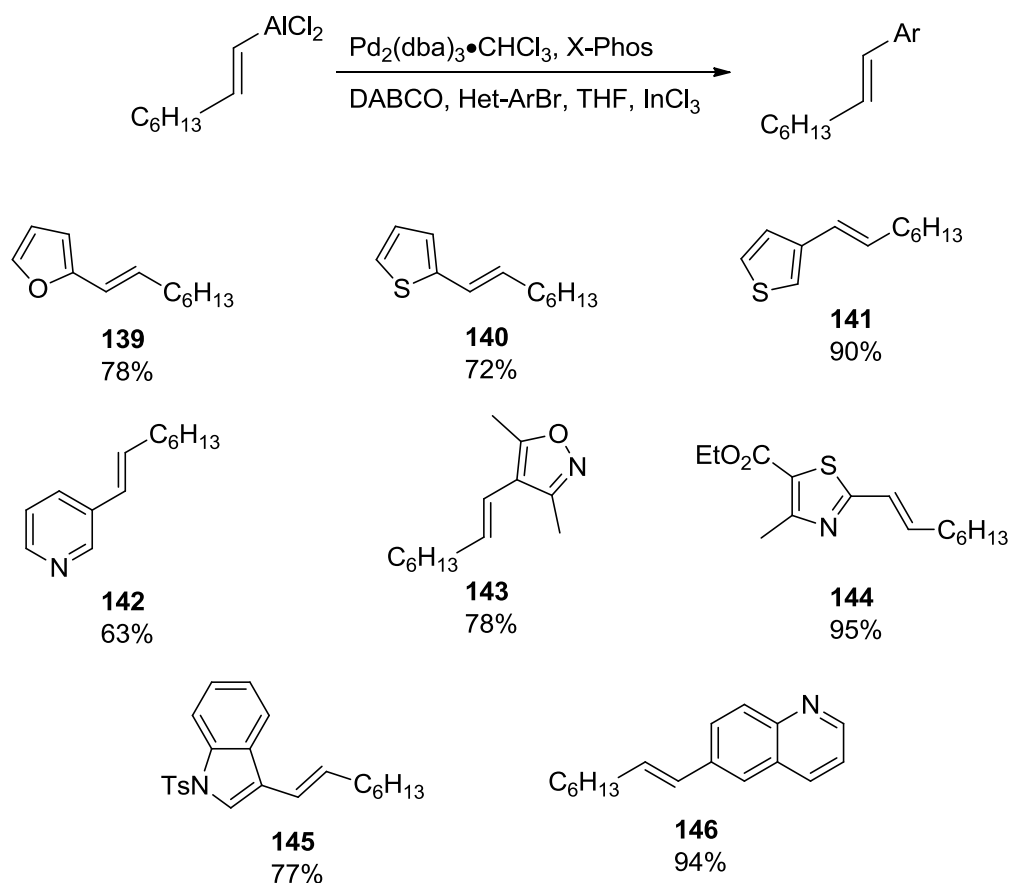
electron-donating groups with different levels of steric bulk also underwent cross-coupling, producing the desired products in excellent yields (up to 99%). When the position of the alkyl substituent was explored, high yields were still observed (**133**, **134** and **135**).



Scheme 35 Aryl bromide screen for the cross-coupling of alkenylalanes.

When aryl halides containing a nucleophilic centre were screened, **138** was obtained in good yields with no biaryl self-coupled product observed.

The use of heteroaryl halides in the Negishi cross-coupling of alkenylalanes is underrepresented in the literature, therefore to see the generality of the cross-coupling such systems were explored (**Scheme 36**).

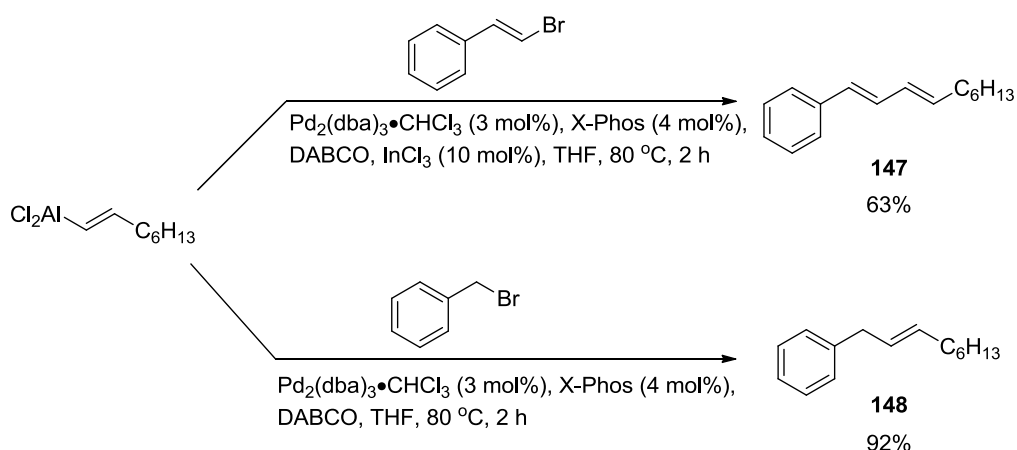


Scheme 36 Hetero-aryl bromide screen in the cross-coupling reaction.

Oxygen and sulfur containing heterocycles underwent cross-coupling in good to excellent yields, with the 3-substituted heterocycles producing the desired product in higher yields than the corresponding 2-halo heterocycle. However, the cross coupling of nitrogen containing heterocycles required further optimization due to the Lewis basicity of the nitrogen moieties.

Amines and pyridine functionalities are known to be able to complex the alkenylaluminium reagents strongly, potentially deactivating at least one equivalent of the alane. It was found that the cross coupling of 3-bromopyridine with 1.4 equivalents of octenylalane gave a low yield, but when 2.1 equivalents of (*E*)-octenylalane was used, a more synthetically useful yield of 3-octenylpyridine was achieved (63%, **142**). The cross coupling of other nitrogen containing heterocycles, such as isoxazoles (**143**) thiazoles (**144**), indoles (**145**) and quinolines (**146**), with 2.1 equivalents of alkenylalane, all proceeded in high yields but indium trichloride (10 mol%) was required as a co-catalyst.

Like the nitrogen containing heterocycles, vinyl halides proved to be particularly challenging, yielding only 7% of the desired product. When indium chloride was used as the co-catalyst again, the reaction proceeds in a cleaner fashion yielding the corresponding diene in 63% yield (**Scheme 37**). Benzylic halides on the other hand reacted cleanly under the optimised conditions to form the allylated arene in excellent yields (up to 92%).



Scheme 37 Cross-coupling to vinyl halides and benzyl bromides.

To see how our dichloroalane tandem protocol fared against the literature procedures, it was compared against the traditional hydroalumination-cross-coupling protocol using diisobutylaluminium hydride (**Figure 27**). In this comparison, only the aluminium hydride was changed and the cross-coupling reagents kept the same.

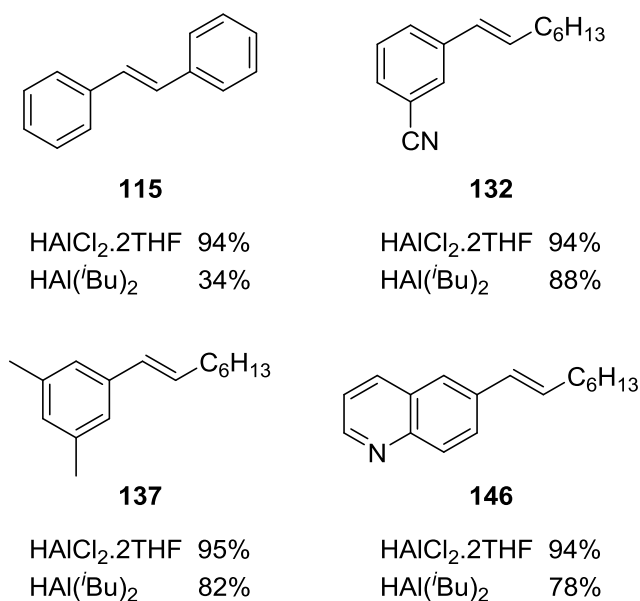


Figure 27 Comparison of hydroalumination procedures.

The results showed that the hydroalumination carried out using dichloroalane led to higher chemical yields in all cases compared to Negishi's diisobutylaluminium hydride hydroalumination. In particular, the hydroalumination of phenylacetylene using diisobutylaluminium hydride, led to large amounts of the alkynyl-cross coupled product (up to 30%) under Negishi's conditions.

2.3 Conclusions

Adducts of dihaloalanes, mainly dichloroalane and dibromoalane can be synthesised with relative ease in a two step process starting from commercial lithium aluminium hydride and aluminium trihalide (X = chloro and bromide). High yields and an ability to work on large scales (up to 50 grams) characterise this procedure. These alanes exhibit low pyrophoricity with effective handling times of up to 30 minutes in air, meaning that they can be weighed out promptly on the bench without the need for special techniques.

Hydroalumination of terminal alkynes proved most effective with the previously unused catalyst, decamethylzirconocene dichloride, which generated the (*E*)-alkenylalanes in high yields with excellent regio- and stereochemistry with minimal acetylide formation.

The tandem hydroalumination/palladium cross-coupling reaction of acetylenes was also been explored in great detail, with the (*E*)-selective alkenylalane cross-coupling, under palladium catalysis in the presence of DABCO, with various aryl halides, sulfur, oxygen and nitrogen containing heterocycles, vinylic and benzylic bromides all proceeding in high yields.

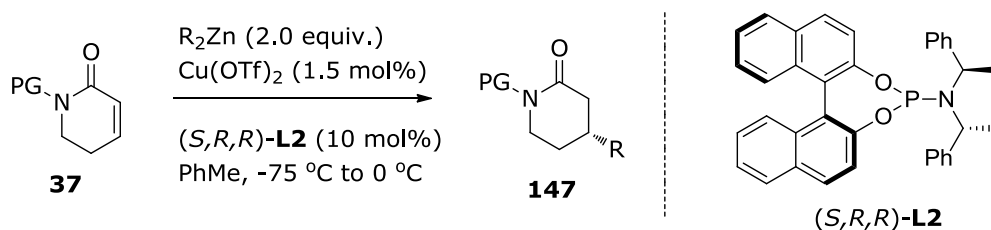
Chapter 3

Conjugate addition of alkenylaluminum reagents to α,β -unsaturated carbonyl compounds

3.1 Introduction

3.1.1 Conjugate addition to diactivated carbonyls

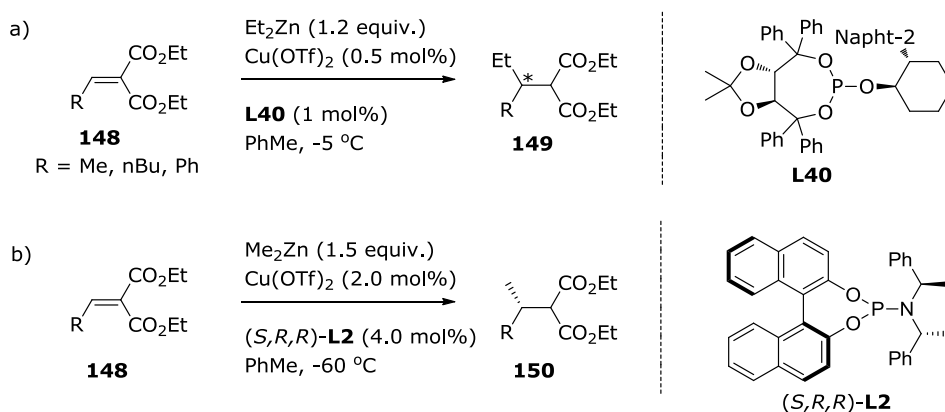
The introduction of a second electron withdrawing group at the 1'-position of an α,β -unsaturated carbonyl compound significantly increases its reactivity towards catalytic conjugate addition of dialkylzinc and trialkylaluminium species. Feringa in 2004 showed that this is indeed the case, by adding a suitable protecting/activating group to the nitrogen of α,β -unsaturated lactams (**29**), the addition of dialkylzincs, under copper catalysis in the presence of **L2**, yielded **147** in good yields (up to 70%) with excellent enantioselectivity (up to 95% ee) (**Scheme 38**).⁸¹



Scheme 38 1,4-addition of dialkylzinc to lactams.

Thus far, only alkyl organometallic reagents and relatively unreactive allylsilanes⁸² have been employed successfully in the enantioselective conjugate addition to 1,1'-diactivated enones.

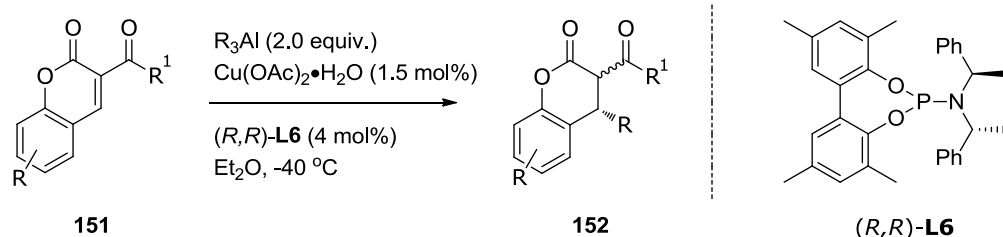
Alexakis investigated the copper-catalysed ACA of dialkylzinc reagents to alkylidene malonates **148**.⁸³ In the presence of copper(II) triflate and ligand **L40**, the 1,4-addition products **149** were obtained in good to excellent yields with enantioselectivities ranging between 64-73% (**Scheme 39a**). When triethylaluminium was used instead of diethylzinc, no enantioselectivity was observed. Feringa also investigated the copper-catalysed conjugate addition to alkylidene malonates using dimethylzinc in the presence of copper(II) triflate and ligand **L2**. The 1,4-adducts were obtained in good to excellent conversions with excellent enantioselectivity up to 98% (**Scheme 39b**).⁸⁴



Scheme 39 1,4-addition of ZnR₂ to alkylidene malonates.

Woodward and co-workers investigated the copper-catalysed conjugate addition of organoalanes to 3-acylcoumarins.⁸⁵ In the presence of copper(II) acetate monohydrate and **L6**, the 1,4-addition product was obtained in high yields (up to 94%) with good to excellent

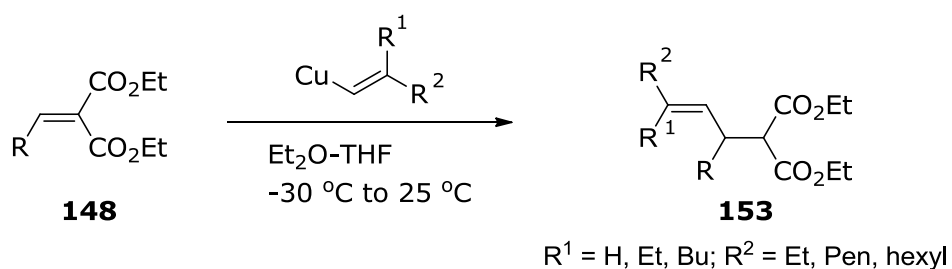
diastereoselectivity (up to 99:1) and enantioselectivity (up to 96%) (**Scheme 40**).



Scheme 40 1,4-addition of trialkylaluminium to 3-acylcoumarins.

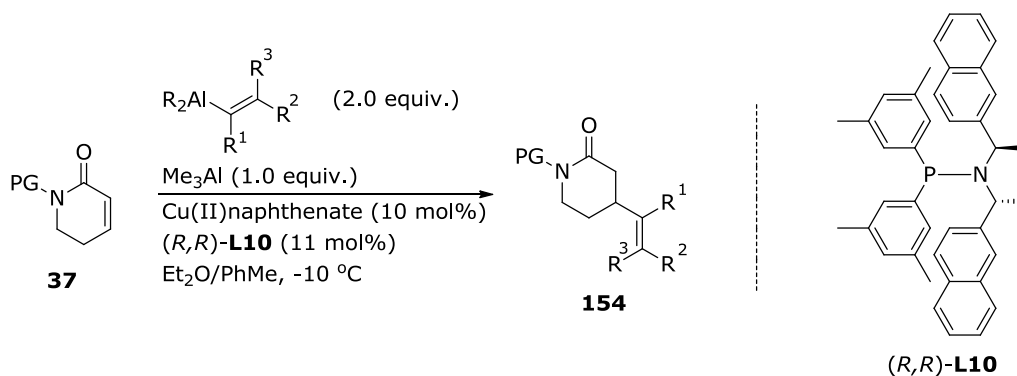
Within this work, the addition of alkenylalanes, derived from the hydroalumination of alkynes with diisobutylaluminium hydride, to acylcoumarins was also investigated. This reaction proceeds in good to excellent yields but with *no* enantioselectivity. The lack of enantioselectivity was attributed to the high background reaction due to the higher reactivity of the sp^2 -hybridised carbon atom compared to an sp^3 carbon.

Apart from this report, there are very few reports of the conjugate addition of alkenyl organometallics to 1,1'-diactivated enones. In the early 1990s, Knochel and Cahiez investigated the conjugate addition of stoichiometric alkenylcopper reagents to alkylidene malonates (**Scheme 41**).⁸⁶ The 1,4-addition products **153** were synthesised in excellent yields.



Scheme 41 1,4-addition of alkenylcopper to alkylidene malonates.

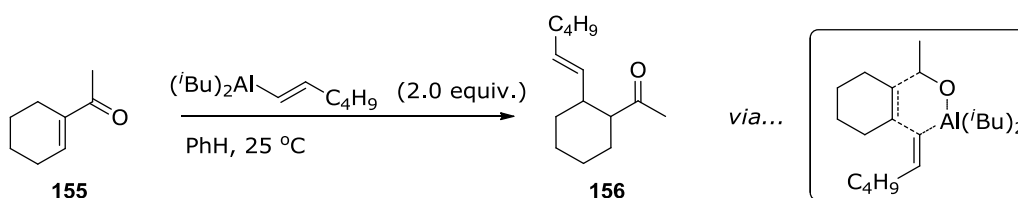
Recently (2013), Alexakis and co-workers have shown that it is possible to add a series of alkenylalanes, derived by transmetallation and hydroalumination, to α,β -unsaturated lactams **29**.⁸⁷ In the presence of 10 mol% copper(II)naphthenate and SimplePhos ligand (*R,R*)-**L10**, moderate to good yields of the 1,4-adduct **154** were achieved (30-70%) with good to excellent enantioselectivities (up to 90%) (**Scheme 42**).



Scheme 42 conjugate alkenylation of lactams.

3.1.2 Uncatalysed conjugate addition of alkenylalanes to enones

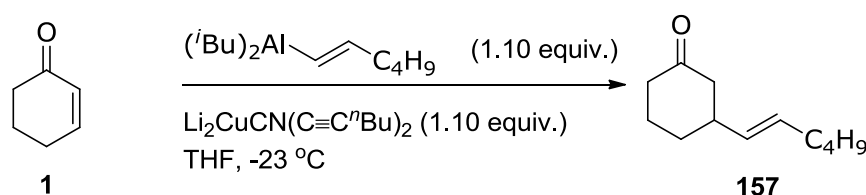
The first use of alkenylalanes, synthesised *via* hydroalumination, in conjugate addition was reported by Hooz and co-workers.⁸⁸ It was noted that only enones which could adopt the cisoidal conformation were active towards conjugate addition (**Scheme 43**). When enones such as cyclohexenone, which adopt the transoidal conformation, were used, the conjugate addition was inefficient.



Scheme 43 1,4-addition to cisoidal enones.

This difference in reactivity between the cisoidal and transoidal conformations of enones is attributed to the formation of a six-membered transition state. This transition state is only possible for enones which are able to adopt the cisoidal conformation. The postulated transition state also explains why the reaction proceeds in non-coordinating or weakly coordinating solvents, because solvents such as tetrahydrofuran, coordinate to the aluminium strongly and prevent the coordination of the carbonyl moiety therefore completely suppressing the reaction.

The first conjugate addition of an alkenylalane to a transoidal enone **1** was reported by Wipf,⁸⁹ where a stoichiometric amount of an elaborate higher order acetylene based cyanocuprate was used to achieve good regioselectivity and yields (up to 95%) of the 1,4-addition adduct **157** (Scheme 44).



Scheme 44 1,4-addition to transoidal enones.

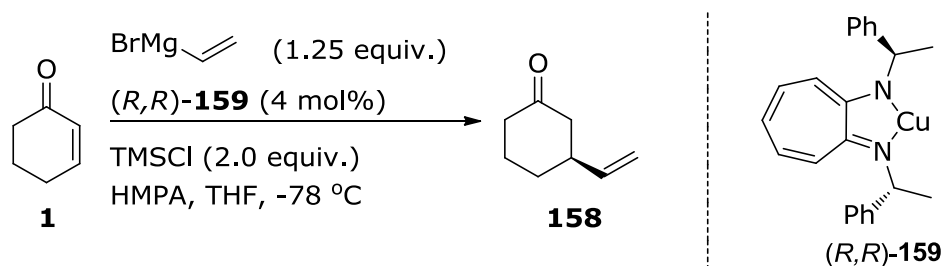
3.1.3 Copper-catalysed conjugate addition of alkenyl organometallics

This section covers reported examples of copper-catalysed conjugate addition of alkenyl organometallics to enones and is divided according to the organometallic nucleophile. Although there are numerous examples of rhodium-catalysed conjugate addition of alkenyl organometallics, they will not be discussed within this section as they are not a topic of this thesis and an excellent recent review is available.⁹⁰

3.1.3.1 Alkenyl magnesium reagents

Lippard and co-workers,⁹¹ reported in their seminal work, the addition of vinylmagnesium bromide to cyclohexenone, using a preformed copper(I) complex **159**, to

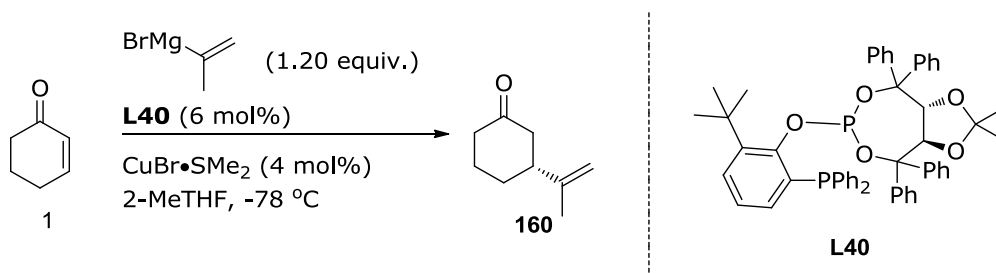
yield the 1,4-adduct in 92% isolated yield but with only 9% enantioselectivity (**Scheme 45**).



Scheme 45 ACA of vinylmagnesium bromide.

Schmalz and co-workers, a couple of decades later, reported the first highly enantioselective copper-catalysed addition of prop-1-en-2-ylmagnesium bromide to **1**.⁹² In this work, it was noticed that a phosphine-phosphite ligand based on TADDOL **L41** in the presence of copper(I) bromide dimethyl sulfide yielded the 1,4-adduct **160** with high enantioselectivity, 92%, but only moderate yield, 49%. An important discovery was the use of 2-methyltetrahydrofuran as solvent, which led to higher enantioselectivities compared to other ethereal solvents. Furthermore, the same author noted that the conjugate addition of prop-1-en-2-ylmagnesium bromide to both cyclopentenone and cycloheptenone could also be achieved in good yields (53 and 62% respectively) and enantioselectivity (up to 89%) (**Scheme 46**).⁹³ The addition of trimethylsilyl chloride was crucial in the conjugate addition to cyclopentenone to obtain good yields, reducing the propensity of the enolate generated

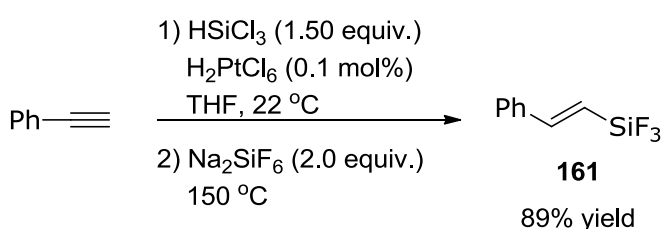
to undergo conjugate addition with another molecule of cyclopentenone.



Scheme 46. ACA of alkenyl Grignard reagents.

3.1.3.2 Alkenyl Silicon reagents

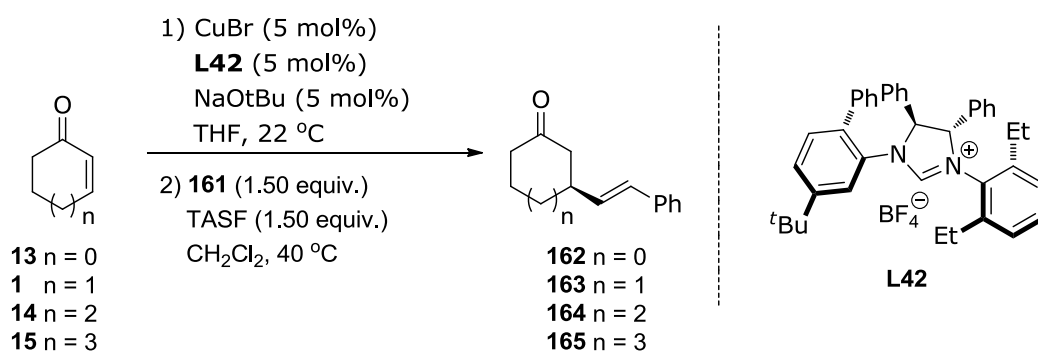
The only report of a copper-catalysed conjugate addition of alkenylsilanes is from Hoveyda.⁹⁴ The alkenyltrifluorosilanes were synthesised *via* a two step procedure i) platinum-catalysed hydrosilylation using trichlorosilane, followed by ii) treatment with sodium fluorosilicate to synthesise the corresponding trifluorosilane in good overall yields (**Scheme 47**).



Scheme 47 Synthesis of alkenyltrifluorosilanes.

Hoveyda showed that these alkenylsilanes can undergo conjugate addition in the presence of a copper-NHC complex, generated from copper(I) bromide and chiral NHC (**L42**), to generate the conjugate addition products **162-165** in good

yields (up to 97%) and moderate to high enantioselectivities (up to 92%) with the highest enantioselectivities being achieved for cycloheptenone and cyclooctenone (**Scheme 48**). The addition of a fluoride source, tris(dimethylamino)sulfonium difluorotrimethylsilicate (TASF), was required to activate the alkenyltrifluorosilane by generating a reactive pentavalent silicon species analogous to the Hosomi-Sakurai reaction. The transmetalation of this activated alkenylsilane onto copper is facile.



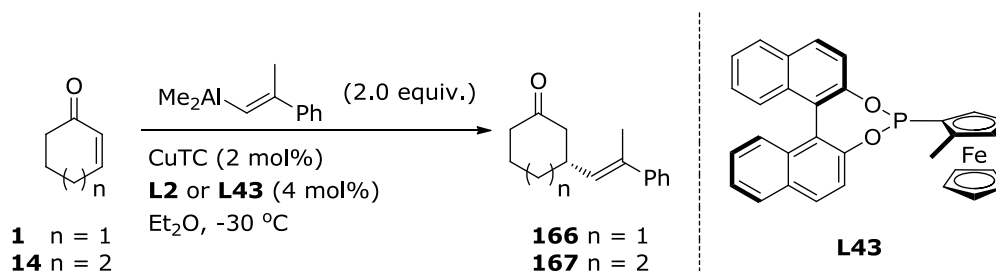
Scheme 48 Copper-catalysed ACA of alkenyltrifluorosilanes.

3.1.3.3 Alkenyl aluminium reagents

As mentioned in Chapter 2, alkenylalanes are readily accessible *via* three main synthetic methods i) carboalumination, ii) hydroalumination and iii) lithium-halogen exchange.

Alexakis, Woodward and co-workers reported the first enantioselective conjugate addition of alkenylalanes to cyclohexenone and cycloheptenone, by a tandem carboalumination-ACA procedure. Moderate yields, up to 54%,

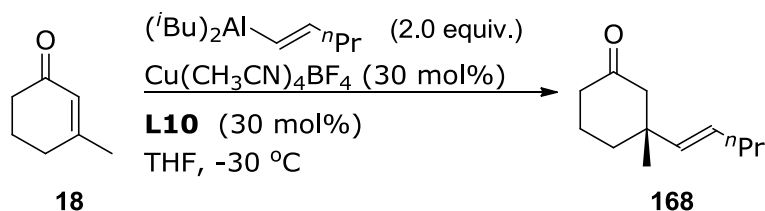
and enantioselectivities, up to 77%, of the addition products **166** and **167** could be achieved using copper(I)thiophenecarboxylate in combination with phosphoramidite **L2**.^{95 a} The enantioselectivity could be increased, to 85%, when copper(I)thiophenecarboxylate was used in combination with chiral ferrophite (**L43**) (**Scheme 49**).^{95b} It was also noted that the carboalumination catalyst (zirconocene dichloride) did not interfere with the conjugate addition.



Scheme 49 Tandem carboalumination-ACA protocol.

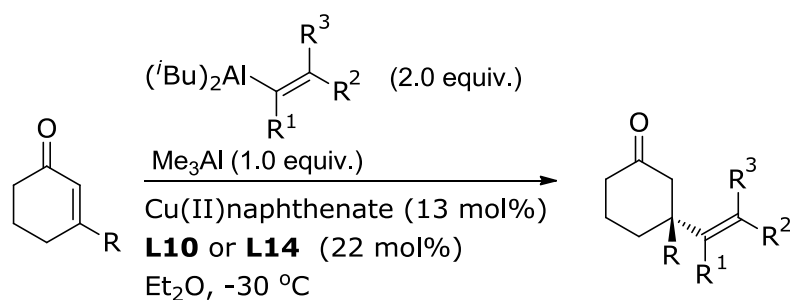
The first example of conjugate addition of an alkenylalane to a trisubstituted enone, forming an all carbon stereogenic centre *via* a tandem hydroalumination-ACA protocol, was reported by Alexakis. It was found that when copper(I) thiophenecarboxylate was used in combination with **L10**, good enantioselectivities was achieved. The choice of solvent was critical, when diethyl ether was used, high enantioselectivities (up to 80%) were obtained but a significant amount of undesired 1,2-addition product was observed. When tetrahydrofuran was used in the presence of

copper(I)*tetrakis*acetonitrile tetrafluoroborate, no undesired 1,2-product was obtained but a decrease in enantioselectivity to 73% ee was observed (**Scheme 50**).



Scheme 50 first reported tandem hydroalumination-ACA.

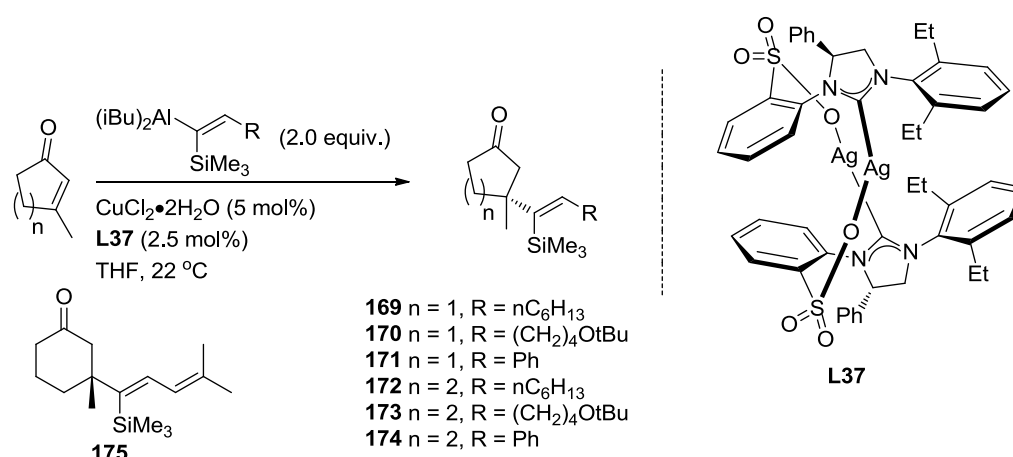
A recent report from Alexakis and co-workers represents a new tandem hydroalumination-ACA protocol using phosphinamine ligands. When these electron rich ligands are used in the presence of copper(II) naphthenate, the reaction proceeds with excellent regio- (up to 91% 1,4-adduct) and enantioselectivity (up to 89%).⁹⁶ Also in this report, the use of co-activation with trimethylaluminium was noted for the first time, which was crucial when sterically demanding alkenylalanes are used. A wide variety of both *E* and *Z*-alkenylalanes could be used in this protocol as well as α - and β -substituted alkenylalanes (**Scheme 51**), which were generated *via* the nickel catalysed hydroalumination.⁹⁷



Scheme 51 Modified tandem hydroalumination-ACA.

What is noticeable within these reports is that a higher catalyst loading is required for the conjugate addition of alkenylalanes compared to alkylalanes, this could be due to trace amounts of aluminium acetylides, produced as an unwanted side product in hydroalumination, which could poison the copper-catalyst by acting as a dummy ligand after transmetallation from aluminium to copper.⁹⁸

One approach to avoid the formation of the problematic aluminium acetylides was reported by Hoveyda and co-workers.⁹⁹ This strategy involved the clean hydroalumination of silyl-protected alkynes without the formation any aluminium acetylides. A strongly donating sulfone-based NHC-copper complex, generated from the corresponding silver carbene complex **L37**, was able to promote the conjugate addition of these alkenylalanes, in moderate to high yields (up to 95%) with excellent enantioselectivities (up to 97%), in short times (0.25 h) and at room temperature (**Scheme 52**).

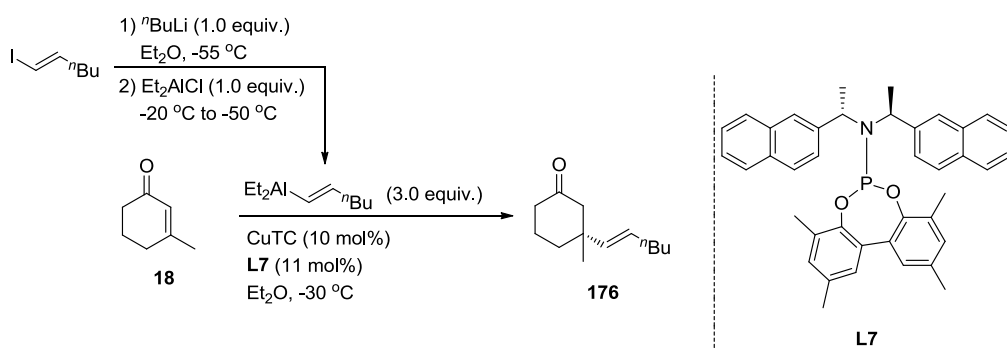


Scheme 52 ACA of silicon substituted alkenylalanes.

This methodology is very general; both in terms of the alkenylalane, with aryl-, alkyl- and conjugated alkynes all being compatible, and also enones, in particular, the addition to notoriously difficult cyclopentenones proceeds with excellent yields of 1,4-products **169-171**. However, for the addition to cyclohexenones, lower chemical yields of the desired products **172-175** were obtained due the transfer of the *iso*-butyl group (up to 33%) and additions to cycloheptenones were inefficient (conv. up to 40%), thought to be attributed by steric hindrance by the silicon moiety.

Another approach to avoid the formation of aluminium acetylides is to synthesise the alkenylalanes *via* a halogen-lithium exchange followed by transmetallation. The first reported use of alkenylalanes generated *via* this sequence in conjugate addition chemistry was by Alexakis and co-workers, where (*E*)-1-iodohexene underwent treatment with *n*-butyllithium to generate the alkenyllithium reagent, which

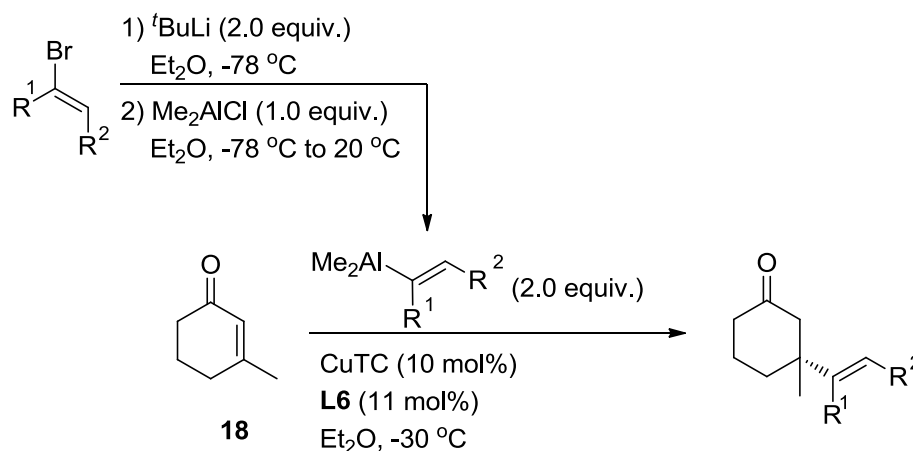
subsequently transmetallated onto diethylaluminium chloride to furnish the corresponding alkenylalane.¹⁰⁰ The formation of the alkenylalane required very precise temperature control. When the alkenylalane was used in conjugate addition, with copper(I) thiophenecarboxylate in combination with phosphoramidite **L7**, the 1,4-adduct **176** was synthesised with good optical purity (82%) in excellent yield (93%). It should be noted that the catalyst loadings could be reduced from 30 mol% in the early attempts to 10 mol% (**Scheme 53**).



Scheme 53 ACA of alkenylalanes generated from alkenyl iodides.

As only a few alkenyliodides are commercially available, the procedure was modified so that alkenylbromides (for which there is greater commercial availability) could be used. Alexakis and co-workers treated the alkenylbromides with *t*-butyllithium in diethyl ether; this was followed by a transmetallation onto dimethylaluminium chloride to yield the corresponding alkenylalane.¹⁰¹ The stoichiometry between *t*-

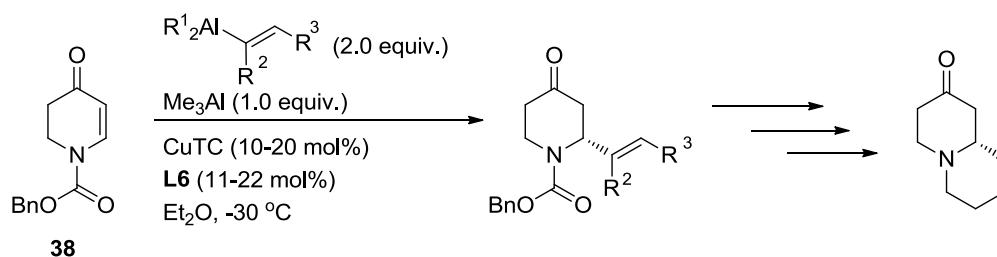
butyllithium and dimethylaluminium chloride is critical as an excess of either reagent decreases the enantioselectivity of the 1,4-addition product, therefore the alane solution was stirred at room temperature for 18 h to ensure complete conversion to the alkenylalane. It was found that copper(I) thiophenecarboxylate in the presence of phosphinamine **L6**, would efficiently add these alkenylalanes to 3-methyl-2-cyclohexenone to generate the 1,4-adduct in good yields with excellent optical purity. Other Michael acceptors were also tried but either low conversion or low enantioselectivity was observed (**Scheme 54**).



Scheme 54 ACA of alkenylalanes derived from alkenylbromides.

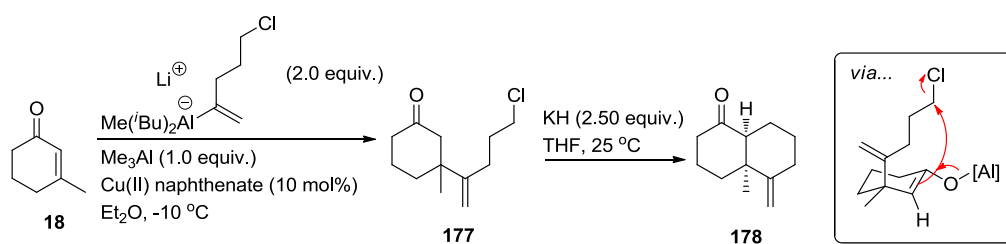
Recently, it was shown that both hydroalumination and transmetallation protocols can be employed to the addition to *N*-substituted-2,3-dehydro-4-piperidones.¹⁰² Alexakis and co-workers showed, that under a catalyst system of Cu(II) naphthenate and ligand **L6**, good to moderate yields of

the 1,4-adduct could be obtained in excellent enantioselectivities (up to 97%). The corresponding piperidones can be used as precursors to pharmaceutically active piperidines and alkaloids (**Scheme 55**). Enantioselective addition of alkenylalanes generated from vinylmagnesium bromide was also reported for the first time.



Scheme 55 ACA to *N*-substituted-2,3-dehydro-4-piperidones.

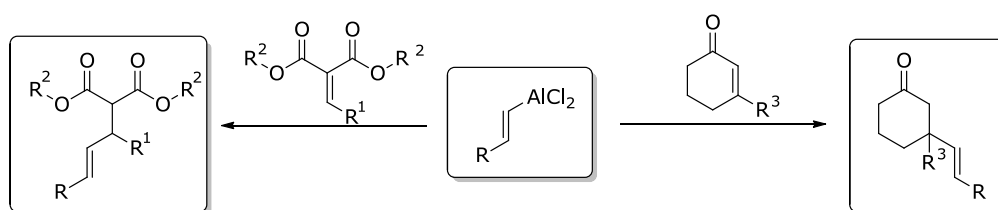
An efficient and practical approach for the conjugate addition of sterically encumbered alkenyl alanes to trisubstituted enones, to generate highly congested quaternary stereogenic centres, such as **177** in good yields (up to 63%), was reported by Alexakis and co-workers.¹⁰³ The alkenyl alanes are generated in high yields *via* a nickel-catalysed hydroalumination of alkynes to generate internal alkenylalanes, which are subsequently reacted with methyllithium. *Cis*-decalin systems can be synthesised from the conjugate addition product **177** by treatment with potassium hydride, resulting in a simple preparation of these bicycles (**Scheme 56**).



Scheme 56 Conjugate addition of alkenyl alanates.

3.2 Aim of research

The success of alkenylaluminium dichlorides in palladium catalysed cross-coupling caused us to consider their use in other metal-promoted transformations, in particular 1,4-additions to Michael acceptors. What particularly caught our attention was the under-representation of the conjugate addition of alkenyl nucleophiles to 1,1'-diactivated enones, particularly alkylidene malonates. Also noted was the lack of use of alkenylalanes in the conjugate addition to simple enones, such as cyclohexenone. Inspired by this lack of literature, we wondered if our alkenylaluminum reagents (generated *via* the methodology developed in Chapter 2) could contribute to these problems in alkenyl additions to such classes of Michael acceptors (**Scheme 57**).



Scheme 57 Objectives of this work.

3.3 Results and discussions

3.3.1 Conjugate addition to alkylidene malonates

It is known that many conjugate addition reactions to 1,1'-diactivated enones are extremely facile. It is known that organoaluminium dihalides are extremely strong Lewis acids and this should promote any reaction. Our initial investigations focused on the effect of temperature on the addition of (*E*)-octenylaluminium dichloride (**179**) to dimethyl 2-ethylidenemalonate (**180**) to see if any background reaction could be minimised (**Table 11**). Diethyl ether was chosen as solvent for this screening due to the literature precedent for its use in conjugate additions to acylcoumarins.⁸⁵

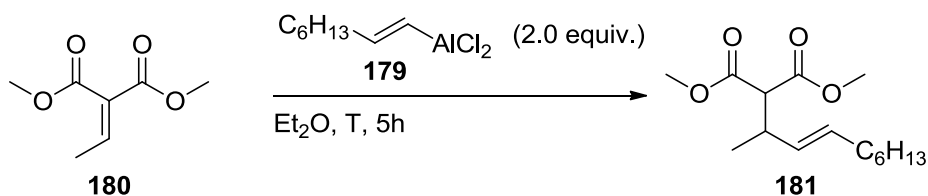


Table 11 Temperature effects in alkenylalane addition to alkylidene malonates.^a

Entry	Temperature °C	Isolated yield %
1	0	76
2	-20 ^b	51
3	-40 ^b	50
4	-78	48

a) reaction carried out on a 0.5 mmol scale; b) temperature controlled using a cryostat.

Although the background reaction was suppressed slightly by decreasing the temperature of the reaction mixture

(entry 1-4), the amount of product obtained in this non-catalytic reaction was still around 50% even at -78 °C, indicating that even at low temperatures the background reaction is facile. When the solvent was changed from diethyl ether to more coordinating solvents such as tetrahydrofuran and 1,4-dioxane at -40 °C, **181** was obtained in similar yield as in diethyl ether (51% and 49% respectively). In order to try and decrease the Lewis acidity at the aluminium centre and thus minimise the background reaction, other Lewis base additives were screened (**Table 12**).

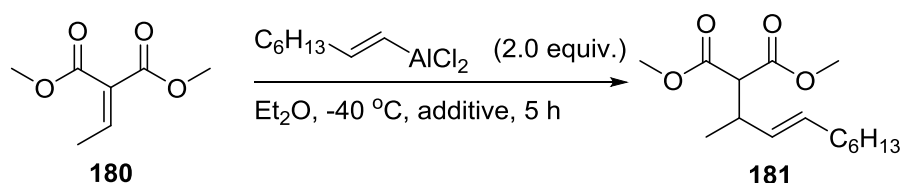


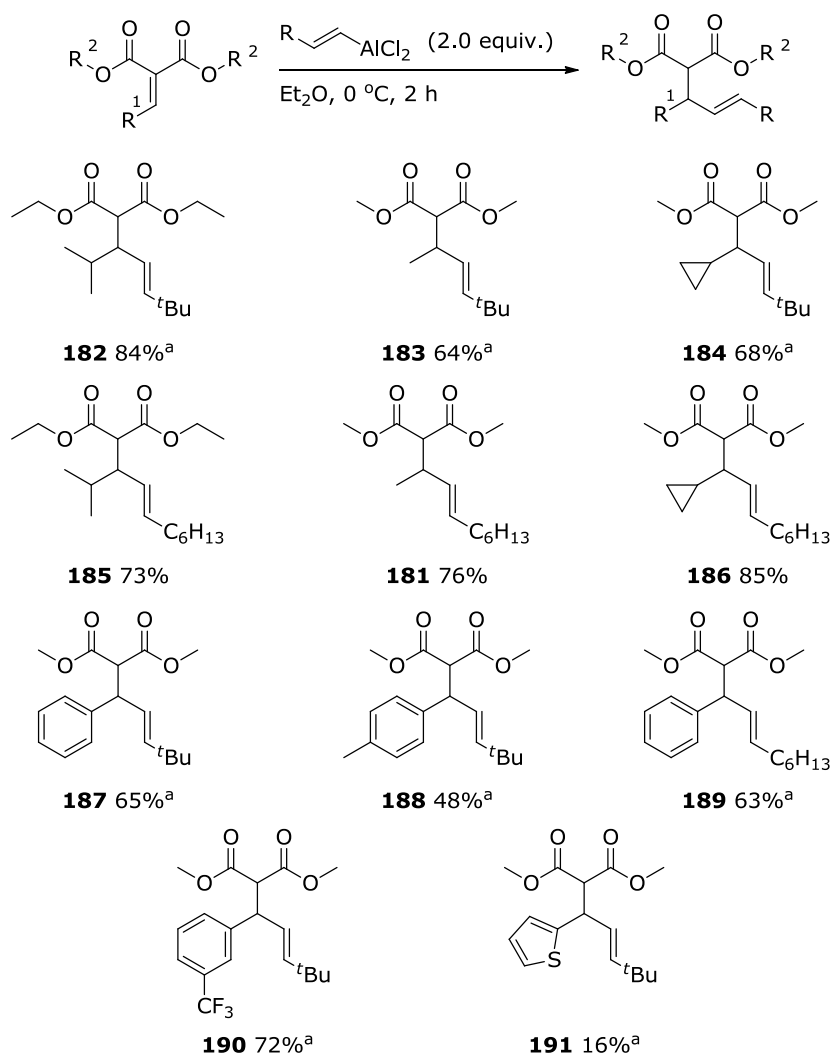
Table 12 Effect of Lewis base on background reaction.^a

Entry	Additive	Isolated yield %
1	Tetrahydrofuran ^b	51
2	1,4-dioxane ^b	49
3	DABCO ^c	46
4	<i>N</i> -methylpyrrolidine	52
5	<i>N</i> -methylmorpholine	49

a) reaction carried out on a 0.5 mmol scale; b) used as solvent; c) 0.5 mmol used to form a 2:1 adduct with organoalane.

Unfortunately, even when nitrogen containing Lewis bases were used, **181** was obtained in similar yields (entry 3-5). This suggests that the chelating carbonyl moieties are better at coordinating an aluminium centre, thus making the alkylidene malonate more electrophilic and consequently the background reaction more facile. What was interesting was

the yield obtained for *N*-methyl morpholine and 1,4-dioxane was the same, and this could be due to aluminium being chelated by the substrate hence binding to the oxygen rather than the nitrogen sites. Due to the unsuccessful attempts to minimise the background reaction, the racemic reaction was optimised at 0 °C in diethylether to see what functional groups could be tolerated (**Scheme 58**).



a) reaction carried out by Marc Garcia.¹⁰⁴

Scheme 58 1,4-Addition to alkylidene malonates by alkenylalanes.

The results showed that both linear and branched alkyl substituents on the alkylidene malonate were well tolerated, producing **181**, **182**, **183** and **185** in good yields. Strained cyclopropyl substituents were also tolerated in good to excellent yields (compounds **184** and **186**) with both a sterically demanding alkenylalane and a linear non-branched alkenylalane. Aryl substituents on the alkylidene malonates were tolerated with both alkenylalanes giving **187** and **189** in 65% and 63% yield respectively. However, when electron-donating substituents were added to the aryl ring in the *para*-position, a lower yield was observed of 48% (**188**). Substituents with a strong positive mesomeric effect, such as a methoxy group in the *para*-position, were not tolerated in the reaction leading to low yields of an inseparable mixture of compounds.

Conversely the addition of an electron-withdrawing group in the electronically disconnected *meta*-position led to good yields of **190** being isolated. When the aromatic moiety was changed from a phenyl derivative to a 2-thiophene group, this compound had very low reactivity towards the alkenylalane, with the corresponding product **191** being isolated in only 16% yield. Because of the high propensity of alkylidene malonates to show background reactions, attention was switched to less activated substrates.

3.3.2 Copper-catalysed conjugate addition of alkenylalanes

3.3.2.1 Initial findings

To begin our investigation into whether alkenylaluminium dichlorides were competent nucleophiles in the copper-catalysed conjugate addition to non-activated enones, the reaction of **179** with 2-cyclohexenone **1** at -30 °C in diethyl ether was used as the model system (**Table 13**). The temperature was chosen based on previous additions of alkenylalanes to cyclohexenone.⁹⁵

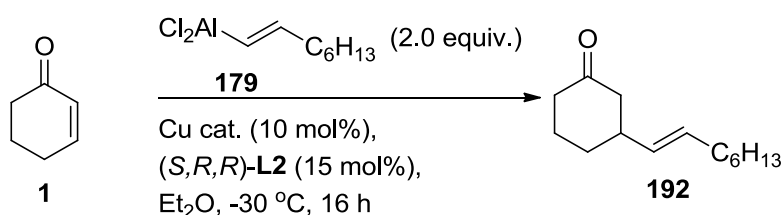


Table 13 Initial screening of conditions for addition to cyclohexenone.^a

Entry	Cu cat.	Conversion % ^b	Yield % ^b
1	none	0	0
2	$\text{Cu}(\text{OAc})_2$	44	<1
3	$\text{Cu}(\text{OAc})_2 \cdot \text{H}_2\text{O}$	54	1
4	CuTC	58	<1
5	$\text{Cu}(\text{OTf})_2$	60	<1
6	$\text{Cu}(\text{MeCN})_4\text{BF}_4$	47	<1
7	$\text{CuBr} \cdot \text{SMe}_2$	78	1
8	$\text{Cu}(\text{II})\text{Np}$	81	<1

a) reaction carried out on a 0.5 mmol scale; b) determined by GC using dodecane as internal standard.

The results showed that in the absence of a catalyst, no background reaction occurred (entry 1). However, when a copper pre-catalyst was added in the presence of (*S,R,R*)-**L2**

the conversion of starting material increased dramatically (up to 81%), but the yield of **192** was extremely low in all cases resulting only in polymerisation products (entries 2-8). The lack of reactivity in run 1 may be due to the electron-withdrawing ability of the chlorides, resulting in a strengthening of the aluminium-carbon bond. Similarly the high conversion of **1** was attributed to its Lewis acid catalysed polymerisation. To overcome the lack of reactivity of **179**, the nucleophilicity of the alkenylalane needed to be increased and its Lewis acidity modified. To increase the reactivity one of the chlorine atoms on the aluminium centre was exchanged with a methyl group. A methyl group was chosen because it is effectively a non-transferrable group on aluminium ($D(\text{Al-Me})$ is 68 kcal mol^{-1}) and the organometallic reagents for carrying out the exchange are readily available. To see if this new reagent was a competent nucleophile, the reaction shown in **Table 13** was explored using copper(I)thiophenecarboxylate (10 mol%) as the copper source (**Table 14**).

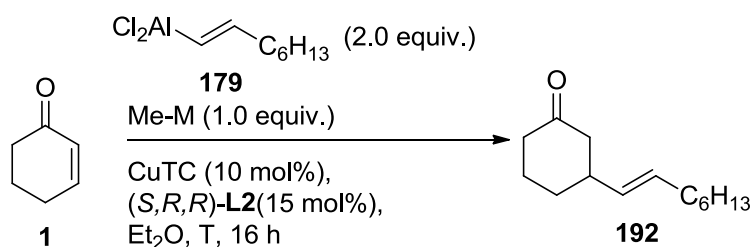


Table 14 Mixed alane addition to cyclohexenone.^a

Entry	Temperature (°C)	MeMet.	Conv. (%) ^b	Yield (%) ^b	ee (%) ^b
1	-30	MeLi (1.0 equiv.)	96	2	n.d
2	-30	MeLi (2.0 equiv.)	97	12	n.d
3	25	MeLi (1.0 equiv.)	81	13	82
4	25	MeMgBr (1.0 equiv.)	-	-	-
5	25	Me ₃ Al (1.0 equiv.)	91	27	12
6	25	MeLi (1.0 equiv.) ^c	90	33 ^d	82

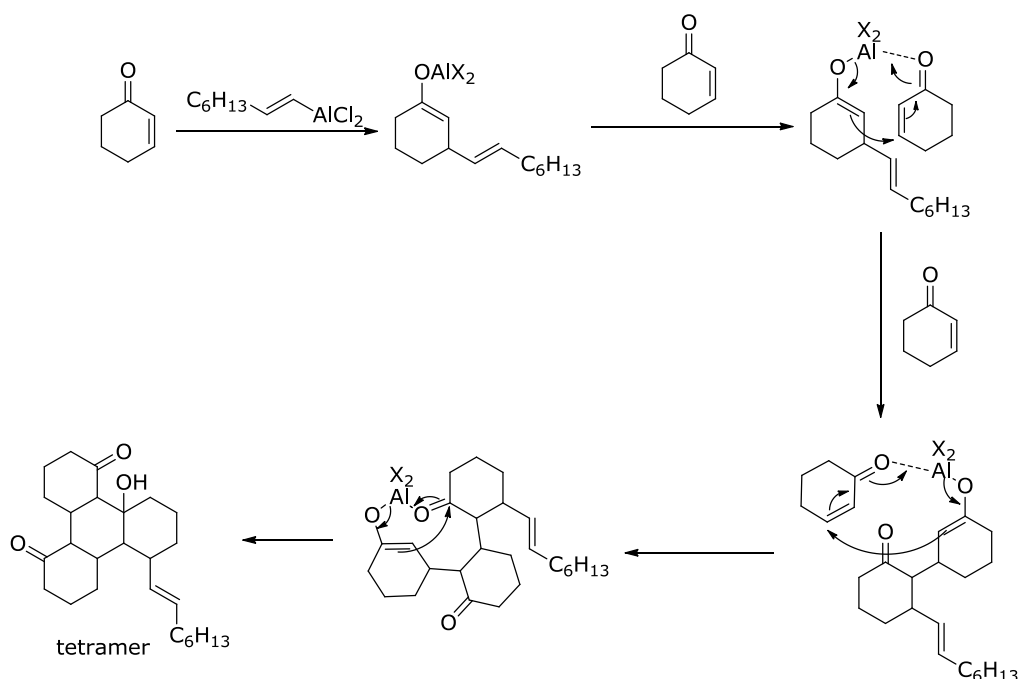
a) reaction carried out on a 0.5 mmol scale; b) determined by chiral GC; c) reaction carried out for 1 h only; d) isolated yield.

The results showed again that the reagent derived from the addition of one equivalent of methyllithium to the alane mixture was unreactive in the conjugate addition at low temperature (**Table 13** entry 1) meaning that the transmetallation from aluminium to copper is extremely slow at this temperature.

Two equivalents of methyllithium were used to generate a similar reagent to that of Alexakis which was demonstrated to be an extremely competent nucleophile for the addition of an alkenyl group.¹⁰¹ Unfortunately, under the same conditions that were reported, the reagent in our hands gave high conversion but only 12% yield (entry 2). When the temperature was increased from -30 °C to +25 °C and one equivalent of methyllithium was used to generate the mixed

alane, the yield of **192** increased from 2% to 13% with an enantioselectivity of 82% (entry 3). If the organometallic reagent was changed from methyllithium to methylmagnesium bromide, no reaction occurred at all (entry 4), whereas changing to trimethylaluminium, the cheapest organometallic available, the conversion remained high and the yield increased to 27% but the enantioselectivity decreased dramatically to only 12% (entry 5). This decrease in enantioselectivity could be due to the cleavage of the BINOL backbone on (*S,R,R*)-**L2** and generating an aminophosphine ligand. From these results it was concluded that methyllithium at +25 °C was the best temperature and organometallic and these conditions were taken forward. When the reaction conversion was monitored for the reaction it was found that after only one hour, 90% of the starting material had been consumed but only 33% of the desired product was isolated with the same enantioselectivity (82%) as for the corresponding reaction left for 16 hours. During the purification process of this reaction, a white solid was also isolated and it was revealed to be the cyclic tetramer of the unaccounted-for starting material (**Scheme 59**). These cyclic tetramers have been identified before in a methylaluminumoxane promoted Schlenk equilibrium to generate diorganozinc

reagents which were subsequently used in conjugate addition.¹⁰⁵



Scheme 59 Formation of the undesired cyclic tetramer.

As can be seen from **Scheme 61** the initial step is a copper-catalysed conjugate addition of the alkenylalane followed by a Lewis acid mediated Michael addition of the corresponding aluminium enolate onto another equivalent of cyclohexenone, where the enolate formed reacts further with an equivalent of cyclohexenone in Michael fashion. The final ring closure occurs *via* an aldol reaction of the enolate onto the ketone to generate a quite complex scaffold in a small number of steps.

3.3.2.2 Equivalents of alkenylalane

Reports by Alexakis and co-workers noted that the number of equivalents of alkenylalane had an effect on the enantioselectivity. Due to this, use of a different number of equivalents of alkenylalane was considered (**Table 15**). Unlike the dramatic effects noted by Alexakis, the enantioselectivity of our model system did not show too much change between 2.0 equivalents and 1.3 equivalents. This could be attributed to our hydroalumination protocol being clean with negligible amounts of acetylide produced, as well as the excess alkyne being removed prior to the addition of methyllithium, thus eliminating the formation of lithium acetylides and subsequent transmetallation onto the copper. However, it was observed that the yield of **192** actually increased with lower equivalents of alkenylalane (entry 1-3).

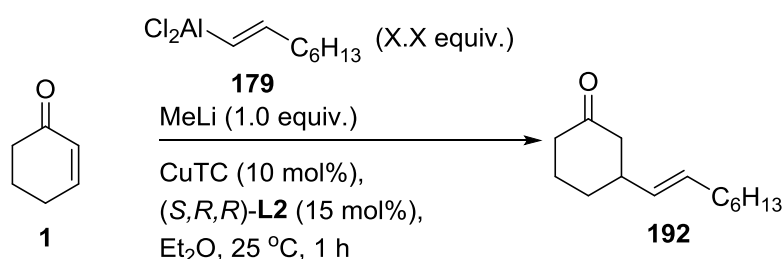


Table 15 Effect of alkenylalane equivalents.^a

Entry	Alane equiv.	Conv. (%) ^b	Yield (%) ^b	ee. (%) ^b
1	2.0	90	33	82
2	1.5	93	37	82
3	1.3	93	39	76

a) reaction carried out on a 0.5 mmol scale; b) determined by chiral GC.

3.3.2.3 Effect of solvent on ACA of alkenylalanes

Encouraged by the results so far, we decided to screen several solvents, both coordinating and non-coordinating, for the copper-catalysed conjugate addition of **179** to substrate **1** (**Table 16**). These results showed that, weakly coordinating or non-coordinating solvents had little effect of the enantioselectivity of the reaction (entries 3 and 4). However, toluene led to a higher yield of **192** compared to diethyl ether, possibly due to the formation of a more reactive species with little coordination from the solvent. When tetrahydrofuran was used as the solvent, the desired product was obtained in only 12% yield and the product was racemic (entry 1). This could be attributed to the strength of the complex formed between tetrahydrofuran and the aluminium centre, leading to an inefficient catalyst of different structure. Although ethyl acetate did produce **192** in 20% yield, no enantioselectivity was observed (entry 2). The precise reason for the lack on enantioselectivity is unclear but it is likely due to similar issues as were seen with tetrahydrofuran.

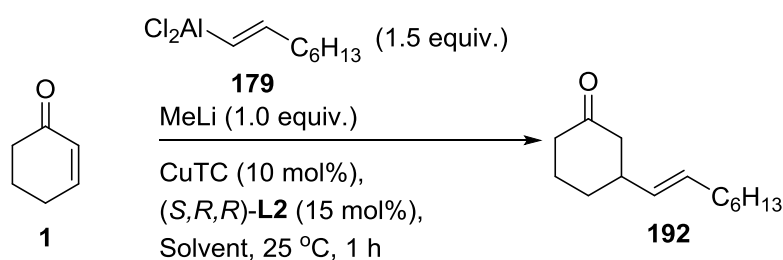


Table 16 solvent screen.^a

Entry	Solvent	Conv. (%) ^b	Yield (%) ^b	ee. (%) ^b
1	THF	92	12	0
2	EtOAc	98	20	0
3	Et ₂ O	93	37	82
4	PhMe	72	43	89
5	PhMe/Et ₂ O (1:1) ^c	82	21	82
6	PhMe/MTBE (1:1) ^c	67	54	84

a) reaction carried out on a 0.5 mmol scale; b) determined by chiral GC; c) alane mixture dissolved in PhMe and copper mixture in diethylether or *t*-butylmethyl ether.

When mixed solvent systems were tried, the alane hydroalumination was dissolved in toluene due to the results obtained (entry 4), whereas the copper mixture was dissolved in the ethereal solvent. It was found that both diethyl ether and *t*-butyl methyl ether led to high enantioselectivities (entries 5 and 6); however, the toluene/*t*-butyl methyl ether system gave far superior yields with lower conversion to the cyclic tetramer. When other non-coordinating solvents were tried in place of toluene such as *n*-hexane or *n*-heptane, the alkenylalane generated was completely insoluble making the mixture non-transferrable to the copper mixture.

3.3.2.4 Effect of addition mode on the ACA of alkenylalanes

In order to increase the yield of the 1,4-product and minimise the formation of the undesired tetracycle, we looked at changing the mode of addition for the reagents (**Table 17**). In the previous reactions we first added the alkenylalane mixture in toluene to the ethereal mixture of copper-salt followed by the Michael acceptor ("normal" addition).

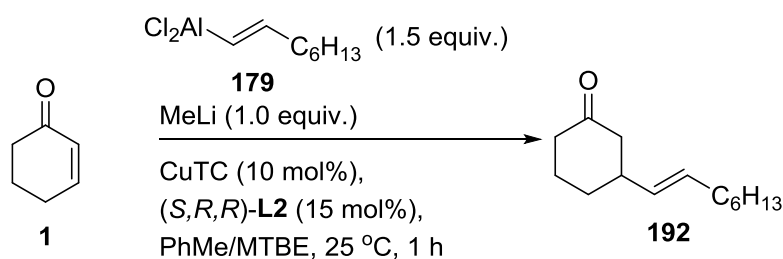


Table 17 Effect of addition mode.^a

Entry	Addition mode	Conv. (%) ^b	Yield (%) ^b	ee. (%) ^b
1	Normal ^c	67	54	84
2	Reverse ^d	88	71	60
3	Slow addition of enone ^e	68	66	76
4	Slow addition of enone and alane ^e	57	20	90

a) reaction carried out on 0.5 mmol scale; b) determined by chiral GC; c) alane then enone; d) enone then alane; e) added over 30 min.

Interestingly, the addition of alkenylalane **179** to the catalyst and substrate ("reverse" addition) had an important effect on the yield of the corresponding product. Whereas the "normal" addition mode afforded **192** in 54% yield and 84% enantioselectivity (entry 1), the "reverse" addition increased the yield to 71% but a significant decrease in

enantioselectivity to 60% was observed (entry 2). When **1** was added slowly over 30 minutes (syringe pump) to a mixture of the alkenylalane and copper catalyst, the conversion was similar to that observed in the "normal" addition; however, a higher yield of 66% was obtained but a lower enantioselectivity 76% was observed (entry 3). Compared to the "reverse" addition, the slow addition gives the product in lower yield but higher enantioselectivity, thus indicating that there are possibly different active copper species formed, one with higher catalyst activity but lower selectivity and another with lower activity but higher selectivity. The slow addition of both the enone and alkenylalane over 30 minutes led to a high level of enantioselectivity, 90%, but unfortunately a 20% yield was obtained with 37% 'missing mass' (entry 4). The result for the slow addition of both enone and alane makes the argument for different catalyst species stronger.

3.3.2.5 Copper salt optimisation

From previous studies on the conjugate addition of organoaluminium reagents, copper thiophene carboxylate gave the best enantioselectivities and yields of the corresponding 1,4-adducts, however other copper salts have successfully been used for the conjugate addition of alkenyl

nucleophiles. Therefore several copper salts were tested for their ability to promote the conjugate addition of our alkenylalane **179** (Table 18).

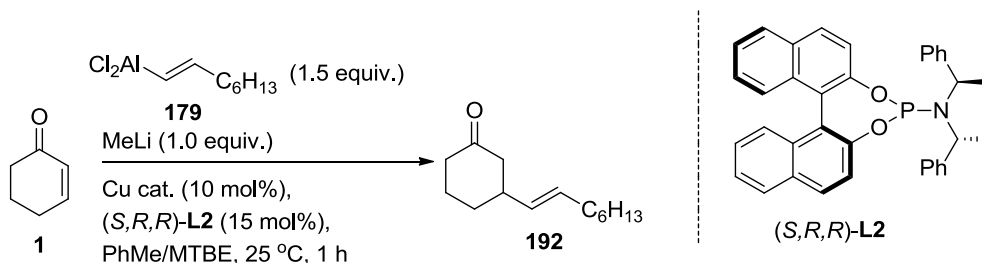


Table 18 screen of copper salts.^a

entry	Cu cat.	Conv. (%) ^b	Yield (%) ^b	ee. (%) ^b
1	Cu(OTf) ₂	89	6	64
2	(CuOTf) ₂ .PhMe	85	47	78
3	Cu(MeCN) ₄ BF ₄	86	34	80
4	CuCl + AgNTf ₂ ^c	93	7	90
5	CuTC	68	66	76

a) reaction carried out on 0.5 mmol; b) determined by chiral GC; c) 15 mol% AgNTf₂ used.

In all cases, with the exception of copper thiophenecarboxylate, the conversion of the starting material was high >80%. Interestingly all copper salts gave moderate to good enantioselectivity. When copper (II) triflate was used, a poor yield was obtained with moderate enantioselectivity (entry 1). This low activity could be due to the alkenylalane being unable to reduce the copper(II) down to copper(I) to enter into the catalytic cycle. When copper(I) triflate was used, the conversion was similar to copper(II) triflate but the yield increased significantly from 6% to 47% as did the enantioselectivity (entry 2). When copper(I)

tetrakis(acetonitrile) tetrafluoroborate, was used, high conversion and enantioselectivity was achieved but the yield was relatively low (entry 3). Copper halides are not commonly used for the conjugate addition of organoaluminium reagents, but a recent publication showed that it is possible to use a combination of copper(I) chloride and silver triflimide to catalyse the conjugate addition of alkylzirconium reagents to trisubstituted enones.¹⁰⁶ However, when this combination was tried a poor yield was obtained in excellent enantioselectivity (entry 4). After screening a few copper salts it was decided copper thiophene carboxylate gave the best results giving the desired product in 66% yield and 76% enantioselectivity.

3.3.2.6. Ligand Screen

With optimised reaction conditions in hand, a range of monodentate and bidentate phosphorus based ligands as well as some *N*-heterocyclic carbenes were screen to see if further improvements were possible (**Figure 28** and **Table 19**).

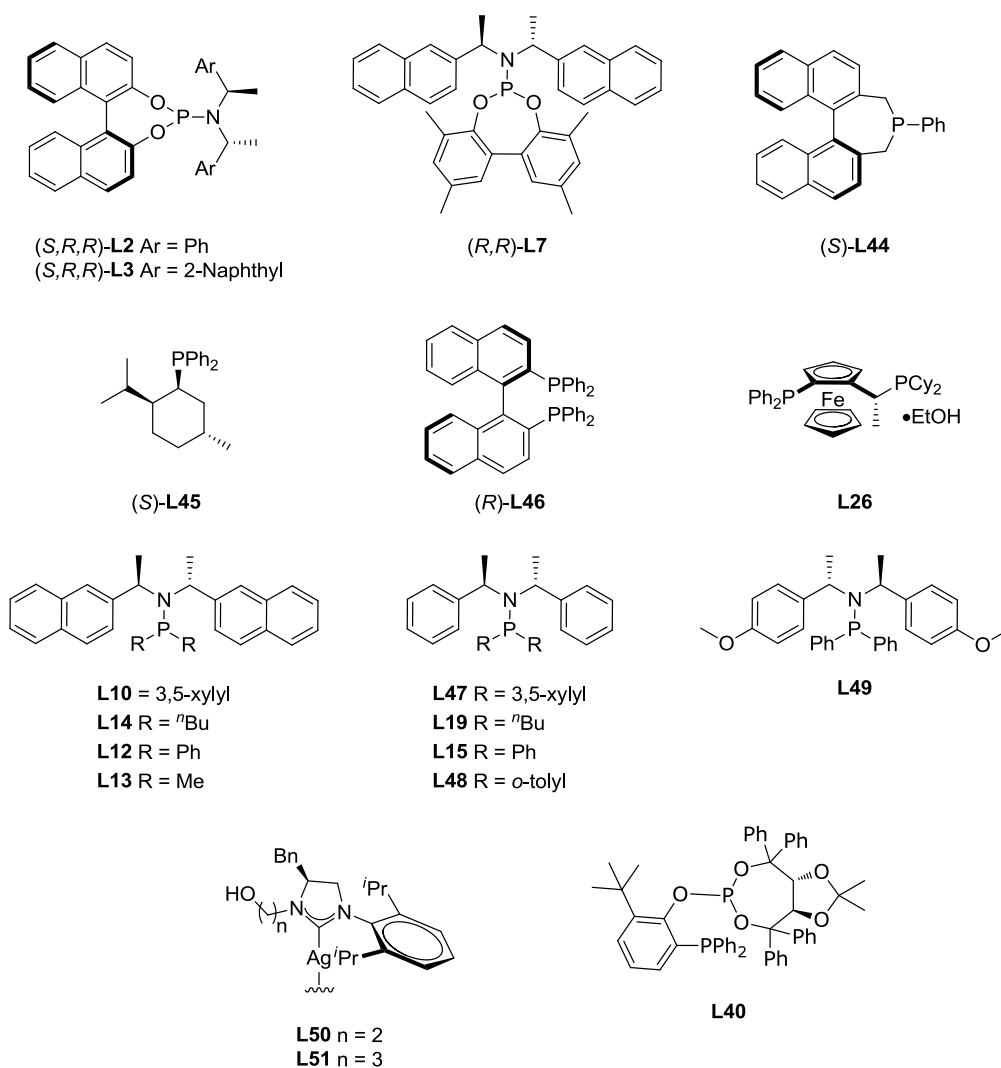


Figure 28 Ligands used in this study.

Several noteworthy findings from the ligand screening were prominent. When bidentate phosphine ligands **L46** and **L26**, which are powerful ligands for the ACA of trimethylaluminium, were used, no reaction was observed (entries 6 and 7). SimplePhos ligands (entries 8 to 16), which have afforded excellent results for the conjugate addition of alkenylalanes to enones, resulted in excellent yields but moderate enantioselectivities. If the R group in the SimplePhos ligands was changed from aryl to alkyl (entries 9,

11 and 13), a significant drop in both yield and enantioselectivity was observed. The reason for this is unclear but it could be due to the change in conformational bias where an aryl group is 'held' in an *atropos* manner due to the lack of flexibility compared to alkyl substituents. Catalyst screening using SimplePhos ligands also indicated that changing the electronics and sterics of the R group had an effect on both the enantioselectivity and yield (entries 12, 14 and 15). Changing the amine moiety of the ligand also had little effect on the enantioselectivity (**L12** vs. **L15** vs. **L49**). Monodentate phosphines (entries 4 and 5), produced **192** in moderate yields, but unfortunately as a racemate (entry 4). The result from ligand (*S*)-**L44** indicates that the *atropos* nature of biaryl systems is not a major contributor to the enantioselectivity delivered to the final product. Phosphoramidite ligands (*S,R,R*)-**L2**, (*S,R,R*)-**L3** and produced the desired products in high optical purity, when a BINOL core was present, and in good yields (entries 1 to 3). When a biphenol core was present (*R,R*)-**L7** (entry 3) the enantioselectivity decreased dramatically. However, unlike the SimplePhos ligands, the amine moiety plays a major role for producing the product in high enantioselectivities. Phosphoramidite ligands which contained the 2-naphthyl- derived amine afforded better optical purity than the corresponding phenyl-derived amine

((*S,R,R*)-**L2** vs. (*S,R,R*)-**L3**). Like phosphoramidite ligands, phosphite ligands could deliver the product in moderate yields but with a lower enantioselectivity (entry 19). *N*-Heterocyclic carbenes bearing pendant coordinating groups (**L50** and **L51**) were ineffective ligands for the addition of alkenyl groups from the monomethyl derivative of **179**.

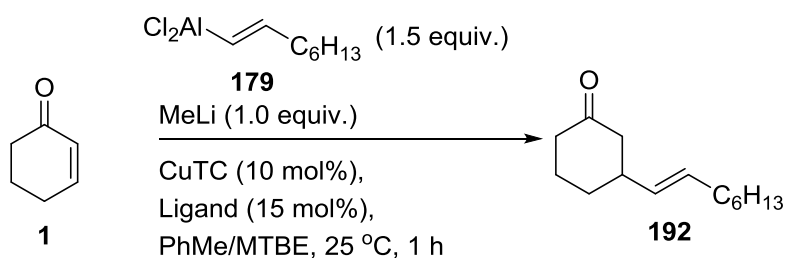


Table 19 ligand screen.^a

Entry	Ligand	Conv. (%) ^b	Yield (%) ^b	ee. (%) ^b
1	(<i>S,R,R</i>)- L2	68	66	76
2	(<i>S,R,R</i>)- L3	95	65	88
3	L4	91	65	38
4	L44	92	56	0
5	L45	87	26	0
6	L46	-	-	-
7	L26	-	-	-
8	L10	84	81	20
9	L14	90	49	6
10	L12	84	63	50
11	L13	>99	19	0
12	L47	90	54	44
13	L19	90	36	10
14	L15	87	81	56
15	L48	93	23	38
16	L49	>99	27	56
17	L50	91	17	10
18	L51	70	16	8
19	L40	90	59	50

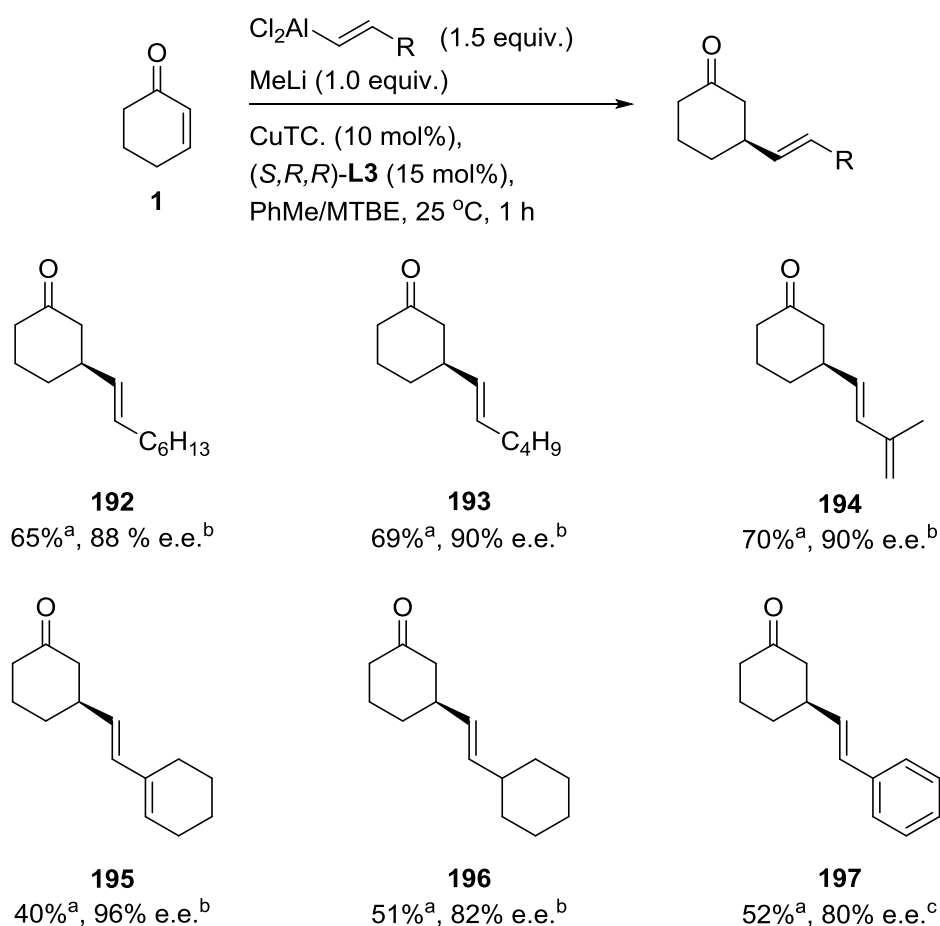
a) reaction carried out on a 0.5 mmol scale; b) determined by chiral GC.

3.3.2.7. Summary of optimisation

The optimisation experiments showed that the nature of the alkenylalane and temperature is, at least, as important as the chiral copper catalyst to afford high yields of the desired product. The combination of all the optimisation reactions had led to a set of conditions which showed that the conjugate addition of alkenylalanes to cyclohexenone can be achieved in high enantiomeric excess.

3.3.2.8. Alkenylalane scope in ACA to cyclohexenone

With the optimised conditions in hand, the scope of alkenylalanes was explored against cyclohexenone (**Scheme 60**). Volatile alkynes behaved capriciously under the original hydroalumination conditions when carried out at smaller scales (<5 mmol). Over vigorous initial heating can cause significant alkyne to escape leading to variable yields in normal Schlenkware. However, this issue could be overcome using a GC septa equipped 1.0 mL vials which has minimum headspace. This change worked well for both volatile and non-volatile alkynes up to a one mmol scale.



a) isolated yield; b) determined by chiral GC; c) determined by chiral HPLC. Absolute stereochemistry confirmed by analogy.

Scheme 60 Alkenylalane scope for the addition to cyclohexenone..

The results showed that a range of alkenyl substituents could be introduced. Alkenylalanes generated from linear, non-branched alkynes could add to cyclohexenone in good yields (**192** and **193**) with high levels of enantioselectivity up to 90%. When conjugated alkenylalanes were used, the cyclic derivative (**195**) was obtained in moderate yield (40%) but excellent enantioselectivity (96%), whereas the acyclic variant (**194**) was obtained in good yield (70%) but at a lower

enantioselectivity (90%). When the cyclohexyl derivative was used, **196** was obtained in higher yields than the corresponding cyclohexenyl derivative (51% vs. 40%), but a significant drop in optical purity was observed. Styrylalanine could also be added to cyclohexenone in moderate yield (52%) and good levels of optical purity (80%). These are the first reported enantioselective copper-catalysed conjugate additions of alkenylalanines to cyclohexenone.

Unfortunately when the Michael acceptor was changed to cyclopentenone, high levels of conversion of the starting material was observed (>95%), but, no 1,4-adduct was observed. This could be explained by polymerisation of the starting material *via* successive conjugate additions of the highly reactive enolate to the Michael acceptor. Trapping with trimethylsilyl chloride had no effect on the reaction with high conversion still noticed.

3.3.3. ACA to trisubstituted enones

With the successful addition of alkenylalanines to cyclohexenone, it was decided to see whether these alkenylalanines were competent nucleophiles for the addition to trisubstituted enones to generate all carbon quaternary centres. A very small amount of optimisation was required and that was in the addition mode in which the reagents were

added (**Table 20**). The addition mode was screened because the problem with the cyclic tetramer would not be possible due to the enolate being unable to carry out the subsequent Michael addition.

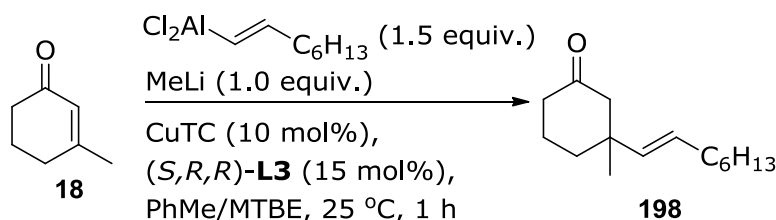
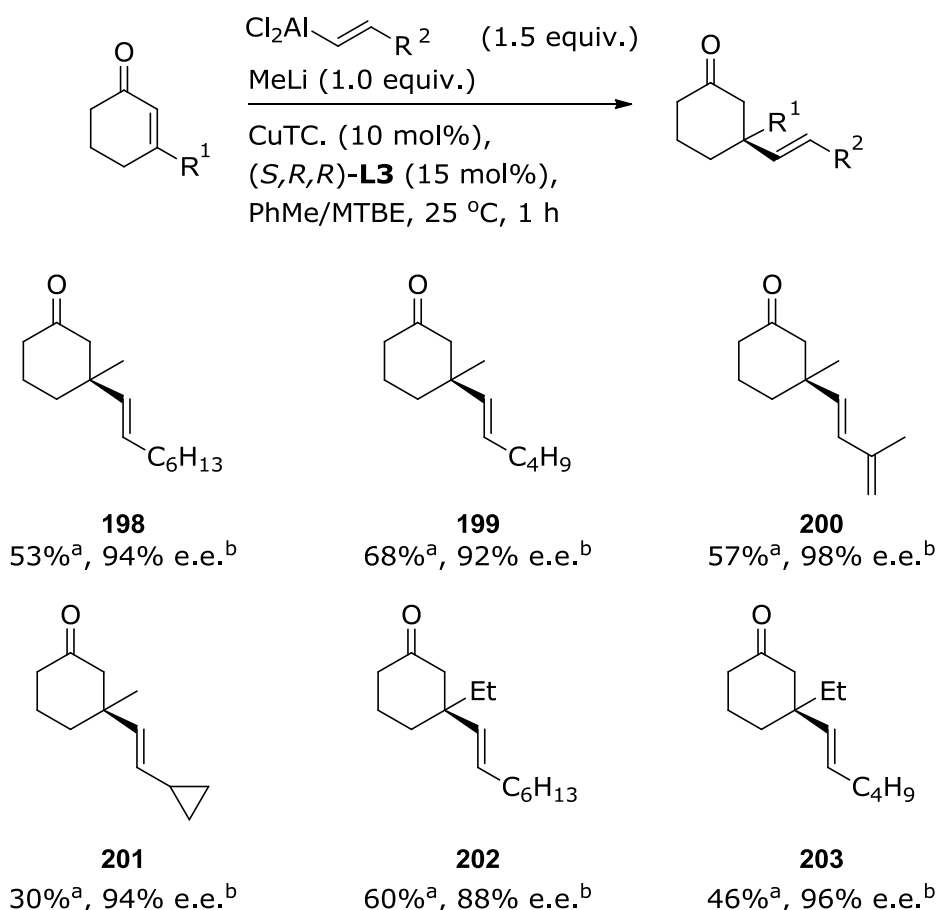


Table 20 Mode of addition to trisubstituted enones.^a

Entry	Addition mode	Yield (%) ^b	ee. (%) ^c
1	Slow addition of enone	48	90
2	Normal	48	89
3	Reverse	53	94

a) Reaction carried out on a 0.5 mmol scale; b) isolated yield; c) determined by chiral GC.

The mode of addition did not make too much difference in terms of chemical yield with the reverse addition giving slightly more of the desired product. However, there was a more pronounced difference in optical purity; with the reverse addition again provide higher levels of enantioselectivity. With the addition mode now optimised for the enantioselective addition of **179** to substrate **18**, the scope of the reaction in terms of nucleophile and electrophile was screened (**Scheme 61**). Cyclopentenones with β -methyl substituents were tried and like the case with unsubstituted cyclopentenones, a high level of conversion was observed, but none of the desired 1,4-adduct was observed.



a) Isolated yield; b) determined by chiral GC. Absolute stereochemistry confirmed by analogy.

Scheme 61 ACA to trisubstituted enones.

What is evident from these results is that the alkenylalanes are competent nucleophiles for the transformation with the enantioselectivities being higher (up to 98%) than for the addition to cyclohexenones (*c.f.* 90%). This increase in enantioselectivity could be due to the steric factor of the β -substituents being larger (methyl > hydrogen) and creating better facial selectivity. Again alkenylalanes derived from linear alkynes could be added to both methyl and ethyl substituted enones generating the 1,4-adducts (**198**,

199, **202** and **203**) with high levels of enantioselectivity (up to 96%) in moderate yields. In the case of (*E*)-hexenylalane, the yield of **203** (46%) was lower than that of **199** (68%) indicating that the steric profile of the substituent plays a major role on the chemical yield. Challenging alkenylalanes, those derived from conjugated alkynes and cyclopropylacetylene, were also added to methyl substituted enones to generate **200** and **201** in moderate to good yields with excellent enantioselectivity.

Preliminary studies indicate that the scope of the reaction could be extended to (in the racemic sense) products **204-206**, derived from linear enones (**Figure 29**) and to hydroalumination of problematic ethynyltrimethylsilane (leading to **207**). However, the present conditions do not provide synthetically useful enantioselectivities (39%) or yields (11%).

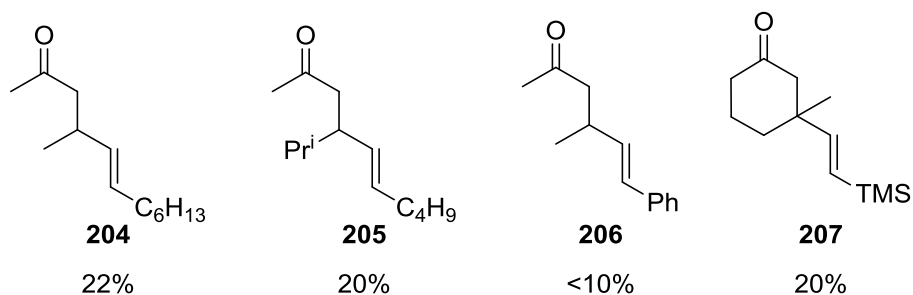


Figure 29 Conjugate addition to linear enones.

3.4. Conclusion

A protocol has been developed which allows the addition of alkenylalanes, derived from air-stabilised aluminium hydrides, to cyclohexenones and β -substituted cyclohexenones in excellent enantioselectivities (up to 98%) using commercially available phosphoramidite ligands, with moderate to good yields. This protocol unfortunately requires more optimisation to be compatible with cyclopentenones and linear aliphatic enones.¹⁰⁷

Chapter 4

Experimental Section

General remarks

Infrared spectra were recorded using Bruker Tensor 27 FT-IR spectrometer with absorptions given in wavenumbers (cm^{-1}). Proton, ^{13}C , ^{19}F and ^{31}P NMR spectra were recorded on Bruker (DPX400, AV400 or AV(III)400) spectrometers and ^2H NMR spectra were recorded on Bruker AV400 spectrometer. Proton and ^{13}C NMR chemical shifts are given in ppm relative to tetramethylsilane (0.00 ppm). Proton-NMR spectra were referenced to CDCl_3 (7.26 ppm) or C_6D_6 (7.16) and carbon-13-NMR spectra were referenced to CDCl_3 (77.16 ppm) or C_6D_6 (128.06). ^{108}P Phosphorus-31 NMR chemical shifts were reported in ppm relative to phosphoric acid. Data are reported as follows: chemical shift, integration, multiplicity: s (singlet), d (doublet), t (triplet), q (quartet), or combinations, brs (broad singlet), m = multiplet, and coupling constants (Hz). Mass spectra were obtained on Bruker microTOF spectrometer. Optical rotations were measured at the sodium D-line with a 1 dm path length cell using an ADP400 polarimeter, and are reported as follows: $[\alpha]_{\text{D}}^{\text{T}}$ in degrees, concentration ($\text{g}/100 \text{ cm}^3$), and solvent. Melting points were determined using a Gallenkamp melting point apparatus and are uncorrected. Gas chromatography was performed on either a Varian 430 or Varian 3900 apparatus using either a

Lipodex A or *octakis*(2,6-di-*O*-methyl-3-*O*-pentyl- γ -cyclodextrin stationary phase. Chiral HPLC analysis was performed on a Varian Prostar Chromatograph using Daicel Chiracel OD-H stationary phase.

All procedures involving air or moisture sensitive reagents were performed under atmospheres of argon or nitrogen using standard Schlenk techniques. Reaction solvents were dried and distilled immediately prior to use from appropriate drying agents. Toluene, tetrahydrofuran, diethyl ether and *t*-butyl methyl ether were distilled from sodium-benzophenone ketyl. Dichloromethane and acetonitrile were distilled from calcium hydride.

Analytical thin layer chromatography (TLC) was performed on Merck pre-coated aluminium-backed TLC plates (silica gel 60 F₂₅₄) and visualised by UV lamp (254 nm), potassium permanganate (KMnO₄) stain. Flash chromatography was performed using silica gel 60 (220–240 mesh) from Fluka. Technical grade solvents were employed.

Organolithiums and Grignard reagents were commercial products and titrated using the Gilman double titration method. Solutions of triorganoaluminium and dialkylzinc reagents were purchased from Acros organics or Aldrich. Enones and alkynes were distilled prior to use and stored over 4 Å molecular sieves.

General procedure 1: Kinetic studies using phosphorus ligands

In a flame-dried two-necked flask under argon, phosphorus ligand (0.5-3.0 mol%), copper(II) acetate (18.0 mg, 0.0991 mmol) and nonane (1.0 mL) were added to dried toluene (25.0 mL) and stirred at room temperature for 30 minutes. The solution was cooled to -40 °C and diethylzinc (1.0 M in toluene, 12.0 mL, 12.0 mmol) was added to the mixture and stirred at this temperature for 10 minutes. At time point t_0 , cyclohexenone (1.00 mL, 10.3 mmol) was added. Aliquots were withdrawn under an argon counterflow at regular intervals (using a Pasteur pipette that had been previously cooled to -196 °C in liquid nitrogen) and immediately quenched with hydrochloric acid (2 M). The organic phase of each aliquot was analysed by GC. After 1 hour the residual reaction was quenched with hydrochloric acid (2 M) and extracted with diethyl ether (2 x 3 mL). The organic phase was separated and purified by column chromatography (silica, 4:1 pentane/diethyl ether) to typically provide 3-ethyl cyclohexanone as a colourless oil.

General procedure 2: Kinetic studies Using SIMES

In a flame-dried two-necked flask under argon, **L39** (0.5-3.0 mol%), copper(II) acetate (18.0 mg, 0.0991 mmol) and nonane (1 mL) were added to dried toluene (25 mL) and stirred at room temperature for 30 minutes. The solution was cooled to -40 °C and diethylzinc (1 M in toluene, 12 mL, 12 mmol) was added to the mixture and stirred at this temperature for 10 minutes. At time point t_0 cyclohexenone (1.00 mL, 10.3 mmol) was added. Aliquots were withdrawn under an argon counterflow at regular intervals (using a Pasteur pipette that had been previously cooled to -196 °C in liquid nitrogen) and immediately quenched with hydrochloric acid (2 M). The organic phase of each aliquot was analysed by GC. After 1 hour the reaction was quenched with hydrochloric acid (2 M) and extracted with diethyl ether (2 x 3 mL). The organic phase was separated and purified by column chromatography (silica, 4:1 pentane/diethyl ether) to typically provide 3-ethyl cyclohexanone as a colourless oil.

General procedure 3: Kinetic studies of Triethylaluminium with phosphoramidite ligands

To a flame-dried two-necked flask under argon, phosphorus ligand (0.5-5.0 mol%), copper(II) acetate (18.0 mg, 0.0991 mmol) and nonane (1 mL) were added to diethyl ether (25.0 mL) and stirred at room temperature for 30 minutes. The solution was cooled to -40 °C and triethylaluminium (1.30 M in hexanes, 10.0 mL, 13.0 mmol) was added to the mixture and stirred at this temperature for 10 minutes. At time point t_0 cyclohexenone (1.00 mL, 10.3 mmol) was added. Aliquots were withdrawn under an argon counterflow at regular intervals (using a Pasteur pipette that had been previously cooled in liquid nitrogen) and immediately quenched with hydrochloric acid (2 M). The organic phase of each aliquot was analysed by GC. After 1 hour the reaction was quenched with hydrochloric acid (2 M) and extracted with diethyl ether (2 x 3 mL). The organic phase was separated and purified by column chromatography (silica, 4:1 pentane/diethyl ether) to typically provide 3-ethyl cyclohexanone as a colourless oil.

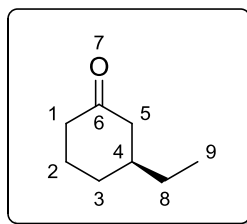
General procedure 4: Kinetic studies of the conjugate addition of ethylmagnesium bromide to methyl crotonate

In a flame-dried and argon filled two necked round bottom flask; copper salt (0.1 mmol, 1 mol%) and ligand (0.25 – 3.0 mol%) and tridecane (1.00 mL internal standard) were stirred at room temperature for 30 minutes in dichloromethane (25.0 mL). The solution was cooled to -78 °C and ethylmagnesium bromide (3.0 M in diethyl ether, 4.00 mL, 12.0 mmol) added. At time point t_0 , methyl crotonate (1.10 mL, 10.0 mmol) was added to the reaction mixture (end volume 31.0 mL, starting concentration of methyl crotonate 0.320 M). Aliquots were withdrawn under an argon counterflow at regular intervals (using a Pasteur pipette that had been previously cooled in liquid nitrogen) and immediately quenched with hydrochloric acid (2 M in methanol). The organic phase of each aliquot was analysed by GC. After 1 hour the overall reaction was quenched with hydrochloric acid (2 M in methanol) and the phases separated. All the ethereal layers were combined and concentrated to afford an orange oil which was purified by column chromatography (silica, 99:1 pentane/diethyl ether) to typically provide methyl 3-methylpentanoate as a colourless oil.

General procedure 5: Kinetic studies of nickel-catalyzed 1,2-addition of trimethylaluminium to benzaldehyde

In a flame-dried, argon filled two-necked round bottom flask; nickel acetoacetate (25.0 mg, 0.10 mmol, 1 mol%), (R,S,S)-**L2** (0.5-4.0 mol%) and tridecane (1.00 mL internal standard) were stirred at room temperature for 30 minutes in tetrahydrofuran (25.0 mL). The solution was cooled to -40 °C and trimethylaluminium (2.0 M in hexanes, 10.0 mL, 20.0 mmol) added. At time point t_0 , distilled benzaldehyde (1.0 mL, 10.0 mmol) was added to the reaction mixture (end volume 37.0 mL, starting concentration of benzaldehyde 0.270 M). Aliquots were withdrawn under an argon counter flow at regular intervals (using a Pasteur pipette that had been previously cooled to -196 °C in liquid nitrogen) and immediately quenched with hydrochloric acid (2 M). The organic phase of each aliquot was analysed by GC. After 1 h the overall reaction was quenched with hydrochloric acid (2 M) and the phases separated. All the ethereal layers were combined and concentrated to afford an orange oil, which was purified by column chromatography (hexanes/ ethyl acetate 5:1) to typically provide 2-phenylethanol as a colourless oil.

(S)-3-Ethyl-cyclohexanone (37)¹⁰⁹



Prepared *via* general procedures **1-3** using ligand (*R,S,S*)-**L2** to give the title compound as a colourless oil in 96% ee.

¹H NMR (400 MHz, CDCl₃) δ_{H} : 0.89 (3H, t, $J = 7.5$ Hz, C⁹H₃), 1.26-1.39 (3H, m, C⁸H₂ and C⁴H), 1.60-1.69 (2H, m, C³H₂), 1.87-1.97 (1H, m, C⁵H), 1.95-2.05 (2H, m, C²H₂), 2.19-2.28 (2H, m, C¹H₂), 2.31-2.42 (1H, m, C₅H').

¹³C NMR (100 MHz, CDCl₃) δ_{C} : 11.1 (C9), 25.3 (C2), 29.3 (C8), 30.9 (C3), 40.8 (C4), 41.5 (C1), 47.8 (C5), 212.2 (C6).

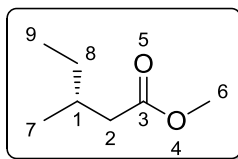
HRMS (ESI) C₈H₁₄O [M]⁺ requires m/z 126.1045, found [M]⁺ 126.1044.

IR (CHCl₃) ν_{max} : 2965, 2875, 1706, 1460, 1448, 1421, 1397, 1313, 1116 cm⁻¹.

[α]_D ($c = 1.00$, CH₂Cl₂): -19.6. (lit. -11.2, $c = 1.0$, CH₂Cl₂)¹⁰⁸

GC: (Lipodex A); $T_{\text{inj}} = 250$ °C, $T_{\text{det}} = 275$ °C, flow = 2.0 mL min⁻¹, $t_{\text{i}} = 75$ °C isothermal: (*R*)-isomer: $t_{\text{R}} = 8.4$ min; (*S*)-isomer: $t_{\text{R}} = 8.6$ min.

(*R*)-3-Methyl-methylpentanoate (54)^{28b}



Prepared *via* general procedure **4** from copper(I) iodide and (*R*)-Tolyl-BINAP to give the title compound as a colourless oil in 90% ee. and purified by column chromatography (99:1 pentane/diethyl ether).

¹H NMR (400 MHz, CDCl₃) δ_{H} : 0.87 (3H, t, J = 7.0 Hz, C⁹H₃), 0.90 (3H, d, J = 7.0 Hz, C⁷H₃), 1.25-1.20 (1H, m, C⁸H₂), 1.37-1.32 (1H, m, C⁸H₂), 1.89-1.84 (1H, m, C¹H), 2.07 (1H, dd, J = 15.0, 8.0 Hz, C²H₂), 2.27 (1H, dd, J = 15.0, 6.0 Hz, C²H₂), 3.65 (3H, s, C⁶H₃).

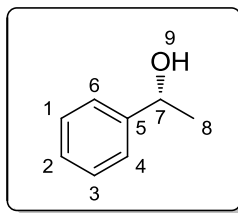
¹³C NMR (100 MHz, CDCl₃) δ_{C} : 11.2 (C⁹), 19.2 (C⁷), 29.3 (C⁸), 31.9 (C⁶), 41.2 (C¹), 51.2 (C²), 173.7 (C³).

HRMS: (EI) C₇H₁₄O₂ [M]⁺ requires m/z 130.0988, found [M]⁺ 130.0994.

IR (CHCl₃) ν_{max} : 3630, 3011, 2927, 2855, 1729, 1465, 1171, 1016 cm⁻¹.

GC: (*Octakis* (2,6-di-*O*-methyl-3-*O*-pentyl)- γ -cyclodextrin); T_{inj} = 250 °C, T_{det} = 275 °C, flow = 2.0 mL min⁻¹, t_{i} = 60 °C (11.0 min), (20.0 °C min⁻¹) t_{f} = 160 °C (20.0 °C min⁻¹): (*R*)-isomer: t_{R} = 5.24 min; (*S*)-isomer: t_{R} = 5.50 min.

(R)-1-Phenylethanol (57)¹¹⁰



Prepared *via* general procedure **5** to yield a colourless oil with 86% *ee*.

¹H NMR (400 MHz, CDCl₃) δ_{H} : 1.53 (3H, d, J = 6.5 Hz, C⁸H₃), 2.01 (1H, brd s, OH), 4.92 (1H, q, J = 6.5 Hz, C⁷H), 7.29-7.42 (5H, m, CH_{Ar}).

¹³C NMR (100 MHz, CDCl₃) δ_{C} : 25.2 (C8), 70.4 (C7), 125.6 (C1 & C3), 127.1 (C2), 127.4 (C4 and C6), 128.5 (C5).

HRMS: (EI) C₈H₁₀O [M]⁺ requires m/z 122.0726, found [M]⁺ 122.0729.

IR (CHCl₃) ν_{max} : 3528, 3065, 3011, 1454, 1378, 1254, 1075, 896, 650 cm⁻¹.

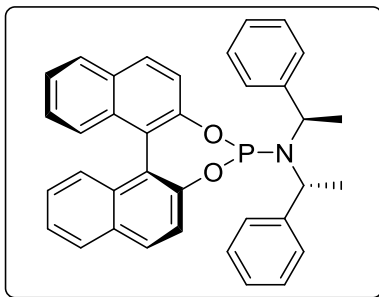
$[\alpha]_{\text{D}}$ (c = 0.50, MeOH): +39.6. (lit. +45, c = 0.5, MeOH)¹⁰⁹

GC: (Lipodex A); T_{inj} = 250 °C, T_{det} = 275 °C, flow = 2.0 mL min⁻¹, t_{i} = 75 °C isothermal: (*S*)-isomer: t_{R} = 21.3 min; (*R*)-isomer: t_{R} = 22.3 min.

General procedure 6: Phosphoramidite synthesis

A flame dried round-bottom flask was charged with anhydrous dichloromethane (8.0 mL) and freshly distilled phosphorus trichloride (348 μ L, 4.10 mmol, 1.0 equiv.). The reaction was cooled to 0 °C and neat triethylamine (2.80 mL, 20.0 mmol, 5.0 equiv.) was added dropwise over 5 min to the vigorously stirred solution (the reaction becomes cloudy). Then C₂-symmetrical chiral amine (1.0 equiv.) was added to the reaction mixture while maintaining the temperature at 0 °C. After addition of the amine was complete the ice bath was removed and the resulting suspension was allowed warm to ambient temperature and stirred for an additional 4 h. After 4 h binol or phenol (1 equiv.) was slowly added to the reaction mixture at 0 °C and then the suspension was stirred at ambient temperature overnight. The reaction mixture was quenched with water (20 mL), the organic layer was removed and the aqueous layer extracted with dichloromethane (2 x 30 mL). The combined organic phases were dried over anhydrous sodium sulfate and concentrated to afford a yellow foam which was purified by column chromatography on neutral alumina (4:1 pentane/diethyl ether).

***O,O'* -(*S*)-(1,1' -Dinaphthyl-2,2' -diyl)-*N,N'*
-di-(*R,R*)-1-phenylethylphosphoramidite (**L2**)¹¹¹**



Prepared according to general procedure 6 from (*R*)-bis((*R*)-1-phenylethyl)amine (914 μ l, 4.00 mmol) and (*S*)-1,1'-bi-2-naphthol (1.15 g, 4.0 mmol) to yield **L2** as a white solid (1.67 g, 3.10 mmol, 78%); **R_F** (4:1 pentane/diethylether) 0.67.

¹H NMR (400 MHz, CDCl₃) δ_{H} : 1.75 (6H, d, J = 7.0 Hz, 2 x CH₃), 4.50–4.58 (2H, m, CH_{amide}), 7.11–7.16 (10H, m, Ar), 7.22–7.27 (2H, m, Ar), 7.31 (1H, d, J = 8.5 Hz, Ar), 7.39–7.47 (4H, m, Ar), 7.62 (1H, d, J = 8.5 Hz, Ar), 7.92 (2H, dd, J = 8.5, 4.5 Hz, Ar), 7.96 (2H, d, J = 8.5 Hz, Ar).

¹³C NMR (100 MHz, CDCl₃) δ_{C} : 22.1 (d, J = 7.0 Hz), 52.4 (d, J = 12.0 Hz), 122.5 (d, J = 1.5 Hz), 122.6, 124.6, 124.9, 126.1 (d, J = 3.0 Hz), 126.7, 127.3 (d, J = 5.5 Hz), 127.9, 128.1 (d, J = 2.0 Hz), 128.4 (d, J = 20.0 Hz), 129.6, 130.4, 130.6, 131.5, 132.9 (d, J = 4.0 Hz), 149.7, 150.2 (d, J = 7.5 Hz).

³¹P NMR (100 MHz, CDCl₃) δ_{P} : 145.4.

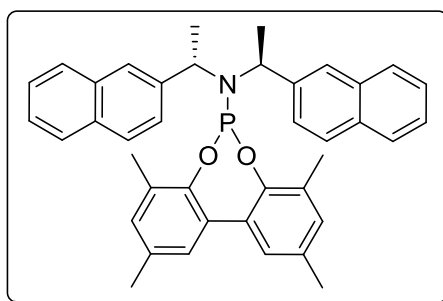
IR (CHCl₃) ν_{max} : 3062, 3011, 2975, 2935, 2877, 1686, 1507, 1070, 949 cm⁻¹.

HMRS: (ESI) $C_{44}H_{34}NO_2P$ $[M+H]^+$ requires m/z 540.2070, found $[M+H]^+$ 540.2077.

m.p. 90-92 °C (lit 88-90 °C)¹¹¹.

$[\alpha]_D^{25}$ ($c = 1.00$, $CHCl_3$) +432.7. (lit. +456, $c = 0.8$, $CHCl_3$)¹¹¹

2,4,8,10-tetramethyl-*N,N*-bis((*R*)-1-(naphthalen-2-yl)ethyl)dibenzo[d,f][1,3,2]dioxaphosphepin-6-amine (L7)¹¹²



Prepared according to general procedure 6 from (*R*)-bis((*R*)-1-(naphthalen-2-yl)ethyl)amine (651 mg, 2.00 mmol), phosphorus trichloride (174 mL, 2.05 mmol) and 3,3',5,5'-tetramethyl-[1,1'-biphenyl]-2,2'-diol (484 mg, 2.0 mmol) to yield **L7** as a white solid (692 mg, 1.16 mmol, 58%); R_F (4:1 pentane/diethyl ether) 0.59.

1H NMR (400 MHz, $CDCl_3$) δ_H : 1.83 (6H, d, $J = 7.0$ Hz, 2x CH_3), 2.08 (3H, s, CH_3), 2.33 (3H, s, CH_3), 2.36 (3H, s, CH_3), 2.52 (3H, s, CH_3), 4.83–4.91 (2H, m, 2 X CH_{amide}), 7.00 (1H, s, CH_{Ar}), 7.04–7.05 (2H, m, Ar), 7.08–7.10 (2H, m, Ar),

7.26–7.32 (1H, m, Ar), 7.32–7.38 (4H, m, Ar), 7.48 (6H, app d, $J = 8.5$ Hz, Ar), 7.64–7.66 (2H, m, Ar).

^{13}C NMR (100 MHz, CDCl_3) δ_{C} : 16.6 (2 x CH_3), 17.6 (2 x CH_3), 21.0 (2 x $\text{CH}_{3\text{amide}}$), 52.7 (2 x CH_{amide}), 125.6, 125.7, 126.3, 126.9, 127.3, 127.4, 127.9, 128.3, 128.4, 129.4, 130.3, 130.4, 131.1, 131.3, 132.4, 132.8, 133.1, 133.5.

^{31}P NMR (100 MHz, CDCl_3) δ_{P} : 141.3.

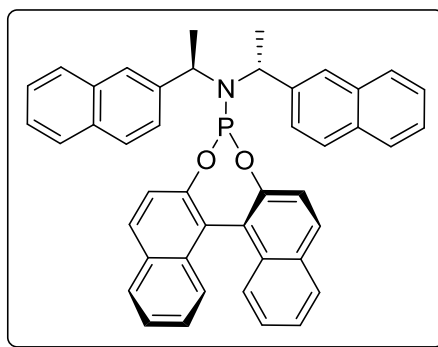
IR (CHCl_3) ν_{max} : 3059, 3010, 2974, 2924, 2863, 1477, 1192 cm^{-1} .

HMRS: (ESI) $\text{C}_{40}\text{H}_{38}\text{NO}_2\text{P}$ $[\text{M}+\text{H}]^+$ requires m/z 596.2758, found $[\text{M}+\text{H}]^+$ 596.2748.

m.p. 108–110 $^{\circ}\text{C}$.

$[\alpha]_{\text{D}}^{25}$ ($c = 1.00$, CHCl_3): +318.7.

***O,O'* -(*S*)-(1,1' -Dinaphthyl-2,2' -diyl)-*N,N'* -di-(*R,R*)-1-naphthylethylphosphoramidite (**L3**)¹¹¹**



Prepared according to general procedure 6 from (*R*)-bis((*R*)-1-(naphthalen-2-yl)ethyl)amine (1.30 g, 4.00 mmol) and (*S*)-1,1'-bi-2-naphthol (1.14 g, 4.0 mmol) to yield **L3** as a white

solid (1.48 g, 2.31 mmol, 58%); **R_F** (4:1 pentane/diethyl ether) 0.61.

¹H NMR (400 MHz, CDCl₃) δ_H: 1.87 (6H, d, *J* = 7.0 Hz, 2xCH₃), 4.65–4.73 (2H, m, CH_{amide}), 7.24–7.34 (5H, m, Ar), 7.37–7.47 (10H, m, Ar), 7.51 (4H, d, *J* = 8.5 Hz, Ar), 7.67–7.73 (3H, m, Ar), 7.92–8.01 (4H, m, Ar).

¹³C NMR (100 MHz, CDCl₃) δ_C: 31.1 (2 x CH₃), 52.5 (2 x CH_{amide}), 121.9, 122.5, 124.17, 124.6, 124.9, 125.7, 126.1, 127.2, 127.3, 127.5, 128.0, 128.3, 129.6, 130.5, 131.5, 132.4, 133.01, 149.6.

³¹P NMR (100 MHz, CDCl₃) δ_P: 145.0.

IR (CHCl₃) ν_{max}: 3062, 3011, 2975, 2935, 2877, 1686, 1507, 1070, 949 cm⁻¹.

HMRS: (ESI) C₄₀H₃₈NO₂P [M+H]⁺ requires *m/z* 640.2430, found [M+H]⁺ 640.2438.

m.p. 210–212 °C.

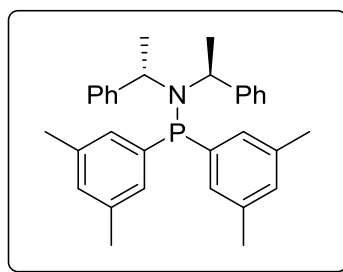
[α]_D²⁵ (*c* = 1.00, CHCl₃): +531.1. (lit. +497, *c* = 0.9, CHCl₃)¹¹¹

General Procedure 7: Synthesis of Aryl SimplePhos ligands

To a solution of C₂-symmetric amine (2.12 mmol, 1.05 equiv.) in tetrahydrofuran (6 mL) was slowly added *n*-butyllithium (1.30 mL, 2.12 mmol, 1.05 equiv.) at -78 °C and stirred for 5

min resulting in a pale pink solution. To the amide solution was added neat phosphorus trichloride (174 μ L, 2.00 mmol, 1.0 equiv.) at -78 $^{\circ}$ C upon which the solution turned yellow. After 5 min the complete consumption of phosphorus trichloride was verified by ^{31}P NMR (single peak at 166.5 ppm in C_6D_6). To this was added aryl Grignard reagents (3.00 equiv.) and the reaction mixture was allowed to warm up to room temperature and then was heated to reflux overnight. An aliquot was taken and ^{31}P NMR confirmed the formation of desired ligand as the major peak. The mixture was diluted with pentane to remove solubilised magnesium salts and filtered through a pad of Celite eluting with diethyl ether (2 x 10 mL), concentrated and purified by column chromatography (Acros organics Brockmann basic alumina, activity 1) to yield the compounds as colourless solids.

**1,1-Dixylyl-*N,N*-bis((*S*)-1-phenylethyl)phosphinamine
(L47)¹¹³**



Prepared according to general procedure 7 from (*S*)-bis((*S*)-1-phenylethyl)amine (484 μ L, 2.12 mmol), *n*-butyllithium (1.30 mL, 2.12 mmol), phosphorus trichloride (174 μ L, 2.00 mmol)

and 3,5-dimethylphenylmagnesium bromide (9.0 mL, 6 mmol, 0.7 M in THF) to yield **L47** as a colourless solid (309 mg, 0.66 mmol, 33%). **R_F** (pentane/diethyl ether 15:1) 0.69.

¹H NMR (400 MHz, CDCl₃) δ_H: 1.48 (6H, d, *J* = 7.0 Hz, 2 x CH₃), 2.15 (6H, s, 2 x Ar-CH₃), 2.37 (6H, s, Ar-CH₃), 4.48-4.56 (2H, m, ArCH(Me)), 6.64 (2H, d, *J* = 7.0 Hz, Ar), 6.85 (1H, s, Ar), 6.94-6.96 (4H, m, Ar), 7.06 (1H, s, Ar), 7.15-7.16 (6H, m, Ar), 7.41 (2H, d, *J* = 7.5 Hz, Ar).

¹³C NMR (100 MHz, CDCl₃) δ_C: 21.2 (ArCH₃), 21.5 (2 x ArCH₃), 56.2 (2 x CH₃), 126.7 (2 x C_{xylyl}-P), 127.8 (4 x Ph_{ortho}), 128.4 (4 x xylyl_{ortho}), 129.3, 129.9, 130.1, 130.7, 131.5, 131.7, 137.0, 137.1, 137.7, 137.8, 139.1, 139.3, 139.7, 139.8, 144.4.

³¹P NMR (162 MHz, CDCl₃) δ_P: 42.4.

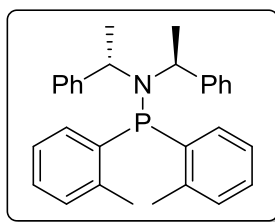
HRMS: (ESI) C₃₂H₃₆NP [M+H]⁺ requires *m/z* 466.2655, found [M+H]⁺ 466.2654.

IR (CHCl₃) ν_{max}: 3059, 3011, 2961, 2929, 2873, 1631, 1507, 1465, 1375, 1127 cm⁻¹.

m.p. 104-106 °C (lit. 105 °C)¹¹³

[α]_D²⁵ (*c* = 1.00, CHCl₃): -198.1.

**1,1-Di-*o*-tolyl-*N,N*-bis((*S*)-1-phenylethyl)
phosphinamine (L48)**



Prepared according to general procedure 7 from (*S*)-bis((*S*)-1-phenylethyl)amine (484 μ L, 2.12 mmol), *n*-butyllithium (1.30 mL, 2.12 mmol), phosphorus trichloride (174 μ L, 2.00 mmol) and *o*-tolylmagnesium bromide (6.0 mL, 6 mmol, 1.0 M in diethyl ether) to yield **L48** as a colourless low melting solid (236 mg, 0.54 mmol, 27%); R_F (pentane) 0.14.

^1H NMR (400 MHz, CDCl_3) δ_{H} : 1.64 (6H, d, $J = 7.0$ Hz 2 x CH_3), 1.72 (3H, s, Ar- CH_3), 2.42 (3H, s, Ar- CH_3), 4.59-4.67 (2H, m, ArCH(Me)), 6.90 (1H, t, $J = 7.0$ Hz, Ar), 6.95 - 7.03 (2H, m, ArCH(Me)), 6.90 (1H, t, $J = 7.0$ Hz, Ar), 6.95 - 7.03 (6H, m, Ar), 7.10-7.15 (7H, m, Ar), 7.19-7.24 (2H, m, Ar), 7.27-7.31 (1H, m, Ar), 7.57 - 7.60 (1H, m, Ar).

^{13}C NMR (100 MHz, CDCl_3) δ_{C} : 20.7 (d, $J = 20.0$ Hz), 21.4 (d, $J = 21.0$ Hz), 22.2 (d, $J = 7.0$ Hz), 56.2 (d, $J = 7.0$ Hz), 125.0, 125.6, 126.7, 127.7, 128.1, 128.5 (d, $J = 2.0$ Hz), 129.9 (d, $J = 4.0$ Hz), 130.5 (d, $J = 4.0$ Hz), 132.6 (d, $J = 2.5$ Hz), 133.1 (d, $J = 3.0$ Hz), 138.3 (d, $J = 13.0$ Hz), 139.3 (d, $J = 18.0$ Hz), 141.1 (d, $J = 3.0$ Hz), 141.4 (d, $J = 2.0$ Hz), 144.4

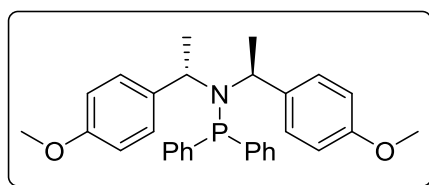
^{31}P NMR (162 MHz, CDCl_3) δ_{P} : 27.6.

HRMS: (ESI) $C_{30}H_{32}NP$ $[M+H]^+$ requires m/z 438.2336, found $[M+H]^+$ 438.2335.

IR ($CHCl_3$) ν_{max} : 3059, 3011, 2961, 2929, 2873, 1631, 1507, 1465, 1375, 1127 cm^{-1} .

$[\alpha]_D^{25}$ ($c = 1.00$, $CHCl_3$): -209.4.

***N,N*-bis((*S*)-1-(4-Methoxyphenyl)ethyl)-1,1-diphenylphosphinamine (**L49**)¹¹³**



Prepared according to general procedure 7 from (*S*)-bis((*S*)-1-(4-methoxyphenyl)ethyl)amine (302 mg, 1.06 mmol), *n*-butyllithium (0.65 mL, 1.06 mmol), phosphorus trichloride (87 μ L, 1.00 mmol) and phenylmagnesium bromide (1.0 mL, 3 mmol, 2.8 M in diethyl ether) to yield **L49** as a colourless solid (159 mg, 0.33 mmol, 34%); R_F (pentane/diethyl ether 15:1) 0.19.

1H NMR (400 MHz, $CDCl_3$) δ_H : 1.52 (6H, d, $J = 7.0$ Hz, 2 x CH_3), 3.81 (6H, s, 2 x OCH_3), 4.52-4.57 (2H, m, $ArCH(Me)$), 6.77 (4H, app d, $J = 8.5$ Hz, Ar), 6.94 (4H, app d, $J = 8.5$ Hz, Ar), 7.18-7.22 (2H, m, Ar), 7.24-7.30 (3H, m, Ar), 7.43-7.49 (3H, m, Ar), 7.81 (2H, td, $J = 7.5, 1.6$ Hz, Ar).

^{13}C NMR (100 MHz, $CDCl_3$) δ_C : 21.9 (d, $J = 8.0$ Hz), 55.5 (d, $J = 8.0$ Hz), 113.2, 127.8 (d, $J = 5.0$ Hz), 127.9, 128.4 (d, $J =$

6.5 Hz), 129.3 (d, $J = 1.5$ Hz), 132.6 (d, $J = 19.0$ Hz), 133.7 (d, $J = 22.5$ Hz), 136.8, 139.9 (d, $J = 6.0$ Hz), 140.1, 158.3

^{31}P NMR (162 MHz, CDCl_3) δ_{P} : 41.2.

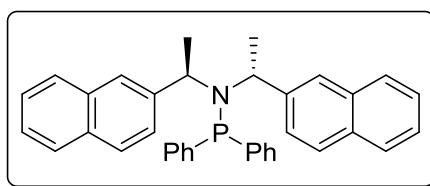
HRMS: (ESI) $\text{C}_{30}\text{H}_{32}\text{NO}_2\text{P}$ $[\text{M}+\text{H}]^+$ requires m/z 470.2238, found $[\text{M}+\text{H}]^+$ 470.2240.

IR (CHCl_3) ν_{max} : 3059, 3011, 2961, 2929, 2873, 1631, 1507, 1465, 1375, 1127 cm^{-1} .

$[\alpha]_{\text{D}}^{25}$ ($c = 1.00$, CHCl_3): -287.4.

m.p. 102-104 $^{\circ}\text{C}$.

***N,N*-bis((*R*)-1-(4-methoxyphenyl)ethyl)-1,1-diphenylphosphinamine (L12)**²⁵



Prepared according to general procedure 7 from (*R*)-bis((*R*)-1-(naphthalen-2-yl)ethyl)amine (346 mg, 1.06 mmol), *n*-butyllithium (0.65 mL, 1.06 mmol), phosphorus trichloride (87 μL , 1.00 mmol) and phenylmagnesium bromide (1.0 mL, 3 mmol, 2.8M in tetrahydrofuran) to yield **L12** as a colourless solid (138 mg, 0.27 mmol, 27%). **R_F** (pentane/diethyl ether 15:1) 0.22.

^1H NMR (400 MHz, CDCl_3) δ_{H} : 1.72 (6H, d, $J = 7.0$ Hz, 2 x CH_3), 4.83-4.91 (2H, m, $\text{ArCH}(\text{Me})$), 7.03 - 7.05 (3H, m, Ar), 7.26 - 7.36 (10H, m, Ar), 7.41 - 7.46 (2H, m, Ar), 7.53 - 7.56 (5H, m, Ar), 7.66 - 7.69 (2H, m, Ar), 7.91 - 7.96 (2H, m, Ar).

¹³C NMR (100 MHz, CDCl₃) δ_C: 21.8 (d, *J* = 8.0 Hz), 56.8 (d, *J* = 8.0 Hz), 125.7 (d, *J* = 15.5 Hz), 126.8 (d, *J* = 1.0 Hz), 126.9 (d, *J* = 2.0 Hz), 127.4 (d, *J* = 6.0 Hz), 128.0 (d, *J* = 5.5 Hz), 128.1, 128.3, 128.4 (d, *J* = 6.0 Hz), 128.8, 132.5, 132.9, 133.2 (d, *J* = 9.5 Hz), 133.5 (d, *J* = 22.0 Hz), 139.7 (d, *J* = 10.0 Hz), 139.9 (d, *J* = 18.0 Hz), 141.8.

³¹P NMR (162 MHz, CDCl₃) δ_P: 42.5.

HRMS: (ESI) C₃₆H₃₂NP [M+H]⁺ requires *m/z* 510.2350, found [M]⁺ 510.2352.

IR (CHCl₃) ν_{max}: 3058, 3010, 2971, 2932, 2873, 1599, 1434, 1375, 1127 cm⁻¹.

m.p. 58-60 °C (lit 60 °C).²⁵

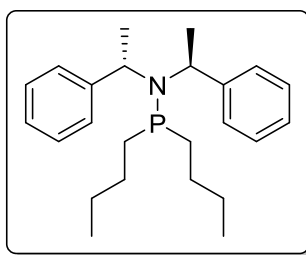
[α]_D²⁵ (*c* = 1.00, CHCl₃): +515.2.

General Procedure 8: synthesis of alkyl SimplePhos ligands¹¹⁴

A flame dried Schlenk tube was charged with bis((*S*)-1-phenylethyl)amine (484 μL, 2.12 mmol, 1.06 equiv.) and tetrahydrofuran (6 mL) was added. The solution was cooled down to -78 °C and *n*-butyllithium (1.3 mL, 2.1 mmol, 1.6 M solution in hexane) was added which resulted in a pale pink solution. After 5 min phosphorus trichloride (174 μL, 2.0 mmol, 1.0 equiv.) was added whereupon the solution turned pale yellow. After 5 min the complete consumption of

phosphorus trichloride was verified by ^{31}P NMR spectroscopy (single peak at 166.5 in C_6D_6). Alkyl Grignard (3.0 equiv.) was added which resulted in a thick slurry. The slurry was then let warm to room temperature and an aliquot was taken showing the formation of the product *via* ^{31}P NMR analysis. The reaction mixture was diluted with pentane (10 mL) to precipitate solubilised magnesium salts and the suspension was passed through celite and thoroughly rinsed with ether (2 x 10 mL). Then the solvents were removed *in vacuo* and the crude compound was purified by column chromatography (Acros Organics Brockmann basic alumina; pentane/diethyl ether).

1,1-dibutyl-*N,N*-bis((*S*)-1-phenylethyl)phosphinamine
(L19)¹¹³



Prepared according to general procedure 8 from bis((*S*)-1-phenylethyl)amine (484 μL , 2.12 mmol, 1.06 equiv.), *n*-butyllithium (1.30 mL, 2.12 mmol, 1.6 M solution in hexane), phosphorus trichloride (174 μL , 2.0 mmol, 1.0 equiv.) and *n*-butylmagnesium chloride (3.4 mL, 6.0 mmol, 3.0 equiv, 1.76 M solution in tetrahydrofuran) to yield **L19** as a colourless oil

which solidified in the freezer (596 mg, 1.61 mmol, 81%). **R_F** (pentane/diethyl ether 15:1) 0.81.

¹H NMR (400 MHz, CDCl₃) δ_H: 0.71 (3H, t, *J* = 7.0 Hz, CH₃), 0.76-0.87 (1H, m), 0.96 (3H, t, *J* = 7.0 Hz), 1.10-1.20 (2H, m), 1.22-1.30 (1H, m), 1.38-1.42 (2H, m), 1.45-1.51 (3H, m), 1.59 (6H, d, *J* = 7.0 Hz CH₃), 1.61-1.63 (1H, m), 1.64-1.70 (1H, m), 1.70-1.76 (1H, m), 4.30-4.38 (2H, m, CMe(H)), 6.95-6.96 (4H, m, Ar), 7.13-7.16 (6H, m, Ar).

¹³C NMR (100 MHz, CDCl₃) δ_C: 14.0 (d, *J* = 15.0 Hz), 21.7 (d, *J* = 7.0 Hz), 24.2 (d, *J* = 13.0 Hz), 24.8 (d, *J* = 13.0 Hz), 27.3 (d, *J* = 17.5 Hz), 28.6 (d, *J* = 19.0 Hz), 29.7 (d, *J* = 15.0 Hz), 29.9 (d, *J* = 13.0 Hz), 53.3, 53.4, 126.4, 127.7, 128.0 (d, *J* = 2.0 Hz), 144.7

³¹P NMR (162 MHz, CDCl₃) δ_P: 30.7.

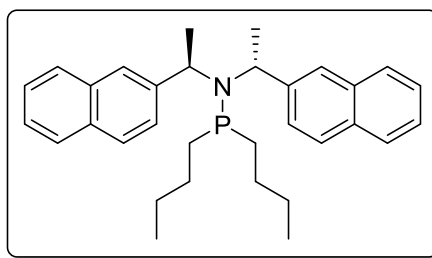
HRMS: (ESI) C₂₄H₃₆NP [M]⁺ requires *m/z* 370.2664, found [M]⁺ 370.2653.

IR (CHCl₃) ν_{max}: 2960, 2930, 2873, 1490, 1464, 1450, 1126 cm⁻¹.

m.p. 50-52 °C (lit. 48 °C).¹¹⁴

[α]_D²⁵ (*c* = 1.00, CHCl₃): -127.7.

1,1-Dibutyl-*N,N*-bis((*S*)-2-naphthylethyl)phosphinamine (L14**)**¹¹⁴



Prepared according to general procedure 8 from bis((*S*)-1-naphthylethyl)amine (306 mg, 0.94 mmol, 1.06 equiv.), *n*-butyllithium (0.6 mL, 0.9 mmol, 1.6 M solution in hexane), phosphorus trichloride (77 μ L, 0.88 mmol, 1.0 equiv.) and *n*-butylmagnesium chloride (1.5 mL, 2.6 mmol, 3.0 equiv., 1.76 M solution in tetrahydrofuran) to yield **L14** as a colourless oil which solidified in the freezer (304 mg, 0.65 mmol, 74%). **R_F** (pentane/diethyl ether 4:1) 0.80.

¹H NMR (400 MHz, CDCl₃) δ_{H} : 0.71 (3H, t, J = 7.0 Hz, CH₃), 0.76-0.87 (1H, m), 0.96 (3H, t, J = 7.0 Hz), 1.10-1.20 (2H, m), 1.22-1.30 (1H, m), 1.38-1.42 (2H, m), 1.45-1.51 (3H, m), 1.59 (6H, d, J = 7.0 Hz CH₃), 1.61-1.63 (1H, m), 1.64-1.70 (1H, m), 1.70-1.76 (1H, m), 4.30-4.38 (2H, m, CMe(**H**)), 7.04 (2H, d, J = 8.0 Hz, Ar), 7.37-7.41 (6H, m, Ar), 7.50 (2H, d, J = 7.5 Hz, Ar), 7.54 (2H, d, 8.0 Hz, Ar), 7.71-7.73 (2H, m, Ar).

¹³C NMR (100 MHz, CDCl₃) δ_{C} : 13.7, 14.1, 21.6 (d, J = 7.5 Hz), 24.2 (d, J = 13.0 Hz), 24.8 (d, J = 13.0 Hz), 27.5 (d, J

= 17.5 Hz), 28.7 (d, J = 19.0 Hz), 29.6 (d, J = 15.0 Hz), 29.9 (d, J = 13.0 Hz), 53.7 (d, J = 6.0 Hz), 125.6 (d, J = 21.0 Hz), 126.4 (d, J = 1.0 Hz), 127.1, 127.3, 127.4 (d, J = 2.0 Hz), 128.0, 132.4, 133.2, 142.1

^{31}P NMR (162 MHz, CDCl_3) δ_{P} : 30.7.

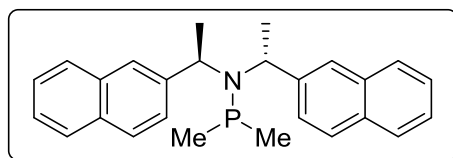
HRMS: (ESI) $\text{C}_{32}\text{H}_{41}\text{NP}$ $[\text{M}]^+$ requires m/z 470.2976, found $[\text{M}]^+$ 470.2980.

IR (CHCl_3) ν_{max} : 3059, 3009, 2960, 2929, 2873, 1375, 1127, 1119 cm^{-1} .

$[\alpha]_{\text{D}}^{25}$ (c = 1.00, CHCl_3): +366.7.

m.p. 36-38 $^{\circ}\text{C}$.

1,1-Dimethyl-*N,N*-bis((*S*)-1-(naphthalen-2-yl)ethyl)phosphinamine (L13)¹¹³



Prepared according to general procedure 8 from bis((*S*)-1-naphthylethyl)amine (306 mg, 0.94 mmol, 1.06 equiv.), *n*-butyllithium (0.6 mL, 0.9 mmol, 1.6 M solution in hexane), phosphorus trichloride (77 μL , 0.88 mmol, 1.0 equiv.) and methylmagnesium bromide (1.0 mL, 3.0 mmol, 3.0 equiv., 3.0 M solution in tetrahydrofuran) to yield **L13** as a colourless oil which solidified in the freezer (329 mg, 0.85 mmol, 85%). **R_{F}** (pentane/diethyl ether 5:1) 0.61.

^1H NMR (400 MHz, CDCl_3) δ_{H} : 1.19 (3H, d, $J = 6.0$ Hz, P- CH_3), 1.31 (3H, d, $J = 6.0$ Hz, P- CH_3), 1.74 (6H, d, $J = 7.0$ Hz $\text{CH}_{3\text{amide}}$), 4.48–4.56 (2H, m, CH_{amide}), 7.12–7.14 (2H, d, $J = 8.5$ Hz, Ar), 7.37–7.43 (5H, m, Ar), 7.51–7.58 (4H, m, Ar), 7.70–7.72 (2H, m, Ar), 7.87–7.92 (1H, m, Ar).

^{13}C NMR (100 MHz, CDCl_3) δ_{C} : 17.0 (d, $J = 14.0$ Hz), 17.5 (d, $J = 17.5$ Hz), 21.3 (d, $J = 9.0$ Hz), 53.3 (d, $J = 7.5$ Hz), 125.4, 125.6, 125.8 (d, $J = 1.5$ Hz), 127.2, 127.3, 127.9, 132.2, 133.0, 141.9.

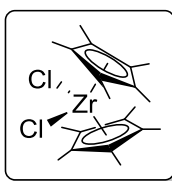
^{31}P NMR (162 MHz, CDCl_3) δ_{P} : 12.9.

HRMS: (ESI) $\text{C}_{26}\text{H}_{28}\text{NP}$ $[\text{M}+\text{H}]^+$ requires m/z 386.2029, found $[\text{M}+\text{H}]^+$ 386.2028.

IR (CHCl_3) ν_{max} : 3059, 3009, 2970, 1355, 1129 cm^{-1} .

$[\alpha]_{\text{D}}^{25}$ ($c = 1.00$, CHCl_3): +420.36.

Bis(pentamethylcyclopentadienyl)zirconium dichloride¹¹⁵



To a solution of pentamethylcyclopentadiene (5.00 mL, 32.0 mmol) in toluene (70 mL) was added *n*-butyllithium (20 mL, 32 mmol, 1.6M in hexane) at 0 °C. The mixture was warmed to ambient temperature and stirred for a further 0.5 h. To this solution was added zirconium tetrachloride (3.40 g, 15.0

mmol) in one portion and the brown heterogeneous solution was refluxed for 72 h. The mixture was cooled and aqueous hydrochloric acid (50 mL, 2 M) added and the mixture stirred overnight in air. The phases were separated and aqueous layer extracted with chloroform (3 x 30 mL). The combined organic layers were concentrated then redissolved in chloroform (50 mL) and filtered through Celite (to remove lithium chloride) and re-concentrated. The crude material was recrystallised (toluene) to yield the title compound as yellow needles (3.23 g, 7.46 mmol, 50%).

¹H NMR (400 MHz, CDCl₃) δ_H: 1.99 (30H, s).

¹³C NMR (100 MHz, CDCl₃) δ_C: 12.0 (CH₃), 123.7 (C_{quat}).

IR (CHCl₃) ν_{max}: 3008, 2910, 1488, 1453, 1427, 1380, 1023 cm⁻¹.

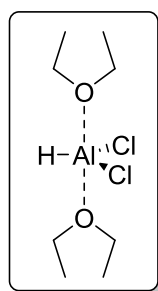
m.p. 310-312 °C (lit. 311 °C).¹¹⁵

General procedure 9: Synthesis of dichloroalane adducts^{51b}

Aluminium trichloride (11.0 g, 82.5 mmol) was dissolved in diethyl ether (40 mL) and added, *via* cannula to a suspension of lithium aluminium hydride (1.04 g, 27.5 mmol) in diethyl ether (40 mL) and the mixture stirred for 20 min at ambient temperature. The mixture filtered *via* cannula and the corresponding Lewis base adduct added dropwise (2.0

equivalents for monodentate ligands or 1.0 equivalent for bidentate ligands) to the filtrate. The solvent was removed under vacuum and product washed with anhydrous pentane (3 x 10 mL). After drying under vacuum (5 h) it was stored in a glove box.

Dichloroalane•bis(diethyl ether) (67)⁴⁹

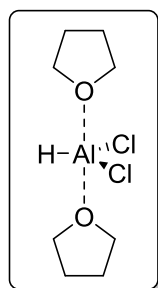


Prepared as above, with the solvent concentration *in vacuo* to yield **67** as a low melting solid (3.08 g, 91%).

¹H NMR (C₆D₆, 400 MHz) δ_{H} : 0.91 (12H, t, J = 7.2 Hz, 4 x CH₃), 3.67 (8H, m, 4 x CH₂), 4.23 (1H, broad, Al-H).

¹³C NMR (C₆D₆, 100 MHz) δ_{C} : 13.5 (CH₃), 69.6 (CH₂).

Dichloroalane•bis(tetrahydrofuran) (68)^{51b}



Prepared from dichloroalane•*bis*(diethyl etherate) (40 mL, 100.1 mmol, 2.5 M solution) and tetrahydrofuran (17.8 mL, 216.3 mmol) to yield **68** as a colourless solid (22.03 g, 90%).

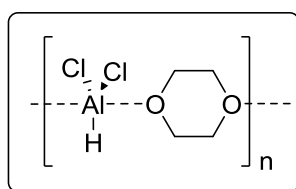
¹H NMR (C₆D₆, 400 MHz) δ_{C} : 1.38 (8 H, 4 x CH₂), 3.97 (8 H, 4 x OCH₂). The Al-H signal could not be detected in spectra.

¹³C NMR (C₆D₆, 100 MHz) δ_{C} : 69.9 (OCH₂), 24.9 (CH₂).

IR (nujol) ν_{max} : 1841, 1600 cm⁻¹.

m.p. 74 - 76 °C.

Dichloroalane•(Dioxane) adduct (70)^{51a}



Prepared from dichloroalane•*bis*(diethyl etherate) (6.0 mL, 8.25 mmol, 1.37 M solution) and dioxane (0.8 mL, 9.07 mmol) to yield **70** as a colourless solid (1.49 g, 96%).

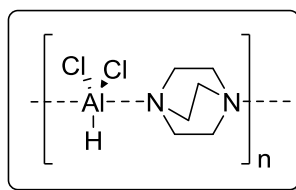
¹H NMR (C₆D₆, 400 MHz) δ_{H} : 3.42 (8H, s, CH₂). The Al-H signal could not be detected in spectra.

¹³C NMR (C₆D₆, 100 MHz) δ_{C} : 67.3 (OCH₂).

IR (nujol) ν_{max} : 1884, 1685 cm⁻¹.

m.p. 170 - 172 °C.

Dichloroalane•(DABCO) adduct (**99**)



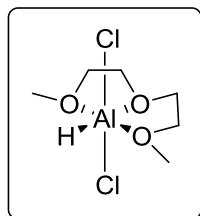
Prepared from dichloroalane•*bis*(diethyl etherate) (6.0 mL, 8.25 mmol, 1.37 M solution) and a toluene solution (8 mL) of DABCO (925 mg, 8.25 mmol) to yield **99** as a colourless solid (1.59 g, 91%).

No NMR data could be assigned due to insolubility of complex.

IR (nujol) ν_{max} : 1930, 1633 cm^{-1} .

m.p. 270 - 272 °C.

Dichloroalane•(Diglyme) adduct (**102**)



Prepared from dichloroalane•*bis*(diethyl etherate) (10.0 mL, 17.90 mmol, 1.79 M solution) and diglyme (2.5 mL, 17.5 mmol) to yield **102** as a colourless solid (3.492 g, 89%).

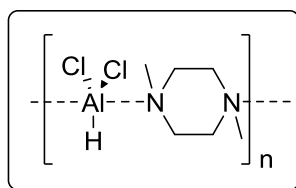
^1H NMR (d_8 -THF, 400 MHz) δ_{H} : 1.46 (6H, s, OCH_3), 1.63 (4H, m, CH_2OCH_2), 1.71 (4H, m, MeOCH_2). The Al-H signal could not be detected in spectra.

^{13}C NMR (d_8 -THF, 100 MHz) δ_{C} : 71.9 (OCH_2), 70.3 (OCH_2), 57.9 (OCH_3).

IR (nujol) ν_{max} : 1899, 1841 cm^{-1} .

m.p. 105 - 107 $^{\circ}\text{C}$.

Dichloroalane•(*N,N*-dimethylpiperazine) adduct (**98**)



Prepared from dichloroalane•*bis*(diethyl etherate) (10.0 mL, 12.7 mmol, 1.27 M solution) and *N,N'*-dimethylpiperazine (1.72 mL, 12.7 mmol) to yield **98** as a colourless solid (2.45 g, 92%).

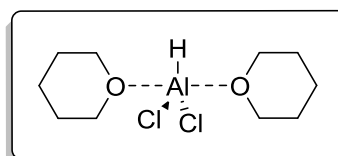
^1H NMR (d_8 -THF, 400 MHz) δ_{H} : 0.34 (4H, s, CH_2), 0.48 (3H, s, NCH_3). The Al-H signal could not be detected in spectra.

^{13}C NMR (d_8 -THF, 100 MHz) δ_{C} : 55.0 (NCH_2), 45.4 (NCH_3).

IR (nujol) ν_{max} : 1797 cm^{-1} .

m.p. 216 - 218 $^{\circ}\text{C}$.

Dichloroalane•*bis*(tetrahydropyran) (**73**)^{51a}

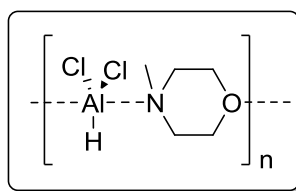


Prepared from dichloroalane•*bis*(diethyl etherate) (10 mL, 12.7 mmol, 1.27M solution) and tetrahydropyran (2.5 mL, 25.4 mmol) to yield **73** as a waxy colourless solid (2.67 g, 79%).

^1H NMR (C_6D_6 , 400 MHz) δ_{H} : 1.81 (2H, m, C^4H_2), 1.28 (4H, m, C^3H_2 & C^5H_2), 3.80 (4H, t, $J = 5.0$ Hz, C^2H_2 and C^6H_2). The Al-H signal could not be detected in spectra.

^{13}C NMR (C_6D_6 , 100 MHz) δ_{C} : 22.2 (C^4H_2), 25.4 (C^3H_2 and C^5H_2), 70.7 (C^2H_2 and C^6H_2).

Dichloroalane•(*N*-methylmorpholine) adduct (**100**)



Prepared from dichloroalane•*bis*(diethyl etherate) (10 mL, 12.5 mmol, 1.25 M solution) and *N*-methylmorpholine (1.40 mL, 12.5 mmol) to yield **100** as a colourless solid (2.27 g, 91%).

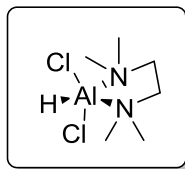
^1H NMR (C_6D_6 , 400 MHz) δ_{H} : 1.94 (3H, s, CH_3), 2.28 (4H, s, NCH_2), 3.18 (4H, s, OCH_2). The Al-H signal could not be detected in spectra.

^{13}C NMR (C_6D_6 100 MHz) δ_{C} : 61.4 (CH_2O), 52.4 (CH_2N), 41.0 (NCH_3).

IR (nujol) ν_{max} : 1843 cm^{-1} .

m.p. 140 - 142 °C.

Dichloroalane•(teteamethylethylene diamine) adduct (103)



Prepared from dichloroalane•*bis*(diethyl etherate) (10 mL, 12.5 mmol, 1.25M solution) and anhydrous *N,N'*-tetramethylethylenediamine (1.90 mL, 12.5 mmol) to yield **103** as a colourless solid (2.11 g, 78%).

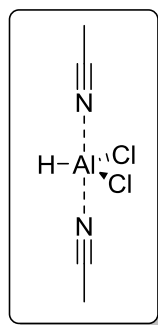
¹H NMR (d₈-THF, 400 MHz) δ_{H} : 0.41 (12H, s, NCH₃), 0.58 (4H, s, NCH₂). The Al-H signal could not be detected in spectra.

¹³C NMR (d₈-THF, 100 MHz) δ_{C} : 56.0 (NCH₂), 43.4 (N(CH₃)₂).

IR (nujol) ν_{max} : 1841, 1641 cm⁻¹.

m.p. 162 - 164 °C.

Dichloroalane•bis(acetonitrile) adduct (101)

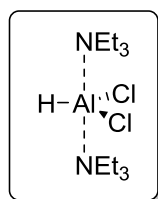


Prepared from dichloroalane•*bis*(diethyl etherate) (10 mL, 12.5 mmol, 1.25M solution) and anhydrous acetonitrile (1.3 mL, 25.0 mmol) to yield **101** as a yellow oil (2.10 g, 93%).

¹H NMR (d₃-MeCN, 400 MHz) δ_H: 1.99 (6H, s, CH₃). The Al-H signal could not be detected in spectra.

¹³C NMR (d₃-MeCN) δ_C: 117.3 (CN), 14.0 (CH₃).

Dichloroalane•*bis*(triethylamine) adduct (**104**)



Prepared from dichloroalane•*bis*(diethyl etherate) (10 mL, 12.5 mmol, 1.25 M solution) and anhydrous triethylamine (3.5 mL, 25.0 mmol) to yield **104** as a colourless solid (3.15 g, 84%).

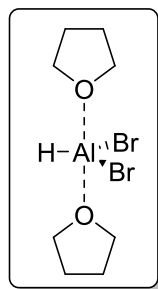
¹H NMR (C₆D₆, 400 MHz) δ_H: 0.86 (12H, s, 4 x CH₃), 2.46 (4H, s, 4 x CH₂). The Al-H signal could not be detected in spectra.

¹³C NMR (C₆D₆, 100 MHz) δ_C: 47.2 (NCH₂), 8.5 (CH₃).

IR (nujol) ν_{max}: 1872, 1638 cm⁻¹.

m.p. 94 - 96 °C.

Dibromoalane•bis(tetrahydrofuran) (105)^{51b}



A solution of aluminium chloride (609 mg, 4.5 mmol) in diethylether (20 mL) was added to a solution of lithium aluminium hydride (520 mg, 13.7 mmol) in diethyl ether (20 mL) and stirred for 20 min. The lithium chloride was removed *via* cannula filtration under argon and a solution of aluminium tribromide (9.76 g, 36.6 mmol) in diethyl ether (20 mL) was added to the filtrate and the mixture stirred for 15 min. Anhydrous THF (8.9 mL, 110 mmol) was added and mixture stored at -20 °C overnight to yield a white solid. The mother liquor was removed *via* cannula and the solid dried in *vacuo* for 5 h to yield **105** as a white solid (13.13 g, 72%).

¹H NMR (C₆D₆, 400 MHz) δ_{H} : 1.14 (8H, m, 4 x CH₂), 3.72 (8H, m, 4 x OCH₂). The Al-H signal could not be detected in spectra.

¹³C NMR (C₆D₆, 100 MHz) δ_{C} : 24.9 (CH₂), 69.8 (OCH₂).

IR (nujol) ν_{max} : 1851 cm⁻¹.

m.p. 58 - 60 °C.

General Procedure 10: $\text{Cp}^*_2\text{ZrCl}_2$ -catalysed hydroalumination-cross coupling

A Radley's carousel reaction tube was charged with dichloroalane•*bis*(tetrahydrofuran) (1.02 g, 4.20 mmol, 2.1 equiv.) and *bis*(pentamethylcyclopentadienyl)zirconium dichloride (60 mg, 0.14 mmol, 5.0 mol% based on alkyne) in the glove box. Under an inert atmosphere, tetrahydrofuran (4 mL) and alkyne (2.80 mmol, 1.4 equiv.) were added, the reaction mixture stirred at reflux for 4 h and then removed from the heat. In a flame-dried, stirrer-equipped Schlenk tube under an inert atmosphere, X-Phos (38 mg, 0.08 mmol, 4.0 mol% based on ArX), tris(dibenzylideneacetone)dipalladium(0)-chloroform adduct (31 mg, 0.030 mmol, 1.5 mol% based on ArX) and 1,4-diazabicyclo[2.2.2]octane (0.160 g, 1.40 mmol, 0.7 equiv.) were dissolved in tetrahydrofuran (4 mL) and transferred to the reaction mixture *via* cannula. Aryl halide (2.00 mmol, 1.0 equiv.) was added and the reaction mixture was heated at reflux for 2 h. Hydrochloric acid (2 M, 6 mL) was added, the layers were separated and the aqueous phase was extracted with dichloromethane (3 x 5 mL). The combined organic extracts were evaporated under reduced pressure to give the crude product, which was purified by flash column chromatography (solid load). Alternatively, for acid sensitive

substrates the reaction was quenched with aqueous Rochelle's salt (saturated, 6 mL) and the same extraction procedure as above used.

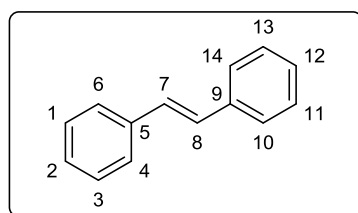
General Procedure 11: $^2\text{H}\{^1\text{H}\}$ and ^1H NMR monitoring of hydroalumination

Hydroaluminations were carried out as described above. The crude mixture of alanes (from alkyne (2.80 mmol) and dichloroalane bis(tetrahydrofuran) (4.20 mmol) in tetrahydrofuran (4 mL) was quenched with deuterium oxide (0.50 mL) at room temperature. The crude reaction mixture was apportioned into two equal parts. To the first part deuterated chloroform (50 μL , internal standard) was added and the $^2\text{H}\{^1\text{H}\}$ spectrum acquired.

The $^2\text{H}\{^1\text{H}\}$ spectra were run unlocked and the signals were recorded on the lock channel. Samples were shimmed by means of gradient shimming using the ^1H signal of the solvent. The 'zgig2h' pulse sequence of a Bruker AVANCE I type instrument was used and the ^2H spectra acquired using power gated ^1H decoupling. Use of coupled ^2H spectra was ineffective due to signal overlaps in the alkene region. The relative populations of (*E*)-**109**:(*Z*)-**109**:**110**:**111**:**112**:**113** (R = C₈H₁₇, Y = Cl) were determined by the integrals of the singlets at δ_{D} 4.97 (=C(1)D), 5.03 (=C(1)D'), 5.85 (=C(2)D),

1.95 ($\equiv\text{CD}$), 0.93 ($-\text{CD}_2\text{H}$), 1.31 ($-\text{CHD}-$) respectively of the D-quenched products. No evidence for the formation of *n*- $\text{C}_8\text{H}_{17}\text{CD}_2\text{CH}_3$ (potentially from double C(2)-Al addition) was detected and its concentration was assumed minimal. The second part of the reaction mixture was evaporated to a crude oil. The alkyne conversion was determined by comparison of the ^1H NMR spectrum of the residual 1-decyne $\equiv\text{CH}$ integral at δ_{H} 1.95 to integral of the non-terminal alkene signal at δ_{H} 5.85 after correction for deuterium incorporation. Total deuterium incorporation in the 1-decene was determined by GC-MS, while the fraction at C(1)/C(2) was available from the $^2\text{H}\{^1\text{H}\}$ studies above.

(*E*)-stilbene (115)¹¹⁶



Prepared by general procedure 10, dichloroalane bis(tetrahydrofuran) (1.02 g, 4.20 mmol), bis(pentamethylcyclopentadienyl)zirconium dichloride (59 mg, 0.14 mmol), phenylacetylene (310 μL , 2.80 mmol), X-Phos (39 mg, 0.080 mmol), tris(dibenzylideneacetone)dipalladium(0)-chloroform adduct (31 mg, 0.03 mmol), 1,4-diazabicyclo[2.2.2]octane (157 mg,

1.40 mmol) and bromobenzene (210 μ L, 2.00 mmol) to yield **115** (338 mg, 94 %) as a white crystalline solid; **R_f** (pentane) 0.30.

¹H NMR (400 MHz, CDCl₃): δ_{H} 7.14 (2H, s, C⁷H & C⁸H), 7.32-7.26 (2H, m, C²H & C¹²H), 7.41-7.35 (4H, m, C¹H, C³H, C¹¹H & C¹³H), 7.56-7.50 (4H, m, C⁴H, C⁶H, C¹⁰H & C¹⁴H).

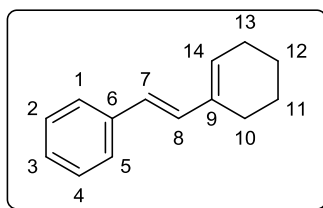
¹³C NMR (100.6 MHz, CDCl₃): δ_{C} 126.5 (Ar), 127.6 (Ar), 128.7 (C7 & C8), 137.3 (Ar).

IR (CHCl₃) ν_{max} : 3081, 3062, 3011, 1600, 1497, 1452, 961 cm⁻¹.

m.p. 122-124 °C (lit. 122 °C).¹¹⁶

HRMS: (EI) C₁₄H₁₂ [M]⁺ requires m/z 180.0939, found [M]⁺ 180.0943.

(*E*)-(2-(Cyclohex-1-en-1-yl)vinyl)benzene (116)¹¹⁷



Prepared by general procedure 10, dichloroalane bis(tetrahydrofuran) (510 mg, 2.10 mmol), bis(pentamethylcyclopentadienyl)zirconium dichloride (45 mg, 0.10 mmol), 1-ethynylcyclohexene (164 μ L, 1.40 mmol), X-Phos (19 mg, 0.040 mmol), tris(dibenzylideneacetone)dipalladium(0)-chloroform adduct

(15 mg, 0.015 mmol), 1,4-diazabicyclo[2.2.2]octane (79 mg, 0.70 mmol), and bromobenzene (100 μ L, 1.00 mmol) and quenched with Rochelle's salt (3 mL of saturated aqueous solution) afforded **116** (125 mg, 68%) as a colourless oil; R_F (pentane) 0.25.

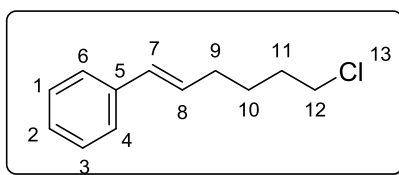
^1H NMR (400 MHz, CDCl_3): δ_{H} 1.65 – 1.71 (2H, m, c-hex), 1.74 – 1.80 (2H, m, c-hex), 2.22 – 2.24 (2H, m, c-hex), 2.33–2.39 (2H, m, c-hex), 5.94 (1H, t, J = 4.5 Hz, C^{14}H), 6.49 (1H, d, J = 16.5 Hz, C^8H), 6.82 (1H, d, J = 16.5 Hz, C^9H), 7.22 (1H, tt, J = 7.0, 1.5 Hz, $\text{C}^3\text{H}(\text{Ar})$), 7.33 (2H, tt, J = 7.5, 1.5 Hz, $\text{C}^1\text{H}(\text{Ar})$, $\text{C}^5\text{H}(\text{Ar})$), 7.44 (2H, dt, J = 7.0, 1.5 Hz, $\text{C}^2\text{H}(\text{Ar})$ and $\text{C}^4\text{H}(\text{Ar})$).

^{13}C NMR (100.6 MHz, CDCl_3): δ_{C} 22.5 ($\text{CH}_2(\text{c-hex})$), 22.6 ($\text{CH}_2(\text{c-hex})$), 24.6 ($\text{CH}_2(\text{c-hex})$), 26.2 ($\text{CH}_2(\text{c-hex})$), 124.6 (C^{14}), 126.1 (C^1 and C^5), 126.8 (C^3), 128.5 (C^2 and C^4), 130.8 (C^7), 132.6 (C^8), 135.8 (C^9), 138.0 (C^6).

IR (CHCl_3) ν_{max} : 3010, 2930, 2861, 1632, 1616, 1494, 1447, 962 cm^{-1} .

HRMS: (EI) $\text{C}_{14}\text{H}_{16}$ $[\text{M}]^+$ requires m/z 184.1252, found $[\text{M}]^+$ 184.1254.

(E)-(6-Chlorohex-1-en-1-yl)benzene (117)



Prepared by general procedure 10, dichloroalane bis(tetrahydrofuran) (510 mg, 2.10 mmol), bis(pentamethylcyclopentadienyl)zirconium dichloride (30 mg, 0.07 mmol), 6-chlorohexyne (169 μ L, 1.40 mmol), X-Phos (19 mg, 0.040 mmol), tris(dibenzylideneacetone)dipalladium(0)-chloroform adduct (15 mg, 0.015 mmol), 1,4-diazabicyclo[2.2.2]octane (117 mg, 0.700 mmol), and bromobenzene (100 μ L, 1.00 mmol) and quenched with Rochelle's salt (3 mL of saturated aqueous solution) afforded **117** (125 mg, 68%) as a colourless oil; R_F (pentane) 0.49.

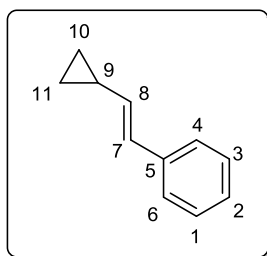
^1H NMR (400 MHz, CDCl_3): δ_{H} 1.60–1.67 (2H, m, C^{10}H_2), 1.80–1.88 (2H, m, C^{11}H_2), 2.22–2.28 (2H, m, C^9H_2), 3.57 (2H, t, $J = 7.0$ Hz, C^{12}H_2), 6.25 (1H, dt, $J = 16.0, 7.0$ Hz, C^8H), 6.40 (1H, d, $J = 16.0$ Hz, C^7H), 7.18–7.22 (1H, m, C^2H), 7.27–7.31 (2H, m, C^1H & C^3H), 7.31–7.35 (2H, m, C^6H & C^4H).

^{13}C NMR (100.6 MHz, CDCl_3): δ_{C} 26.5 (C^{10}), 32.1 (C^{11}), 32.2 (C^9), 44.9 (C^{12}), 125.9 (C^4 & C^6), 126.9 (C^8), 128.5 (C^1 & C^3), 130.1 (C^2), 130.5 (C^7), 137.7 (C^5).

IR (CHCl₃) ν_{max} : 3058, 3025, 2935, 2860, 1493, 1447, 965 cm⁻¹.

HRMS: (EI) C₁₂H₁₅³⁵Cl [M]⁺ requires m/z 194.0862, found [M]⁺ 194.0875.

(*E*)-(2-Cyclopropylvinyl)benzene (118**)**¹¹⁸



Prepared by general procedure 10, dichloroalane bis(tetrahydrofuran) (510 mg, 2.10 mmol), bis(pentamethylcyclopentadienyl)zirconium dichloride (30 mg, 0.07 mmol), cyclopropylacetylene (118 μ L, 1.40 mmol), X-Phos (19 mg, 0.040 mmol), tris(dibenzylideneacetone)dipalladium(0)-chloroform adduct (15 mg, 0.015 mmol), 1,4-diazabicyclo[2.2.2]octane (117 mg, 0.700 mmol), and bromobenzene (100 μ L, 1.00 mmol) and quenched with Rochelle's salt (3 mL of saturated aqueous solution) afforded **118** (140 mg, 97%) as a colourless oil; R_F (pentane) 0.44.

¹H NMR (400 MHz, CDCl₃): δ_H 0.44–0.63 (2H, m, cyclopropyl), 0.72–0.96 (2H, m, cyclopropyl), 1.50–1.68 (1H, m, C⁹H), 5.76 (1H, dd, J = 16.0, 9.0 Hz, C⁸H), 6.50 (1H, d, J

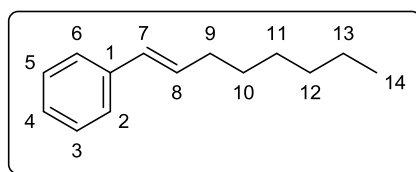
= 16.0 Hz, C⁷H), 7.17–7.21 (1H, m, C²H), 2.28–7.34 (4H, m, C¹H, C³H, C⁴H, C⁶H).

¹³C NMR (100.6 MHz, CDCl₃): δ_C 7.2 (C10 and C11), 14.5 (C9), 125.6 (C4 & C6), 126.5 (C2), 127.4 (C7), 128.5 (C1 & C3), 134.9 (C8), 137.8 (C5).

IR (CHCl₃) ν_{max}: 3081, 3024, 3004, 1650, 1489, 1428, 954 cm⁻¹.

HRMS: (EI) C₁₁H₁₂ [M]⁺ requires *m/z* 144.0939, found [M]⁺ 144.0940.

(*E*)-1-Phenyl-1-octene (119**)**¹¹⁹



Prepared by general procedure 10, dichloroalane bis(tetrahydrofuran) (1.02 g, 4.20 mmol), bis(pentamethylcyclopentadienyl)zirconium dichloride (64 mg, 0.15 mmol), 1-octyne (410 μL, 2.80 mmol), X-Phos (38 mg, 0.080 mmol), tris(dibenzylideneacetone)dipalladium(0)-chloroform adduct (31 mg, 0.030 mmol), 1,4-diazabicyclo[2.2.2]octane (164 mg, 1.46 mmol) and bromobenzene (210 μL, 2.00 mmol) afforded **119** (367 mg, 98%) as a colourless oil; *R_F* (pentane) 0.70.

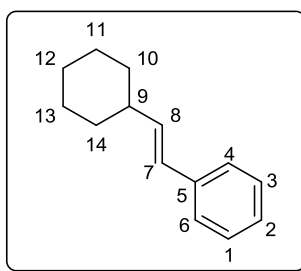
^1H NMR (400 MHz, CDCl_3): δ_{H} 0.97-0.87 (3H, m, C^{14}H_3), 1.43-1.22 (6H, m, $\text{C}^{11}\text{H}_2\text{-C}^{13}\text{H}_2$), 1.55-1.44 (2H, m, C^{10}H_2), 2.24 (2H, q, $J = 7.0$ Hz, C^9H_2), 6.26 (1H, dt, $J = 16.0, 7.0$ Hz, C^8H), 6.41 (1H, d, $J = 16.0$ Hz, C^7H), 7.22 (1H, t, $J = 8.0$ Hz, C^4H), 7.32 (2H, t, $J = 8.0$ Hz, C^5H & C^3H), 7.38 (2H, d, $J = 8.0$ Hz, C^6H & C^2H).

^{13}C NMR (100.6 MHz, CDCl_3): δ_{C} 14.1 (C^{14}), 22.6 (C^{13}), 28.9 (C^{12}), 29.4 (C^{11}), 31.8 (C^{10}), 33.1 (C^9), 125.9 (C^5 and C^3), 126.7 (C^1), 128.4 (C^2 and C^6), 129.7 (C^7), 131.2 (C^8), 138.0 (C^4).

IR (CHCl_3) ν_{max} : 3062, 3009, 2958, 2928, 2856, 1494, 956 cm^{-1} .

HRMS: (EI) $\text{C}_{14}\text{H}_{20}$ $[\text{M}]^+$ requires m/z 188.1565, found $[\text{M}]^+$ 188.1564.

(*E*)-(2-Cyclohexylvinyl)benzene (121)



Prepared by general procedure 10, dichloroalane bis(tetrahydrofuran) (510 mg, 2.10 mmol), bis(pentamethylcyclopentadienyl)zirconium dichloride (45 mg, 0.14 mmol), cyclohexylacetylene (183 μL , 1.40 mmol), X-Phos

(19 mg, 0.040 mmol), tris(dibenzylideneacetone)dipalladium(0)-chloroform adduct (15 mg, 0.015 mmol), 1,4-diazabicyclo[2.2.2]octane (158 mg, 1.41 mmol) and bromobenzene (100 μ L, 1.00 mmol) afforded **121** (175 mg, 94 %) as a pale yellow oil; **R_F** (pentane) 0.42.

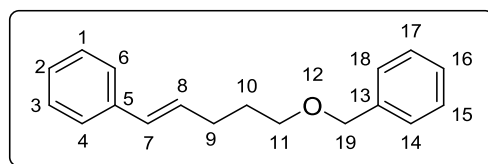
¹H NMR (400 MHz, CDCl₃): δ_{H} 1.17–1.25 (3H, m, c-hex), 1.27–1.36 (2H, m, c-hex), 1.66–1.71 (1H, m, c-hex), 1.75–1.83 (4H, m, c-hex), 2.10–2.23 (1H, m, c-hex), 6.21 (1H, dd, J = 16.0, 7.0 Hz, C⁸H), 6.38 (1H, d, J = 16.0 Hz, C⁷H), 7.18–7.20 (1H, m, C²H), 7.27–7.30 (2H, m, C¹H & C³H), 7.34–7.36 (2H, m, C⁴H & C⁶H).

¹³C NMR (100.6 MHz, CDCl₃): δ_{C} 26.1 (C11 and C13), 26.3 (C12), 33.1 (C10 & C14), 41.3 (C9), 126.1 (C7), 126.8 (C6), 127.4 (C1), 128.6 (C3), 130.4 (C8), 137.6 (C2).

IR (CHCl₃) ν_{max} : 3736, 3690, 2928, 2853, 1647, 1600, 1490, 909 cm⁻¹.

HRMS: (EI) C₁₄H₁₆ [M]⁺ requires m/z 186.1409, found [M]⁺ 186.1415.

(*E*)-(5-(Benzyloxy)pent-1-en-1-yl)benzene (124**)**¹²⁰



Prepared by general procedure 10, dichloroalane bis(tetrahydrofuran) (1.02 g, 4.20 mmol), bis(pentamethylcyclopentadienyl)zirconium dichloride (61 mg, 0.14 mmol), ((pent-4-yn-1-yloxy)methyl)benzene (487 mg, 2.80 mmol), X-Phos (38 mg, 0.080 mmol), tris(dibenzylideneacetone)dipalladium(0)-chloroform adduct (31 mg, 0.030 mmol), 1,4-diazabicyclo[2.2.2]octane (157 mg, 1.40 mmol) and bromobenzene (210 μ L, 2.00 mmol) to afforded **124** (356.2 mg, 75%) as a colourless oil; R_F (pentane/diethyl ether 1:1) 0.36.

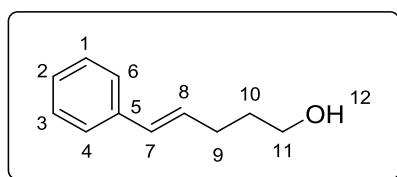
¹H NMR (400 MHz, CDCl₃): δ_H 1.91 - 1.94 (2H, m, C¹⁰H₂), 2.40 (2H, dtd, J = 8.0, 7.0, 1.0 Hz, C⁹H₂), 3.60 (2H, t, J = 6.5 Hz, C¹¹H₂), 4.60 (2H, s, C¹⁹H₂) 6.28 (1H, dt, J = 16.0, 7.0 Hz, C⁸H), 6.45 (1H, dt, J = 16.0, 1.0 Hz, C⁷H), 7.40 - 7.48 (10H, m, Ar).

¹³C NMR (100.6 MHz, CDCl₃): δ_C 29.0 (C10), 29.5 (C9), 69.7 (C11), 73.0 (C19), 125.7 (C4 and C6), 126.1 (C7), 127.9 (C14 and C16 and C18), 128.2 (C15 and C17), 128.3 (C1 and C3), 128.9 (C2), 130.3 (C8), 137.8 (C5), 138.6 (C13).

IR (CHCl₃) ν_{max} : 3065, 3009, 2940, 2862, 1495, 1453, 1100, 965, 909 cm⁻¹.

HRMS: (EI) C₁₈H₂₀O [M]⁺ requires m/z 252.1514, found [M]⁺ 252.1524

(*E*)-5-Phenylpent-4-en-1-ol (125**)**¹²¹



Prepared by general procedure 10, dichloroalane bis(tetrahydrofuran) (1.02 g, 4.20 mmol), bis(pentamethylcyclopentadienyl)zirconium dichloride (31 mg, 0.070 mmol), 5-pentynol (130 μ L, 1.40 mmol), X-Phos (19 mg, 0.040 mmol), tris(dibenzylideneacetone)dipalladium(0)-chloroform adduct (16 mg, 0.015 mmol), 1,4-diazabicyclo[2.2.2]octane (79 mg, 0.70 mmol), indium(III) chloride (31 mg, 0.14 mmol) and bromobenzene (110 μ L, 1.00 mmol) afforded **125** (99.1 mg, 61%) as a yellow oil; R_F (pentane/diethyl ether 1:1) 0.44.

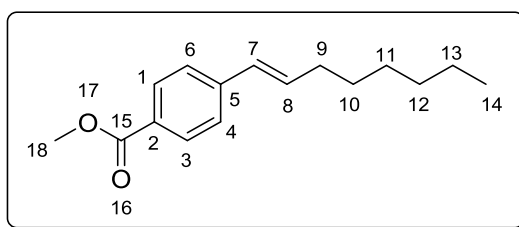
¹H NMR (400 MHz, CDCl₃): δ_H 1.81 - 1.87 (2H, m, C¹⁰H₂), 2.35 (2H, dtd, J = 8.0, 7.0, 1.5 Hz, C⁹H₂), 3.75 (2H, t, J = 6.5 Hz, C¹¹H₂), 6.27 (1H, dt, J = 16.0, 7.0 Hz, C⁸H), 6.45 (1H, dt, J = 16.0, 1.5 Hz, C⁷H), 7.23 - 7.28 (1H, m, C²H), 7.35 - 7.40 (4H, m, C¹H, C³H, C⁴H and C⁶H).

^{13}C NMR (100.6 MHz, CDCl_3): δ_{C} 29.3 (C9), 32.3 (C10), 62.4 (C11), 125.9 (C4 and C6), 126.9 (C2), 128.5 (C1 and C3), 130.3 (C7), 130.0 (C8), 137.6 (C5).

IR (CHCl_3) ν_{max} : 3624, 2938, 2255, 1599, 1056, 966 cm^{-1} .

HRMS: (EI) $\text{C}_{11}\text{H}_{14}\text{O}$ $[\text{M}]^+$ requires m/z 162.1045, found $[\text{M}]^+$ 162.1045.

(*E*)-Methyl 4-(oct-1-en-1-yl)benzoate (128**)**¹²²



Prepared by general procedure 10, dichloroalane bis(tetrahydrofuran) (1.02 g, 4.20 mmol), bis(pentamethylcyclopentadienyl)zirconium dichloride (61 mg, 0.14 mmol), 1-octyne (410 μL , 2.80 mmol), X-Phos (38 mg, 0.080 mmol), tris(dibenzylideneacetone)dipalladium(0)-chloroform adduct (31 mg, 0.030 mmol), 1,4-diazabicyclo[2.2.2]octane (157 mg, 1.40 mmol) and methyl-4-bromobenzoate (430 mg, 2.00 mmol) afforded **128** (417.8 mg, 85%) as a yellow oil; R_{F} (pentane/diethyl ether 10:1) 0.44.

^1H NMR (400 MHz, CDCl_3): δ_{H} 0.92 (3H, t, J = 7.0 Hz, C^{14}H_3), 1.33 - 1.38 (6H, m, $\text{C}^{11}\text{H}_2\text{-C}^{13}\text{H}_2$), 1.48 - 1.50 (2H, m, C^{10}H_2), 2.26 (2H, dtd, J = 7.6, 5.5, 2.0 Hz, C^9H_2), 3.92 (3H, s, C^{18}H_3)

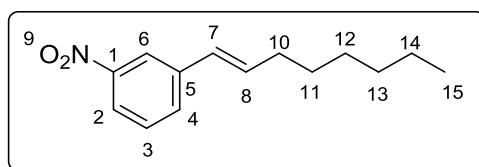
6.37 (1H, dt, $J = 16.0, 5.5$ Hz, C⁸H), 6.44, (1H, d, $J = 16.0$ Hz, C⁷H), 7.41 (2H, d, $J = 8.5$ Hz, C⁴H and C⁶H), 7.98 (2H, d, $J = 8.5$ Hz, C¹H and C³H).

¹³C NMR (100.6 MHz, CDCl₃): δ_{C} 14.1 (C14), 22.6 (C13), 28.9 (C12), 29.1 (C11), 31.7 (C10), 33.2 (C9), 51.9 (C18), 125.7 (C4 and C6), 128.2 (C5), 128.9 (C8), 129.9 (C1 and C3), 134.3 (C7), 142.5 (C2), 167.0 (C15).

IR (CHCl₃) ν_{max} : 3008, 2955, 2929, 2857, 1715, 1606, 1436, 1328, 1112, 969 cm⁻¹.

HRMS: (EI) C₁₆H₂₂O₂ [M]⁺ requires m/z 246.1620, found [M]⁺ 246.1621.

(*E*)-1-Nitro-3-(oct-1-en-1-yl)benzene (129)¹²²



Prepared by general procedure 10, dichloroalane bis(tetrahydrofuran) (1.02 g, 4.20 mmol), bis(pentamethylcyclopentadienyl)zirconium dichloride (61 mg, 0.14 mmol), 1-octyne (410 μ L, 2.80 mmol), X-Phos (38 mg, 0.080 mmol), tris(dibenzylideneacetone)dipalladium(0)-chloroform adduct (31 mg, 0.030 mmol), 1,4-diazabicyclo[2.2.2]octane (157 mg, 1.40 mmol) and 3-nitrobromobenzene (404 mg, 2.00 mmol) afforded **129** (215

mg, 55%) as a light brown oil; **R_F** (pentane/diethyl ether 49:1) 0.36.

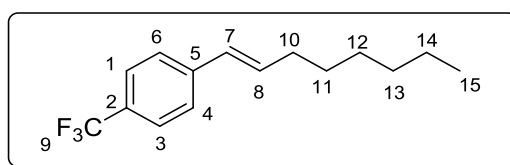
¹H NMR (400 MHz, CDCl₃): δ_H 0.92 (3H, t, *J* = 7.0 Hz, C¹⁵H₃), 1.34 - 1.38 (6H, m, C¹²H₂-C¹⁴H₂), 1.51 - 1.55 (2H, m, C¹¹H₂), 2.27 (2H, dtd, *J* = 7.0, 6.0, 2.0 Hz, C¹⁰H₂), 6.38 (1H, dt, *J* = 16.0, 6.0 Hz, C⁸H), 6.44, (1H, d, *J* = 16.0 Hz, C⁷H), 7.46 (1H, app t, *J* = 8.0 Hz, C³H), 7.63 (1H, dt, *J* = 7.0, 1.0 Hz, C²H), 8.04 (1H, m, C⁴H), 8.20 (1H, app t, *J* = 2.0 Hz, C⁶H).

¹³C NMR (100.6 MHz, CDCl₃): δ_C 14.1 (C15), 22.6 (C14), 28.9 (C13), 29.0 (C12), 31.7 (C11), 33.0 (C10), 120.5 (C4), 121.4 (C6), 127.6 (C5), 129.3 (C8), 131.8 (C2), 134.7 (C7), 139.7 (C3), 147.2 (C1).

IR (CHCl₃) ν_{max}: 2958, 2929, 2857, 1529, 1352, 964 cm⁻¹.

HRMS: (EI) C₁₄H₁₉NO₂ [M]⁺ requires *m/z* 233.1416, found [M]⁺ 233.1407.

(*E*)-1-(Oct-1-en-1-yl)-4-(trifluoromethyl)benzene (130)
123



Prepared by general procedure 10, dichloroalane bis(tetrahydrofuran) (1.02 g, 4.20 mmol), bis(pentamethylcyclopentadienyl)zirconium dichloride (61 mg, 0.14 mmol), 1-octyne (410 μL, 2.80 mmol), X-Phos (38 mg,

0.080 mmol), tris(dibenzylideneacetone)dipalladium(0)-chloroform adduct (31 mg, 0.030 mmol), 1,4-diazabicyclo[2.2.2]octane (157 mg, 1.40 mmol) and 4-(trifluoromethyl)bromobenzene (280 μ L, 2.00 mmol) afforded **130** (484.1 mg, 94%) as a colourless oil; **R_F** (pentane) 0.52.

¹H NMR (400 MHz, CDCl₃): δ_{H} 0.93 (3H, t, J = 7.0 Hz, C¹⁵H₃), 1.34 - 1.38 (6H, m, C¹²H₂-C¹⁴H₂), 1.51 - 1.55 (2H, m, C¹¹H₂), 2.27 (2H, dtd, J = 7.5, 7.0, 1.0 Hz, C¹⁰H₂), 6.35 (1H, dt, J = 16.0, 7.5 Hz, C⁸H), 6.42 - 6.44, (1H, m, C⁷H), 7.44 (2H, d, J = 8.5 Hz, C¹H and C³H), 7.55 (2H, d, J = 8.5 Hz, C⁴H and C⁶H).

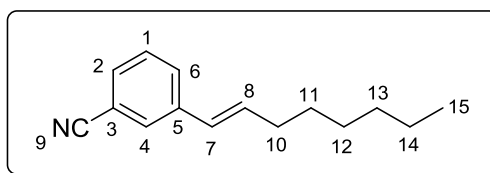
¹³C NMR (100.6 MHz, CDCl₃): δ_{C} 14.1 (C15), 22.6 (C14), 28.9 (C13), 29.3 (C12), 31.7 (C11), 33.0 (C10), 118.6 (C1 and C3), 123.5 (q, J = 272.0 Hz, CF₃), 129.4 (C4 and C6), 129.5 (C7), 130.5 (C5), 131.6 (C8), 139.4 (C2).

¹⁹F NMR (376.5 MHz, CDCl₃): δ_{F} -69.3.

IR (CHCl₃) ν_{max} : 2958, 2929, 2857, 1615, 1329, 1166, 1124, 968 cm⁻¹.

HRMS: (EI) C₁₅H₁₉F₃ [M]⁺ requires m/z 256.1439, found [M]⁺ 256.1441.

(E)-3-(Oct-1-en-1-yl)benzonitrile (132)



Prepared by general procedure 10, dichloroalane bis(tetrahydrofuran) (1.02 g, 4.20 mmol), bis(pentamethylcyclopentadienyl)zirconium dichloride (61 mg, 0.14 mmol), 1-octyne (410 μ L, 2.80 mmol), X-Phos (38 mg, 0.080 mmol), tris(dibenzylideneacetone)dipalladium(0)-chloroform adduct (31 mg, 0.030 mmol), 1,4-diazabicyclo[2.2.2]octane (157 mg, 1.40 mmol) and 3-bromobenzonitrile (364 mg, 2.00 mmol) afforded **132** (398.1 mg, 94%) as a yellow oil; R_F (pentane/diethyl ether 19:1) 0.14.

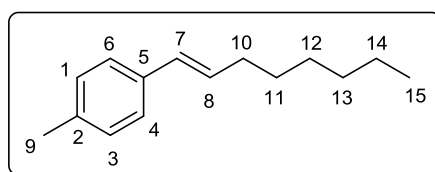
^1H NMR (400 MHz, CDCl_3): δ_{H} 0.92 (3H, t, $J = 7.0$ Hz, C^{15}H_3), 1.33 - 1.38 (6H, m, $\text{C}^{12}\text{H}_2\text{-C}^{14}\text{H}_2$), 1.50 - 1.55 (2H, m, C^{11}H_2), 2.24 (2H, dtd, $J = 7.0, 6.0, 1.0$ Hz, C^{10}H_2), 6.32 (1H, dt, $J = 16.0, 6.0$ Hz, C^8H), 6.36, (1H, dt, $J = 16.0, 1.0$ Hz, C^7H), 7.40 (1H, t, $J = 8.0$ Hz, C^1H), 7.47 (1H, dt, $J = 8.0, 1.5$ Hz, C^2H), 7.55 (1H, dt, $J = 8.0, 1.5$ Hz, C^6H), 7.62 (1H, s, C^4H).

^{13}C NMR (100.6 MHz, CDCl_3): δ_{C} 14.1 (C^{15}), 22.6 (C^{14}), 28.9 (C^{13}), 29.0 (C^{12}), 31.7 (C^{11}), 33.0 (C^{10}), 112.6 (C^5), 118.9 (CN), 127.7 (C^1), 129.2 (C^2), 129.4 (C^8), 130.0 (C^4), 130.1 (C^6), 134.3 (C^7), 139.2 (C^3).

IR (CHCl₃) ν_{max} : 3009, 2958, 2929, 2857, 2232, 1651, 1598, 1466, 964 cm⁻¹.

HRMS: (EI) C₁₅H₁₉N [M]⁺ requires m/z 213.1517, found [M]⁺ 213.1517.

(*E*)-1-Methyl-4-(oct-1-en-1-yl)benzene (133)¹²⁴



Prepared by general procedure 10, dichloroalane bis(tetrahydrofuran) (1.02 g, 4.20 mmol), bis(pentamethylcyclopentadienyl)zirconium dichloride (61 mg, 0.14 mmol), 1-octyne (410 μ L, 2.80 mmol), X-Phos (38 mg, 0.080 mmol), tris(dibenzylideneacetone)dipalladium(0)-chloroform adduct (31 mg, 0.030 mmol), 1,4-diazabicyclo[2.2.2]octane (157 mg, 1.40 mmol) and from 4-bromotoluene (342 mg, 2.00 mmol) afforded **133** (375.3 mg, 87%) as a colourless oil; **R_F** (pentane) 0.50.

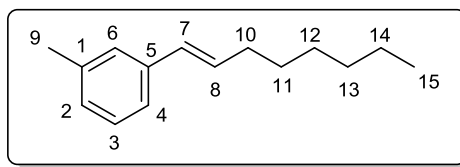
¹H NMR (400 MHz, CDCl₃): δ_{H} 0.93 (3H, t, J = 7.0 Hz, C¹⁵H₃), 1.33 - 1.38 (6H, m, C¹²H₂-C¹⁴H₂), 1.42 - 1.45 (2H, m, C¹¹H₂), 2.20 (2H, dtd, J = 7.5, 7.0, 1.0 Hz, C¹⁰H₂), 2.35 (3H, s, C⁹H₃) 6.20 (1H, dt, J = 15.0, 7.0 Hz, C⁸H), 6.35, (1H, d, J = 15.0 Hz, C⁷H), 7.13 (2H, d, J = 8.0 Hz, C⁴H and C⁶H), 7.25 (2H, d, J = 8.0, C¹H and C³H).

^{13}C NMR (100.6 MHz, CDCl_3): δ_{C} 14.1 (C15), 21.1 (C9), 22.6 (C14), 28.9 (C13), 29.4 (C12), 31.7 (C11), 33.0 (C10), 125.8 (C1 and C3), 129.1 (C4 and C6), 129.5 (C8), 130.2 (C7), 136.4 (C2), 135.1 (C1).

IR (CHCl_3) ν_{max} : 3009, 2958, 2928, 2857, 2735, 1702, 1512, 1019 cm^{-1} .

HRMS: (EI) $\text{C}_{15}\text{H}_{22}$ $[\text{M}]^+$ requires m/z 202.1722, found $[\text{M}]^+$ 202.1726.

(*E*)-1-Methyl-3-(oct-1-en-1-yl)benzene (134)



Prepared by general procedure 10, dichloroalane bis(tetrahydrofuran) (1.02 g, 4.20 mmol), bis(pentamethylcyclopentadienyl)zirconium dichloride (61 mg, 0.14 mmol), 1-octyne (410 μL , 2.80 mmol), X-Phos (38 mg, 0.080 mmol), tris(dibenzylideneacetone)dipalladium(0)-chloroform adduct (31 mg, 0.030 mmol), 1,4-diazabicyclo[2.2.2]octane (157 mg, 1.40 mmol) and 3-bromotoluene (240 μL , 2.00 mmol) afforded **134** (384 mg, 95 %) as a colourless oil; R_{F} (pentane) 0.47.

^1H NMR (400 MHz, CDCl_3): δ_{H} 0.93 (3H, t, $J = 7.0$ Hz, C^{15}H_3), 1.33 - 1.37 (6H, m, $\text{C}^{12}\text{H}_2\text{-C}^{14}\text{H}_2$), 1.55 - 1.58 (2H, m, C^{11}H_2),

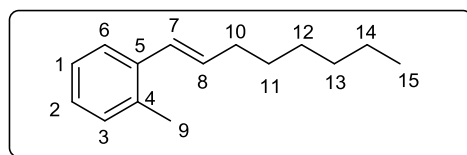
2.22 (2H, dtd, $J = 7.5, 7.0, 1.0$ Hz, $C^{10}H_2$), 2.36 (3H, s, C^9H_3)
 6.24 (1H, dt, $J = 16.0, 7.0$ Hz, C^8H), 6.37, (1H, dt, $J = 16.0,$
 1.0 Hz, C^7H), 7.03 (1H, d, $J = 8.0$ Hz, C^2H , 7.17 - 7.19 (1H,
 m, C^3H), 7.20 (1H, s, C^6H), 7.22 (1H, d, $J = 8.0$ Hz, C^4H).

^{13}C NMR (100.6 MHz, $CDCl_3$): δ_C 14.1 (C15), 21.4 (C9), 22.6
 (C14), 28.9 (C13), 29.3 (C12), 31.7 (C11) 33.1 (C10), 123.1
 (C2), 126.6 (C4), 127.7 (C3), 128.4 (C8), 129.7 (C7), 131.0
 (C6), 137.9 (C1), 137.9 (C3).

IR ($CHCl_3$) ν_{max} : 3009, 2958, 2928, 2857, 2735, 1702, 1512,
 1019 cm^{-1} .

HRMS: (EI) $C_{15}H_{22}$ $[M]^+$ requires m/z 202.1722, found $[M]^+$
 202.1718.

(*E*)-1-Methyl-2-(oct-1-en-1-yl)benzene (135)¹²²



Prepared by general procedure 10, dichloroalane
 bis(tetrahydrofuran) (1.02 g, 4.20 mmol),
 bis(pentamethylcyclopentadienyl)zirconium dichloride (61 mg,
 0.14 mmol), 1-octyne (410 μ L, 2.80 mmol), X-Phos (38 mg,
 0.080 mmol), tris(dibenzylideneacetone)dipalladium(0)-
 chloroform adduct (31 mg, 0.030 mmol), 1,4-
 diazabicyclo[2.2.2]octane (157 mg, 1.40 mmol) and 2-

bromotoluene (240 μ L, 2.00 mmol) afforded **135** (370.9 mg, 92%) a colourless oil; R_F (pentane) 0.54.

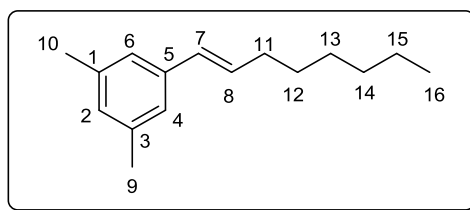
^1H NMR (400 MHz, CDCl_3): δ_{H} 0.91 (3H, t, $J = 7.0$ Hz, C^{15}H_3), 1.35 - 1.38 (6H, m, $\text{C}^{12}\text{H}_2\text{-C}^{14}\text{H}_2$), 1.55 - 1.58 (2H, m, C^{11}H_2), 2.25 (2H, dtd, $J = 7.5, 7.0, 1.0$ Hz, C^{10}H_2), 2.35 (3H, s, C^9H_3) 6.12 (1H, dt, $J = 15.5, 7.5$ Hz, C^8H), 6.60 (1H, dt, $J = 15.5, 1.0$ Hz, C^7H), 7.14 - 7.20 (3H, m, C^1H and C^2H and C^6H), 7.43 - 7.45 (m, 1H, C^3H).

^{13}C NMR (100.6 MHz, CDCl_3): δ_{C} 14.1 (C^{15}), 19.8 (C^9), 22.6 (C^{14}), 28.7 (C^{13}), 29.4 (C^{12}), 31.7 (C^{11}), 33.3 (C^{10}), 125.4 (C^2), 125.9 (C^1), 126.7 (C^8), 127.5 (C^3), 130.1 (C^6), 132.6 (C^7), 134.8 (C^4), 137.1 (C^5).

IR (CHCl_3) ν_{max} : 3009, 2958, 2928, 2857, 2735, 1702, 1512, 1019 cm^{-1} .

HRMS: (EI) $\text{C}_{15}\text{H}_{22}$ $[\text{M}]^+$ requires m/z 202.1722, found $[\text{M}]^+$ 202.1726.

(*E*)-1,3-Dimethyl-5-(oct-1-en-1-yl)benzene (137)



Prepared by general procedure 10, dichloroalane bis(tetrahydrofuran) (1.02 g, 4.20 mmol), bis(pentamethylcyclopentadienyl)zirconium dichloride (61 mg,

0.14 mmol), 1-octyne (410 μ L, 2.80 mmol), X-Phos (38 mg, 0.080 mmol), tris(dibenzylideneacetone)dipalladium(0)-chloroform adduct (31 mg, 0.030 mmol), 1,4-diazabicyclo[2.2.2]octane (157 mg, 1.40 mmol) and 5-bromo-*m*-xylene (368 mg, 2.00 mmol) afforded **137** (412 mg, 95%) as a colourless oil; R_F (pentane) 0.44.

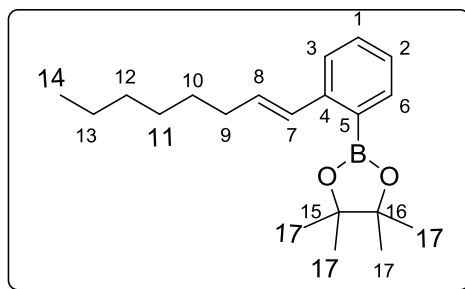
^1H NMR (400 MHz, CDCl_3): δ_{H} 0.93 (3H, t, $J = 7.0$ Hz, C^{16}H_3), 1.34 - 1.38 (6H, m, $\text{C}^{13}\text{H}_2\text{-C}^{15}\text{H}_2$), 1.50 - 1.55 (2H, m, C^{12}H_2), 2.21 (2H, dtd, $J = 7.5, 7.0, 1.0$ Hz, C^{11}H_2), 2.33 (6H, s, C^9H_3 & C^{10}H_3), 6.25 (1H, dt, $J = 16.0, 7.5$ Hz, C^8H), 6.37 (1H, dt, $J = 16.0, 1.0$ Hz, C^7H), 6.57 (1H, s, C^2H), 7.00 (2H, s, C^4H and C^6H).

^{13}C NMR (100.6 MHz, CDCl_3): δ_{C} 14.1 (C^{16}), 21.3 (C^9 and C^{10}), 22.6 (C^{15}), 28.9 (C^{14}), 29.4 (C^{13}), 31.8 (C^{12}), 33.0 (C^{11}), 123.8 (C^4 and C^6), 128.5 (C^8), 129.8 (C^2), 130.9 (C^7), 137.8 (C^5), 137.9 (C^1 and C^3).

IR (CHCl_3) ν_{max} : 3010, 2958, 2928, 2856, 1600, 1466, 1378, 966 cm^{-1} .

HRMS: (EI) $\text{C}_{16}\text{H}_{24}$ $[\text{M}]^+$ requires m/z 216.1878, found $[\text{M}]^+$ 216.1880.

(*E*)-4,4,5,5-Tetramethyl-2-(2-(oct-1-en-1-yl)phenyl)-1,3,2-dioxaborolane (138**)**



Prepared by general procedure 10, dichloroalane bis(tetrahydrofuran) (510 mg, 2.10 mmol), bis(pentamethylcyclopentadienyl)zirconium dichloride (45 mg, 0.10 mmol), 1-octyne (205 μ L, 1.40 mmol), X-Phos (19 mg, 0.040 mmol), tris(dibenzylideneacetone)dipalladium(0)-chloroform adduct (19 mg, 0.015 mmol), 1,4-diazabicyclo[2.2.2]octane (117 mg, 0.700 mmol) and 2-(2-bromophenyl)-4,4,5,5-tetramethyl-1,3,2-dioxaborolane (219 μ L, 1.00 mmol) afforded **138** (258 mg, 82%) as an orange oil; R_F (pentane/diethyl ether 9:1) 0.69.

^1H NMR (400 MHz, CDCl_3): δ_{H} 0.90 (3H, t, J = 7.0 Hz, C^{14}H_3), 1.29–1.33 (6H, m, C^{11}H_2 - C^{13}H_2), 1.36 (12H, s, C^{17}H_3), 1.44–1.54 (2H, m, C^{10}H_2), 2.19–2.26 (2H, m, C^9H_2), 6.16 (1H, dt, J = 16.0, 7.0 Hz, C^8H), 7.14–7.20 (2H, m, C^7H & C^6H), 7.32–7.38 (1H, m, C^2H), 7.54 (1H, d, J = 8.0 Hz, C^3H), 7.74 (1H, dd, J = 8.0, 1.0 Hz, C^1H)

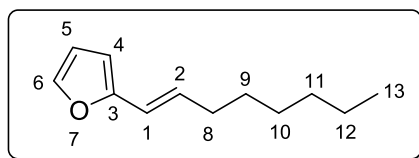
^{13}C NMR (100.6 MHz, CDCl_3): δ_{C} 14.1 (C^{14}), 22.6 (C^{13}), 24.9 (C^{17}), 28.9 (C^{11}), 29.1 (C^{10}), 31.8 (C^{12}), 33.1 (C^9), 83.6

(C15 and C16), 124.6 (C8), 125.8 (C7), 130.5 (C6), 130.8 (C2), 131.9 (C1), 135.8 (C3), 144.2 (C5), 191.9 (C4).

IR (CHCl₃) ν_{\max} : 2978, 2957, 2926, 2855, 1596, 1561, 1482, 1466, 1379, 1347, 1314, 1272, 1214, 1145, 1109, 1066, 1041 cm⁻¹.

HRMS: (ESI) C₂₀H₃₁¹⁰BO₂ [M+Na]⁺ requires m/z 337.2320, found [M+Na]⁺ 337.2319.

(*E*)-2-(Oct-1-en-1-yl)furan (139)



Prepared by general procedure 10, dichloroalane bis(tetrahydrofuran) (1.02 g, 4.20 mmol), bis(pentamethylcyclopentadienyl)zirconium dichloride (61 mg, 0.14 mmol), 1-octyne (410 μ L, 2.80 mmol), X-Phos (38 mg, 0.080 mmol), tris(dibenzylideneacetone)dipalladium(0)-chloroform adduct (31 mg, 0.030 mmol), 1,4-diazabicyclo[2.2.2]octane (157 mg, 1.40 mmol) and 2-bromofuran (180 μ L, 2.00 mmol) to afford **139** (291.6 mg, 78%) as a yellow oil; **R_F** (pentane) 0.48.

¹H NMR (400 MHz, CDCl₃): δ_{H} 0.95 (3H, t, J = 7.0 Hz, C¹³H₃), 1.35 - 1.40 (6H, m, C¹⁰H₂-C¹²H₂), 1.48 (2H, m, C⁹H₂), 2.21 (2H, dt, J = 8.5, 7.0 Hz, C⁸H₂), 6.10 (1H, d, J = 3.0 Hz, C⁴H),

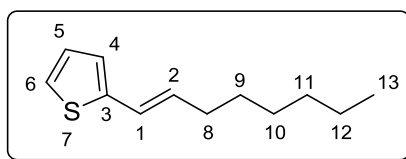
6.22 - 6.25 (2H, m, C¹H and C²H), 6.39 (1H, dd, $J = 3.0, 2.0$ Hz, C⁵H), 7.29 (1H, d, $J = 2.0$ Hz C⁶H).

¹³C NMR (100.6 MHz, CDCl₃): δ_{C} 14.1 (C13), 22.6 (C12), 28.9 (C11), 29.3 (C10), 31.8 (C9), 33.8 (C8), 105.8 (C4), 111.1 (C5), 118.4 (C2), 130.3 (C1), 141.3 (C6), 153.3 (C3).

IR (CHCl₃) ν_{max} : 2957, 2930, 2858, 1722, 1677, 1466, 1016 cm⁻¹.

HRMS: (EI) C₁₂H₁₈O [M]⁺ requires m/z 178.1358, found [M]⁺ 178.1358.

(*E*)-2-(oct-1-en-1-yl)thiophene (140**)**¹²⁵



Prepared by general procedure 10, dichloroalane bis(tetrahydrofuran) (1.02 g, 4.20 mmol), bis(pentamethylcyclopentadienyl)zirconium dichloride (61 mg, 0.14 mmol), 1-octyne (410 μ L, 2.80 mmol), X-Phos (38 mg, 0.080 mmol), tris(dibenzylideneacetone)dipalladium(0)-chloroform adduct (31 mg, 0.030 mmol), 1,4-diazabicyclo[2.2.2]octane (157 mg, 1.40 mmol) and 2-bromothiophene (190 μ L, 2.00 mmol) afforded **140** (280.5 mg, 72%) as a colourless oil; R_{F} = (pentane) 0.56.

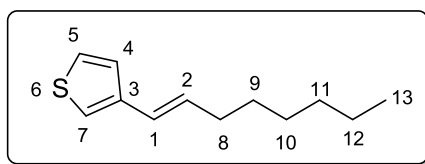
^1H NMR (400 MHz, CDCl_3): δ_{H} 0.92 (3H, t, $J = 7.0$ Hz, C^{13}H_3), 1.33 - 1.40 (6H, m, $\text{C}^{10}\text{H}_2\text{-C}^{12}\text{H}_2$), 1.48 - 1.52 (2H, m, C^9H_2), 2.19 (2H, dtd, $J = 7.5, 7.0, 1.5$ Hz, C^8H_2), 6.10 (1H, dt, $J = 16.0, 7.0$ Hz, C^2H), 6.53 (1H, ddt, $J = 16.0, 1.5, 1.0$ Hz, C^1H), 6.89 (1H, d, $J = 3.0$ Hz, C^4H), 6.96 (1H, dd, $J = 5.0, 3.0$ Hz, C^5H) 7.11 (1H, dt, $J = 5.0, 1.0$ Hz, C^6H).

^{13}C NMR (100.6 MHz, CDCl_3): δ_{C} 14.1 (C^{13}), 22.6 (C^{12}), 28.7 (C^{11}), 29.4 (C^{10}), 31.7 (C^9), 33.3 (C^8), 122.8 (C^2), 123.0 (C^6), 124.1 (C^4), 127.2 (C^5), 131.3 (C^1), 143.3 (C^3).

IR (CHCl_3) ν_{max} : 3074, 3009, 2958, 2929, 2857, 1466, 955 cm^{-1} ;

HRMS: (EI) $\text{C}_{12}\text{H}_{18}\text{S}$ $[\text{M}]^+$ requires m/z 194.1129, found $[\text{M}]^+$ 194.1123.

(*E*)-3-(Oct-1-en-1-yl)thiophene (141)



Prepared by general procedure 10, dichloroalane bis(tetrahydrofuran) (1.02 g, 4.20 mmol), bis(pentamethylcyclopentadienyl)zirconium dichloride (61 mg, 0.14 mmol), 1-octyne (410 μL , 2.80 mmol), X-Phos (38 mg, 0.080 mmol), tris(dibenzylideneacetone)dipalladium(0)-chloroform adduct (31 mg, 0.030 mmol), 1,4-

diazabicyclo[2.2.2]octane (157 mg, 1.40 mmol) and 3-bromothiophene (190 μ L, 2.00 mmol) afforded **141** (350.8 mg, 90%) as a colourless oil; R_F (pentane) 0.48.

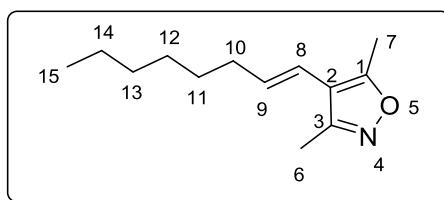
^1H NMR (400 MHz, CDCl_3): δ_{H} 0.92 (3H, t, $J = 7.0$ Hz, C^{13}H_3), 1.32 - 1.36 (6H, m, $\text{C}^{10}\text{H}_2\text{-C}^{12}\text{H}_2$), 1.47 - 1.50 (2H, m, C^9H_2), 2.19 (2H, dtd, $J = 7.0, 6.0, 1.5$ Hz, C^8H_2), 6.10 (1H, dt, $J = 16.0, 7.0$ Hz, C^2H), 6.41 (1H, dd, $J = 16.0, 3.0$ Hz, C^1H), 7.07 (1H, dd, $J = 3.0, 1.5$ Hz, C^7H), 7.21 (1H, dd, $J = 1.5, 0.5$ Hz, C^4H), 7.27 - 7.30 (1H, m, C^5H).

^{13}C NMR (100.6 MHz, CDCl_3): δ_{C} 14.1 (C^{13}), 22.6 (C^{12}), 28.9 (C^{11}), 29.3 (C^{10}), 31.7 (C^9), 32.9 (C^8), 120.2 (C^4), 123.9 (C^5), 124.9 (C^7), 125.7 (C^2), 131.2 (C^1), 143.3 (C^3).

IR (CHCl_3) ν_{max} : 3009, 2958, 2928, 2856, 1495, 963 cm^{-1} .

HRMS: (EI) $\text{C}_{12}\text{H}_{18}\text{S}$ $[\text{M}]^+$ requires m/z 194.1129, found $[\text{M}]^+$ 194.1131.

(*E*)-3,5-Dimethyl-4-(oct-1-en-1-yl)isoxazole (143)



Prepared by general procedure 10, dichloroalane bis(tetrahydrofuran) (510 mg, 2.10 mmol), bis(pentamethylcyclopentadienyl)zirconium dichloride (45 mg, 0.10 mmol), 1-octyne (205 μ L, 1.40 mmol), X-Phos (19 mg,

0.040 mmol), tris(dibenzylideneacetone)dipalladium(0)-chloroform adduct (15 mg, 0.015 mmol), 1,4-diazabicyclo[2.2.2]octane (117 mg, 0.700 mmol) and 4-bromo-3,5-dimethylisoxazole (119 μ L, 1.00 mmol) and indium trichloride (46 mg, 0.21 mmol) afforded **143** (161 mg, 78%) as a colourless oil; R_F (pentane) 0.25.

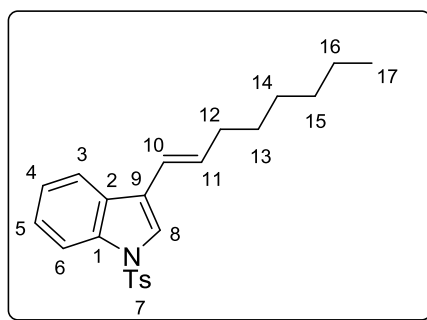
^1H NMR (400 MHz, CDCl_3): δ_{H} : 0.89 (3H, t, $J = 8.0$ Hz, C^{15}H_3), 1.26–1.37 (6H, m, $\text{C}^{12}\text{H}_2\text{--C}^{14}\text{H}_2$), 1.40–1.48 (2H, m, C^{11}H_2), 2.15–2.21 (2H, m, C^{10}H_2), 2.28 (3H, s, C^7H_3), 2.38 (3H, s, C^6H_3), 5.85 (1H, dt, $J = 16.0, 7.0$ Hz, C^9H), 6.00 (1H, dt, $J = 16.0, 1.0$ Hz, C^8H).

^{13}C NMR (100.6 MHz, CDCl_3): δ_{C} : 11.4 (C6), 11.6 (C7), 14.1 (C15), 22.6 (C14), 28.8 (C12), 29.4 (C11), 31.6 (C13), 33.6 (C10), 113.0 (C2), 117.3 (C8), 133.3 (C9), 158.3 (C3), 164.4 (C1)

IR (CHCl_3) ν_{max} : 2957, 2930, 2858, 1722, 1677, 1466, 1016 cm^{-1} .

HRMS: (EI) $\text{C}_{13}\text{H}_{21}\text{NO}$ $[\text{M}]^+$ requires m/z 207.1613, found $[\text{M}]^+$ 207.1623.

(*E*)-3-(Oct-1-en-1-yl)-1-tosyl-1H-indole (145)



Prepared by general procedure 10, dichloroalane bis(tetrahydrofuran) (766 mg, 3.15 mmol), bis(pentamethylcyclopentadienyl)zirconium dichloride (45 mg, 0.11 mmol), 1-octyne (310 μ L, 2.10 mmol), X-Phos (19 mg, 0.080 mmol), tris(dibenzylideneacetone)dipalladium(0)-chloroform adduct (16 mg, 0.015 mmol), 1,4-diazabicyclo[2.2.2]octane (117 mg, 1.05 mmol), indium (III) chloride (46 mg, 0.21 mmol) and *N*-tosyl-3-bromoindole (350 mg, 1.00 mmol) and quenching with Rochelle's salt (3 mL of saturated aqueous solution) afforded **145** (220 mg, 77%) as a yellow oil; **R_F** (pentane/diethyl ether 6:1) 0.51.

¹H NMR (400 MHz, CDCl₃): δ_{H} 0.94 (3H, t, J = 7.0 Hz, C¹⁷H₃), 1.43 - 1.47 (6H, m, C¹⁴H₂-C¹⁶H₂), 1.50 - 1.55 (2H, m, C¹³H₂), 2.25 (2H, dtd, J = 7.5, 7.0, 1.5 Hz, C¹²H₂), 2.35 (3H, s, CH₃(tosyl)), 6.30 (1H, dt, J = 16.0, 7.0 Hz, C¹¹H), 6.45 (1H, d, J = 16.0 Hz, C¹⁰H), 7.20 (2H, d, J = 8.5 Hz, CH(tol)) 7.30 - 7.40 (2H, m, C⁴H and C⁵H), 7.53 (1H, s, 1H, C⁸H), 7.70 (1H,

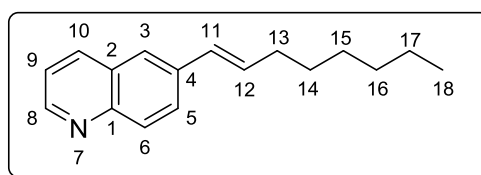
d, $J = 7.0$ Hz, C^3H), 7.80 (2H, d, $J = 8.5$ Hz, CH(tosyl)), 8.02 (1H, d, $J = 7.0$ Hz, C^6H).

^{13}C NMR (100.6 MHz, $CDCl_3$): δ_c 14.1 (C17), 21.5 (CH_3 (tosyl)), 22.6 (C16), 28.9 (C15), 29.4 (C14), 31.7 (C13), 33.5 (12), 113.7 (C6), 120.0 (C3), 120.3 (C4), 122.6 (C9), 123.3 (C10), 124.7 (C8), 126.8 (C5), 126.9 (CH(tosyl) and CH(tosyl)), 129.3 (C2), 129.8 (CH(tosyl) and CH(tosyl)), 132.9 (C11), 125.2 (CH(tosyl)), 135.5 (C1), 144.0 (CH(tosyl)).

IR ($CHCl_3$) ν_{max} : 3133, 3011, 2958, 2928, 2856, 1644, 1446, 1373, 1188, 976 cm^{-1} .

HRMS: (EI) $C_{23}H_{27}NO_2S$ $[M]^+$ requires m/z 381.1763, found $[M]^+$ 381.1770.

(*E*)-6-(Oct-1-en-1-yl)quinolone (146)



Prepared by general procedure 10, dichloroalane bis(tetrahydrofuran) (766 mg, 3.15 mmol), bis(pentamethylcyclopentadienyl)zirconium dichloride (45 mg, 0.11 mmol), 1-octyne (310 μ L, 2.10 mmol), X-Phos (38 mg, 0.080 mmol), tris(dibenzylideneacetone)dipalladium(0)-chloroform adduct (31 mg, 0.030 mmol), 1,4-diazabicyclo[2.2.2]octane (157 mg, 1.40 mmol), indium(III)

chloride (46 mg, 0.21 mmol) and 6-bromoquinoline (130 μ L, 1.00 mmol) and quenched with Rochelle's salt (3 mL of saturated aqueous solution) afforded **146** (226 mg, 94%) as a yellow oil; **R_F** (pentane/diethyl ether 1:1) 0.25.

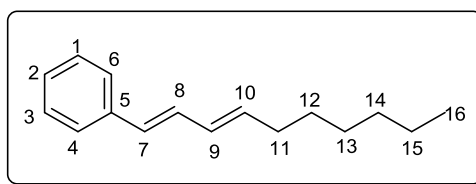
¹H NMR (400 MHz, CDCl₃): δ_{H} 0.94 (3H, t, J = 7.0 Hz, C¹⁸H₃), 1.38 - 1.42 (6H, m, C¹⁵H₂-C¹⁷H₂), 1.55 - 1.60 (2H, m, C¹⁴H₂), 2.31 (2H, dtd, J = 8.0, 7.0, 1.0 Hz, C¹³H₂), 6.45 (1H, dt, J = 16.0, 7.0 Hz, C¹²H), 6.58 (1H, d, J = 16.0 Hz, C¹¹H), 7.42 (1H, dd, J = 8.0, 4.0 Hz, C⁹H) 7.58 (1H, d, J = 1.5 Hz C³H), 7.87 (1H, d, J = 8.5 Hz, C⁵H) 8.10 (1H, d, J = 8.5 Hz, C⁶H), 8.18 (1H, d, J = 8.0 Hz, C⁸H), 8.85 (1H, dd, J = 4.0, 1.5 Hz, C¹⁰H).

¹³C NMR (100.6 MHz, CDCl₃): δ_{C} 14.1 (C18), 22.6 (C17), 31.3 (C16), 31.7 (C15), 33.1 (C14), 35.3 (C13), 124.3 (C9), 124.6 (C4), 128.0 (C6), 128.5 (C3), 129.0 (C2), 129.3 (C11), 132.5 (C12), 135.5 (C10), 136.2 (C5), 147.7 (C1), 149.6 (C8).

IR (CHCl₃) ν_{max} : 3011, 2959, 2929, 2857, 1500, 962 cm⁻¹.

HRMS: (EI) C₁₇H₂₁N [M]⁺ requires m/z 239.1674, found [M]⁺ 239.1675.

(1*E*,3*E*)-Deca-1,3-dien-1-ylbenzene (147**)**¹²⁶



Prepared by general procedure 10, dichloroalane bis(tetrahydrofuran) (1.02 g, 4.20 mmol), bis(pentamethylcyclopentadienyl)zirconium dichloride (61 mg, 0.14 mmol), 1-octyne (410 μ L, 2.80 mmol), X-Phos (38 mg, 0.080 mmol), tris(dibenzylideneacetone)dipalladium(0)-chloroform adduct (31 mg, 0.030 mmol), 1,4-diazabicyclo[2.2.2]octane (157 mg, 1.40 mmol), indium(III) chloride (69 mg, 0.28 mmol) and β -bromostyrene (260 μ L, 2.00 mmol) afforded **147** (271 mg, 63%) as a yellow oil; R_F (pentane) 0.46.

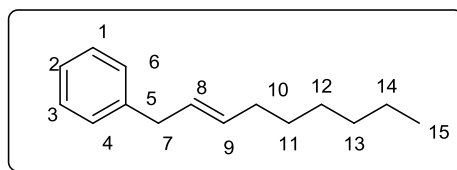
¹H NMR (400 MHz, CDCl₃): δ_H 0.91 (3H, t, J = 7.0 Hz, C¹⁶H₃), 1.31 - 1.35 (6H, m, C¹³H₂-C¹⁵H₂), 1.45 - 1.50 (2H, m, C¹²H₂), 2.17 (2H, dtd, J = 8.0, 7.0, 1.0 Hz, C¹¹H₂), 5.86 (1H, dt, J = 15.5, 7.0 Hz, C¹⁰H), 6.25 (1H, dd, J = 15.5, 11.0 Hz, C⁹H), 6.46 (1H, d, J = 15.5 Hz, C⁷H), 6.78 (1H, dd, J = 15.5, 11.0 Hz, C⁸H) 7.28 - 7.35 (5H, m, Ar).

¹³C NMR (100.6 MHz, CDCl₃): δ_C 14.1 (C16), 22.6 (C15), 29.4 (C14), 29.7 (C13), 31.7 (C12), 33.1 (C11), 125.4 (C4) and C6), 126.1 (C2), 128.2 (C1) and C3), 129.9 (C8), 130.4 (C7), 131.9 (C9), 131.3 (C10), 137.7 (C5).

IR (CHCl₃) ν_{max} : 2957, 2930, 2958, 1676, 1451, 1167, 970 cm⁻¹;

HRMS: (EI) C₁₆H₂₂ [M]⁺ requires m/z 214.1722, found [M]⁺ 214.1720.

(*E*)-Non-2-en-1-ylbenzene (148)



Prepared by general procedure 10, dichloroalane bis(tetrahydrofuran) (510 mg, 2.10 mmol), bis(pentamethylcyclopentadienyl)zirconium dichloride (45 mg, 0.10 mmol), 1-octyne (410 μ L, 1.40 mmol), X-Phos (19 mg, 0.040 mmol), tris(dibenzylideneacetone)dipalladium(0)-chloroform adduct (15 mg, 0.015 mmol), 1,4-diazabicyclo[2.2.2]octane (78 mg, 0.70 mmol), and benzylbromide (119 μ L, 1.00 mmol) afforded **148** (186 mg, 92%) as a colourless oil; **R_F** (pentane) 0.60.

¹H NMR (400 MHz, CDCl₃): δ_{H} 0.91 (3H, t, J = 7.0 Hz, C¹⁵H₃), 1.29–1.41 (8H, m, C¹¹H₂–C¹⁴H₂), 2.05 (2H, app dd, J = 14.0, 7.0 Hz, C¹⁰H₂), 3.35 (2H, d, J = 6.0 Hz, C⁷H₂), 5.49–5.62 (2H, m, C⁸H & C⁹H), 7.19–7.22 (3H, m, C¹H, C²H, C³H), 7.29–7.32 (2H, m, C⁴H & C⁶H).

^{13}C NMR (100.6 MHz, CDCl_3): δ_{C} 14.1 (C15), 22.6 (C14), 28.9 (C12), 29.5 (C11), 32.6 (C10), 34.2 (C13), 39.1 (C7), 126.9 (C2), 128.4 (C4 & C6), 128.6 (C1 & C3), 128.8 (C9), 132.3 (C8), 141.3 (C5).

IR (CHCl_3) ν_{max} : 3084, 3064, 3009, 2958, 2928, 2855, 1602, 1494, 1453, 969, 909 cm^{-1} ;

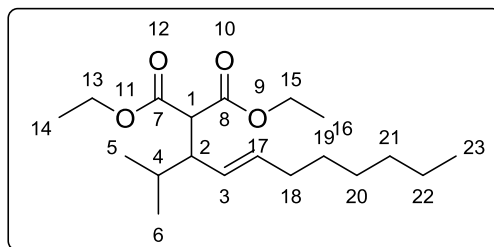
HRMS: (EI) $\text{C}_{15}\text{H}_{22}$ $[\text{M}]^+$ requires m/z 202.1728, found $[\text{M}]^+$ 202.1722.

General procedure 12: Zirconium-catalysed hydroalumination and conjugate addition

Dichloroalane *bis*(tetrahydrofuran) (243 mg, 1.00 mmol, 1.0 equiv.), decamethylzirconocene dichloride (22 mg, 0.05 mmol, 0.05 equiv.) and 1-octyne (206 μL , 1.40 mmol, 1.4 equiv.) and a stir bar were added to a Schlenk tube and mixture heated at 80 $^{\circ}\text{C}$ for 1.5 h. Excess 1-octyne and THF was removed *in vacuo* and the mixture diluted with anhydrous deoxygenated diethyl ether (1.0 mL). The mixture was cooled to 0 $^{\circ}\text{C}$ and alkylidene malonate (0.50 mmol, 0.5 equiv.) added in one portion. After stirring the mixture at 0 $^{\circ}\text{C}$ (2 h) it was quenched with water (3.0 mL) and phases separated. The aqueous phase was re-extracted with dichloromethane (3 x 3.0 mL) and the combined organics dried (sodium sulfate), filtered and concentrated to a crude oil. The product was

purified by column chromatography (silica: 9:1 cyclohexane/ethyl acetate).

(E)-Diethyl 2-(2-methylundec-4-en-3-yl)malonate (185)



Prepared according to general procedure 12 from diethyl 2-(2-methylpropylidene) malonate (108 μ L, 0.500 mmol) to yield **185** as a yellow oil (118 mg, 73%) R_F (cyclohexane/ ethyl acetate 9:1) 0.33.

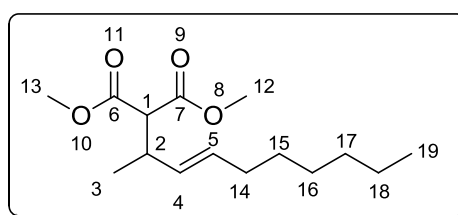
^1H NMR (400 MHz, CDCl_3): δ_{H} : 0.81–0.90 (9H, m, C^5H_3 , C^6H_3 and C^{23}H_3); 1.21–1.29 (14H, m, C^{19}H_2 – C^{22}H_2 , C^{14}H_3 and C^{16}H_3), 1.67–1.75 (1H, m C^4H), 1.96–2.00 (2H, m, C^{18}H_2); 2.61 (1H, td, $J = 10.0, 5.0$ Hz, C^2H); 3.48 (1H, d, $J = 10.0$ Hz, C^1H); 4.10–4.23 (4H, m, C^{13}H_2 & C^{15}H_2); 5.26 (1H, dd, $J = 15.0, 10.0$ Hz, C^3H); 5.47 (1H, dt, $J = 15.0, 7.0$ Hz, C^{17}H).

^{13}C NMR (100 MHz, CDCl_3) δ_{C} : 14.2 (C^{14}), 14.3 (C^{16}), 17.6 (C^{23}), 21.7 (C^5 and C^6), 22.8 (C^{20}), 28.9 (C^{21}), 29.3 (C^{22}), 29.6 (C^4), 31.8 (C^{19}), 32.7 (C^{18}), 49.3 (C^2), 55.6 (C^1), 61.1 (C^{13}), 61.4 (C^{15}), 125.9 (C^3), 135.2 (C^{17}), 168.8 and 169.9 (C^7 and C^8).

IR (CHCl₃) ν_{max} : 3045, 2962, 2929, 2573, 2356, 1749, 1726 (C=O), 1466, 1388, 1301, 1178 cm⁻¹.

HRMS: (EI) C₁₉H₃₄O₄ [M]⁺ requires m/z 326.2457, found [M]⁺ 326.2454.

(E)-Dimethyl 2-(dec-3-en-2-yl)malonate (181)



Prepared according to general procedure 12 from dimethyl 2-ethylidenemalonate (79.1 mg, 0.500 mmol) to yield **181** as a colourless oil (103 mg, 76%), **R_F** (cyclohexane/ethyl acetate 9:1) 0.44.

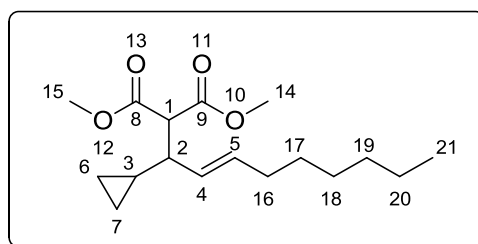
¹H NMR (400 MHz, CDCl₃) δ_{H} : 0.86 (3H, t, J = 7.0 Hz, C¹⁹H₃), 1.05 (3H, d, J = 7.0 Hz, C³H₃), 1.20–1.36 (8H, m, C¹⁵H₂–C¹⁸H₂), 1.93 (2H, dt, J = 7.5, 7.0 Hz, C¹⁴H₂), 2.88 – 2.95 (1H, m, C²H), 3.25 (1H, d, J = 9.0 Hz, C¹H), 3.67 (3H, s, C¹²H), 3.71 (3H, s, C¹³H), 5.29 (1H, dd, J = 15.0, 8.0 Hz, C⁴H), 5.49 (dt, 1H, J = 15.5, 7.5 Hz, C⁵H).

¹³C NMR (100 MHz, CDCl₃) δ_{C} : 14.1 (C¹⁹), 18.7 (C³), 22.6 (C¹⁸), 28.7 (C¹⁷), 29.4 (C¹⁶), 31.7 (C¹⁵), 32.4 (C¹⁴), 37.5 (C²), 52.1 (C¹²); 52.3 (C¹³), 58.1 (C¹); 131.1 (C⁵), 132.0 (C⁴), 168.7 and 168.9 (C⁶ & C⁷).

IR (CHCl₃) ν_{max} : 3042, 2957, 2929, 2856, 2434, 2412, 1753, 1732 (C=O), 1521, 1424 cm⁻¹.

HRMS: (EI+) C₁₅H₂₆O₄ requires m/z 270.1831, found [M]⁺ 270.1822.

(E)-Dimethyl 2-(1-cyclopropylnon-2-en-1-yl)malonate (186)



Prepared according to general procedure 12 from dimethyl 2-(cyclopropylmethylene) malonate (92.1 mg, 0.500 mmol) to yield **186** as a colourless oil (126 mg, 85%) **R_F** (cyclohexane/ethyl acetate 9:1) 0.39

¹H NMR (400 MHz, CDCl₃): δ_{H} : 0.06–0.13 (1H, m, C⁶H or C⁷H), 0.17–0.23 (1H, m, C⁶H or C⁷H), 0.42–0.46 (2H, m, C⁶H or C⁷H), 0.79–0.84 (1H, m, C³H), 0.87 (3H, t, J = 7.0 Hz, C²¹H₃), 1.23–1.32 (8H, m, C¹⁷H₂–C²⁰H₂), 1.94–1.99 (2H, m, C¹⁶H₂), 2.07–2.13 (1H, m, C²H), 3.49 (1H, d, J = 9.0 Hz, C¹H), 3.69 (3H, s, C¹⁴H₃), 3.75 (3H, s, C¹⁵H₃), 5.35 (1H, ddt, J = 15.0, 8.0, 1.0 Hz, C⁴H), 5.48 (1H, dt, J = 15.0, 6.0 Hz, C⁵H).

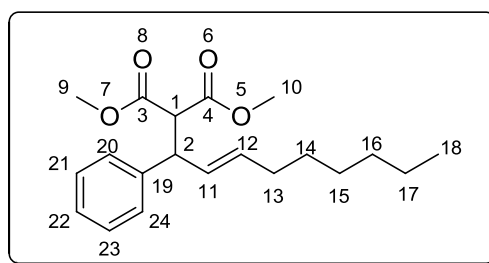
¹³C NMR (100 MHz, CDCl₃) δ_{C} : 3.2 and 4.8 (C6), 14.1 (C21), 14.2 (C3), 22.7 (C20), 28.8 (C19), 29.5 (C18), 31.8 (C17),

32.6 (C16), 47.6 (C2), 52.3 (C14), 52.4 (C15), 57.4 (C1), 128.8 (C4), 133.3 (C5), 168.8, (C8), 169.1 (C9).

IR (CHCl₃) ν_{max} : 3082, 3007, 2955, 2928, 2872, 2856, 1753, 1733 (C=O), 1435, 1336 cm⁻¹.

HRMS: (EI) C₁₇H₂₈O₄ [M]⁺ requires m/z 296.1988; found [M]⁺ 296.1977.

(E)-Dimethyl 2-(1-phenylnon-2-en-1-yl)malonate (189)



Prepared according to general procedure 12 from dimethyl 2-benzylidenemalonate (110 mg, 0.500 mmol) to yield **189** as a yellow oil (105 mg, 63%) **R_F** (cyclohexane/ ethyl acetate 9:1) 0.25.

¹H NMR (400 MHz, CDCl₃): δ_{H} : 0.86 (3H, t, J = 7.0 Hz, C¹⁸H₃), 1.21–1.29 (8H, m, C¹⁴H²-C¹⁷H²), 1.93–1.98 (2H, m, C¹³H₂), 3.48 (3H, s, C⁹H₃), 3.72 (3H, s, C¹⁰H₃), 3.82 (1H, d, J = 11.0 Hz, C¹H), 4.02–4.07 (1H, m, C²H), 5.55–5.57 (2H, m, C¹¹H and C¹²H), 7.20–7.22 (3H, m, C²¹H-C²³H), 7.26–7.29 (2H, m, C²⁰H and C²⁴H).

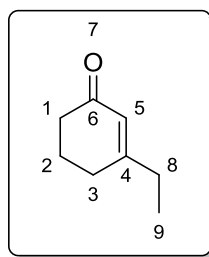
¹³C NMR (100 MHz, CDCl₃): δ_{C} : 14.2 (C18), 22.7 (C17), 28.8 (C16), 29.4 (C15), 31.8 (C14), 32.6 (C13), 49.2 (C2), 52.5

(C9), 52.6 (C10), 58.1 (C1), 127.0 (C22), 127.9 (C20 and C24), 128.7 (C20 and C24), 129.3 (C11), 133.4 (C12), 141.0 (C19), 168.1 (C3), 168.4 (C4).

IR (CHCl_3) ν_{max} : 3006, 2955, 2929, 2856, 1756, 1735 ($\text{C}=\text{O}$), 1454, 1435, 1318, 1260 cm^{-1} .

HRMS: (EI) $\text{C}_{20}\text{H}_{28}\text{O}_4$ $[\text{M}]^+$ requires m/z 332.1988, found $[\text{M}]^+$ 332.1994.

3-Ethylcyclohex-2-enone (**8**)¹²⁷



A flame-dried flask was charged with ethylmagnesium bromide (3.60 mL, 10.0 mmol) and cooled to 0 °C. The ethoxycyclohex-2-en-1-one (726 μL , 5.00 mmol) in tetrahydrofuran (4 mL) was added dropwise. Once the addition was complete the reaction mixture was left at room temperature until complete disappearance of the starting material (1 h). The reaction was hydrolyzed by addition of aqueous sulfuric acid (5% w/w). Diethyl ether (5 mL) was added and the aqueous phase was separated and extracted further with diethylether (3 x 5 mL). The combined organic fractions were washed with aqueous sodium bicarbonate,

brine and water, dried over sodium sulfate, filtered and concentrated in *vacuo*. The oily residue was purified by column chromatography to yield **8** as a yellow oil (579 mg, 93%); **R_F** (pentane/diethyl ether 4:1) 0.50.

¹H NMR (400 MHz, CDCl₃) δ_{H} : 1.13 (3H, t, J = 7.5 Hz, C⁹H₃), 1.95-2.01 (2H, m, C²H₂), 2.20-2.30 (4H, m, C⁸H₂ & C³H₂), 2.35 (2H, app t, J = 6.5 Hz, C¹H₂), 5.87 (1H, app t, J = 1.3 Hz, C⁵H).

¹³C NMR (100 MHz, CDCl₃) δ_{C} : 11.2 (C₉), 22.7 (C₂), 29.7 (C₈), 30.9 (C₃), 37.4 (C₁), 124.5 (C₅), 168.0 (C₄), 200.0 (C₆).

HRMS: (ESI) C₈H₁₂ONa [M+Na]⁺ requires 147.0764, found [M+Na]⁺ 147.0761.

IR (CHCl₃) ν_{max} : 2937, 1668, 1625, 1458, 1428, 1283, 1192, 887 cm⁻¹

General procedure 13: volatile alkyne hydroalumination and conjugate addition

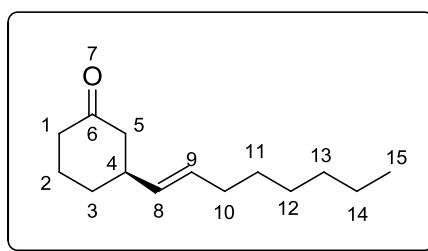
A 1.5 mL vial (glass screw cap vial, 854171, Supelco) was charged with decamethylzirconocene dichloride (21.6 mg, 0.050 mmol, 0.05 equiv.) and dichloroalane *bis*(tetrahydrofuran) (340 mg, 1.40 mmol, 1.4 equiv.) under an inert atmosphere. Neat alkyne (1.00 mmol) and tetrahydrofuran (1.0 mL) were injected through the septum (9mm AG3 CenterGuide, CR246713, Varian) and mixture was

heated for 2 h at 80 °C. The solution was transferred to a flame-dried Schlenk tube and solvent removed *in vacuo* and replaced with toluene (1.0 mL). To this was added methyllithium (330 µL, 0.650 mmol, 2 M in diethyl ether) and the mixture stirred for 30 min. In a Radleys carousel tube, copper(I) thiophenecarboxylate (9.50 mg, 0.05 mmol) and ligand **L3** (48 mg, 0.075 mmol) were dissolved in *t*-butylmethyl ether (1.0 mL) and stirred for 15 mins. The alane mixture was transferred to the copper mixture *via* syringe and enone (0.5 mmol) in toluene (0.5 mL) was added over 0.5 h. The reaction was stirred for a further 0.5 h at 25 °C and then quenched with water and hydrochloric (1 M). The organic layer was separated and the aqueous phase was extracted with dichloromethane (3 x 5 mL). The combined organic phases were dried (sodium sulfate), filtered, and concentrated. The crude was purified by flash chromatography (pentane/diethyl ether 4:1).

General procedure 14: Zirconium-catalysed hydroalumination and conjugate addition (neat conditions)

A dried Schlenk tube was charged dichloroalane bis(tetrahydrofuran) (158 mg, 0.650 mmol), decamethylzirconocene dichloride (14.0 mg, 0.030 mmol) and 1-octyne (134 μ L, 1.40 mmol) and the mixture melted at 80 °C for 1.5 h. The excess alkyne was removed under vacuum (0.1 mmHg). The resulting alane was diluted with toluene (1.0 mL) and methyllithium added (330 μ L, 0.650 mmol, 2M in diethyl ether) and the mixture stirred for 30 min. In a Radleys carousel tube, copper(I) thiophenecarboxylate (9.50 mg, 0.050 mmol) and ligand **L3** (48 mg, 0.075 mmol) were and stirred for 15 mins in *t*-butylmethyl ether (1.0 mL). The previously prepared alane mixture was transferred to the copper(I) thiophenecarboxylate/**L3** catalyst *via* syringe and enone (0.5 mmol) in toluene (0.5 mL) was added over 0.5 h. The reaction was stirred for a further 0.5 h at 25 °C and then quenched with water and hydrochloric acid (1 M). The organic layer was separated and the aqueous phase was extracted with dichloromethane (3 x 5 mL). The combined organic phases were dried (sodium sulfate), filtered, and concentrated. The crude was purified by flash chromatography (pentane/diethyl ether 4:1).

(S)-(E)-3-(Oct-1-en-1-yl)cyclohexanone (192)¹²⁸



Prepared according to general procedure 14 from 1-octyne (134 μ L, 1.40 mmol) and cyclohexenone (48 μ L, 0.50 mmol) to yield **192** as a colourless oil in 88% ee. (68 mg, 65%,) **R_F** (pentane/diethyl ether 4:1) 0.56.

¹H NMR δ_{H} : 0.83 (3H, t, J = 7.0 Hz, C¹⁵H₃), 1.20–1.32 (8H, m, C¹¹H₂–C¹⁴H₂), 1.39–1.49 (1H, m, c-hex), 1.58–1.69 (1H, m, c-hex), 1.83–1.92 (1H, m, c-hex), 1.91–2.02 (3H, m, c-hex), 2.11–2.17 (1H, m, c-hex), 2.19–2.25 (1H, m, c-hex), 2.26–2.44 (3H, m, c-hex and C¹⁰H₂), 5.31 (1H, dd, J = 16.0, 6.0 Hz, C⁸H), 5.38 (1H, dt, J = 16.0, 6.5 Hz, C⁹H).

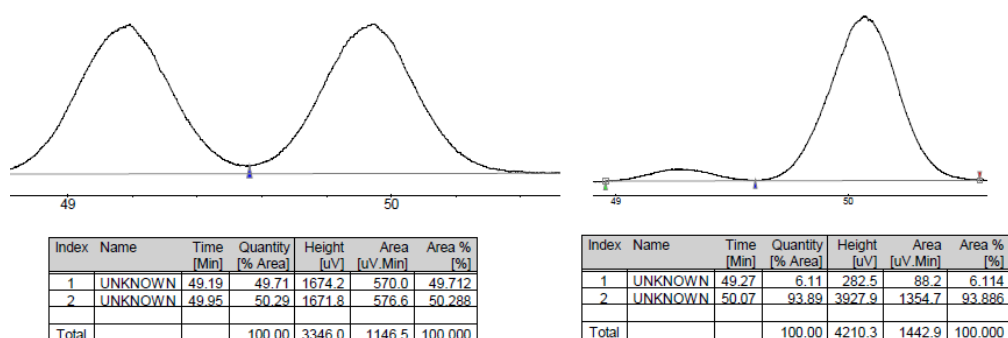
¹³C NMR δ_{C} : 14.1 (C15), 22.6 (C2), 25.0 (C14), 28.8 (C12), 29.4 (C11), 31.6 (C3), 31.7 (C13), 32.5 (C10), 41.3 (C1), 41.6 (C4), 47.7 (C5), 130.0 (C9), 133.0 (C8), 211.4 (C6).

IR (CHCl₃) ν_{max} : 2956, 2927, 2855, 1713, 1455, 1226, 975, 737 cm⁻¹.

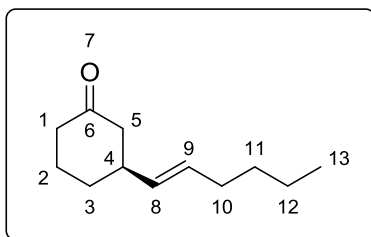
HRMS: (EI) C₁₄H₂₄O [M]⁺ requires m/z 208.1827, found [M]⁺ 208.1833.

GC: (Lipodex A); $T_{\text{inj}} = 250\text{ }^{\circ}\text{C}$, $T_{\text{det}} = 250\text{ }^{\circ}\text{C}$, flow = 2.0 mL min⁻¹, $t_i = 75\text{ }^{\circ}\text{C}$ (7 min), $(5\text{ }^{\circ}\text{C min}^{-1}) t_f = 115\text{ }^{\circ}\text{C}$ (90 min), $(0.7\text{ }^{\circ}\text{C min}^{-1}) t_f = 140\text{ }^{\circ}\text{C}$: (*R*)-enantiomer: $t_R = 49.19\text{ min}$; (*S*)-enantiomer: $t_R = 49.95\text{ min}$.

$[\alpha]_D^{25}$: +104.9 ($c = 2.00$, CHCl₃).



(*S*)-(E)-3-(Hex-1-en-1-yl)cyclohexanone (193)¹²⁹



Prepared according to general procedure 13 from 1-hexyne (91 μL , 0.75 mmol) and cyclohexenone (48 μL , 0.50 mmol) to yield **193** as a colourless oil in 90% ee. (62 mg, 69%) R_F (pentane/diethyl ether 4:1) 0.58.

¹H NMR (CDCl₃) δ_H : 0.87 (3H, t, $J = 7.0\text{ Hz}$, C¹³H₃), 1.25–1.33 (4H, m, C¹¹H₂ & C¹²H₂), 1.42–1.51 (1H, m, c-hex), 1.61–1.71 (1H, m, c-hex), 1.85–1.90 (1H, m, c-hex), 1.96–1.99

(2H, m, C¹⁰H₂), 2.01–2.06 (1H, m, *c*-hex), 2.14–2.28 (2H, m, *c*-hex), 2.30–2.41 (3H, m, *c*-hex), 5.34 (1H, dd, *J* = 15.0, 6.0 Hz, C⁸H), 5.41 (1H, dt, *J* = 15.0, 6.0 Hz, C⁹H).

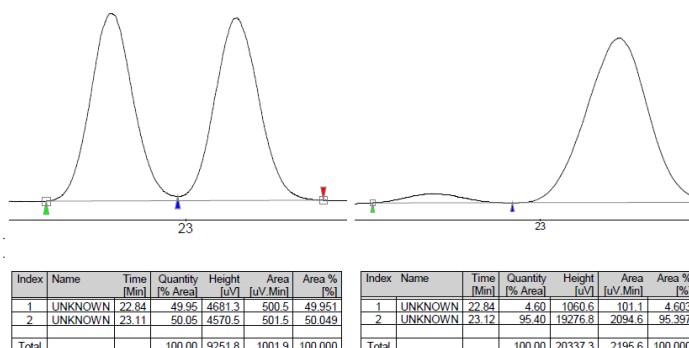
¹³C NMR (CDCl₃) δ_C: 14.0 (C13), 22.2 (C12), 25.1 (C2), 31.6 (C11), 31.7 (C3), 32.3 (C10), 41.4 (C4), 41.7 (C1), 47.8 (C5), 130.1 (C9), 133 (C8), 211.8 (C6).

IR (CHCl₃) ν_{max}: 2956, 2927, 2855, 1713, 1455, 1226, 975, 737 cm⁻¹.

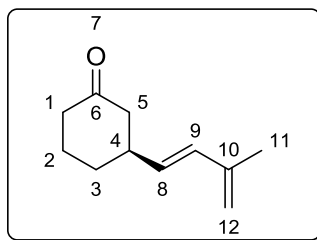
HRMS: (EI) C₁₂H₂₀O [M]⁺ requires *m/z* 180.1514, found [M]⁺ 180.1511.

GC: (Lipodex A); *T*_{inj} = 250 °C, *T*_{det} = 250 °C, flow = 2.0 mL min⁻¹, *t*_i = 75 °C (7 min), (5 °C min⁻¹) *t*_f = 115 °C (90 min), (0.7 °C min⁻¹) *t*_f = 140 °C: (*R*)-enantiomer: *t*_R = 22.84 min; (*S*)-enantiomer: *t*_R = 23.12 min.

[α]_D²⁵: -7.8 (*c* = 2.00, CHCl₃).



(S)-(E)-3-(3-Methylbuta-1,3-dien-1-yl)cyclohexanone
(194)¹³⁰



Prepared according to general procedure 13 from 2-methyl-1-buten-3-yne (71 μ L, 0.75 mmol) and cyclohexenone (48 μ L, 0.50 mmol) to yield **194** as a colourless oil in 90% ee. (57.5 mg, 70%) **R_F** (pentane/diethyl ether 4:1) 0.35.

¹H NMR (CDCl₃) δ_{H} : 1.49–1.59 (1H, m, c-hex), 1.64–1.76 (1H, m, c-hex), 1.83 (3H, s, C¹¹H₃), 1.92–1.97 (1H, m, c-hex), 2.04–2.10 (1H, m, c-hex), 2.20–2.30 (2H, m, c-hex), 2.36–2.40 (1H, m, c-hex), 2.43–2.48 (1H, m, c-hex), 2.52–2.61 (1H, m, c-hex), 4.92 (2H, app. s, C¹²H₂), 5.58 (1H, dd, J = 16.0, 7.0 Hz, C⁸H), 6.14 (1H, d, J = 16.0 Hz, C⁹H).

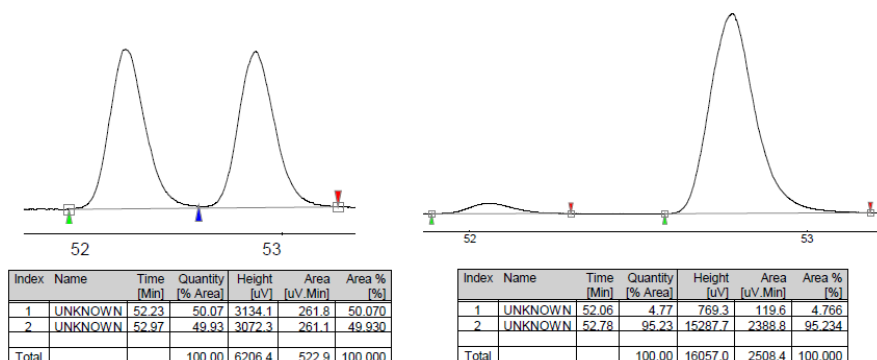
¹³C NMR (CDCl₃) δ_{C} : 18.6 (C11), 25.0 (C2), 31.5 (C3), 41.3 (C4), 41.7 (C1), 47.4 (C5), 115.8 (C12), 132.0 (C8), 132.8 (C9), 141.6 (C10), 210.9 (C6).

IR (CHCl₃) ν_{max} : 3083, 2942, 1707, 1608, 1448 cm⁻¹.

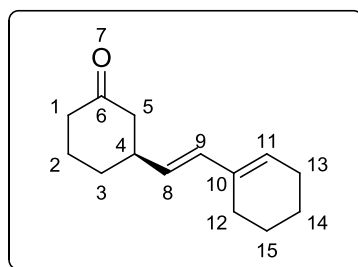
HRMS: (EI) C₁₁H₁₆O [M]⁺ requires m/z 164.1201, found [M]⁺ 164.1199.

GC: (Lipodex A); $T_{\text{inj}} = 250\text{ }^{\circ}\text{C}$, $T_{\text{det}} = 250\text{ }^{\circ}\text{C}$, flow = 2.0 mL min⁻¹, $t_i = 50\text{ }^{\circ}\text{C}$, (1.0 $^{\circ}\text{C min}^{-1}$) $t_f = 160$ (30 min): (*R*-enantiomer: $t_R = 38.56$ min; (*S*)-enantiomer: $t_R = 38.70$ min.

$[\alpha]_{\text{D}}^{25}$: -5.2 ($c = 2.00$, CHCl_3).



(*S*)-(E)-3-(2-(Cyclohex-1-en-1-yl)vinyl)cyclohexanone (195)



Prepared according to general procedure 13 from 1-ethynylcyclohexene (88 μL , 0.75 mmol) and cyclohexenone (48 μL , 0.50 mmol) to yield **195** as a colourless oil in 82% ee. (41 mg, 40%) R_F (pentane/diethyl ether 4:1) 0.31.

$^1\text{H NMR}$ (CDCl_3) δ_{H} : 1.50 - 1.54 (1H, m, c-hex), 1.56 - 1.68 (5H, m, c-hex), 1.89 - 1.96 (1H, m, c-hex), 2.06 - 2.11 (5H, m, c-hex), 2.18 - 2.31 (2H, m, c-hex), 2.32 - 2.39 (1H, m, c-hex), 2.41 - 2.46 (1H, m, c-hex), 2.49 - 2.55 (1H, m, c-hex),

5.46 (1H, dd, $J = 16.0, 7.0$ Hz, C⁸H), 5.69 (1H, app. s, C¹¹H),
6.02 (1H, d, $J = 16.0$ Hz, C⁹H).

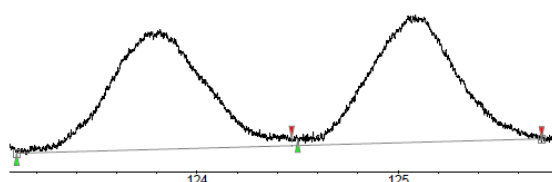
¹³C NMR (CDCl₃) δ_C : 22.6 (C15), 22.7 (C2), 24.7 (C14), 25.2 (C13), 25.9 (C12), 31.8 (C3), 41.2 (C4), 42.0 (C1), 47.8 (C5), 128.8 (C11), 129.0 (C9), 132.8 (C8), 135.3 (C10), 211.4 (C6).

IR (CHCl₃) ν_{\max} : 3011, 2935, 2861, 2837, 1706, 1448 cm⁻¹.

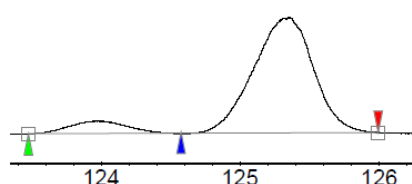
HRMS: (EI) C₁₄H₂₀O [M]⁺ requires m/z 204.1514, found [M]⁺ 204.1522.

GC: (Lipodex A); $T_{\text{inj}} = 250$ °C, $T_{\text{det}} = 250$ °C, flow = 2.0 mL min⁻¹, $t_i = 75$ °C (7 min), (5 °C min⁻¹) $t_f = 115$ °C (90 min), (0.7 °C min⁻¹) $t_f = 140$ °C: (*R*)-enantiomer: $t_R = 123.96$ min; (*S*)- enantiomer: $t_R = 125.36$ min.

[α]_D²⁵: +5.5 ($c = 2.00$, CHCl₃).



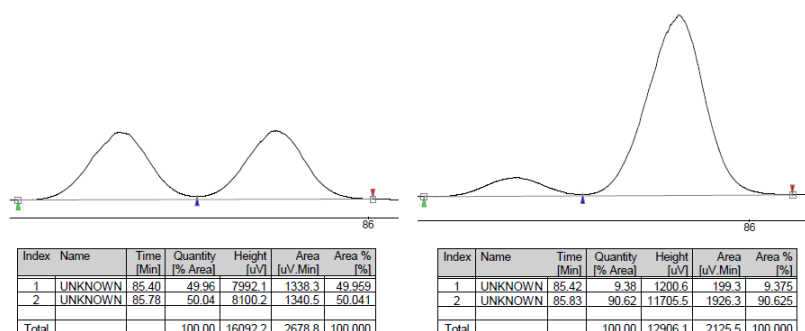
Index	Name	Time [Min]	Quantity [% Area]	Height [uV]	Area [uV.Min]	Area % [%]
1	UNKNOWN	123.82	50.61	284.9	159.2	50.612
2	UNKNOWN	125.09	49.39	310.8	155.3	49.388
Total			100.00	595.7	314.5	100.000



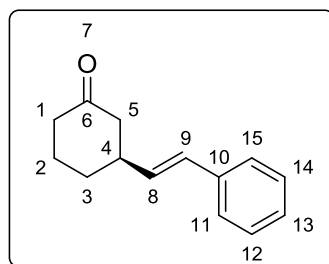
Index	Name	Time [Min]	Quantity [% Area]	Height [uV]	Area [uV.Min]	Area % [%]
1	UNKNOWN	123.96	9.23	586.8	280.0	9.228
2	UNKNOWN	125.36	90.77	5541.3	2753.9	90.772
Total			100.00	6128.2	3033.9	100.000

GC: (Lipodex A); $T_{\text{inj}} = 250\text{ }^{\circ}\text{C}$, $T_{\text{det}} = 250\text{ }^{\circ}\text{C}$, flow = 2.0 mL min^{-1} , $t_i = 50\text{ }^{\circ}\text{C}$, $(1.0\text{ }^{\circ}\text{C min}^{-1}) t_f = 160$ (30 min): (*R*)-enantiomer: $t_R = 85.42\text{ min}$; (*S*)-enantiomer: $t_R = 85.83\text{ min}$.

$[\alpha]_D^{25}$: +3.6 ($c = 2.00$, CHCl_3).



(*S*)-(*E*)-3-Styrylcyclohexanone (**197**)



Prepared according to general procedure 13 from phenylacetylene (82 μL , 0.75 mmol) and cyclohexenone (48 μL , 0.50 mmol) to yield **197** as a colourless oil in 80% ee. (52 mg, 52%) R_F (pentane/diethyl ether 4:1) 0.36.

$^1\text{H NMR}$ (CDCl_3) δ_H : 1.60–1.67 (1H, m, c-hex), 1.70–1.80 (1H, m, c-hex), 1.99–2.06 (1H, m, c-hex), 2.07–2.14 (1H, m, c-hex), 2.27–2.45 (3H, m, c-hex), 2.51–2.56 (1H, m, c-hex), 2.66–2.70 (1H, m, c-hex), 6.16 (1H, dd, $J = 16.0, 7.0\text{ Hz}$,

C⁸H), 6.39 (1H, d, $J = 16.0$ Hz, C⁹H), 7.21–7.24 (1H, m, C¹³H), 7.29–7.36 (4H, m, C¹¹H, C¹²H, C¹⁴H, C¹⁵H).

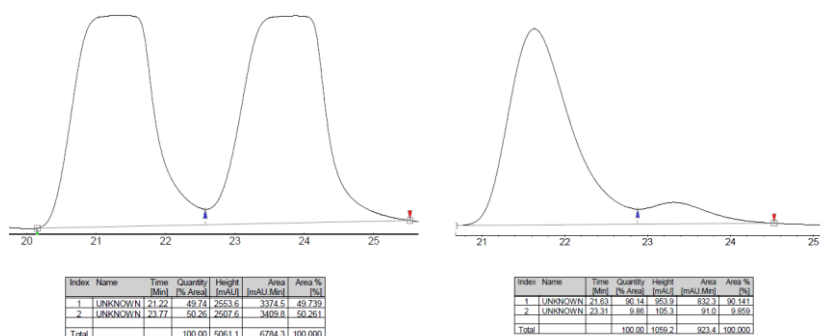
¹³C NMR (CDCl₃) δ_c : 25.1 (C2), 31.5 (C3), 41.4 (C1), 42.1 (C4), 47.5 (C5), 126.3 (C11 and C15), 127.5 (C13), 129.2 (C12 & C14), 129.7 (C9), 133.0 (C8), 137.2 (C10), 211.1 (C6).

IR (CHCl₃) ν_{\max} : 3402, 3058, 3026, 2936, 2865, 1711, 1598, 1493, 1448, 1223 cm⁻¹.

HRMS: (EI) C₁₄H₁₆O [M]⁺ requires m/z 200.1201, found [M]⁺ 200.1203.

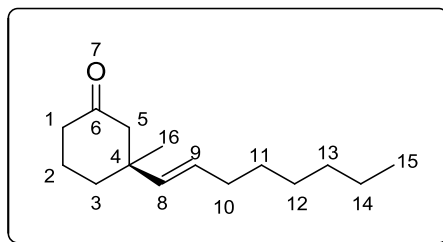
HPLC: (Chircel OD-H); eluent 2% isopropanol/hexane, 1.0 mL/min, 254 nm: (*S*)-enantiomer: $t_R = 21.6$ min; (*R*)-enantiomer: $t_R = 23.3$ min.

$[\alpha]_D^{25}$: +85.5 ($c = 2.00$, CHCl₃).



(S)-(E)-3-Methyl-3-(oct-1-en-1-yl)cyclohexanone (198)

132



Prepared according to general procedure 14 from 1-octyne (134 μL , 1.40 mmol) and 3-methyl-cyclohexenone (55 μL , 0.50 mmol) to yield **198** as a colourless oil in 94% ee. (59 mg, 53%) **R_F** (pentane/diethyl ether 4:1) 0.44.

¹H NMR (CDCl_3) δ_{H} : 0.87 (3H, t, $J = 7.0$ Hz, C^{15}H_3), 1.04 (3H, s, C^{16}H_3), 1.25–1.31 (8H, m, $\text{C}^{11}\text{H}_2\text{--C}^{14}\text{H}_2$), 1.57–1.62 (1H, m, c-hex), 1.66–1.72 (1H, m, c-hex), 1.79–1.86 (2H, m, c-hex), 1.94–1.99 (2H, m, c-hex), 2.14 (1H, d, $J = 14.0$ Hz, C^5H), 2.19–2.32 (2H, m, C^{10}H_2), 2.42 (1H, dt, $J = 14.0, 1.5$ Hz, C^5H), 5.28 (1H, d, $J = 16.0$ Hz, C^8H), 5.35 (1H, dt, $J = 16.0, 6.0$ Hz, C^9H).

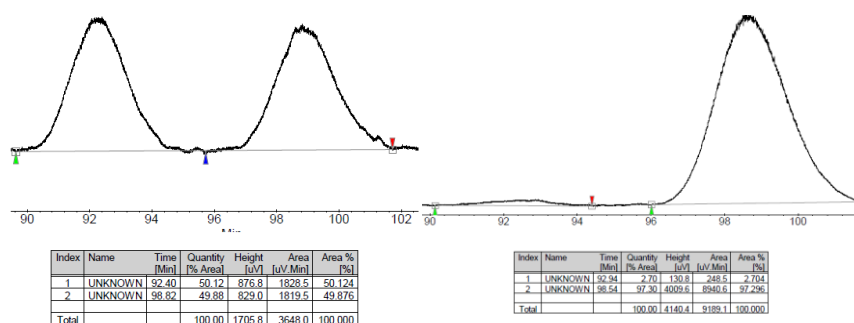
¹³C NMR (CDCl_3) δ_{C} : 14.2 (C^{15}), 22.3 (C^2), 22.7 (C^{14}), 28.2 (C^{16}), 28.8 (C^{12}), 29.5 (C^{11}), 31.7 (C^{13}), 32.8 (C^{10}), 37.2 (C^3), 40.9 (C^4), 41.0 (C^1), 52.4 (C^5), 128.9 (C^9), 137.7 (C^8), 211.9 (C^6).

IR (CHCl_3) ν_{max} : 2956, 2927, 2855, 1713, 1455, 1226, 975, 737 cm^{-1} .

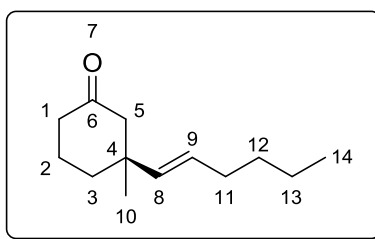
HRMS: (EI) $\text{C}_{15}\text{H}_{26}\text{O}$ $[\text{M}]^+$ requires m/z 222.1984, found $[\text{M}]^+$ 222.1980.

GC: (octakis(2,6-di-*O*-methyl-3-*O*-pentyl- γ -cyclodextrin); $T_{\text{inj}} = 250\text{ }^{\circ}\text{C}$, $T_{\text{det}} = 250\text{ }^{\circ}\text{C}$, flow = 2.0 mL min^{-1} , $t_i = 75\text{ }^{\circ}\text{C}$ (7 min), ($5\text{ }^{\circ}\text{C min}^{-1}$) $t_f = 115\text{ }^{\circ}\text{C}$ (90 min), ($0.7\text{ }^{\circ}\text{C min}^{-1}$) $t_f = 170\text{ }^{\circ}\text{C}$ (*R*)- enantiomer: $t_R = 92.94\text{ min}$; (*S*)-enantiomer: $t_R = 98.54\text{ min}$.

$[\alpha]_D^{25}$: +12.7 ($c = 2.00$, CHCl_3).



(*S*)-(*E*)-3-(Hex-1-en-1-yl)-3-methylcyclohexanone
(199)¹³³



Prepared according to general procedure 13 from 1-hexyne (91 μL , 0.75 mmol) and 3-methyl-cyclohexenone (55 μL , 0.50 mmol) to yield **199** as a colourless oil in 92% ee. (66 mg, 68%) R_F (pentane/diethyl ether 4:1) 0.47.

$^1\text{H NMR}$ (CDCl_3) δ_H : 0.90 (3H, t, $J = 7.0\text{ Hz}$, C^{14}H_3), 1.06 (3H, s, C^{10}H), 1.28–1.38 (4H, m, C^{12}H_2 & C^{13}H_2), 1.57–1.65 (1H, m, c-hex), 1.65–1.74 (1H, m, c-hex), 1.81–1.90 (2H, m, c-

hex), 1.97–2.02 (2H, m, c-hex), 2.17 (1H, d, $J = 14.0$ Hz, C^5H), 2.22–2.33 (2H, m, $C^{11}H_2$), 2.44 (1H, dt, $J = 14.0, 1.0$ Hz, C^5H), 5.30 (1H, d, $J = 16.0$ Hz, C^8H), 5.37 (1H, dt, $J = 16.0, 6.0$ Hz, C^9H).

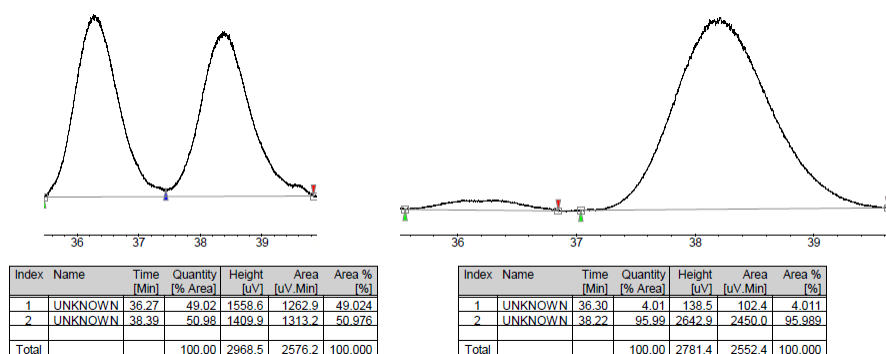
^{13}C NMR ($CDCl_3$) δ_C : 13.9 (C14), 22.1 (C2), 22.2 (C13), 28.1 (C10), 31.6 (C12), 32.4 (C11), 37.1 (C3), 40.7 (C4), 40.9 (C1), 52.4 (C5), 128.7 (C9), 137.5 (C8), 211.7 (C6).

IR ($CHCl_3$) ν_{max} : 2956, 2927, 2855, 1713, 1455, 1226, 975, 737 cm^{-1} .

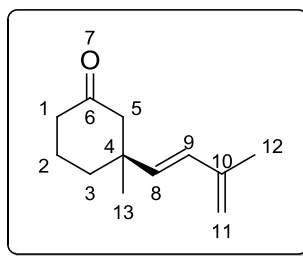
HRMS: (EI) $C_{13}H_{22}O$ $[M]^+$ requires m/z 194.1671, found $[M]^+$ 194.1666.

GC: (octakis(2,6-di-*O*-methyl-3-*O*-pentyl- γ -cyclodextrin); $T_{inj} = 250$ °C, $T_{det} = 25$ °C, flow = 2.0 mL min^{-1} , $t_i = 50$ °C, (1.0 °C min^{-1}) $t_f = 160$ (30 min): (*R*)-enantiomer: $t_R = 36.30$ min; (*S*)-enantiomer: $t_R = 38.22$ min.

$[\alpha]_D^{25}$: +59.6 ($c = 2.0$, $CHCl_3$).



(S)-(E)-3-Methyl-3-(3-methylbuta-1,3-dien-1-yl)cyclohexanone (200)



Prepared according to general procedure 13 from 2-methyl-1-buten-3-yne (71 μL , 0.75 mmol) and 3-methylcyclohexenone (55 μL , 0.50 mmol) to yield **200** as a colourless oil in 98% ee. (51 mg, 57%); **R_F** (pentane/diethyl ether 4:1) 0.31.

¹H NMR (CDCl_3) δ_{H} : 1.09 (3H, s, C^{13}H_3), 1.60–1.69 (1H, m, c-hex), 1.74–1.79 (1H, m, c-hex), 1.81 (3H, s, C^{12}H_3), 1.83–1.92 (2H, m, c-hex), 2.20 (1H, d, $J = 14.0$ Hz, C^5H), 2.24–2.34 (2H, m, c-hex), 2.47 (1H, dt, $J = 14.0, 1.0$ Hz, C^5H), 4.93 (2H, app. s, C^{11}H_2), 5.52 (1H, d, $J = 16.0$ Hz, C^8H), 6.08 (1H, d, $J = 16.0$ Hz, C^9H).

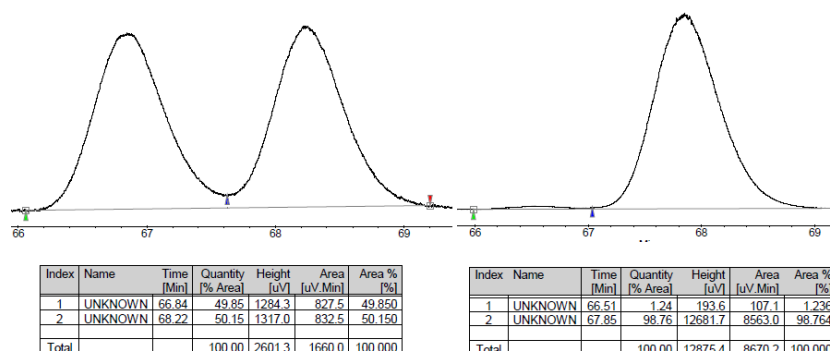
¹³C NMR (CDCl_3) δ_{C} : 18.7 (C^{12}), 22.3 (C^2), 22.7 (C^{13}), 37.2 (C^3), 41.0 (C^1), 41.1 (C^4), 52.5 (C^5), 116.0 (C^{11}), 130.7 (C^9), 137.5 (C^8), 141.7 (C^{10}), 211.4 (C^6).

IR (CHCl_3) ν_{max} : 3010, 2959, 2929, 2872, 1704, 1455, 1378, 972, 892 cm^{-1} .

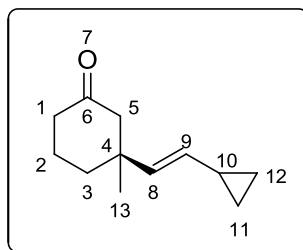
HRMS: (EI) $\text{C}_{12}\text{H}_{18}\text{O}$ $[\text{M}]^+$ requires m/z 178.1358, found $[\text{M}]^+$ 178.1356.

GC:(octakis(2,6-di-*O*-methyl-3-*O*-pentyl- γ -cyclodextrin); T_{inj} = 250 °C, T_{det} = 250 °C, flow = 2.0 mL min⁻¹, t_i = 50 °C, (1.0 °C min⁻¹) t_f = 160 (30 min): (*R*)- enantiomer: t_R = 66.51 min; (*S*)- enantiomer: t_R = 67.85 min.

$[\alpha]_D^{25}$: +29.0 (c = 2.00, CHCl₃).



(*S*)-(*E*)-3-(2-Cyclopropylvinyl)-3-methylcyclohexanone (**201**)



Prepared according to general procedure 13 from cyclopropylacetylene (71 μ L, 0.75 mmol) and 3-methylcyclohexenone (55 μ L, 0.50 mmol) to yield **201** as a colourless oil in 94% ee. (26 mg, 30%); R_F (pentane/diethyl ether 4:1) 0.42.

¹H NMR (CDCl₃) δ_H : 0.29–0.32 (2H, m, *c*-propyl), 0.63–0.67 (2H, m, *c*-propyl), 1.03 (3H, s, C¹³H₃), 1.24–1.34 (1H, m, C¹⁰H), 1.55–1.61 (1H, m, *c*-hex), 1.66–1.71 (1H, m, *c*-hex),

1.80–1.87 (2H, m, c-hex), 2.13 (1H, d, $J = 14.0$ Hz, C⁵H), 2.17–2.31 (2H, m, c-hex), 2.37 (1H, dt, $J = 14.0, 1.5$ Hz, C⁵H), 4.86 (1H, dd, $J = 16.0, 8.5$ Hz, C⁹H), 5.38 (1H, d, $J = 16.0$ Hz, C⁸H).

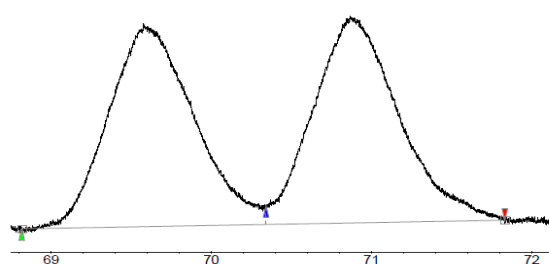
¹³C NMR (CDCl₃) δ_C : 6.72 (C11 & C12), 13.9 (C10), 22.3 (C2), 28.0 (C13), 37.2 (C3), 40.8 (C4), 41.0 (C1), 52.5 (C5), 132.3 (C9), 136.4 (C8), 211.8 (C6).

IR (CHCl₃) ν_{\max} : 3038, 3010, 2959, 2873, 1704, 1454, 1426, 1313, 1291, 1241, 968 cm⁻¹.

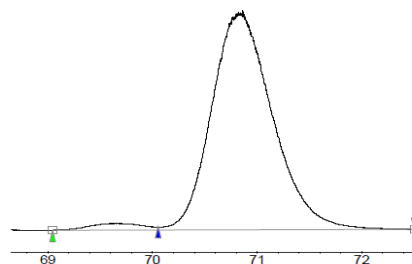
HRMS: (EI) C₁₂H₁₈O [M]⁺ requires m/z 178.1358, found [M]⁺ 178.1361.

GC: (octakis(2,6-di-*O*-methyl-3-*O*-pentyl- γ -cyclodextrin); $T_{\text{inj}} = 250$ °C, $T_{\text{det}} = 250$ °C, flow = 2.0 mL min⁻¹, $t_i = 50$ °C, (1.0 °C min⁻¹) $t_f = 160$ (30 min): (*R*)-enantiomer: $t_R = 69.64$ min; (*S*)-enantiomer: $t_R = 70.86$ min.

[α]_D²⁵: +37.4 ($c = 2.00$, CHCl₃).

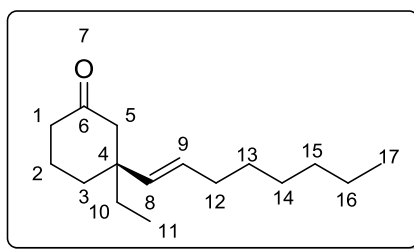


Index	Name	Time (Min)	Quantity [% Area]	Height [uV]	Area [uV.Min]	Area % [%]
1	UNKNOWN	69.64	49.30	677.1	421.0	49.305
2	UNKNOWN	70.86	50.70	699.0	432.9	50.695
Total			100.00	1376.1	853.9	100.000



Index	Name	Time (Min)	Quantity [% Area]	Height [uV]	Area [uV.Min]	Area % [%]
1	UNKNOWN	69.64	2.63	668.5	391.7	2.625
2	UNKNOWN	70.86	97.37	21766.6	14527.7	97.375
Total			100.00	22435.0	14919.4	100.000

(S)-(E)-3-Ethyl-3-(oct-1-en-1-yl)cyclohexanone (202)



Prepared according to general procedure 14 from 1-octyne (134 μ L, 0.750 mmol) and 3-ethyl-cyclohexenone (59 μ L, 0.50 mmol) to yield **202** as a colourless oil in 88% ee. (71 mg, 60%); **R_F** (pentane/diethyl ether 4:1) 0.50.

¹H NMR (CDCl₃) δ_{H} : 0.78 (3H, t, J = 7.5 Hz, C¹¹H₃), 0.87 (3H, t, J = 7.0 Hz, C¹⁷H₃), 1.19–1.32 (8H, m, C¹³H₂–C¹⁶H₂), 1.34–1.40 (2H, m, C¹⁰H₂), 1.60–1.69 (2H, m, c-hex), 1.76–1.86 (2H, m, c-hex), 1.96–2.02 (2H, m, c-hex), 2.10 (1H, d, J = 14.0 Hz, C⁵H), 2.16–2.32 (2H, m, C¹²H₂), 2.49 (1H, d, J = 14.0 Hz, C⁵H), 5.12 (1H, d, J = 16.0 Hz, C⁸H), 5.31 (1H, dt, J = 16.0, 7.0 Hz, C⁹H).

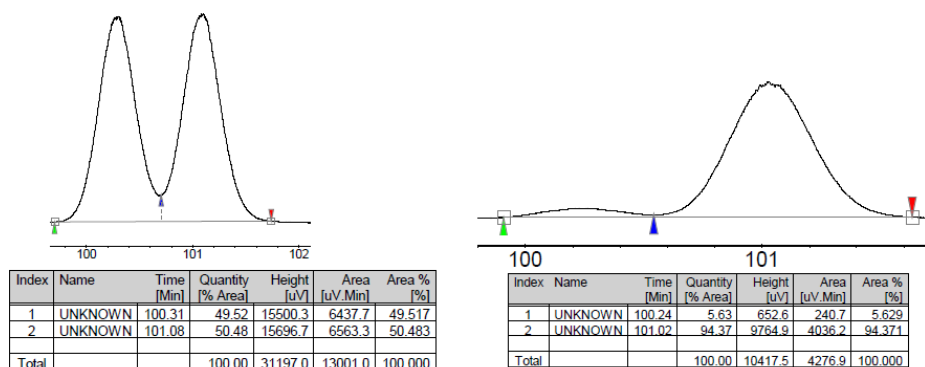
¹³C NMR (CDCl₃) δ_{C} : 7.9 (C11), 14.1 (C17), 21.7 (C2), 22.6 (C16), 28.7 (C14), 29.5 (C13), 31.7 (C10), 32.9 (C15), 34.2 (C3), 35.3 (C12), 41.2 (C1), 44.1 (C4), 49.8 (C5), 131.1 (C9), 135.3 (C8), 211.9 (C6).

IR (CHCl₃) ν_{max} : 3038, 3010, 2959, 2873, 1704, 1454, 1426, 1313, 1291, 1241, 968 cm⁻¹

HRMS: (EI) C₁₆H₂₈O [M]⁺ requires m/z 236.2140, found [M]⁺ 236.2138.

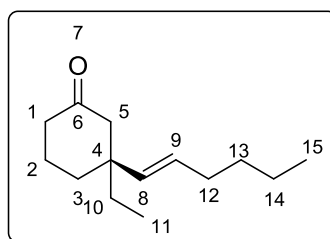
GC: (*octakis*(2,6-di-*O*-methyl-3-*O*-pentyl- γ -cyclodextrin)); $T_{\text{inj}} = 250\text{ }^{\circ}\text{C}$, $T_{\text{det}} = 250\text{ }^{\circ}\text{C}$, flow = 2.0 mL min^{-1} , $t_{\text{i}} = 50\text{ }^{\circ}\text{C}$, ($1.0\text{ }^{\circ}\text{C min}^{-1}$) $t_{\text{f}} = 160$ (30 min): (*R*)-enantiomer: $t_{\text{R}} = 100.24\text{ min}$; (*S*)- enantiomer: $t_{\text{R}} = 101.02\text{ min}$.

$[\alpha]_{\text{D}}^{25}$: +69.1 ($c=2.00$, CHCl_3).



(*S*)-(*E*)-3-Ethyl-3-(hex-1-en-1-yl)cyclohexanone (**203**)

134



Prepared according to general procedure 13 from 1-hexyne (71 μL , 0.75 mmol) and 3-ethyl-cyclohexenone (59 μL , 0.50 mmol) to yield **203** as a colourless oil in 96% ee. (48 mg, 46%); R_{F} (pentane/diethyl ether 4:1) 0.55.

$^1\text{H NMR}$ (CDCl_3) δ_{H} : 0.80 (3H, t, $J = 7.0\text{ Hz}$, C^{11}H_3), 0.90 (3H, t, $J = 7.0\text{ Hz}$, C^{15}H_3), 1.25–1.36 (4H, m, C^{13}H_2 and C^{14}H_2), 1.36–1.42 (2H, m, C^{10}H_2), 1.60–1.71 (2H, m, c-hex), 1.79–1.90 (2H, m, c-hex), 2.00–2.06 (2H, m, c-hex), 2.13 (1H, d, J

= 14.0 Hz, C⁵H), 2.18–2.33 (2H, m, C¹²H₂), 2.49 (1H, dt, *J* = 14.0, 1.5 Hz, C⁵H), 5.14 (1H, d, *J* = 16.0 Hz, C⁸H), 5.34 (1H, dt, *J* = 16.0, 6.5 Hz, C⁹H).

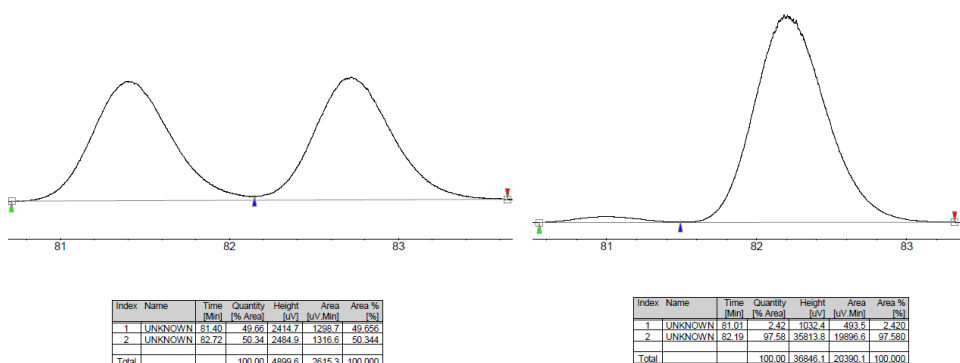
¹³C NMR (CDCl₃) δ_C: 7.8 (C11), 13.9 (C15), 21.7 (C2), 22.1 (C14), 31.7 (C10), 32.6 (C13), 34.2 (C3), 35.3 (C12), 41.2 (C1), 44.1 (C4), 49.8 (C5), 131.0 (C9), 135.3 (C8), 211.9 (C6).

IR (CHCl₃) ν_{max}: 3038, 3010, 2959, 2873, 1704, 1454, 1426, 1313, 1291, 1241, 968 cm⁻¹.

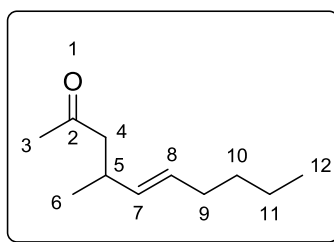
HRMS: (EI) C₁₄H₂₄O [M]⁺ requires *m/z* 208.1827, found [M]⁺ 208.1820.

GC:(octakis(2,6-di-*O*-methyl-3-*O*-pentyl-γ-cyclodextrin); *T*_{inj} = 250 °C, *T*_{det} = 250 °C, flow = 2.0 mL min⁻¹, *t*_i=50 °C, (1.0 °C min⁻¹) *t*_f = 160 (30 min): (*R*)- enantiomer: *t*_R = 81.01 min; (*S*)- enantiomer: *t*_R = 82.19 min.

[α]_D²⁵: +31.8 (*c* = 2.00, CHCl₃).



(E)-4-Methyldec-5-en-2-one (204)



Prepared according to general procedure 13 from 1-hexyne (71 μL , 0.75 mmol), 3-penten-2-one (49 μL , 0.50 mmol), trimethylaluminium (0.37 mL, 0.75 mmol) and tricyclohexylphosphine (25 mg, 0.075 mmol) to yield **204** as a yellow oil (19 mg, 22%); **R_F** (pentane/diethyl ether 4:1) 0.64.

¹H NMR (CDCl_3) δ_{H} : 0.58 (3H, t, $J = 7.0$ Hz, C^{12}H_3), 0.99 (3H, d, $J = 6.5$ Hz, C^6H_3), 1.25-1.34 (4H, m, C^{10}H_2 & C^{11}H_2), 1.96 (2H, app q, $J = 6.0$ Hz, C^9H_2), 2.11 (3H, s, C^3H_3), 2.33 (1H, dd, $J = 15.5, 7.0$ Hz, C^4H), 2.42 (1H, dd, $J = 15.5, 7.0$ Hz, C^4H), 5.30 (1H, dd, $J = 15.5, 7.0$ Hz, C^7H), 5.40 (1H, dt, $J = 15.5, 6.0$ Hz, C^8H).

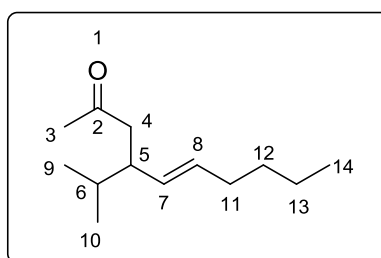
¹³C NMR (CDCl_3) δ_{C} : 14.1 (C^{12}), 20.7 (C^6), 22.3 (C^{11}), 30.7 (C^5), 31.8 (C^3), 32.9 (C^9), 51.3 (C^4), 129.6 (C^8), 134.4 (C^7), 208.6 (C^2).

IR (CHCl_3) ν_{max} : 3010, 2961, 2930, 2873, 1710, 1457, 1360, 971 cm^{-1} .

HRMS: (EI) $\text{C}_{12}\text{H}_{24}\text{O}_3$ [$\text{M}+\text{MeOH}+\text{H}_2\text{O}+\text{H}^+$] requires m/z 219.1710, found [$\text{M}+\text{MeOH}+\text{H}_2\text{O}+\text{H}$] 219.1717.

GC:(*octakis*(6-*O*-pentyl-2,3-di-*O*-methyl- γ -cyclodextrin)); $T_{\text{inj}} = 250\text{ }^{\circ}\text{C}$, $T_{\text{det}} = 250\text{ }^{\circ}\text{C}$, flow = 2.0 mL min^{-1} , $t_i = 70\text{ }^{\circ}\text{C}$, (45 min)($20\text{ }^{\circ}\text{C min}^{-1}$) $t_f = 170$ (10 min): enantiomer 1: $t_R = 29.37$ min; enantiomer 2: $t_R = 30.39$ min.

(*E*)-4-Isopropyldec-5-en-2-one (205)



Prepared according to general procedure 13 from 1-hexyne (71 μL , 0.75 mmol), 5-methyl-3-hexen-2-one (66 μL , 0.50 mmol), trimethylaluminium (0.37 mL, 0.75 mmol) and tricyclohexylphosphine (25 mg, 0.075 mmol) to yield **205** as a yellow oil (19 mg, 22%); R_F (pentane/diethyl ether 4:1) 0.60.

^1H NMR (CDCl_3) δ_H : 0.82-0.92 (9H, m, C^9H_3 , C^{10}H_3 , C^{14}H_3), 1.19-1.34 (4H, m, C^{12}H_2 & C^{13}H_2), 1.54-1.60 (1H, m, C^6H), 1.97 (2H, app q, $J = 6.5\text{ Hz}$, C^{11}H_2), 2.10 (3H, s, C^3H_3), 2.31-2.47 (3H, m, C^4H_2 & C^5H), 5.19 (1H, dd, $J = 15.0, 8.5\text{ Hz}$, C^7H), 5.38 (1H, dt, $J = 15.0, 6.5\text{ Hz}$, C^8H).

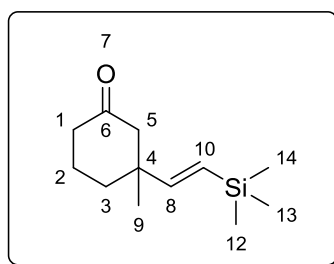
^{13}C NMR (CDCl_3) δ_C : 14.1 (C^{14}), 18.9 (C^{10}), 20.6 (C^9), 22.3 (C^{13}), 30.7 (C^5), 31.8 (C^3), 32.0 (C^{12}), 32.4 (C^{11}), 45.2 (C^6), 47.3 (C^4), 130.3 (C^8), 132.5 (C^7), 209.3 (C^2).

IR (CHCl₃) ν_{max} : 3010, 2961, 2930, 2873, 1706, 1466, 1369, 1358, 973 cm⁻¹.

HRMS: (ESI) C₁₃H₂₅O [M+H]⁺ requires m/z 197.1900, found [M+H]⁺ 197.1907.

GC:(*octakis*(6-*O*-pentyl-2,3-di-*O*-methyl- γ -cyclodextrin); T_{inj} = 250 °C, T_{det} = 250 °C, flow = 2.0 mL min⁻¹, t_{i} = 70 °C, (45 min)(20 °C min⁻¹) t_{f} = 170 (10 min): enantiomer 1: t_{R} = 69.26 min; enantiomer 2: t_{R} = 69.92 min.

(*E*)-3-Methyl-3-(2-(trimethylsilyl)vinyl)cyclohexanone (207)



Prepared according to general procedure 13 from trimethylsilylacetylene (104 μ L, 0.750 mmol) and 3-methylcyclohexenone (55 μ L, 0.50 mmol) trimethylaluminium (0.37 mL, 0.75 mmol) and tricyclohexylphosphine (25 mg, 0.075 mmol) to yield **207** as a colourless oil (21.1 mg, 20%); R_{F} (pentane/diethyl ether 4:1) 0.36.

¹H NMR (CDCl₃) δ_{H} : 0.06 (9H, s, Si(CH₃)₃), 1.05 (3H, s, C⁹H₃), 1.56-1.62 (1H, m, c-hex), 1.69-1.85 (3H, m, c-hex), 2.16 (1H, d, J = 14.0 Hz, C⁵H), 2.20-2.30 (2H, m, c-hex),

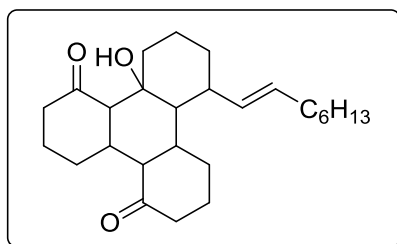
2.47 (1H, dt, $J = 14.0, 1.0$ Hz, C⁵H), 5.60 (1H, d, $J = 19.0$ Hz, C¹⁰H), 5.88 (1H, d, $J = 19.0$ Hz, C⁸H).

¹³C NMR (CDCl₃) δ_C : 1.06 (Si(CH₃)₃), 22.2 (C9), 27.1 (C2), 36.5 (C3), 41.0 (C1), 42.9 (C4), 51.8 (C5), 127.1 (C10), 153.3 (C8), 211.6 (C6).

IR (CHCl₃) ν_{\max} : 3010, 2958, 1705, 1612, 1248, 867, 841 cm⁻¹.

HRMS: (EI) C₁₂H₂₂OSi [M]⁺ requires m/z 210.1440, found [M]⁺ 210.1436.

Tetracyclic compound



Racemic tetracycle was identified in early optimisation studies using copper(I) thiophenecarboxylate/tricyclohexylphosphine or **L3** as the major mass balance element. It was purified by flash chromatography (pentane/diethyl ether 4:1) **R_F** 0.28.

¹H NMR (CDCl₃) δ_H : 0.89 (3H, t, $J = 7.0$ Hz, CH₃), 0.99–1.18 (3H, m), 1.27–1.32 (8H, m, CH₂), 1.41–1.54 (3H, m), 1.66–2.45 (16H, m), 2.50 (1H, d, $J = 10.5$ Hz), 2.61 (1H, m), 2.97 (1H, app t, $J = 11.0$ Hz), 4.42 (1H, s), 5.20 (1H, app dd, $J = 15.0, 8.0$ Hz), 5.45 (1H, dt, $J = 15.0, 7.0$ Hz).

^{13}C NMR (CDCl_3) δ_{C} : 14.2, 20.6, 20.7, 22.7, 27.6, 28.8, 29.8, 31.8, 32.8, 34.4, 38.1, 41.9, 45.5, 55.1, 55.9, 75.5, 130.7, 134.8, 213.7, 219.3.

IR (CHCl_3) ν_{max} : 3598, 3546, 3047, 3005, 2976, 2950, 2925, 2862, 1705, 1478, 1436, 1323, 1118 cm^{-1} .

HRMS: (ESI) $\text{C}_{26}\text{H}_{40}\text{O}_3$ $[\text{M}]^+$ requires m/z 422.2989, found $[\text{M}]^+$ 422.2982.

References

- [1] A. Michael, *J. Prak. Chem.* **1887**, 35, 349–356.
- [2] G. H. Posner, *Org. React.* **1972**, 19, 1–113.
- [3] B. E. Rossiter, N. M. Swingle, *Chem. Rev.* **1992**, 92, 771–806.
- [4] S. R. Krauss, S. G. Smith, *J. Am. Chem. Soc.* **1981**, 103, 141–148.
- [5] J. Canisius, A. Gerold, N. Krause, *Angew. Chem. Int. Ed.*, **1999**, 38, 1644–1646.
- [6] a) S. H. Bertz, R. A. J. Smith, *J. Am. Chem. Soc.* **1989**, 111, 8276–8277. b) N. Krause, *J. Org. Chem.* **1992**, 57, 3509–3512. (c) N. Krause, R. Wagner, A. Gerold, *J. Am. Chem. Soc.* **1994**, 116, 381–382. (d) J. Canisius, T. A. Mobley, S. Berger, N. Krause, *Chem. Eur. J.* **2001**, 7, 2671–2675. e) S. H. Bertz, C. M. Carlin, D. A. Deadwyler, M. D. Murphy, C. A. Ogle, P. H. Seagle, *J. Am. Chem. Soc.* **2002**, 124, 13650–13651. (f) M. D. Murphy, C. A. Ogle, S. H. Bertz, *Chem. Commun.* **2005**, 854–856. g) K. Nilsson, C. Ullenius, N. Krause, *J. Am. Chem. Soc.* **1996**, 118, 4194–4195.
- [7] S. H. Bertz, S. Cope, M. Murphy, C. A. Ogle, B. J. Taylor, *J. Am. Chem. Soc.* **2007**, 129, 7208–7209.
- [8] N. Yoshikai, E. Nakamura, *Chem. Rev.* **2012**, 2339–2372.
- [9] D. J. Berrisford, C. Bolm, K. B. Sharpless, *Angew. Chem. Int. Ed. Engl.* **1995**, 34, 1050–1064.
- [10] A. Alexakis, J. Frutos, P. Mangeney, *Tetrahedron: Asymm.* **1993**, 4, 2427–2430.

-
- [11] B. L. Feringa, M. Pineschi, L. A. Arnold, R. Imbos, A. H. de Vries, *Angew Chem. Int. Ed.* **1997**, 36, 2620–2623.
- [12] T. Hayashi, K. Yamasaki, *Chem. Rev.* **2003**, 103, 2829–2844.
- [13] P. Wipf, *Synthesis*, **1993**, 537–557.
- [14] S. J. Degrado, H. Mizutani, A. H. Hoveyda, *J. Am. Chem. Soc.* **2001**, 123, 755–756.
- [15] M. K. Brown, S. J. Degrado, A. H. Hoveyda, *Angew. Chem. Int. Ed.* **2005**, 44, 5306–5310.
- [16] H. Clavier, L. Coutable, J.-C. Guillemin, M. Mauduit, *Tetrahedron: Asymmetry*, **2005**, 16, 921–924.
- [17] T. L. May, M. K. Brown, A. H. Hoveyda, *Angew. Chem. Int. Ed.* **2008**, 47, 7358–7361.
- [18] M. S. Kharash, P. O. Tawney, *J. Am. Chem. Soc.* **1941**, 63, 2308–2316.
- [19] B. E. Rossiter, N. M. Swingle, *Chem. Rev.* **1992**, 92, 771–806.
- [20] R. M. Maksymowicz, P. M. C. Roth, S. P. Fletcher, *Nature Chem.* **2012**, 4, 649–654.
- [21] R. M. Maksymowicz, S. Mireia, P. M. C. Roth, S. P. Fletcher, *Synthesis*, **2013**, 45, 2662–2668.
- [22] A. D. J. Calow, A. Whiting, *Org. Biol. Chem.* **2012**, 10, 5485–5497.
- [23] a) A. Alexakis, J. E. Bäckvall, N. Krause, O. Pàmies, M. Diéguez, *Chem. Rev.* **2008**, 108, 2796–2823. b) A. Alexakis, N. Krause, S. Woodward, *Copper-Catalyzed Asymmetric Synthesis*, Wiley-VCH Verlag GmbH, Weinheim, **2014**, 33–68.

-
- [24] J. F. Teichert, B. L. Feringa, *Angew. Chem. Int. Ed.* **2010**, 49, 2486–2528.
- [25] L. Palais, I. S. Mikhel, C. Bournaud, L. Micouin, C. A. Falciola, M. Vuagnoux-d'Augustin, S. Rosset, G. Bernardinelli, A. Alexakis, *Angew. Chem. Int. Ed.* **2007**, 46, 7462–7465.
- [26] Y. Yamanoi, T. Imamoto, *J. Org. Chem.* **1999**, 64, 2988–2989.
- [27] F. Valleix, K. Nagai, T. Soeta, M. Kuriyama, K.-I. Yamada and K. Tomioka, *Tetrahedron*, **2005**, 61, 7420–7424.
- [28] a) F. López, S. R. Harutyunyan, A. Meetsma, A. J. Minnaard, B. L. Feringa, *Angew. Chem. Int. Ed.*, **2005**, 44, 2752–2756. b) S.-Y. Wang, S.-J. Ji, T.-P. Loh, *J. Am. Chem. Soc.* **2007**, 129, 276–277.
- [29] P. K. Fraser, S. Woodward, *Tetrahedron Lett.* **2001**, 42, 2747–2749.
- [30] F. Guillen, C. L. Winn, A. Alexakis, *Tetrahedron: Asymmetry*, **2001**, 12, 2083–2086.
- [31] A. Alexakis, C. L. Winn, F. Guillen, J. Pytkowicz, S. Roland, P. Mangeney, *Adv. Synth. Catal.*, **2003**, 345, 345–348.
- [32] T. Pfretzschner, L. Kleemann, B. Janza, K. Harms, T. Schrader, *Chem. Eur. J.* **2004**, 10, 6048–6057.
- [33] H. O. House, W. L. Respess, G. M. Whitesides, *J. Org. Chem.* **1966**, 31, 3128–3141.
- [34] H. Zhang, R. M. Gschwind, *Angew. Chem. Int. Ed.* **2006**, 45, 6391–6394. b) K. Schober, H. Zhang, R. M. Gschwind, *J. Am. Chem. Soc.* **2008**, 130, 12310–12317.

-
- [35] S. R. Harutyunyan, F. López, W. R. Browne, A. Correa, D. Peña, R. Badorrey, A. Meetsma, A. J. Minnaard, B. L. Feringa, *J. Am. Chem. Soc.* **2006**, *128*, 9103–9118.
- [36] L. F. Veiros, M. Welker, S. Woodward. *Chem. Eur. J.* **2010**, *16*, 5620–5629.
- [37] J. R. Chipperfield, *J. Orgmet. Chem.* **1989**, *363*, 253–263.
- [38] For details of using SOLVER see: J. E. Billo, *Excel for Chemists*, Wiley-VCH, Weinheim, 2nd edition, **2004**, 201
- [39] (a) M. R. Wilson, D. C. Woska, A. Prock, W. P. Giering, *Organometallics* **1993**, *12*, 1742–1752. (b) Complete details of the QALE approach are given at: www.bu.edu/qale/
- [40] D. Willcox, S. Woodward, L. Verios, *Adv. Synth. Catal.*, **2014**, manuscript submitted.
- [41] S. Wang, P. Song, T. P. Loh, *Adv. Synth. Catal.* **2010**, *352*, 3185–3189.
- [42] K. Biswas, A. Chapron, T. Cooper, P. Fraser, A. Novak, O. Prieto, S. Woodward, *Pure Appl. Chem.* **2006**, *78*, 511–518.
- [43] S. Aldridge, A. J. Downs, *Chem. Rev.* **2001**, *101*, 3305–3366.
- [44] K. Ouzounis, H. Riffel, H. Hess, U. Kohler, J. Weidlein, Z. *Anorg. Allg. Chem.* **1983**, *504*, 67–76.
- [45] K. N. Semenenko, E. B. Lobkovskii, A. L. Dorosinskii, *Zh. Strukt. Khim.* **1972**, *13*, 743.
- [46] C. Klein, H. Nöth, M. Tacke, M. Thomann, M. *Angew. Chem., Int. Ed. Engl.* **1993**, *32*, 886–888.

-
- [47] G. Del Piero, M. Cesari, G. Dozzi, A. Mazzei, *J. Organomet. Chem.* **1977**, 129, 281–288. b) M. Cesari, G. Perego, G. Del Piero *et al.* *J. Organomet. Chem.* **1974**, 78, 203–213.
- [48] B. M. Bulychiev, *Polyhedron*, **1990**, 9, 387–408.
- [49] J. K. Ruff, *Inorg. Synth.* **1967**, 9, 30–37.
- [50] K. N. Semenenko, E. B. Lobkovskii, V. N. Fokin, *Zh. Neorg. Khim.* **1973**, 18, 2718–2722.
- [51] a) J. K. Ruff, *J. Am. Chem. Soc.* **1961**, 83, 1798–1800; b) E. Wiberg, K. Modritzer, R. U. Lacal, *Rev. Acad. Cienc. Exact. Fis. Quim. Nat. Zaragoza* **1954**, 9, 95–116; c) E. Wiberg, R. U. Lacal, *Rev. Acad. Cienc. Exact. Fis. Quim. Nat. Zaragoza* **1954**, 9, 91–95; d) E. C. Ashby, J. Prather, *J. Am. Chem. Soc.* **1996**, 88, 729–733; e) R. Ehrlich, A. R. Young, D. D. Perry, *Inorg. Chem.* **1965**, 4, 758–759; f) T. H. Pearson, US Patent, 2992248, 1961, 3pp.
- [52] a) W. Marconi, A. Mazzei, S. Cucinella, M. Greco, *Annali di chimica*, **1965**, 55, 897–910; b) D. L. Schmidt, E. E. Flagg, *Inorg. Chem.* **1967**, 6, 1262–1265.
- [53] S. G. Alexander, M. L. Cole, M. Hilder, J. C. Morris, J. B. Patrick, *Dalton Trans.* **2008**, 6361–6363.
- [54] S. G. Alexander, M. L. Cole, S. K. Furfari, M. Kloth, *Dalton Trans.* **2009**, 2909–2911.
- [55] S. R. Snow, R. S. Paley, *Tetrahedron Lett.* **1990**, 31, 5853–5856.
- [56] M. C. Carreño, M. P. Gonzalez, R. Ribagorda, H. Fischer, *J. Org. Chem.* **1996**, 61, 6758–6759.

-
- [57] G. Wilke, H. Müller, *Justus Liebig Ann. Chem.* **1960**, 629, 222–240.
- [58] G. Zweifel, J. A. Miller, *Org. React.* **1984**, 32, 375–517.
- [59] J. J. Eisch, M. W. Foxton, *J. Org. Chem.* **1971**, 36, 3520–3526.
- [60] J. J. Eisch, M. W. Foxton, *J. Organomet. Chem.* **1968**, 12, P33–P36.
- [61] F. Gao, A. H. Hoveyda, *J. Am. Chem. Soc.* **2010**, 132, 10961–10963.
- [62] T. Taapken, S. Blechert, *Tetrahedron Lett.* **1995**, 36, 6659–6662.
- [63] E. C. Ashby, S. A. Noding, *Tetrahedron Lett.* **1977**, 18, 4579–4582.
- [64] G. Zweifel, R. B. Steele, *J. Am. Chem. Soc.* **1967**, 89, 5085–5086.
- [65] E. Negishi, D. E. Van Horn, *J. Am. Chem. Soc.* **1978**, 100, 2252–2254.
- [66] E. Negishi, D. E. Van Horn, T. Yoshida, *J. Am. Chem. Soc.* **1985**, 107, 6639–6647; b) T. Yoshida, E. Negishi, *J. Am. Chem. Soc.* **1981**, 103, 1276–1277; c) E. Negishi, T. Yoshida, *J. Am. Chem. Soc.* **1981**, 103, 4985–4987.
- [67] a) N. Okukado, E. Negishi, *Tetrahedron Lett.* **1978**, 19, 2357–2360; b) E. Negishi, A. O. King, W. L. Klima, *J. Org. Chem.* **1980**, 45, 2526–2528; c) E. Negishi, L. Valente, M. Kobayashi, *J. Am. Chem. Soc.* **1980**, 102, 3298–3299.
- [68] P. Wipf, S. Lim, *Angew. Chem. Int. Ed. Engl.* **1993**, 32, 1068–1071.

-
- [69] S. Baba, E. Negishi, *J. Am. Chem. Soc.* **1976**, 98, 6729–6731.
- [70] E. Negishi, S. Baba, *J. Chem. Soc. Chem. Commun.* **1976**, 596–597.
- [71] T. Hayashi, Y. Katsuo, Y. Okamoto, M. Kumada, *Tetrahedron Lett.* **1981**, 22, 4449–4452.
- [72] E. Negishi, N. Okukado, A. O. King, D. E. Van Horn, B. I. Spiegel, *J. Am. Chem. Soc.* **1978**, 100, 2254–2256.
- [73] F. Zeng, E. Negishi, *Org. Lett.* **2004**, 6, 1531–1534.
- [74] H. Matsushita, E. Negishi, *J. Am. Chem. Soc.* **1981**, 103, 2882–2884.
- [75] E. Negishi, H. Matsushita, N. Okukado, *Tetrahedron Lett.* **1981**, 22, 2715–2718.
- [76] B. H. Lipshutz, G. Bulow, R. F. Lowe, K. L. Stevens, *Tetrahedron*, **1996**, 52, 7265–7276.
- [77] D. B. Biradar, H. M. Gau, *Org. Biomol. Chem.* **2012**, 10, 4243–4248.
- [78] H. Schumann, J. Kaufmann, H. G. Schmalz, A. Bottcher, B. Gotov, *Synlett*, **2003**, 1783–1788.
- [79] E. C. Ashby, S. A. Noding, *J. Org. Chem.* **1979**, 44, 4365–4371.
- [80] T. Cooper, A. Novak, L. D. Humphreys, M. D. Walker, Simon Woodward, *Ad. Synth. Catal.* **2006**, 348, 691–695.
- [81] M. Pineschi, F. Del Moro, F. Gini, A. J. Minnaard, B. L. Feringa, *Chem. Commun.* **2004**, 1244–1245.
- [82] M. Shizuki, M. L. Snapper, *Angew. Chem. Int. Ed.* **2008**, 47, 5049–5051.

-
- [83] A. Alexakis, C. Benhaim, *Tetrahedron: Asymmetry*, **2001**, *12*, 1151–1157.
- [84] J. Schuppan, A. J. Minnaard, B. L. Feringa, *Chem. Commun.*, **2004**, 792–793.
- [85] X. Tang, A. J. Blake, W. Lewis, S. Woodward, *Tetrahedron: Asymmetry*, **2009**, *20*, 1881–1891.
- [86] G. Cahiez, P. Venegas, C. E. Tucker, T. N. Majid, P. Knochel, *J. Chem. Soc., Chem. Commun.*, **1992**, 1406–1408.
- [87] P. Cottet, D. Müller, A. Alexakis, *Org. Lett*, **2013**, *15*, 828–831.
- [88] J. Hooz, R. B. Layton, *Can. J. Chem.* **1973**, *51*, 2098–2101.
- [89] R. E. Ireland, P. Wipf, *J. Org. Chem.* **1990**, *55*, 1425–1426.
- [90] D. Müller, A. Alexakis, *Chem. Commun.*, **2012**, *48*, 12037–12049; and references there in.
- [91] K. H. Ahn, R. B. Klassen, S. J. Lippard, *Organometallics*, **1990**, *9*, 3178–3181.
- [92] T. Robert, J. Velder, H. G. Schmalz, *Angew. Chem. Int. Ed.* **2008**, *47*, 7718–7721.
- [93] Q. Naeemi, T. Robert, D. Kranz, J. Velder, H. G. Schmalz, *Tetrahedron: Asymmetry*. **2011**, *22*, 887–892.
- [94] K. Lee, A. H. Hoveyda, *J. Org. Chem.* **2009**, *74*, 4455–4462.
- [95] a) A. Alexakis, V. Albrow, K. Biswas, M. d’Augustin, O. Prieto, S. Woodward, *Chem. Commun.* **2005**, 2843–2845. b) V. E. Albrow, A. J. Blake, R. Fryatt, C. Wilson, S. Woodward, *Eur. J. Org. Chem.* **2006**, 2549–2557.

-
- [96] D. Müller, M. Tissot, A. Alexakis, *Org. Lett.*, **2011**, *13*, 3040–3043.
- [97] F. Gao, A. H. Hoveyda, *J. Am. Chem. Soc.*, **2010**, *132*, 10961–10963.
- [98] E. J. Corey, D. J. Beames, *J. Am. Chem. Soc.* **1972**, *94*, 7210–1211.
- [99] T. L. May, J. A. Dabrowski, A. H. Hoveyda, *J. Am. Chem. Soc.* **2011**, *133*, 736–739.
- [100] C. Hawner, K. Li, V. Cirriez, A. Alexakis, *Angew. Chem., Int. Ed.*, **2008**, *47*, 8211–8214.
- [101] D. Müller, C. Hawner, M. Tissot, L. Palais, A. Alexakis, *Synlett*, **2010**, 1694–1698.
- [102] D. Müller, A. Alexakis, *Org. Lett.* **2012**, *14*, 1842–1845.
- [103] D. Müller, A. Alexakis, *Org. Lett.* **2013**, *15*, 1594–1597.
- [104] D. Willcox, M. Garcia, H. Gondal, S. Woodward, *Tetrahedron Lett.* **2014**, in press.
- [105] A. J. Blake, J. Shannon, J. C. Stephens, S. Woodward, *Chem. Eur. J.* **2007**, *13*, 2462–2472.
- [106] M. Sidera, P. Roth, R. M. Maksymowicz, S. P. Fletcher, *Angew. Chem. Int. Ed.* **2013**, *52*, 7995–7999.
- [107] D. Willcox, S. Woodward, A. Alexakis, *Chem. Commun.* 2014, in press.
- [108] H. E. Gottlieb, V. Kotlyar, A. Nudelman, *J. Org. Chem.* **1997**, *62*, 7512–7515.
- [109] S. Gao, Z. Ye, L. Shi, D. Qing, Y. Wang, *Appl. Organomet. Chem.* **2010**, *24*, 517–522.

-
- [110] N. Mamidi, D. Manna, *J. Org. Chem.* **2013**, *78*, 2356–2396.
- [111] L. A. Arnold, R. Imbos, A. Mandoli, A. H. M. de Vries, R. Naasz, B. L. Feringa, *Tetrahedron*, **2000**, *56*, 2865–2878.
- [112] Magali Vuagnoux-d'Augustin and Alexandre Alexakis, *Chem. Eur. J.* **2007**, *13*, 9647–9662.
- [113] L. Palais, A. Alexakis, *Chem. Eur. J.* **2009**, *15*, 10473–10485.
- [114] D. Müller, L. Guénée, A. Alexakis, *Eur. J. Org. Chem.* **2013**, 6335–6343.
- [115] J. Hiller, U. Thewalt, M. Polášek, L. Petrusová, V. Varga, P. Sedmera, K. Mach, *Organometallics*, **1996**, *15*, 3752–3759.
- [116] D. Maiti, A. Modak, T. Naveen, *Chem. Commun.* **2013**, *49*, 252–254.
- [117] C-M. Ting, Y-L. Hsu, R-S. Liu, *Chem. Commun.* **2012**, *48*, 6577–6579.
- [118] G. Zuo, J. Louie, *Angew. Chem. Int. Ed.* **2004**, *43*, 2277–2279.
- [119] G. Cahiez, O. Gager, F. Lecomte, *F. Org. Lett.* **2008**, *10*, 5255–5256.
- [120] I. Uchida, Y. Itoh, T. Namiki, M. Nishikawa, M. Hashimoto, *Tetrahedron Lett.* **1986**, *27*, 2015–2018.
- [121] G. Lui, S. S. Stahl, *J. Am. Chem. Soc.* **2007**, *129*, 6328–6335.
- [122] Y. Fall, F. Berthiol, H. Doucet, M. Santelli, *Synthesis*, **2007**, 1683–1696.

-
- [123] B. H. Lipshutz, B. Frieman, *Tetrahedron*, **2004**, *60*, 1309–1316.
- [124] B. Huang, W. Hao, M-Z. Cai, P. Wang, *J. Organomet. Chem.* **2011**, *696*, 2685–2688.
- [125] E. Schulz, P. Kinderli, A. Perrard, M. Lemaire, *Applied Catalysis, A: General*, **1996**, *144*, 293–304.
- [126] M. G. Organ, J. T. Cooper, L. R. Rogers, F. Soleymanzadeh, T. Payl, *J. Org. Chem.* **2000**, *65*, 7959–7970.
- [127] B.-D. Chong, Y.-I. Ji, S.-S. Oh, J.-D. Yang, W. Baik, S. Koo, *J. Org. Chem.* **1997**, *62*, 9323–9325.
- [128] S. Oi, T. Sato and Y. Inoue, *Tetrahedron Lett.* **2004**, *45*, 5051–5056.
- [129] M .K. Brown and E. J. Corey, *Org. Lett.* **2010**, *12*, 172–175.
- [130] Y. Nakao, J. Chen, H. Imanaka, T. Hiyama, Y. Ichikawa, W-L. Duan, R. Shintani, and T. Hayashi, *J. Am. Chem. Soc.*, **2007**, *129*, 9137–9143.
- [131] K. S. Lee and A. H. Hoveyda, *J. Org. Chem.*, **2009**, *74*, 4455–4462.
- [132] T. L. May, J. A. Dabrowski and A. H. Hoveyda, *J. Am. Chem. Soc.*, **2011**, *133*, 736–739.
- [133] C. Hawner, K. Li, V. Cirriez and A. Alexakis, *Angew. Chem. Int. Ed.*, **2008**, *47*, 8211–8214.
- [134] D. Müller, M. Tissot, A. Alexakis, *Org. Lett.* **2011**, *13*, 3040–3043.

Ligand optimisation plot primary data

Copper(II) acetate (1 mol%), **L39** (0.5 – 2.5 mol%), ZnEt₂ (12 mmol), cyclohexenone (10 mmol), PhMe

0.5 mol%			1.0 mol%		
t sec	integ Prod	integ SM	t sec	integ Prod	integ SM
60	17.966	24.986	60	4.565	31.479
180	32.138	13.548	180	16.939	20.626
300	36.877	11.101	300	23.169	19.515
540	41.278	8.509	540	31.092	10.482
900	43.784	6.781	900	34.029	13.944
1200	46.294	6.457	1200	37.02	11.319
1500	47.873	5.783	1500	39.706	7.352
2100	47.759	4.035	2100	41.852	8.304
2700	48.212	3.968	2700	43.077	7.375
3600	48.273	4.304	3600	45.287	6.27
1.5 mol%			2.0 mol%		
t sec	integ Prod	integ SM	t sec	integ Prod	integ SM
60	8.721	30.971	60	7.444	26.136
180	20.322	18.866	180	19.525	21.661
300	26.302	16.647	300	22.541	21.339
540	32.637	13.949	540	28.752	16.131
900	37.3	12.862	900	33.734	13.959
1200	40.339	9.301	1200	34.625	14.343
1500	41.438	10.041	1500	38.631	12.732
2100	43.939	8.668	2100	40.405	10.145
2700	45.195	6.715	2700	43.055	9.443
3600	46.722	6.326	3600	44.105	7.528
2.5 mol%					
60	4.099	30.011			
180	9.912	24.049			
300	12.271	24.288			
540	17.918	21.232			
900	23.538	17.656			
1200	26.546	18.085			
1500	29.473	16.116			
2100	32.93	15.437			
2700	35.92	12.024			
3600	41.848	6.776			
60	4.099	30.011			
180	9.912	24.049			

Copper(II) acetate (1 mol%), **PMe₃** (0.5 – 2.5 mol%), ZnEt₂ (12 mmol), cyclohexenone (10 mmol), PhMe

0.5 mol%			1.0 mol%		
t sec	integ Prod	integ SM	t sec	integ Prod	integ SM
60	6.161	30.158	60	4.736	35.447
180	17.179	26.592	180	10.224	30.317
300	26.023	21.824	300	17.116	24.533
540	38.374	13.999	540	26.188	17.495
900	48.424	8.093	900	36.631	14.33
1200	49.252	6.047	1200	41.478	10.036
1500	51.38	5.033	1500	44.392	8.317
2100	53.505	4.13	2100	47.186	7.227
2700	53.539	3.666	2700	48.495	5.875
3600	53.899	2.895	3600	47.903	6.365
1.5 mol%			2.0 mol%		
t sec	integ Prod	integ SM	t sec	integ Prod	integ SM
60	9.628	26.949	60	7.074	33.834
180	27.43	13.672	180	25.94	20.704
300	39.847	11.317	300	41.067	9.628
540	49.223	5.987	540	48.606	6.66
900	53.242	3.336	900	52.87	4.243
1200	52.894	3.04	1200	53.491	3.233
1500	54.691	2.632	1500	53.44	3.529
2100	55.779	2.259	2100	56.283	2.774
2700	55.21	2.066	2700	56.249	2.523
			3600	55.939	2.53
2.5 mol%					
t sec	integ Prod	integ SM			
60	6.978	31.755			
180	24.12	22.059			
300	38.002	14.128			
540	48.605	6.979			
900	52.123	4.283			
1200	55.435	3.424			
1500	54.904	2.842			
2100	53.975	2.304			
2700	55.435	2.636			
3600	56.508	2.355			

Copper(II) acetate (1 mol%), **PMe₃** (0.5 – 2.5 mol%), ZnEt₂ (12 mmol), cyclohexenone (10 mmol), PhMe

0.5 mol%			1.0 mol%		
t sec	integ Prod	integ SM	t sec	integ Prod	integ SM
60	6.161	30.158	60	4.736	35.447
180	17.179	26.592	180	10.224	30.317
300	26.023	21.824	300	17.116	24.533
540	38.374	13.999	540	26.188	17.495
900	48.424	8.093	900	36.631	14.33
1200	49.252	6.047	1200	41.478	10.036
1500	51.38	5.033	1500	44.392	8.317
2100	53.505	4.13	2100	47.186	7.227
2700	53.539	3.666	2700	48.495	5.875
3600	53.899	2.895	3600	47.903	6.365
1.5 mol%			2.0 mol%		
t sec	integ Prod	integ SM	t sec	integ Prod	integ SM
60	9.628	26.949	60	7.074	33.834
180	27.43	13.672	180	25.94	20.704
300	39.847	11.317	300	41.067	9.628
540	49.223	5.987	540	48.606	6.66
900	53.242	3.336	900	52.87	4.243
1200	52.894	3.04	1200	53.491	3.233
1500	54.691	2.632	1500	53.44	3.529
2100	55.779	2.259	2100	56.283	2.774
2700	55.21	2.066	2700	56.249	2.523
			3600	55.939	2.53
2.5 mol%					
t sec	integ Prod	integ SM			
60	6.978	31.755			
180	24.12	22.059			
300	38.002	14.128			
540	48.605	6.979			
900	52.123	4.283			
1200	55.435	3.424			
1500	54.904	2.842			
2100	53.975	2.304			
2700	55.435	2.636			
3600	56.508	2.355			

Copper(II) acetate (1 mol%), **PCy₃** (1.0 – 2.5 mol%), ZnEt₂ (12 mmol), cyclohexenone (10 mmol), PhMe

1.0 mol%			1.5 mol%		
t sec	integ Prod	integ SM	t sec	integ Prod	integ SM
60	3.673	32.785	60	7.994	31.889
180	12.182	27.799	180	29.015	17.49
300	24.298	20.459	300	40.86	10.472
540	38.598	12.096	540	49.137	5.92
900	48.622	5.132	900	53.257	3.073
1200	48.807	4.32	1200	52.921	2.841
1500	52.063	5	1500	55.116	2.204
2100	55.097	3.761	2100	56.17	2.07
2700	53.782	3.713	2700	56.653	1.645
3600	57.681	3.12	3600	57.339	1.25
2.0 mol%			2.5 mol%		
t sec	integ Prod	integ SM	t sec	integ Prod	integ SM
60	8.206	32.261	60	8.541	29.534
180	29.305	16.493	180	26.437	20.443
300	39.769	12.053	300	38.857	11.714
540	48.381	6.264	540	47.811	6.771
900	51.904	3.768	900	51.3	3.373
1200	53.779	2.624	1200	55.915	3.315
1500	57.834	2.404	1500	56.472	2.379
2100	57.608	2.017	2100	56.918	2.091
2700	58.057	1.56	2700	56.382	1.616
3600	40.265	0.943	3600	59.366	1.51

Copper(II) acetate (1 mol%), **PPh₃** (1.0 – 3.0 mol%), ZnEt₂ (12 mmol), cyclohexenone (10 mmol), PhMe

1.0 mol%			1.5 mol%		
t sec	Integ. Pro	Integ. SM	t sec	Integ. Pro	Integ. SM
60	3.912	40.067	60	2.587	43.162
180	9.957	38.698	180	7.199	41.563
300	25.713	23.942	300	18.107	23.794
540	48.625	7.571	540	40.583	11.593
900	55.431	3.869	900	52.239	3.692
1200	56.347	3.200	1200	53.692	2.955
1500	57.646	2.638	1500	54.285	1.695
2100	55.121	1.434	2100	56.047	2.459
2700	52.735	1.38	2700	56.274	1.994
3600	59.888	1.045	3600	57.412	0.819
2.0 mol%			2.5 mol%		
t sec	Integ. Pro	Integ. SM	t sec	Integ. Pro	Integ. SM
60	1.681	42.283	60	5.081	37.068
180	3.279	33.425	180	1.336	42.175
300	6.379	32.021	300	4.389	43.059
540	14.369	32.796	540	4.181	40.027
900	30.073	20.643	900	7.095	33.521
1200	39.238	10.752	1200	10.305	38.042
1500	44.074	9.751	1500	14.128	38.034
2100	49.244	6.359	2100	23.355	29.663
2700	53.597	4.087	2700	29.575	22.446
3600	52.594	3.114	3600	34.662	20.753
3.0 mol%					
t sec	Integ. Pro	Integ. SM			
60	4.079	37.49			
180	3.02	40.963			
300	4.267	32.656			
540	11.196	32.931			
900	11.225	36.775			
1200	17.985	25.987			
1500	23.103	26.045			
2100	31.351	17.374			
2700	40.264	17.34			
3600	44.16	10.243			

Copper(II) acetate (1 mol%), **P(2-furanyl)₃** (1.0 – 3.0 mol%), ZnEt₂ (12 mmol), cyclohexenone (10 mmol), PhMe

1.0 mol%			1.5 mol%		
t sec	integ Prod	integ SM	t sec	integ Prod	integ SM
60	2.032	34.198	60	2.26	36.572
180	2.466	33.487	180	2.467	36.534
300	2.709	33.188	300	3.621	37.06
540	3.213	29.902	540	6.432	31.58
900	4.539	33.262	900	9.829	29.565
1200	5.791	30.389	1200	14.445	26.554
1500	6.894	29.513	1500	18.632	23.685
2100	10.086	26.096	2100	25.754	18.546
2700	12.475	25.275	2700	32.161	15.672
3600	16.625	25.474	3600	43.406	8.108
2.0 mol%			2.5 mol%		
t sec	integ Prod	integ SM	t sec	integ Prod	integ SM
60	1.526	38.879	60	1.763	36.698
180	2.612	33.855	180	2.328	34.171
300	3.105	32.175	300	2.185	33.942
540	5.014	32.288	540	3.044	29.758
900	8.494	34.243	900	4.014	32.085
1200	11.241	31.872	1200	5.968	31.455
1500	15.872	21.499	1500	7.401	30.42
2100	22.278	18.092	2100	12.387	27.958
2700	28.415	18.308	2700	17.432	21.744
3600	38.458	10.995	3600	22.395	22.008
3.0 mol%					
t sec	integ Prod	integ SM			
60	1.015	35.163			
180	1.394	33.696			
300	1.147	38.205			
540	1.465	34.711			
900	2.348	34.941			
1200	2.516	36.087			
1500	2.946	32.973			
2100	4.756	29.634			
2700	6.293	31.607			
3600	10.24	32.38			

Copper(II) acetate (1 mol%), **P(4-FC₆H₄)₃** (0.5 – 2.0 mol%), ZnEt₂ (12 mmol), cyclohexenone (10 mmol), PhMe

0.5 mol%			1.0 mol%		
t sec	integ Prod	integ SM	t sec	integ Prod	integ SM
60	2.297	33.774	60	6.958	32.536
180	6.915	28.975	180	28.472	20.72
300	15.005	24.509	300	42.374	11.482
540	29.298	18.131	540	52.094	7.033
900	41.607	10.561	900	57.521	3.637
1200	45.242	7.478	1200	56.89	3.521
1500	46.761	8.528	1500	60.024	2.729
2100	50.035	5.755	2100	61.251	2.403
2700	53.336	5.231	2700	60.508	2.255
3600	56.661	4.42	3600	61.875	2.058
1.5 mol%			2.0 mol%		
t sec	integ Prod	integ SM	t sec	integ Prod	integ SM
60	12.994	29.771	60	1.716	41.885
180	37.213	14.901	180	4.656	34.806
300	46.058	9.565	300	9.818	29.664
540	53.39	4.966	540	28.062	16.311
900	56.348	2.481	900	42.099	10.718
1200	52.921	3.172	1200	46.723	7.851
1500	57.948	3.065	1500	41.97	7.497
2100	60.039	1.617	2100	55.024	4.682
2700	60.271	1.959	-	-	-
3600	60.734	1.86	3600	56.281	3.119

Copper(II) acetate (1 mol%), **L2** (0.5 – 3.0 mol%), ZnEt₂ (12 mmol), cyclohexenone (10 mmol), PhMe

0.5 mol%				1.0 mol%			
t sec	integ Prod	integ SM	ee	t sec	integ Prod	integ SM	ee
60	17.966	24.986	68	60	17.498	52.666	94
180	32.138	13.548	76	180	26.923	43.478	96
300	36.877	11.101	80	300	31.526	37.325	96
540	41.278	8.509	86	540	43.222	31.226	96
900	43.784	6.781	90	900	47.877	24.834	97
1200	46.294	6.457	92	1200	54.048	21.602	98
1500	47.873	5.783	94	1500	58.067	15.888	98
2100	47.759	4.035	96	2100	61.099	10.859	98
2700	48.212	3.968	96	2700	64.675	12.631	98
3600	48.273	4.304	96	3600	52.006	6.596	98
1.5 mol%				2.0 mol%			
t sec	integ Prod	integ SM	ee	t sec	integ Prod	integ SM	ee
60	10.85	89.15	70	60	17.193	46.907	90
180	29.13	70.87	85	180	22.524	39.744	94
300	34.61	65.39	88	300	28.777	31.309	94
540	57.38	42.62	92	540	36.238	29.365	94
900	84.93	15.07	-	900	43.192	20.2	94
1200	99.82	0.18	96	1200	49.403	19.14	94
1500	87.21	12.79	96	1500	55.27	16.843	94
2100	99.77	0.23	96	2100	58.297	12.089	94
2700	96.54	3.46	96	2700	66.26	8.655	94
3600	99.04	0.96	96	3600	72.424	3.573	94
2.5 mol%				3.0 mol%			
t sec	integ Prod	integ SM	ee	t sec	integ Prod	integ SM	ee
60	16.197	47.197	86	60	14.744	53.821	96
180	32.901	33.533	92	180	29.003	43.538	98
300	43.619	24.885	94	300	36.367	36.016	98
540	57.724	14.903	94	540	45.353	30.292	98
900	62.109	12.041	94	900	55.696	20.652	98
1200	75.147	6.242	94	1200	58.979	16.545	98
1500	70.955	6.239	94	1500	61.917	13.648	98
2100	74.013	4.362	94	2100	65.652	8.765	98
2700	72.084	4.83	94	2700	69.803	7.879	98
3600	72.233	3.996	94	3600	69.235	6.762	98

Copper(II) acetate (1 mol%), **P(OPh)₃** (1.0 – 3.0 mol%), ZnEt₂ (12 mmol), cyclohexenone (10 mmol), PhMe

1.0 mol%			1.5 mol%		
t sec	Integ. Pro	Integ. SM	t sec	Integ. Pro	Integ. SM
60	3.364	43.173	60	3.613	40.437
180	5.004	42.539	180	4.423	40.663
300	4.161	42.273	300	6.090	40.390
540	7.352	40.977	540	10.360	36.644
900	10.931	37.493	900	20.582	29.892
1200	13.357	33.814	1200	32.634	21.167
1500	16.803	34.386	1500	41.307	13.556
			2100	45.645	7.201
2700	30.284	22.616	2700	52.187	4.465
3600	45.018	12.972	3600	48.268	2.745
2.0 mol%			3.0 mol%		
t sec	Integ. Pro	Integ. SM	t sec	Integ. Pro	Integ. SM
60	5.514	38.087	60	4.044	42.930
180	7.443	29.876	180	9.536	40.353
300	10.687	37.167	360	11.966	36.601
540	25.960	23.989	540		
900	44.591	13.271	900	40.350	13.550
1200	48.032	7.507	1200	50.011	6.172
1500	54.614	4.366	1500	57.235	4.536
2100	58.774	2.560	2100	65.631	2.539
2700	55.422	1.593	2700	63.803	1.914
3600	59.215	1.439	3600	63.118	1.273

Copper(II) triflate (1 mol%), **PPh₃** (1.0 – 2.5 mol%), ZnEt₂ (12 mmol), cyclohexenone (10 mmol), PhMe

1.0 mol%			1.5 mol%		
t sec	integ Prod	integ SM	t sec	integ Prod	integ SM
60	7.32	27.913	60	10.572	30.46
180	17.101	25.376	180	29.059	16.116
300	26.009	20.253	300	41.597	9.434
540	43.198	10.292	540	54.81	2.057
900	50.968	4.316	900	56.091	2.125
1200	54.166	4.84	1200	56.759	2.049
1500	50.882	4.216	1500	55.61	2.385
2100	51.189	4.321	2700	57.457	1.451
2700	51.293	3.881	3300	56.228	1.672
3600	51.697	4.948	3600	53.546	1.823
2.0 mol%			2.5 mol%		
t sec	integ Prod	integ SM	t sec	integ Prod	integ SM
60	16.466	25.049	60	2.963	32.65
180	38.965	12.919	180	6.737	30.711
300	52.277	4.524	300	11.727	26.303
540	58.997	1.357	540	24.29	18.983
900	59.717	1.425	900	37.485	12.511
1200	56.532	1.363	1200	47.511	6.924
1500	56.596	1.503	1500	50.641	4.565
2100	59.241	0.939	2100	52.42	2.259
2700	58.885	1.157	2700	55.582	2.207
3600	55.698	1.228	3600	56.295	2.554

Copper(II) acetate (1 mol%), **L2** (1.0 – 2.5 mol%), AlEt₃ (12 mmol), cyclohexenone (10 mmol), Et₂O

0.5 mol%				1.0 mol%			
t sec	integ Pro	integ SM	ee	t sec	integ Pro	integ SM	ee
60	19.107	31.659	46	60	11.314	44.075	54
180	21.145	37.116	66	180	28.893	34.369	72
300	28.705	28.782	72	300	37.647	23.911	78
540	39.908	19.937	78	540	51.369	13.321	82
900	53.972	12.106	80	900	61.014	7.303	82
1200	59.27	8.098	82	1200	31.48	3.86	82
1500	70.959	5.719	82	1500	65.795	3.497	82
2100	67.644	3.012	82	2100	66.852	3.445	82
2700	67.209	3.399	82	2700	66.139	3.162	82
3600	67.659	4.237	82	3600	67.108	2.825	82
1.5 mol%				2.0 mol%			
t sec	integ Pro	integ SM	ee	t sec	integ Pro	integ SM	ee
60	17.832	37.196	40	60	10.666	40.679	52
180	30.226	29.9	70	180	25.361	34.041	72
300	43.405	21.337	76	300	40.115	20.178	78
540	58.87	9.951	80	540	56.926	7.502	82
900	65.483	5.384	82	900	65.458	3.095	82
1200	67.622	2.93	82	1200	65.024	2.976	82
1500	66.447	3.536	82	1500	64.925	2.69	82
2100	68.137	3.427	82	2100	65.642	2.496	82
2700	68.32	3.455	82	2700	65.87	2.304	82
3600	67.959	2.705	82	3600	65.729	2.306	82
2.5 mol%				3.0 mol%			
t sec	integ Pro	integ SM	ee	t sec	integ Pro	integ SM	ee
60	18.535	23.036	46	60	24.515	37.557	42
180	21.531	24.531	62	180	34.948	28.586	60
300	30.573	17.076	70	300	47.348	17.634	70
540	46.084	9.023	76	540	63.42	5.357	76
900	53.723	3.221	78	900	66.866	3.622	76
1200	52.807	2.821	78	1200	66.955	2.917	76
1500	57.586	2.344	78	1500	74.525	2.846	76
2100	55.658	2.828	78	2100	67.469	2.841	76
2700	55.007	2.14	78	2700	67.432	2.907	76
3600	56.336	2.199	78	3600	66.932	2.724	76
3.5 mol%				4.5 mol%			
t sec	integ Pro	integ SM	ee	t sec	integ Pro	integ SM	ee
60	5.078	15.370	70	60	3.498	29.986	58
180	11.483	10.168	78	180	7.630	24.782	72
300	16.382	8.941	80	300	12.081	23.161	74
540	24.259	4.589	82	540	20.607	13.554	78
900	26.983	1.814	84	900	28.101	10.210	80
1200	28.496	1.341	84	1200	30.609	6.192	80
1500	29.223	1.761	84	1500	32.591	5.781	80
2100	28.809	1.669	84	2100	30.622	2.998	80
2700	28.918	1.589	84	2700	35.473	4.999	80
3600	28.893	1.459	84	3600	33.844	3.346	80

5.0 mol%			
t sec	integ Pro	integ SM	ee
60	5.737	19.171	20
180	10.116	18.270	32
300	11.840	11.926	40
540	18.024	11.505	52
900	26.268	10.134	58
1200	31.852	7.994	64
1500	35.564	5.535	66
2100	39.260	2.841	70
2700	41.013	3.118	70
3600	39.961	1.987	70

Copper(I) bromide dimethylsulfide (1 mol%), **L27** (0.5 – 1.5 mol%), EtMgBr (12 mmol), methylcrotonate (10 mmol), CH₂Cl₂

0.5 mol%			0.75 mol%		
t sec	integ Pro	integ SM	t sec	integ Pro	integ SM
60	21.338	19.324	60	35.398	11.627
180	30.484	16.701	180	29.428	15.806
300	30.271	14.644	300	36.861	10.056
540	35.985	15.549	540	36.901	8.07
900	36.449	13.447	900	39.832	7.118
1200	35.13	11.082	1200	43.034	6.433
1500	34.483	10.088	1500	37.228	5.069
2100	34.42	9.321	2100	39.203	4.687
2700	34.568	8.859	2700	38.927	4.254
3600	35.119	8.13	3600	40.025	4.234
1.0 mol%			1.25 mol%		
t sec	integ Pro	integ SM	t sec	integ Pro	integ SM
60	35.851	8.21	60	35.246	6.582
180	41.592	6.137	180	43.143	5.084
300	43.207	5.843	300	43.291	4.477
540	42.572	5.144	540	42.638	3.605
900	41.137	4.736	900	44.215	3.356
1200	39.129	4.24	1200	45.781	3.219
1500	39.305	4.386	1500	45.41	3.225
2100	39.988	4.465	2100	41.72	3.212
2700	37.718	3.843	2700	40.7	2.829
3600	38.908	4.437	3600	40.997	2.814
1.5 mol%					
t sec	integ Pro	integ SM			
180	39.684	12.172			
300	38.237	10.303			
540	39.875	8.767			
900	46.633	9.162			
1200	47.604	8.569			
1500	48.827	8.702			
2100	47.561	8.056			
2700	47.606	8.165			
3600	48.34	8.234			

Copper(I) iodide (1 mol%), **L28** (0.5 – 2.5 mol%), EtMgBr (12 mmol), methylcrotonate (10 mmol), CH₂Cl₂

0.5 mol%			1.0 mol%		
t sec	integ Pro	integ SM	t sec	integ Pro	integ SM
60	4.367	39.464	60	9.676	28.651
180	6.754	35.515	180	11.146	18.35
300	8.543	38.129	300	12.774	17.055
540	9.611	32.446	540	14.441	15.89
900	10.473	28.392	900	16.2	15.759
1200	11.966	28.574	1200	16.598	14.38
1500	12.856	27.716	1500	16.352	13.625
2100	14.574	28.359	2100	18.384	14.311
2700	16.292	28.686	2700	18.802	13.63
3600	19.57	31.422	3600	19.573	13.221
1.5 mol%			2.0 mol%		
t sec	integ Pro	integ SM	t sec	integ Pro	integ SM
60	2.428	29.512	60	5.15	40.174
180	3.755	24.874	180	8.561	36.962
300	4.522	21.645	300	9.185	37.692
540	5.745	21.102	540	10.53	37.753
900	7.092	21.178	900	9.541	31.396
1200	7.71	19.557	1200	10.248	31.813
1500	7.968	17.865	1500	11.396	30.72
2100	10.274	20.408	2100	10.734	28.306
2700	9.956	16.601	2700	11.694	28.38
3600	11.206	17.053	3600	12.359	28.088
2.5 mol%					
t sec	integ Pro	integ SM			
60	0.632	42.004			
180	0.951	39.436			
300	1.341	39.084			
540	1.697	39.396			
900	2.44	40.581			
1200	2.211	37.404			
1500	2.472	37.674			
2100	2.571	37.223			
2700	2.95	37.005			
3600	3.4	36.631			

Ni(acac)₂ (1 mol%), **L2** (0.5 – 4.0 mol%), AlMe₃ (12 mmol), benzaldehyde (10 mmol), THF

0.5 mol%			1.0 mol%		
t sec	integ Pro	integ SM	t sec	integ Pro	integ SM
60	0	38.635	60	2.547	48.556
180	0.737	43.146	180	5.284	45.827
300	0.764	42.973	300	7.319	44.595
540	2.64	40.983	540	11.989	40.43
900	7.538	34.924	900	25.619	26.53
1200	14.683	31.082	1200	40.383	11.195
1500	22.271	21	1500	53.924	0.128
2100	42.424	0.393	2100	54.23	0.11
2700	44.232	0.1	2700	48.673	0.102
3600	45.04	0.093	3600	52.307	0.088
2.0 mol%			3.0 mol%		
t sec	integ Pro	integ SM	t sec	integ Pro	integ SM
60	0.192	43.689	60	0.573	40.254
180	1.722	43.065	180	1.637	42.167
300	1.182	37.667	300	2.126	37.308
540	7.136	34.546	540	5.667	38.969
900	19.385	20.432	900	11.923	30.683
1200	33.506	12.132	1200	17.703	24.212
1500	37.762	2.584	1500	24.537	23.056
2100	42.487	0.097	2100	30.428	12.224
2700	42.651	0.102	2700	41.361	6.081
3600	39.989	0.089			
4.0 mol%					
t sec	integ Pro	integ SM			
180	1.659	36.728			
300	2.474	35.195			
540	2.776	32.858			
900	5.57	30.85			
1200	6.321	25.971			
1500	8.383	24.61			
2100	16.252	20.605			
2700	21.133	16.021			
3600	27.384	14.456			

Effect of dichloromethane

Copper(II) acetate (1 mol%), **L2** (2.0 mol%), ZnEt₂ (12 mmol), cyclohexenone (10 mmol), PhMe, CH₂Cl₂ (2 mL – 10 mL)

2 mL CH ₂ Cl ₂				5 mL CH ₂ Cl ₂			
t sec	integ Pro	integ SM	ee	t sec	integ Pro	integ SM	ee
60	28.831	18.654	92	60	15.99	35.256	93
180	40.454	3.296	96	180	19.857	37.839	95
300	48.111	14.178	96	300	38.813	22.595	96
540	49.17	16.761	96	540	39.267	15.329	97
900	56.8	5.66	96	900	54.694	8.37	98
1200	57.139	4.561	97	1200	55.95	3.725	98
1500	63.162	9.095	98	1500	59.499	4.101	98
2100	63.221	2.996	98	2100	57.174	0.927	98
2700	68.841	4.827	98	2700	66.83	1.558	98
3600	68.33	1.64	98				
10 mL CH ₂ Cl ₂							
t sec	integ Pro	integ SM	ee				
60	24.96	35.158	95				
180	34.813	14.543	97				
300	56.663	10.908	98				
540	65.082	5.766	98				
900	59.287	2.377	98				
1200	70.445	3.204	98				
1500	66.292	2.776	98				
2100	67.118	2.603	98				
2700	65.29	2.285	98				
4500	61.917	2.411	98				

Kinetic data for activation derivation

Copper(II) acetate (1 mol%), **L2** (2.0 mol%, 50% ee), ZnEt₂ (12 mmol), cyclohexenone (10 mmol), PhMe.

-50 °C			-45 °C		
t sec	integ Pro	integ SM	t sec	integ Pro	integ SM
60	16.147	83.853	60	23.169	32.805
180	30.665	69.335	180	26.639	21.85
300	59.777	40.223	300	30.923	32.05
540	40.152	59.848	540	32.403	34.773
900	56.012	43.988	900	40.454	25.221
1200	77.875	22.125	1200	40.205	16.935
1500	73.276	26.724	1500	44.063	27.578
2100	79.228	20.772	2100	48.644	18.999
2700	89.982	10.018	2700	53.152	17.565
3600	86.966	13.034	3600	55.9	15.215
-40 °C			-35 °C		
t sec	integ Pro	integ SM	t sec	integ Pro	integ SM
60	17.193	46.907	60	12.184	47.552
180	22.524	39.744	180	15.144	46.22
300	28.777	31.309	300	21.567	44.829
540	36.238	29.365	540	33.512	17.284
900	43.192	20.2	900	45.418	26.558
1200	49.403	19.14	1200	51.273	17.875
1500	55.27	16.843	1500	55.571	3.232
2100	58.297	12.089	2100	60.063	8.316
2700	66.26	8.655	2700	54.265	0.418
3600	72.424	3.573	3600	73.655	4.885

Job's plots analysis

Copper(II) acetate **L39** (4.5 mol% total), ZnEt₂ (12 mmol), cyclohexenone (10 mmol), PhMe.

Cu(OAc) ₂ = 1 mol%, SImes = 3.5 mol% [χ (Cu) =0.22]			Cu(OAc) ₂ = 1.5 mol%, SImes = 3 mol% [χ (Cu) =0.333]		
t sec	integ Pro	integ SM	t sec	integ Pro	integ SM
60	40.101	7.974	60	31.766	18.175
180	39.799	12.062	180	23.987	29.201
300	34.125	15.562	300	22.21	34.073
540	30.769	20.074	540	18.068	39.209
900	29.169	23.981	900	16.762	44.5
1200	30.795	26.614	1200	14.794	48.182
1500	25.264	35.567	1500	12.261	53.842
2100	23.807	33.41	2100	11.303	55.244
2700	22.56	36.872	2700	10.702	56.752
3600	17.376	40.996	3600	9.759	56.913
Cu(OAc) ₂ = 2 mol%, SImes = 2.5 mol% [χ (Cu) =0.44]			Cu(OAc) ₂ = 2.2 mol%, SImes = 2.3 mol% [χ (Cu) =0.48]		
t sec	integ Pro	integ SM	t sec	integ Pro	integ SM
60	25.738	33.47	60	28.113	28.032
180	13.509	47.677	180	22.266	38.684
300	12.959	53.041	300	16.311	46.034
540	8.606	58.083	540	13.121	51.038
900	9.511	57.774	900	11.05	54.716
1200	7.436	62.039	1200	9.902	55.692
1500	7.023	63.929	1500	7.907	59.642
2100	6.574	64.98	2100	7.918	61.779
2700	5.327	63.195	2700	7.572	61.09
3600	4.438	67.884	3600	6.363	62.927

Copper(II) acetate **PPh₃** (4.5 mol% total), ZnEt₂ (12 mmol), cyclohexenone (10 mmol), PhMe.

Cu(OAc) ₂ = 1 mol%, SImes = 3.5 mol% [χ (Cu) =0.22]			Cu(OAc) ₂ = 1.5 mol%, SImes = 3 mol% [χ (Cu) =0.333]		
t sec	integ Pro	integ SM	t sec	integ Prod	integ SM
60	48.045	4.634	60	39.292	4.955
180	45.23	5.283	180	36.826	14.005
300	43.559	9.288	300	29.381	25.062
540	31.634	20.643	540	13.47	52.444
900	22.614	36.104	900	9.431	60.054
1200	19.575	42.608	1200	5.285	64.345
1500	13.233	46.931	1500	4.926	66.483
2100	12.382	55.573	2100	3.531	69.333
2700	9.278	60.217	2700	3.083	69.717
3600	7.075	61.293	3600	3.307	69.877
Cu(OAc) ₂ = 2 mol%, SImes = 2.5 mol% [χ (Cu) =0.44]			Cu(OAc) ₂ = 2.2 mol%, SImes = 2.3 mol% [χ (Cu) =0.48]		
t sec	integ Pro	integ SM	t sec	integ Prod	integ SM
60	19.968	38.674	60	46.653	4.274
180	6.969	63.412	180	39.786	13.12
300	4.021	67.952	300	32.376	25.702
540	1.85	72.958	540	19.575	42.993
900	1.94	77.301	900	13.226	50.695
1200	1.379	72.556	1200	8.066	65.737
1500	1.072	75.91	1500	8.225	58.328
2100	1.121	73.996	2100	5.123	73.595
2700	0.711	71.273	2700	4.483	72.861
3600	0.633	74.26	3600	4.018	73.292

Copper(II) acetate **P(OPh)₃** (4.5 mol% total), ZnEt₂ (12 mmol), cyclohexenone (10 mmol), PhMe.

Cu(OAc) ₂ = 1 mol%, SImes = 3.5 mol% [χ (Cu) = 0.22]			Cu(OAc) ₂ = 1.5 mol%, SImes = 3 mol% [χ (Cu) = 0.333]		
t sec	integ Prod	integ SM	t sec	integ Prod	integ SM
60	41.403	5.022	60	43.181	9.189
180	38.189	14.553	180	33.124	20.009
300	30.046	25.845	300	26.671	34.057
540	16.85	46.078	540	14.112	52.53
900	9.494	56.208	900	8.082	66.116
1200	6.409	64.119	1200	5.991	68.034
1500	5.215	66.139	1500	4.445	70.624
2100	3.976	69.268	2100	3.881	69.606
2700	3.425	68.603	2700	3.848	68.513
3600	3.258	69.711	3600	3.664	69.675
Cu(OAc) ₂ = 2 mol%, SImes = 2.5 mol% [χ (Cu) = 0.44]			Cu(OAc) ₂ = 2.2 mol%, SImes = 2.3 mol% [χ (Cu) = 0.48]		
t sec	integ Prod	integ SM	t sec	integ Prod	integ SM
60	41.814	8.188	60	48.237	3.617
180	32.158	22.357	180	42.397	8.158
300	23.428	36.398	300	39.207	15.562
540	12.632	55.584	540	26.757	32.598
900	5.819	67.378	900	15.587	51.082
1200	3.839	69.738	1200	9.578	58.605
1500	2.339	71.02	1500	5.894	66.526
2100	1.774	72.294	2100	3.2	68.974
2700	1.654	71.456	2700	2.314	70.23
3600	1.524	71.335	3600	2.236	67.143

Copper(II) acetate **P(4-FC₆H₄)₃** (4.5 mol% total), ZnEt₂ (12 mmol), cyclohexenone (10 mmol), PhMe.

Cu(OAc) ₂ = 1 mol%, SImes = 3.5 mol% [χ (Cu) =0.22]			Cu(OAc) ₂ = 1.5 mol%, SImes = 3 mol% [χ (Cu) =0.333]		
t sec	integ Prod	integ SM	t sec	integ Prod	integ SM
60	47.178	1.559	60	29.91	22.575
180	44.421	4.292	180	12.416	49.117
300	37.805	10.222	300	8.602	55.53
540	31.957	26.518	540	4.588	64.727
900	15.655	48.431	900	3.289	68.639
1200	11.782	52.802	1200	2.425	67.62
1500	10.069	58.527	1500	2.093	66.823
2100	7.691	64.767	2100	1.855	69.519
2700	6.928	68.473	2700	1.276	71.655
3600	5.845	69.158	3600	1.283	71.573
Cu(OAc) ₂ = 2 mol%, SImes = 2.5 mol% [χ (Cu) =0.44]			Cu(OAc) ₂ = 2.2 mol%, SImes = 2.3 mol% [χ (Cu) =0.48]		
t sec	integ Prod	integ SM	t sec	integ Prod	integ SM
60	31.113	26.187	60	45.326	6.324
180	12.646	56.117	180	24.205	34.428
300	8.492	61.607	300	17.704	43.698
540	5.509	64.431	540	9.246	59.557
900	4.168	70.606	900	6.341	65.379
1200	3.192	73.689	1200	4.822	71.324
1500	2.797	70.656	1500	4.392	70.82
2100	2.456	72.645	2100	3.808	74.514
2700	1.95	76.689	2700	3.513	72.475
3600	1.997	75.616	3600	2.934	75.294